Low-frequency Bias-tone Effects on Auditory-Nerve Responses to Clicks and Tones: Investigating Multiple Outer-Hair-Cell Actions on Auditory-Nerve Firing

By

Hui S. Nam

B.S. Electrical Science and Engineering
Massachusetts Institute of Technology, 1994

SUBMITTED TO THE HARVARD-MIT DIVISION OF HEALTH SCIENCES AND TECHNOLOGY
IN PARTIAL FULFILLMENT OF THE REQUIREMENTS FOR THE DEGREE OF

DOCTOR OF PHILOSOPHY IN HEALTH SCIENCES AND TECHNOLOGY
AT THE
MASSACHUSETTS INSTITUTE OF TECHOLOGY

SEPTEMBER, 2011

Signature of Author _____
Harvard-MIT Division of Health Sciences and Technology
August 5, 2011

Certified by _____
John J. Guinan, Jr., Ph.D
Professor of Otology and Laryngology, Harvard Medical School
Thesis Supervisor

Accepted by _____
Ram Sasisekharan, Ph.D
Director, Harvard-MIT Division of Health Sciences and Technology
Edward Hood Taplin Professor of Health Sciences & Technology and Biological Engineering

Low-frequency Bias-tone Effects on Auditory-Nerve Responses to Clicks and Tones: Investigating Multiple Outer-Hair-Cell Actions on Auditory-Nerve Firing

By

Hui S. Nam

Submitted to Havard-MIT Division of Health Sciences and Technology
on August, 5 2011 in Partial Fulfillment of the
Requirements for the Degree of Doctor of Philosophy in
Health Sciences and Technology

ABSTRACT

Active motility in outer hair cells (OHCs) amplifies basilar-membrane (BM) and auditory-nerve (AN) responses to low-level sounds. The recent finding that medial olivocochlear (MOC) efferents (which innervate OHCs) inhibit AN initial peak (ANIP) responses from mid-to-high-level clicks, but do not inhibit initial BM responses, suggests a coupling of OHC motility to inner-hair-cell (IHC) stereocilia that is not through the BM. The main thesis objective was to test whether different OHC mechanisms produce AN responses to low-level sounds versus ANIP from mid-to-high-level clicks by comparing the suppressive effects of low-frequency "bias-tones" on these responses. Bias tones suppress by pushing OHC stereocilia into low-slope regions of their mechanoelectric transduction functions thereby lowering OHC amplification, particularly for probe tones near an AN-fiber's characteristic frequency (CF). This suppression occurs at opposite bias-tone phases, with one suppression typically larger than the other. Bias-tone effects were measured on cat AN-fiber responses using 50 Hz bias tones. In the first thesis part, bias-tone suppressive effects on AN responses to low-level clicks and low-level CF-tones were found to be similar, as expected but never previously shown. Then, in the main thesis focus, bias-tone suppressions of AN responses to low-level clicks and ANIP responses were studied. Both responses were suppressed twice each bias-tone cycle, but their major suppressions were at opposite bias-tone phases, which indicates that both ANIP and low-level AN responses depend on the slope of OHC-stereocilia mechanoelectric-transduction, but with some significant difference. In the last thesis part, bias-tone suppression effects on low-CF (<4 kHz) AN-fiber responses to low-level CF and off-CF (by >0.7 octaves) tones were studied. Previous work found differences in AN-response group delays between CF and off-CF frequency regions that might arise from two different IHC-drive mechanisms, and the objective was to test this hypothesis. Our results showed similar bias-tone effects in both regions. Overall, the results demonstrate differences and similarities in the OHC mechanisms that produce ANIP and traditional, low-level cochlear amplification, and the results are consistent with the ANIP drive coupling OHC motility to IHC stereocilia without going through BM motion.

Thesis Supervisor: John J. Guinan, Jr., Ph.D
Title: Professor of Otology and Laryngology, Harvard Medical School

Table of Contents

List of Figures

Chapter 1 . Thesis Introduction and Outline

I. Background

Research in cochlear mechanics aims to explain the biophysical mechanisms behind the sound amplification and transmission pathways in the cochlea that lead to deflections of the inner hair cell (IHC) stereocilia and firings of auditory-nerve (AN) fibers. Today, the theory of the "cochlear amplifier" and the experiments that support it [Rhode, 1971; Rhode and Robles, 1974; Liberman and Kiang, 1984; Brownell et al, 1985] are the dominant conceptual framework in the field of cochlear mechanics [Robles and Ruggero, 2001]. Measurements of basilar membrane (BM) vibration from living animals by [Rhode, 1971] revealed that the frequency tuning of BM motion is significantly sharper than in previously reported BM results thereby starting to close the apparent gap between the sharpness of frequency tuning of BM and neural tuning curves which had been a major dilemma. Also, in [Rhode, 1971; Rhode and Robles, 1974], it was found that BM motion in healthy living animals grows with compressive nonlinearity as sound level increases for tone stimuli with frequencies near the characteristic frequency (CF). Postmortem, the sharpness of tuning and nonlinearity disappear thereby providing support to the idea that there is active mechanical amplification within the cochlea. As for the cellular basis of cochlear amplification, it has been found that healthy outer hair cells (OHCs) are needed for the high sensitivity and sharp frequency tuning of the "cochlear amplifier" as evidenced by the loss of sensitivity and sharp tuning brought on by destruction of OHCs due to acoustic trauma [Liberman and Kiang, 1984; Schoonhoven et al, 1994]. The discovery of OHC electromotility by [Brownell et al, 1985], together with the aforementioned work, has led to the current theory of operation of the "cochlear amplifier". According to this theory, "cochlear amplification" is based on feedback between OHC motility and BM motion whereby the OHC mechano-electric transduction function converts the deflections of OHC stereocilia induced by sound stimuli to OHC transmembrane receptor voltage which returns as changes to BM motion through OHC electromotility [Robles and Ruggero, 2001].

Along with the above developments, and with advances in BM measurement techniques [Ruggero et al, 1997], it has been found that the tuning and sensitivity in the tuning-curve tip region of high-CF AN fibers are indeed found in BM motion measured from the same cochleae [Narayan et al, 1998]. This provides support to the currently prevailing view on the mechanism behind sound transmission to IHCs: (a) the mechanical drive that produces AN firing travels through a single transmission pathway, the BM traveling wave, with only minor signal transformations between BM vibration and IHC stereocilia deflections [Narayan et al, 1998; Robles and Ruggero, 2001], and (b) OHC motility preferentially enhances BM and AN responses to low sound levels through the mechanism of the "cochlear amplifier" [Dallos, 1992].

Alongside this view, however, it has also been long recognized that BM vibration alone may not provide an adequate explanation for certain oddments in AN firing in response to low-frequency tones at high-levels [Kiang, 1984; Cody and Mountain, 1989; Kiang, 1990]. AN responses to low-frequency tones have been found to show drastic shifts in the phase of firing over changes in tone intensity whereby a single phase of excitation at low-levels splits to multiple peaks at higher levels which may revert at even higher sound levels to a single peak with a reversed phase [Kiang, 1984; Kiang, 1990].

These drastic shifts in the phase of excitation were suggested to be explained by level-dependent interference between two drive components to the IHCs that have opposite phases [Kiang, 1990]. The role of BM vibration in these phase reversals of AN responses to low-frequency tones were investigated through a direct comparison of the BM vibrations and AN firings in response to a level series of low-frequency tones at a basal site of chinchilla cochleae in [Ruggero et al, 2000]. This study found phase reversals in AN responses to high-level tones that are not accompanied by corresponding phase shifts in BM vibration. This finding provided direct experimental support to the view that the complex phase response characteristics of AN firing to high–level, low-frequency tones indicate that there are multiple modes of mechanical drive to the IHCs [Ruggero et al, 2000].

Evidence for multiple drives to the IHCs at high-sound-levels has also been found from AN responses to clicks [Lin and Guinan, 2000; Guinan et al, 2005; Guinan and Cooper, 2008]. Clicks are acoustic realizations of impulses, and analysis of AN responses to clicks can reveal the resonant properties of the mechanical drives behind the AN responses. Recent studies on AN responses to click-level series have shown that the mechanical drive to the IHCs for mid-to-high-level clicks (60 – 100 dB SPL) are far more complex than for low-level clicks. AN responses to mid-to-high-level clicks exhibit interactions of multiple resonances and potentially multiple drive mechanisms to the IHC stereocilia [Lin and Guinan, 2000; Lin and Guinan, 2004; Guinan et al, 2005; Guinan, 2009].

Among the complex characteristics of the AN responses to high-level clicks reported in [Lin and Guinan, 2000; Guinan et al, 2005], the AN initial peak (ANIP) and AN second peak (ANSP) responses to mid-to-high-levels of clicks are of particular interest. Fig. 1.1 shows compound post-stimulus histograms (cPSTs) of cat AN responses to a click level series with alternating click polarity. The rarefaction click responses are plotted upward and the condensation click responses are plotted downward at each click level. The data came from a low-CF fiber, CT023_U051, with CF = 1.5 kHz and SR = 45 spikes / s. The click intensity ranged from 30 dB pSPL to 115 dB pSPL, where click intensities are expressed as peak-equivalent SPL (pSPL) which corresponds to the SPL of a tone stimulus with the same peak pressure measured near the tympanic membrane as that generated by the clicks. At 80 dB pSPL, the ANIP responses emerged ahead of the bulk of the response (the bulk of the response can be considered to be an upward extension of the responses found at lower click levels). Electrical stimulation of medial-olivocochlear (MOC) efferents inhibits BM and AN responses driven by the electromotility of OHCs, and has been found to inhibit ANIP responses from mid-to-high click levels as well as AN responses from low-level clicks [Guinan et al, 2005]. Further, the ANSP response, which corresponds to the initial peak of the condensation click response, has also been found to be inhibited by MOC efferent stimulation, but by less than the ANIP inhibition. In Fig. 1.1 , the regions of the click responses labeled as "LL-Clix" at low-level clicks and "ANIP" and "ANSP" at mid-to-high level clicks are the regions that were found to be significantly inhibited by stimulation of MOC efferents while the later peaks following ANIP and ANSP remained largely unaffected by MOC stimulation.

high level clicks are the regions that were found to be significantly inhibited by stimulation of MOC efferents while the later peaks following ANIP and ANSP remained largely unaffected by MOC stimulation.

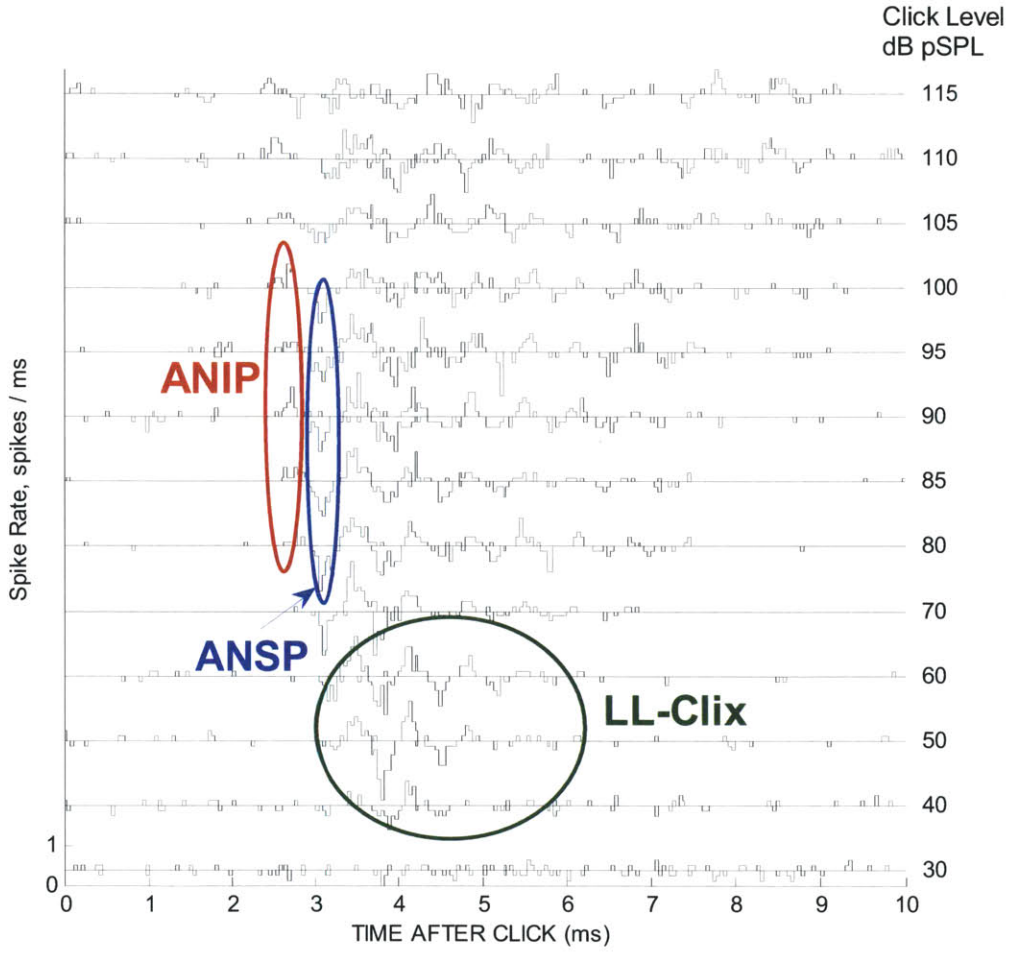

Fig. 1.1. Cat auditory nerve (AN) compound-PST (cPST) histograms showing responses to clicks at different sound levels. A cPST histogram plots responses to rarefaction clicks up and to condensation clicks down. ANIP = AN initial peak, ANSP = AN second peak, LL-Clix is the "low-level click" region. CF = 1.5 kHz. SR=45 sp/s.

Studies of MOC efferent effects on AN responses to clicks have shown that OHC electromotility is unexpectedly involved in response generation of ANIP and ANSP. These responses are invoked by click levels well above the click-response threshold thereby challenging the widely accepted notion that OHCs preferentially affect BM and AN responses to low-level sounds. A question which naturally follows these findings is whether the detailed mechanism whereby OHC electromotility is coupled to AN firing of ANIP and ANSP might be somehow different from the mechanism operating at low click levels. A part of the answer to this question comes from [Guinan and Cooper, 2008] which reported the effects of MOC

stimulation on BM responses to click level series measured in the basal region of the guinea pig's cochlea. Unlike AN responses to mid-to-high-levels of clicks from the apical region of cats, the initial peaks of the BM response to mid-to-high-levels of clicks (and to clicks at all levels) were unaffected by MOC efferent stimulation. Based on these findings, it was hypothesized that the response generation mechanism for ANIP and ANSP involves OHC electromotility, as does the "cochlear amplifier" . However, the coupling of ANIP and ANSP drives to IHC stereocilia must be by a mechanism that is different from the BM cochlear amplification of low-level clicks [Guinan et al, 2005; Guinan, 2009].

The idea that OHC forces can be coupled to deflections of IHC stereocilia through a mechanism other than BM vibration is supported by a multitude of papers [e.g. Mountain and Cody, 1999; Nowotny and Gummer, 2006]. In [Mountain and Cody, 1999], the discrepancy between the complexities in AN responses versus the relatively linear BM motions to high-level tone stimuli was investigated through computational models of the stimulation of IHC stereocilia. Their results demonstrated that incorporating an additional coupling path into the model from OHC forces to IHC stereocilia (possibly through the tectorial membrane) produced significantly closer simulation of the actual measurements of IHC receptor potentials to high-level tones in comparison to a simpler model based on a single transmission path through the BM [Mountain and Cody, 1999]. In the in vitro study on excised guinea-pig cochleae by [Nowotny & Gummer, 2006] for frequencies up to 3 kHz, contraction and elongation of OHCs brought on by their electromotility caused bulging and squeezing of the subtectorial space above the IHC stereocilia thereby resulting in fluid flow that deflected the IHC stereocilia with a sufficient magnitude to stimulate AN firing. Particularly, in [Guinan et al, 2005; Guinan, 2009], a direct fluid coupling mechanism from OHC forces to IHC stereocilia as described in [Nowotny and Gummer, 2006] has been offered as a potential explanation for the mechanical drive behind ANIP.

II. Main Objective of the Thesis

The main objective of this thesis is to test the hypothesis from [Guinan et al, 2005] that the mechanism of OHC involvement in generating ANIP and ANSP responses from cat AN fibers for mid-to-high-levels of clicks is somehow different from the OHC mechanism that produces AN response generation for low-level clicks. Specifically, the focus of the investigation is on the following two key issues:

1) Does the drive mechanism that produces ANIP and ANSP responses involve the OHC mechano-electric transduction function as well as OHC electro-motility in the same was as found in the drive mechanism that produces AN responses to low-level sounds? Answering this question is essential since the MOC efferent study on ANIP and ANSP in [Guinan et al, 2005] only revealed the involvement of OHC electromotility. The involvement of the OHC mechano-electric transduction function in response generation of ANIP and ANSP has not been directly shown. Particularly, it is of interest to determine whether the strength of involvement of OHC mechano-electric transduction function in ANIP and ANSP response generation is as robust as in the generation of AN responses to low-level sounds
2) If the mechano-electric transduction function of OHCs is indeed involved in the generation of ANIP and ANSP responses, are there any significant differences in how the mechano-electric transduction function of OHCs is used in generating ANIP and ANSP responses at mid-to-high click levels versus in the generation of AN responses to low-level sounds, i.e., low-level click responses or low-level CF-tone responses? Further, if there are significant differences in the shapes of the OHC mechano-electric transduction functions in producing ANIP and ANSP versus AN responses to low-level sounds, can we infer any differences in the details of the cochlear mechanisms involved in the generation of ANIP and ANSP responses versus the mechanisms involved in generating responses to low-level sounds?

III. Experimental Strategy

In-vivo measurements of OHC receptor potentials in response to low-frequency tones in guinea pigs have shown that the OHC mechano-electric transduction function can be generally described as a curve with saturating non-linearity at both input ends as shown in Fig. 1.2 [Dallos, 1985; Russell et al, 1986]. The gain of the OHC mechano-electric transduction function that is involved in generating BM and AN responses depends on the local slope at the operating point on the transduction function. Studies have shown that the at-rest location of the operating point on the OHC mechano-electric function varies along the cochlea. Specifically, in the apex of the cochlea the operating point is located asymmetrically in favor of depolarizing output voltage as in Fig. 1.2(b), and in the base the operating point shifts to a more symmetric location as in Fig. 1.2(a) [Cai and Geisler, 1996c]. Further, the operating point of the OHC transduction function has been found to shift in response to the intensity of tone stimuli for low-frequency tones well below the CF in the base of guinea pig cochleae [Cody and Russell, 1987]. These shifts in the operating point of the mechano-electric transduction function of OHCs over cochlear place and stimulus-tone level have been interpreted as indications of significant differences in cochlear mechanics [Russell and Kössl, 1992].

The experimental strategy to uncover whether and how the OHC mechano-electric transduction function is involved in generating AN responses to acoustic stimuli is to study the suppression effects on AN responses brought about by the application of a low-frequency bias-tone [Patuzzi et al, 1984b; Cai and Geisler, 1996a; Cai and Geisler, 1996c]. A low-frequency tone (such as 50 Hz) at high sound levels, presented together with a probe stimulus, can suppress the response of an AN fiber to the probe stimulus, with a temporal pattern of suppression that is synchronized with the phase of the low-frequency bias tone. The mechanism behind the temporal pattern of suppression by a low-frequency bias-tone is now widely accepted to be the modulation of the OHC mechano-electric-transducer operating point so that it traverses through the low gain regions of the transduction curve brought on by sinusoidal deflection of the OHC stereocilia by the bias-tone [Ruggero et al, 1992]. A typical example of a bias-tone-induced suppression pattern is shown in Fig. 1.3 through the effects of a level series of 50 Hz bias-tones on the AN responses to a low-level CF-tone. In this figure, the spike records are binned re. the period of the bias-tone and displayed as bias-tone period histograms. From the level series of period histograms, note the emergence of significant suppression at the bias-tone level of 80 dB SPL with the suppression phase noted as the "Major Suppression Phase". Further, note that at 90 dB SPL, the "Minor Suppression Phase" develops at the opposite phase from the "Major Suppression Phase" and the Major Suppression Phase also further deepens to complete suppression at this level. It is now widely accepted that the oppositely located phases of suppression correspond to phases of peak deflections of the OHC stereocilia, which in turn correspond to the low-slope ends of the OHC mechano-electric transduction function. Accordingly, the phase of the major suppression and the symmetry in suppression depth between the major and minor suppression phases can provide clues to the location of the at-rest operating point of the OHC mechano-electric transduction function. Specifically, in [Cai and Geisler, 1996c] more symmetric depths of the major and minor suppressions from basal AN fibers have been interpreted as showing a more symmetric location of the at-rest OHC mechano-electric transducer operating point in the base of the cochlea.

Consequently, if two oppositely located suppression phases were to be found from the bias-tone effects on ANIP and ANSP responses, it would indicate involvement of the mechano-electric transduction function of OHCs in the response generation mechanism of ANIP and ANSP. Further, comparison of the major suppression phase and the symmetry of suppression phases between ANIP and ANSP versus AN responses to low-level sounds can reveal any significant differences in the shape of the mechano-electric transduction function involved in different types of AN responses.

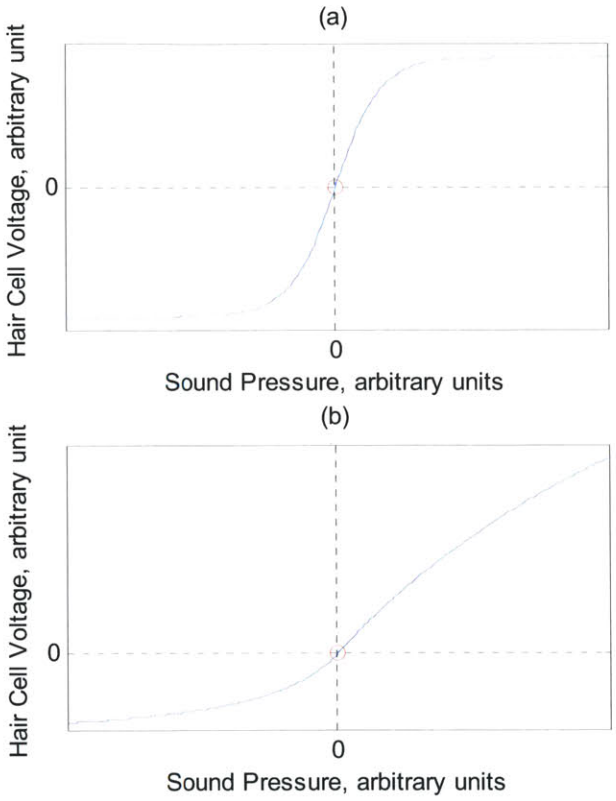

Fig. 1.2. Models of the mechano-electric transduction function of outer hair cells (OHC): the output shows saturating non-linearity at either end of the input. Positive sound pressure indicates rarefaction. The gain of the cochlear amplifier has been linked to the slope of the transduction function at a particular operating point as is indicated by a red circle in the above plots. The operating point at rest has been found to lie at varying degrees of asymmetry between the two saturating ends. (a) a schematized version of the OHC mechano-electric transduction function from the basal region of guinea pigs; (b) a schematized version of the OHC mechano-electric transduction function from the apical region of guinea pigs

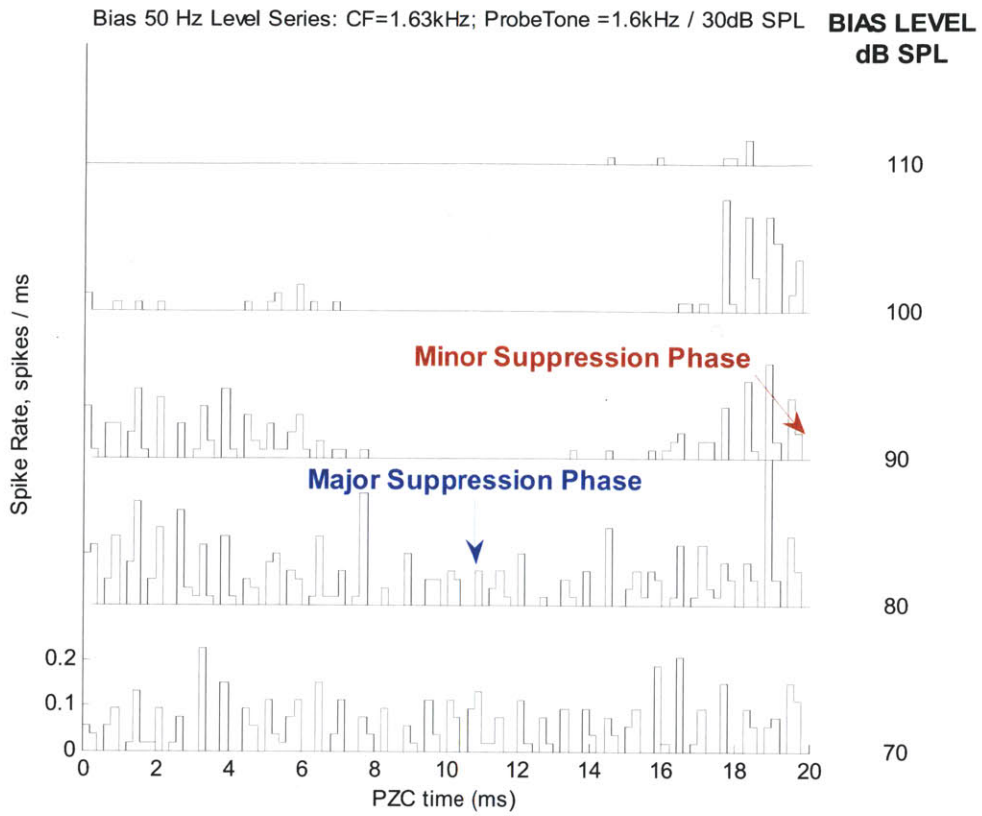

Fig. 1.3. A typical pattern of bias-tone suppression effects on low-level CF-tone responses for a bias-tone level series (bias-tone, 50Hz, level series, 70-110 dB SPL). The CF of the fiber was 1.63 kHz. The probe tone was 1.6 kHz at 6 dB above threshold. The spikes were binned re. the bias-tone-period to form a bias-tone-period histogram. The bias-tone level series of the histograms are shown as vertically stacked plots with the corresponding bias-tone level indicated to the right of each histogram. The scale of the firing rate indicated for the bottom histogram applies to all the plots. Within the bias-tone-period histogram, the spikes are phase-locked to the probe tone frequency. At the bias-tone level of 80 dB SPL, the firing rate is suppressed in the middle of the period histogram (the "Major Suppression Phase"), and at 90 dB SPL, the suppression depth in the middle of the period deepens significantly, and a second suppression phase (the "Minor Suppression Phase") develops at the opposite phase.

IV. Chapter Outline and Significance

This thesis consists of a total of 5 chapters with the first and the last chapters being the introductory and concluding chapters, respectively. The motivation and significance of the three main chapters are outlined as follows.

A. Chapter 2: Bias-tone Effects on Low-level Click Responses and Low-level CF-tone Responses

Currently, studies on bias-tone effects on AN responses to clicks have not been done systematically, and the objective of this chapter is to examine the bias-tone effects on cat AN responses to low-level clicks and to compare them with the bias-tone effects on low-level CF-tone responses. Since it is widely accepted that a common mechanical drive to the IHC stereocilia is behind the low-level CF-tone and low-level click responses, it is expected that the suppression pattern on low-level click responses would be largely similar to the low-level CF-tone responses; however, this has not been shown previously, and the nonlinearity in cochlear mechanics leaves some reservations on the expectations. Furthermore, the experimental techniques developed from this chapter for bias-tone effects on AN response to clicks provide the necessary tools for use in chapter 3 to investigate the OHC involvement in the generation of AN initial-peak responses to high-level clicks.

B. Chapter 3: Bias-tone Effects on AN Responses to Low-level and Mid-to-high-level Clicks

This chapter is the focus of the thesis. It investigates whether and how the OHC mechano-electric transduction function is involved in the mechanisms that produce ANIP and ANSP responses, by measuring the suppressive effects of a low frequency (50 Hz) bias-tone on ANIP and ANSP responses and comparing them to the suppression of low-level click responses. Particularly, the detection of a suppression pattern with two suppression dips at opposite phases will be taken to indicate the involvement of the OHC mechano-electric transduction in the mechanisms that generate ANIP and ANSP responses. Further, comparison of the phases of the major suppressions and the symmetry of the two suppression phases of AN responses to low-level clicks versus ANIP responses versus ANSP responses is expected to uncover any differences in the shape and the at-rest operating point of the OHC mechano-electric transduction function that is involved in producing these click response types.

C. Chapter 4: Bias-tone Effects on Low-level CF-tone and Off-CF-tone Responses from Low-CF Fibers

Prior to the report of OHC involvement in generation of ANIP and ANSP responses [Guinan et al, 2005], it has been hypothesized that interactions between multiple drive mechanisms are involved in tone responses from low-CF AN fibers [Lin and Guinan, 2000]. Studies have found discontinuities in the group delay VS tone frequency measurements from AN responses to tones from low-CF fibers. In tuning curves from AN fibers with CFs < 1 kHz, the CF-centered region had a long group delay, while adjoining "side-lobe" regions had shorter group delays [Pfeiffer & Molnar, 1980; Kiang, 1984]. These characteristics have been interpreted through the hypothesis that these different tuning-curve response regions are likely due to multiple sources driving the IHCs of low-CF fibers [Lin and Guinan, 2000; Guinan et al, 2005]. Further, MOC efferent studies have shown that OHCs are strongly involved in the generation of AN responses to low-level tones from both the CF and the "side-lobe" regions [Gifford and

Guinan, 1988c]. One peculiar finding from this study was that for some fibers with CFs near 1 – 2 kHz, the inhibitory effects of MOC stimulation on near-threshold "side-lobe" tone responses were stronger than near-threshold CF-tone responses thereby resulting in MOC-induced sharpening of tuning. This contrasts with the broadening of tuning due to MOC efferent stimulation as found from most AN fibers [Gifford and Guinan, 1988c]. These findings motivated the hypothesis that the detailed mechanism of OHCs in generating the "side lobe" tone responses may be distinct from the mechanism generating low-level CF-tone responses, i.e., the BM-based cochlear amplifier [Guinan, 2009]. In this chapter, the suppressive effects of a low-frequency (50 Hz) bias-tone on AN responses to low-level CF tones versus "off-CF" tones (tones >0.7 octaves from CF) are compared in order to explore any differences in how the OHC mechano-electric transduction function is involved in generating AN responses to low-level CF-tones versus to side-lobe tones.

V. References

Cai Y, Geisler CD (1996a) Suppression in auditory-nerve fibers of cats using low-side suppressors. I. Temporal aspects. Hear Res. 1996 Jul;96(1-2):94-112

Cai Y, Geisler CD (1996c) Suppression in auditory-nerve fibers of cats using low-side suppressors. III. Model results. Hear Res. 1996 Jul;96(1-2):126-40.

Cody AR, Mountain DC. (1989) Low-frequency responses of inner hair cells: evidence for a mechanical origin of peak splitting. Hear Res. 1989 Sep;41(2-3):89-99.

Cody AR, Russell IJ. (1987) The response of hair cells in the basal turn of the guinea-pig cochlea to tones. J Physiol. 1987 Feb;383:551-69.

Dallos P. (1992) The active cochlea. J Neurosci. 1992 Dec;12(12):4575-85. Review.

Guinan JJ Jr, Lin T, Cheng H. (2005) Medial-olivocochlear-efferent inhibition of the first peak of auditory-nerve responses: evidence for a new motion within the cochlea. J Acoust Soc Am. 2005 Oct;118(4):2421-33

Guinan JJ Jr, Cooper NP. (2008) Medial olivocochlear efferent inhibition of basilar-membrane responses to clicks: evidence for two modes of cochlear mechanical excitation. J Acoust Soc Am. 2008 Aug;124(2):1080-92.

Guinan J.J., Jr. (2009). Bias-tone effects on auditory-nerve responses reveal three mechanical drives, two dependent on outer-hair-cell motility and one passive. Asso. Res. Otolaryngol. Abstr 33, #1109.

Kiang NYS, Watanabe T, Thomas EC, Clark LF (1965) Discharge Patterns of Single Fibers in the Cat's Auditory Nerve (MIT, Cambridge, MA)

Kiang NYS (1984) Peripheral Neural Processing of Auditory Information, Handbook of Physiology, The Nervous System III, Chapter 15

Kiang NYS (1990) Curious oddments of auditory-nerve studies. Hear Res. 1990 Nov;49(1-3):1-16.

Liberman MC, Kiang NY (1984) Single-neuron labeling and chronic cochlear pathology. IV. Stereocilia damage and alterations in rate- and phase-level functions. Hear Res. 1984 Oct;16(1):75-90

Lin T, Guinan JJ Jr. (2000) Auditory-nerve-fiber responses to high-level clicks: interference patterns indicate that excitation is due to the combination of multiple drives. J Acoust Soc Am. 2000 May;107(5 Pt 1):2615-30

Mountain DC, Cody AR. (1999) Multiple modes of inner hair cell stimulation. Hear Res. 1999 Jun;132(1-2):1-14.

Narayan SS, Temchin AN, Recio A, Ruggero MA. Frequency tuning of basilar membrane and auditory nerve fibers in the same cochleae. Science. 1998 Dec 4;282(5395):1882-4

Nowotny M, Gummer AW (2006) Nanomechanics of the subtectorial space caused by electromechanics of cochlear outer hair cells. Proc Natl Acad Sci U S A. 2006 Feb 14;103(7):2120-5. Epub 2006 Feb 6

Rhode WS. (1971) Observations of the vibration of the basilar membrane in squirrel monkeys using the Mössbauer technique. J Acoust Soc Am. 1971 Apr;49(4):Suppl 2:1218+

Rhode WS, Robles L. (1974) Evidence from Mössbauer experiments for nonlinear vibration in the cochlea. J Acoust Soc Am. 1974 Mar;55(3):588-96.

Ruggero MA, Rich NC, Recio A, Narayan SS, Robles L. (1997) Basilar-membrane responses to tones at the base of the chinchilla cochlea.J Acoust Soc Am. 1997 Apr;101(4):2151-63

Ruggero MA, Narayan SS, Temchin AN, Recio A. (2000) Mechanical bases of frequency tuning and neural excitation at the base of the cochlea: comparison of basilar-membrane vibrations and auditory-nerve-fiber responses in chinchilla. Proc Natl Acad Sci U S A. 2000 Oct 24;97(22):11744-50

Russell IJ, Kössl M. (1992) Modulation of hair cell voltage responses to tones by low-frequency biasing of the basilar membrane in the guinea pig cochlea. J Neurosci. 1992 May;12(5):1587-601.

Chapter 2 . Bias-tone Effects on Low-level Click Responses and Low-level CF-tone Responses

I. Introduction

Analysis of auditory nerve (AN) responses to click, (i.e., the acoustic realization of an impulse), can reveal the resonant properties of the mechanical drive to the inner hair cell (IHC) stereocilia. Particularly, recent studies have shown that the AN responses to high-level clicks are quite complex exhibiting interactions of multiple resonances and potentially multiple drives to the IHC stereocilia [Lin and Guinan, 2000; Lin and Guinan, 2004; Guinan et al, 2005; Guinan, 2009]. Despite the complexities at high click levels, the mechanical drive behind the AN responses to low-level clicks can be adequately explained through a single resonant response from the basilar membrane (BM) at the characteristic frequency (CF) of the AN fiber thereby linking the low-level CF-tone responses as the tone response counterpart of the low-level click responses [Kiang et al, 1965; Lin and Guinan, 2000].

It has been found that healthy OHCs are needed to produce the high sensitivity and sharp frequency tuning associated with the low-level CF-tone and low-level click responses as evidenced by their loss brought on by destruction of OHCs due to acoustic trauma [Liberman and Kiang, 1984; Schoonhoven et al, 1994]. Now it is widely accepted that the theory of the OHC based "cochlear amplifier" provides adequate explanations to the mechanism behind the generation of the AN responses to low-level CF-tone and low-level clicks [Robles and Ruggero, 2001]. The critical part of the "cochlear amplifier" lies at the mechanical feedback between the BM and OHCs whereby the stereocilia of OHCs transduce the BM vibration to OHC transmembrane receptor voltage which returns as changes to the BM movement through the electromotility of the OHCs [Robles and Ruggero, 2001].

Further, it is widely accepted that the mechanism behind the various non-linear behaviors such as compressive growth with level, intermodulation distortions and two-tone interactions measured from human psychoacoustic experiments, AN firing patterns, BM motion, and hair cell receptor potentials lies primarily at the OHCs [Robles and Ruggero, 2001]. Particularly, the compressive non-linearity in the mechano-electrical transduction function of the OHCs is cited as the dominant mechanism behind the non-linear behaviors [Patuzzi et al, 1989; Santos-Sacchi, 1993].

In-vivo measurements of the OHC receptor potential in response to low-frequency acoustic tone stimulus from guinea pigs have shown that the mechano-electric transduction function can be generally described as a curve with saturating non-linearity at both ends of the output [Dallos, 1985; Russell et al, 1986]. Further, it has been found that the sharpness of saturation and the location of the transduction operating point on the curve depend on the CF location within the cochlea [Dallos, 1985; Russell et al, 1986]. A schematized version of the transduction function from the basal region of guinea pig cochlea as reported in Fig. 1 of [Russell et al, 1986] is shown in Fig. 2.1(a) where the operating point is located approximately in the middle of the two saturation plateaus. Also, a schematized version of the transduction function from the apical region of guinea pig cochlea as

reported in Fig. 10 of [Dallos, 1985] is shown in Fig. 2.1(b) where the operating point is located closer to the hyperpolarizing saturation plateau.

The shape of the nonlinear transduction function of the OHCs is strikingly well reflected in the two tone interactions between a low-level probe tone and a second low-frequency bias-tone in the BM movement, hair cell receptor voltage as well as firing patterns from AN fibers [Ruggero et al, 1992; Patuzzi et al, 1984b; Cai and Geisler, 1996c]. A low-frequency bias-tone with high enough amplitude sinusoidally deflects the OHC stereocilia over a wide range such that the operating point of the mechano-electric transduction function traverses through the two saturating end regions during each cycle of the low-frequency bias-tone. Further, a bias-tone with frequency below ~100 Hz deflects the OHC stereocilia with significantly larger amplitude than the IHC stereocilia due to the differences in their coupling mechanism to acoustic stimulus [Russell and Sellick, 1983]. Specifically, as shown in Fig. 2.2, the stereocilia of the IHCs are freestanding within the tunnel of Corti whereas the stereocilia of OHCs are embedded into the overlying tectorial membrane. This anatomical difference results in mainly fluid coupling to the stereocilia of IHCs by a low-frequency tone which in turn attenuates low-frequency tone stimulus [Russell and Sellick, 1983]. Therefore, the gain of the cochlear amplifier acting on a low-level near CF probe tone would be diminished as the operating point of the OHC transduction passes through the two saturating regions. In addition, the effect of the low-frequency tone on IHCs should be much less. Consequently, the amplitude of the BM displacement as well as AN firing rate would be suppressed at two opposite phases within the period of the low-frequency bias-tone which correspond to the low-gain saturation plateaus in the OHC transduction function. Further, depending on the location of the operating point of the OHC transduction function at the particular place within the cochlea, one of the suppression phases emerges at a lower level of the bias-tone with a larger depth of modulation [Cai and Geisler, 1996a; Cai and Geisler, 1996c].

Suppression effects on AN responses to a low-level CF-tone by a low-frequency bias-tone are illustrated through the AN firing pattern evoked by the low-level CF-tone at 1.6 kHz and the 50 Hz bias-tone recorded from a cat's AN fiber with the CF of 1.63 kHz. Fig. 2.3 shows the bias-tone level series of bias-tone-period histograms which were constructed by binning the spike records relative to the period of the bias-tone. At the bias-tone level of 80 dB SPL, the firing rate in response to the low-level probe tone begins to be suppressed approximately in the middle of the period which is noted as the "major suppression phase". Then, at 90dB SPL the major suppression phase deepens to complete suppression, and the "minor suppression phase" develops at the opposite phase location. These suppression phases would correspond to the phase of the deflections of the OHC stereocilia into the two saturation plateaus brought on by the 50 Hz bias-tone.

Analysis of the suppression effects by a low-frequency bias-tone on AN firing patterns in response to a low-level CF-tone has been shown to reveal the shape of the OHC transduction function behind generation of AN responses to CF-tone which could not be directly measured in case of high-CF fibers through the in vivo intracellular measurement of the OHC receptor potential [Cai and Geisler, 1996c]. Specifically, the OHC transduction function at the base of the cochlear as shown in Fig. 2.1(a) was done with a low-frequency tone, 600Hz, which is well below the CF of the

recording site [Russell et al, 1986]. Analysis of the suppression pattern on low-level CF-tone response recorded from basal AN fibers of cats has shown that the operating point of the OHC transduction function in response to the low-level CF-tone of the fiber is significantly more symmetric across the saturating ends than the apical fibers [Cai and Geisler, 1996c]. Further, by relating the phase of major suppression with the phase of cochlear microphonic or the phase of excitation by the bias-tone alone, it has been shown that the phase of major suppression on low-level CF-tone responses corresponds to the phase of maximum displacement of the BM toward the scala tympani (ST) in guinea pigs and chinchillas [Patuzzi et al, 1984a; Temchin et al, 1997; Geisler and Nuttall, 1997]. Note, however, that there have been conflicting reports on this topic for cats. Specifically, major suppression phase on BM movement was found to correspond to the peak BM displacement toward ST as in other species [Rhode and Cooper, 1993; Cooper , 1996] whereas the opposite phase, i.e., peak BM displacement toward scalar vestibule (SV), was reported for suppression patterns on AN responses [Cai and Geisler, 1996a].

Currently, studies on the bias-tone effects on AN responses to clicks have not been done systematically, and the main objective of this study is to examine the bias-tone effects on AN responses from cats to low-level clicks and to compare them with the bias-tone effects on low-level CF-tone responses. Since it is widely accepted that a common mechanical drive to the IHC stereocilia is behind the low-level CF-tone and low-level click responses, it is expected that the suppression pattern on low-level click responses would be largely similar to the low-level CF-tone responses. However, since the OHC transduction function has been found to depend subtly on the stimulus parameters [Dallos, 1985; Cody and Russell, 1987], subtle differences may exist. Further, the experimental techniques developed from this study for the bias-tone effects on AN response to clicks would provide the necessary tools to investigate the OHC involvement in generation of the initial peak in the AN responses to high-level click responses where OHCs may be involved through an unknown drive mechanism [Guinan et al, 2005].

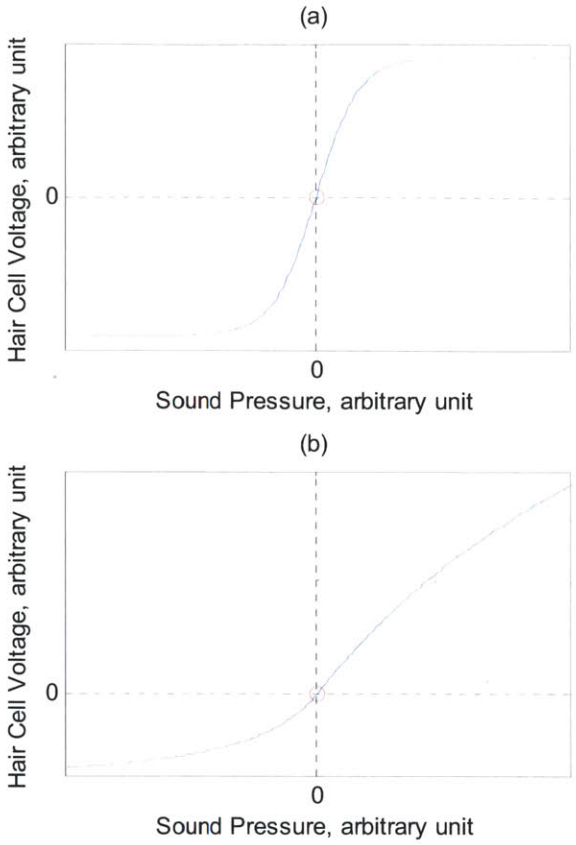

Fig. 2.1. Models of the mechano-electric transduction function of outer hair cells (OHC): they are with saturating non-linearity at either ends of the output. The positive sound pressure indicates rarefaction. The gain of the cochlear amplifier has been linked to the slope of the transduction function at a particular operating point which is indicated by a red dot in the above plots. The operating point has been found to lie at varying degree of asymmetry across the two saturating ends. (a) a schematized version of the OHC mechano-electric transduction function from the basal region of guinea pigs; (b) a schematized version of the OHC mechano-electric transduction function from the apical region of guinea pigs

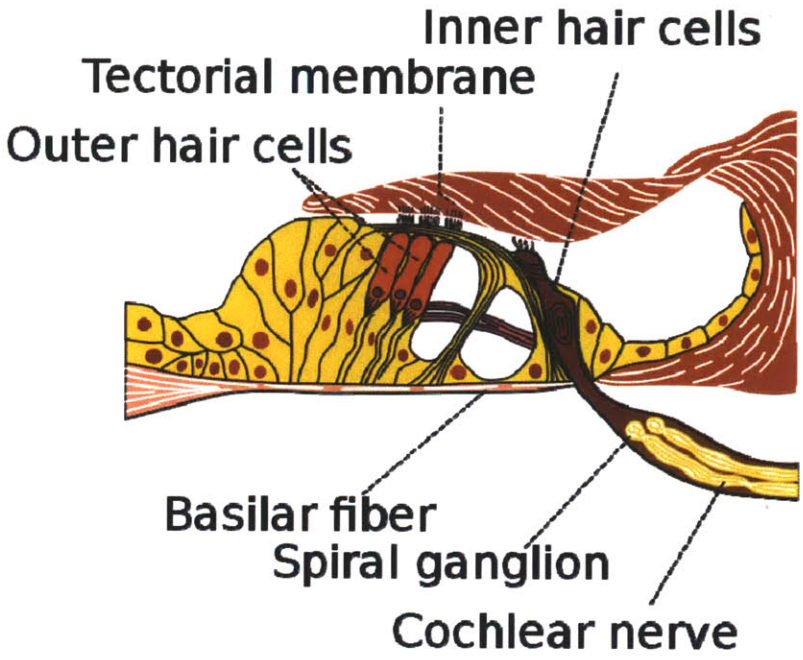

Fig. 2.2. Schematic diagram of the Organ of Corti, the sensory organ within the cochlea. The stereocilia of outer hair cells (OHCs) are embedded into the overlying tectorial membrane whereas the stereocilia of inner hair cells (IHCs) are free-standing within the endolymphatic fluid. Consequently, low-frequency transverse vibrations with frequency below ~100Hz on the Organ of Corti deflect the OHC stereocilia with significantly larger amplitude than the IHC stereocilia.

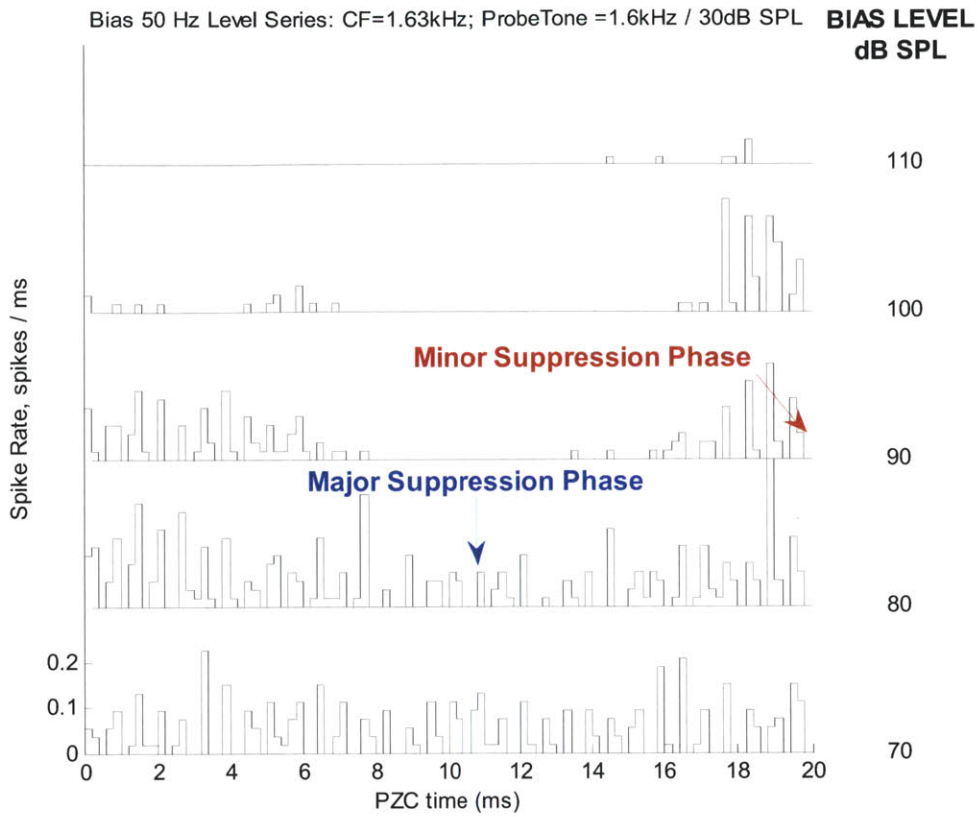

Fig. 2.3. Typical pattern of bias-tone suppression effects on low-level CF-tone responses over a bias-tone level series: a 50 Hz bias-tone at levels, 70-110 dB SPL, was presented together with a low-level CF-tone stimulus. The CF of the fiber was 1.63 kHz. The probe tone was 1.6 kHz at 6 dB above threshold. The spikes were binned re. the bias-tone-period to form bias-tone-period histograms. The bias-tone level series of these histograms are shown as vertically stacked plots with the corresponding bias-tone level indicated to the right of each histogram. The scale of the firing rate indicated for the bottom histogram applies to all the plots. Within each bias-tone-period histogram, the spikes were phase-locked to the probe tone frequency. At the bias-tone level of 80 dB SPL, the firing rate was suppressed in the middle of the period histogram, and at 90 dB SPL, the suppression depth in the middle of the period deepened significantly, and a second suppression phase developed at the opposite phase.

II. Methods

The experiments were done on cats at the Eaton-Peabody Laboratory (EPL) of Auditory Physiology. All experiments were conducted in compliance with protocols approved by the Committee on Animal Care at the Massachusetts Eye and Ear Infirmary.

A. Animal Preparations

23 healthy cats free from ear infections have been used for these experiments. The experimental methods for animal handling, surgical approach to the AN, and methods for recording from AN fibers of cats were as described in [Kiang et al, 1965; Stankovic & Guinan, 1999]. The methods for monitoring the health of hearing during experiments were as described in [Stankovic & Guinan, 1999].

All experiments were acute and began with anaesthetizing the cat with intra-peritoneal (IP) injection of Nembutal in Urethane with the dosage of 150 mg per kg body weight of the animal. Booster injection of the same initial mixture with 1/10 of the initial dose was delivered to maintain the level of the anesthesia. Throughout the duration of the experiment, the depth of anesthesia was monitored based on toe-pinch reflex, heart rate and breathing rate which determine the timing and amounts of the booster injections. The animal's temperature was monitored & maintained at 38 deg C with a rectal thermometer & a heating pad. Experiments typically lasted for 40 to 48 hours during which lactated ringers were dripped to a leg vein through a catheter.

After the initial anesthesia, the bulla cavities of both ears were exposed to reveal the round window. Posterior craniotomy followed by aspiration and retraction of the cerebellar tissues were performed to expose the auditory nerve.

B. Acoustic Setup

All experiments were done inside a double-walled, reduced-reflection chamber. Sound stimuli were delivered with an acoustic assembly consisting of two earphones and a microphone with a probe tube. A DT48 dynamic earphone, capable of high output at low-frequency, was used to generate the low-frequency bias-tone, and all other stimulus types including clicks were generated by the 1-inch condenser earphone. The magnitude and phase of the frequency response of the microphone plus probe tube combination were calibrated over the frequency band 0.02–45 kHz using a reference microphone in a calibration set up to measure the sound pressure near the tip of the probe tube. During the experiment, the assembly was placed inside the external meatus so that the probe-tube tip was a few millimeters away from the eardrum. Then, the magnitude and phase of the frequency response of the earphones were calibrated over the frequency band 0.02–40 kHz using the calibrated microphone plus probe tube.

Throughout all experiments, the frequency of the bias-tone was fixed at 50 Hz which was selected because a low-frequency tone below 200-600 Hz can more selectively deflect the OHC stereocilia compared to the IHC stereocilia [Russell and Sellick, 1983].

C. Data Collection

A silver electrode was inserted through the bulla opening and placed near the round window to measure the cochlear compound action potentials (CAP). An automated tone-pip audiogram was measured over the frequency range from 0.5 kHz to 32 kHz at an octave interval with the criterion of 10

μV pp of the CAP. Tone pip audiograms were run periodically every hour or so, and also after a series of good data in order to ensure good health of the cochlea associated with the collected data.

A glass micropipette electrode filled with 3 M KCL electrolyte with 10 -20 MΩ impedance was driven through the exposed view of the auditory nerve by a remotely controlled microdrive until isolating an AN fiber using a wideband noise burst search stimulus. Spike timings were detected with the resolution of 10 μsec.

Upon isolating a unit, a threshold tuning curve (TC) was measured, the CF of the fiber was determined, and the spontaneous rate (SR) of the fiber was measured from the 20 sec duration recording of spontaneous firing. Then, the following three types of 50 Hz bias-tone paradigms were run:

- Bias-tone alone paradigm
- Bias-tone effects on low-level CF-tone responses
- Bias-tone effects on low-level click responses

Throughout the runs, the quality of spike triggering was monitored & adjusted, and data from recordings with near perfect triggering with no extra or missed triggers have been selected for this thesis. The methods for the above experimental paradigms are described in detail with actual data from the example fiber, CT030_U007, with its CF at 1.88 kHz & SR of 87.2 sps.

D. Bias-tone Only Paradigm: Excitation Threshold & Phase

Acoustic Stimulus and Data Collection

The objective of this paradigm was to measure the neural excitation threshold & phase of excitation of the fiber invoked by 50 Hz bias-tone. A randomized level series of the 50 Hz bias-tone trials over the range from 70 dB SPL to 120 dB SPL was presented. A single trial period was 500 ms with approximately 50% stimulus ON duty cycle. The spike records during the analysis time window of 200 ms duration from the stimulus ON period were binned re. the bias-tone-period in order to form a level series of the bias-tone-period histogram of the spike records. Averaged results from 8 of such trials were used to compute the level series of period histograms. The zero phase reference is the cosine phase of the earphone drive signal. Fig. 2.4 shows the 50 Hz bias-tone level series of period histograms from the example fiber.

Data Analysis

The rate-level function was calculated from the level series of spike records, and the rate threshold was determined with the criterion of one standard deviation, σ, above the baseline rate. The baseline rate was determined as the spike rate at the minimum level of the bias-tone level series which was 60-70 dB SPL. The bias-tone level function of the spike rates including the baseline rate were calculated from the total spike collection time of 1600 ms averaged from 8 trials of 200 ms in each trial. Note that the baseline rate was not the spontaneous rate of the fiber. However, none of the recorded fibers showed a significant upward slope from their rate-level function at the baseline level. The standard deviation was estimated as the square root of the baseline rate under the assumption of Poisson random process behind the spikes.

Vector phase analysis was used to estimate the phase of excitation and synchrony index [Goldberg and Brown, 1969; Johnson, 1980]. Briefly, each spike is represented as a unit vector with its phase as the phase of occurrence of the spike within the period. The magnitude and phase of the average vector representation of all the spikes are the synchrony index and vector phase respectively. Mathematically the average vector corresponds to the first harmonic component of the Fourier series of the period histogram normalized by the total spike count [Goldberg and Brown, 1969].

Further, statistical significance of the phase estimates were evaluated through the standard error of the vector phase estimates. The mathematical model for standard error of the phase estimate, $S.E.\phi$, is described in [Mardia, 2000], and it had been previously applied in AN spike data analysis [Stankovic & Guinan, 2000].

The excitation threshold of the bias-alone alone response was met when both the spike rate exceeded the baseline rate by one standard deviation of the baseline, and the standard error on the phase estimate dropped within 20° ($-20° \leq S.E.\phi \leq 20°$). This criterion allows statistically significant differentiation of the phase data points that are separated by at least 40°.

The detailed analysis of the period histograms in Fig. 2.4 is shown in Fig. 2.5 where the bias-tone level function of the spike rate, synchrony index and estimate of the excitation phase are displayed in the top-down order. In this example, the excitation threshold was met at the bias-tone level of 110 dB SPL. Note that the shape of the histogram moves to a pattern with two modes separated by approximately half a cycle at 110 dB SPL. The vector phase estimate based on the first harmonic component estimated the mid-point of the two peaks as the excitation phase as noted in Fig. 2.4. This phenomenon known as "peak splitting" has been widely reported in previous work for AN response studies on cats particularly from low-CF fibers below 2 kHz in response to low-frequency tone below 200 Hz [Johnson, 1980; Kiang, 1984; Kiang, 1990; Cai & Geisler, 1996].

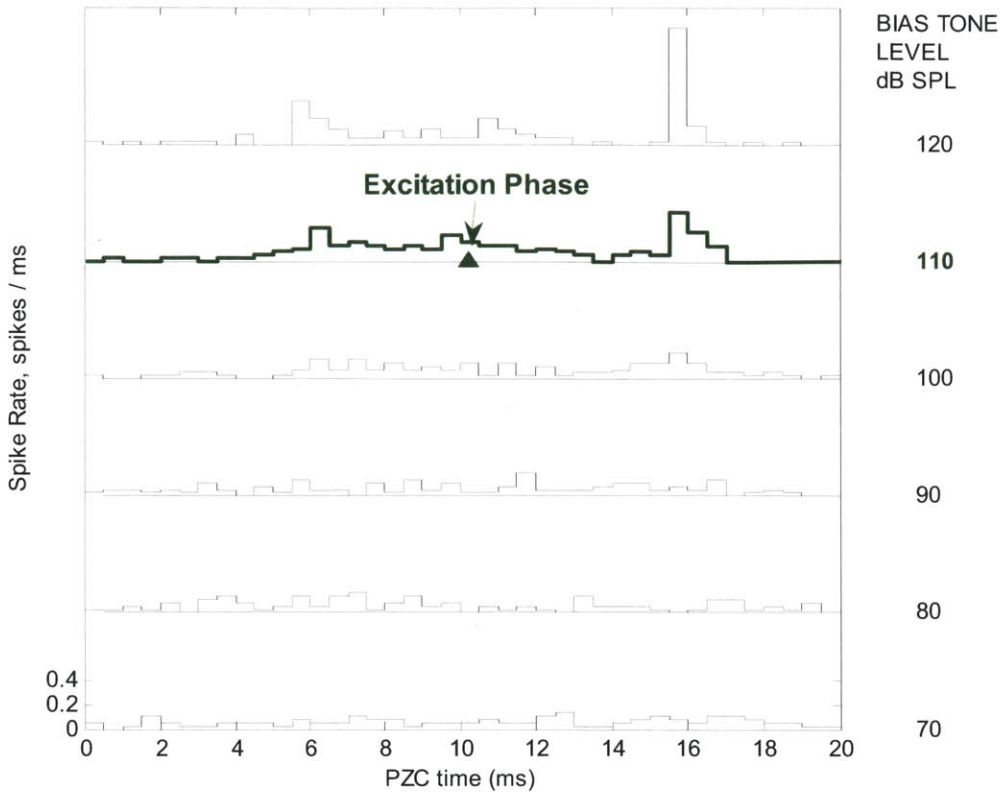

Fig. 2.4. Bias-tone level series of the 50 Hz bias-tone-period histogram of the example fiber, CT030_U007, CF=1.88 kHz & SR=87.2 sps. The excitation threshold level was determined as 110 dB SPL with the excitation phase noted on the period histogram.

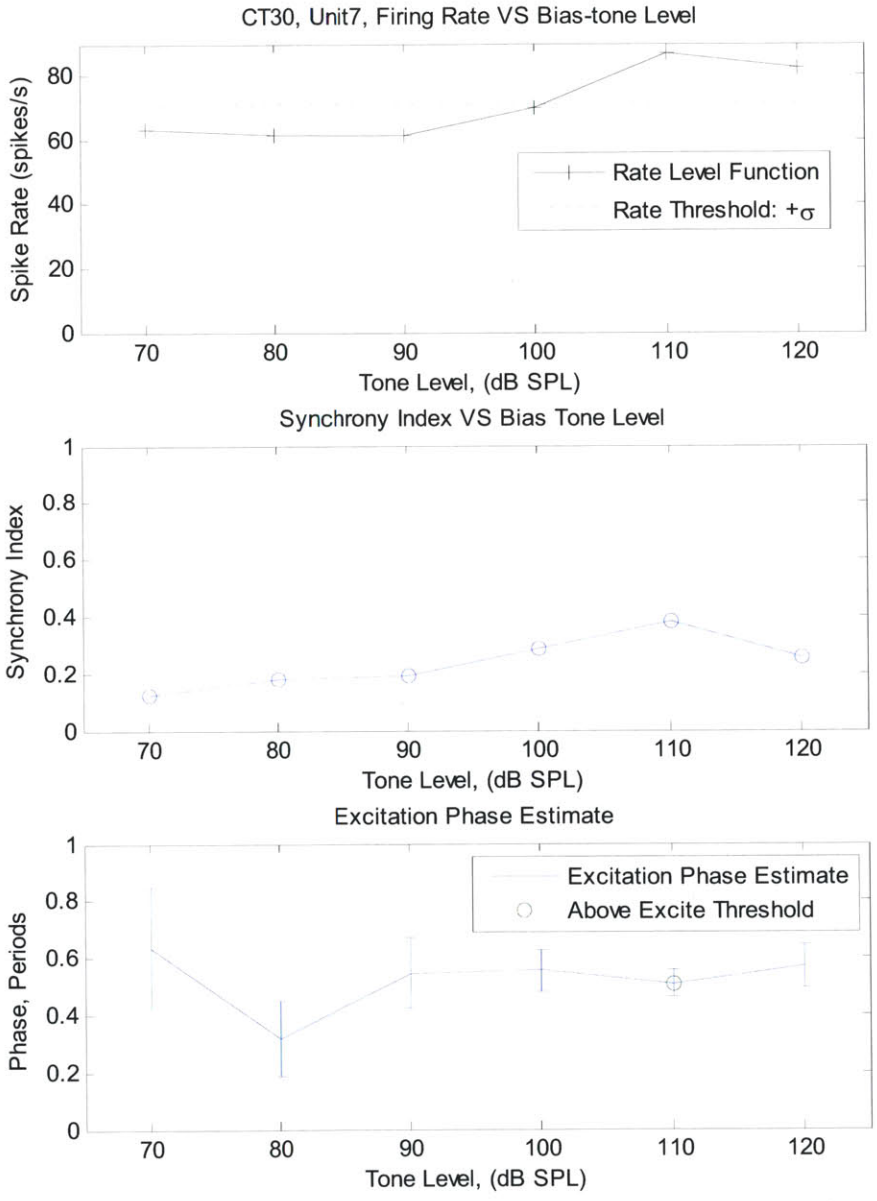

Fig. 2.5. Detailed data analysis metrics to determine bias-tone only response threshold & response phase. *Top*: Rate-level function from which the rate-threshold is determined when the spike rate exceeds one standard deviation; *Middle*: Level function of the synchrony index; *Bottom*: the excitation phase estimates with their standard error. The excitation phase & its standard error is determined by the vector phase method. The excitation threshold is met when both the rate threshold is met and also when the standard error on the phase estimate drops within 20°. In this example, the excitation criteria were met at 110 dB SPL.

E. Experimental Paradigm for Bias-tone Effects on Low-level CF-tone Response

Acoustic Stimulus and Data Collection

A randomized level series of 50 Hz bias-tone over the range of 70 dB SPL to 120 dB SPL was presented together with the CF-tone of the fiber at 10 - 20 dB above the threshold during the 50% ON duty cycle within the 500 ms trial period as shown in Fig. 2.6(a). As for the exact frequency of the CF-tone, it was not necessarily a harmonic of the bias-tone frequency, 50 Hz, as done in previous studies [Sachs and Hubbard, 1981; Cai and Geisler, 1996a]. For the example fiber, the CF-tone was selected as 1.88 kHz at the level of 33.6 dB SPL which is about 16 dB above threshold. Fig. 2.6(b) shows the post-stimulus time histogram (PSTH) resulting from this paradigm at the bias-tone level of 70 dB SPL from the example fiber.

The spike analysis window started at 25 ms for the duration of 220 ms spanning 11 cycles of the 50 Hz bias-tone during which the bias-tone and the low-level CF-tone are presented together for suppression effect analysis. The spike records from 24 of such trials were binned re. the bias-tone-period of 20 ms to form the bias-tone-period histogram. Note that spike records were initially time-stamped with the resolution of 10 μs which would yield bias-tone-period histograms with the sample size of 200000 if left unprocessed. Since spike data analysis for bias-tone effects on period histograms are concerned mainly with low-frequency modulation on the spike records spanning first few harmonics of the bias-tone, the spike records were re-binned at a wider time bin width as follows. The initial time bin width of 10 μs was widened to a value close to the period of the CF-tone in order to reduce the bandwidth of the period histogram below the phase locking frequency to the CF of the fiber. Note that since the CF-tone frequency was not necessarily an integer multiple of the bias-tone frequency, the sample interval of the re-binned histograms was selected to be the bias-tone-period divided by an integer number whereby the resulting time bin width was closest to the period of the CF-tone. Finally, the sample size of the period histograms was limited at the maximum of 40 corresponding to the minimum time bin width of 0.5 ms. Note that the maximum sample size of 40 in this paradigm allowed spectral analysis up to the first 19 harmonics of the bias-tone as discrete Fourier transform was applied on the period histograms. The bias-tone level series of the PSTHs and the corresponding bias-tone-period histograms are shown in Fig. 2.7. In this example with the CF of 1.88 kHz, the period histogram consisted of 38 samples with the time bin width of 0.5263 ms.

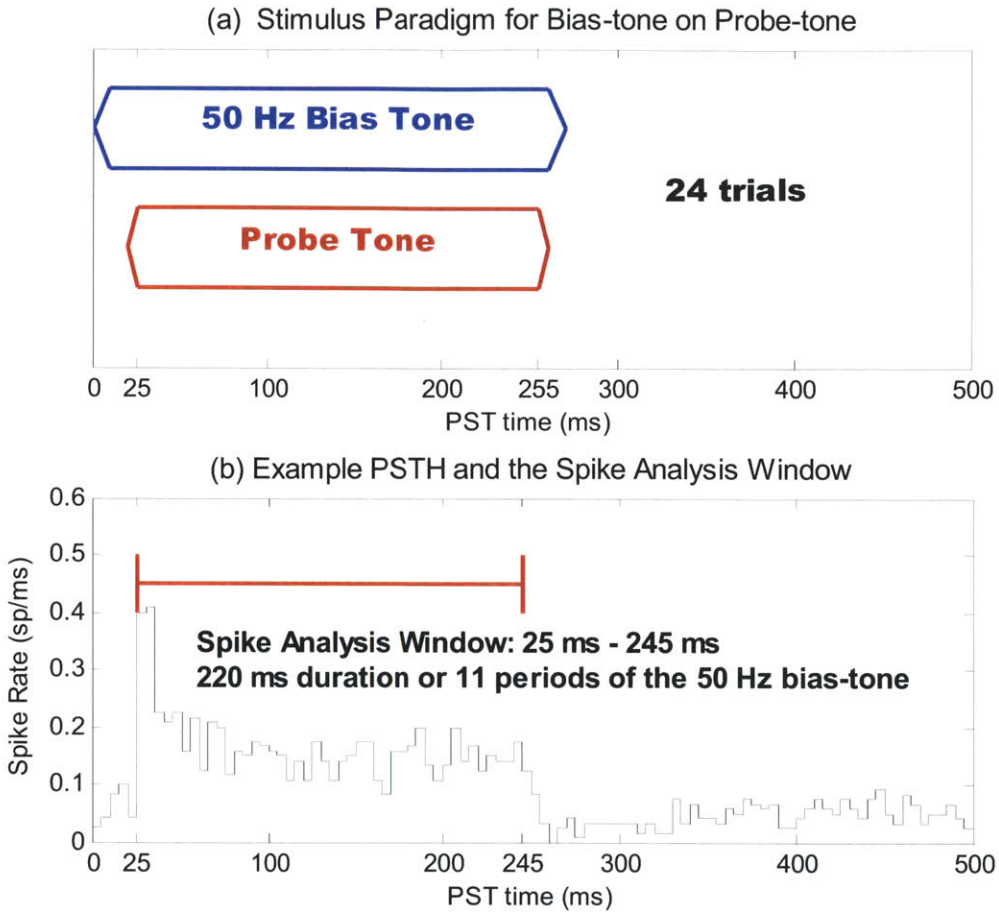

Fig. 2.6. Acoustic Stimulus Setup for the Bias-tone on Tone Burst Paradigm*: Top*: the probe tone & the 50 Hz bias-tone were presented together for 230 ms of spike analysis time within the total trial period of 500 ms. *Bottom*: The post-stimulus time histogram (PSTH) of the spikes over the entire 500 ms trial period. The data come from the example fiber, CT030_U007, CF=1.88 kHz & SR=87.2 sps. Note the ON duty cycle of ~50% corresponding to the stimulus setup diagram above. The spike analysis window covered the duration of 180 ms or 9 periods of the 50 Hz bias-tone. Note that the analysis window starts at 65 ms which was 40 ms after the onset of the probe-tone in order to avoid the onset adaptation time of the probe-tone burst.

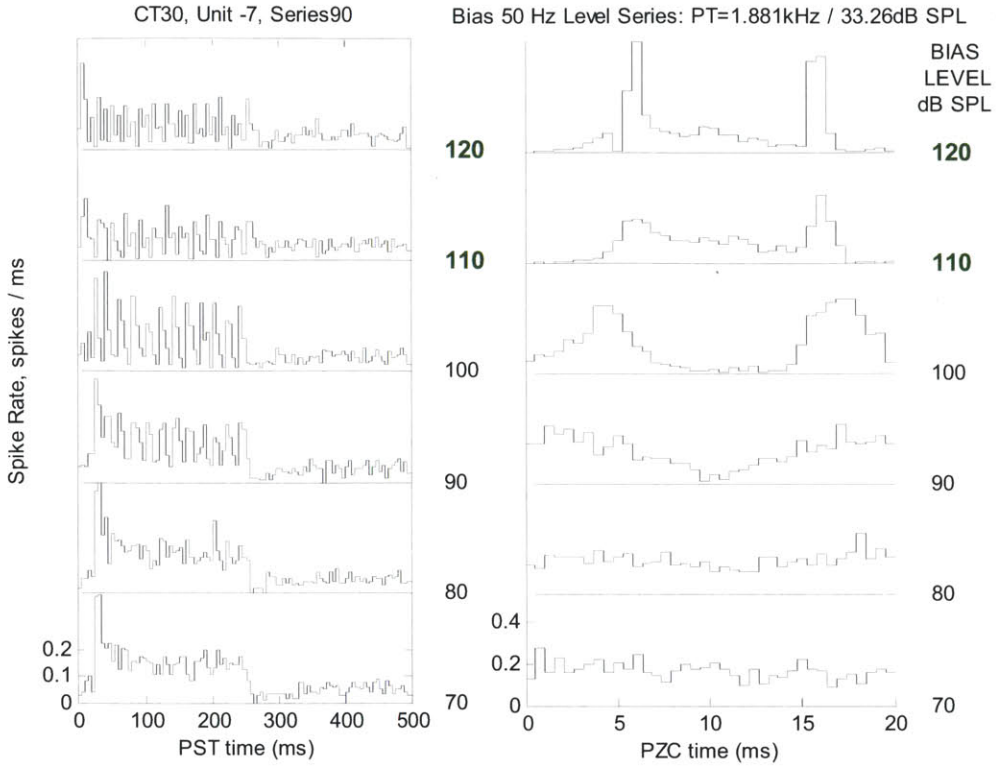

Fig. 2.7. Level series of PST histograms, *Left;* The corresponding the bias-tone-period histogram, *Right*. Spike records from the ON duty cycle from the PST histograms were binned re. the bias-tone-period to form the bias-tone-period histogram. The phase reference of the bias-tone-period histogram was the cosine phase of 50 Hz bias-tone earphone drive signal. Time bin width of the histogram was set at the probe-tone period to reduce the bandwidth of the data below the frequency of the probe tone.

Analysis of the Bias-tone-period Histograms for Suppression Effects

The period histograms were examined to detect significant suppression. Previous studies have shown that that the suppression effects by a low-frequency bias-tone predominantly result in either a single major suppression phase or two suppression phases at opposite phase locations [Patuzzi et al, 1984a; Cai & Geisler, 1996a; Temchin et al, 1997]. Detecting a period histogram with a single major suppression phase was done through the vector phase analysis for the first harmonic component. Specifically, significant suppression was detected when the standard error on phase estimate, $S.E.\phi$, for the first harmonic dropped below 20° (-20°≤ $S.E.\phi \leq 20°$).

Period histograms with two peaks at opposite phase locations can be analyzed with the same basic framework of directional statistical analysis by examining the synchrony index, vector phase and the standard error on the phase estimate with respect to the second harmonic component of the period histogram [Mardia, 2000]. As with the first harmonic, maximum criterion of 40° on the standard error on phase for the second harmonic component, $S.E.\phi_2$, was applied to detect a period histogram with two suppression phases at opposite phase locations; -40°≤ $S.E.\phi_2 \leq 40°$. Since the span of 40° of second

harmonic phase is equivalent to 20° of the first harmonic phase, equivalent detection criteria were applied to the first and second harmonic.

Since the second harmonic phase points to two suppression phases within the period histogram separated by half a cycle, it was necessary to disambiguate major suppression phase between the two. The analysis procedure for this problem termed as "Half-period Synchrony Analysis" was based on the observation that the major suppression phase typically has a higher level of synchrony compared to the minor suppression phase. The analysis procedure first cuts the original period histogram into two half-period histograms of equal-length around the two suppression phase locations. The resultant two half-period histograms would have a single major suppression phase in each, and the depth of suppression in each were calculated as the synchrony index for the first harmonic of each half-period. Finally, the major suppression phase from the original full-period histogram was determined as the suppression phase with higher level of half-period synchrony index. This procedure is illustrated in Fig. 2.8 with the period histogram at the bias-tone level of 100 dB SPL from the example fiber. In Fig. 2.8(a) the two suppression phase locations determined by the second harmonic phase are marked as a blue & red inverted triangle. The resulting two half-period histograms are shown in Fig. 2.8(b). Note that the half-period histogram centered at the blue triangle starts with the wrapped around data from the time window from about 16 ms to 20 ms. The synchrony index for first harmonic of the half-period are shown in each of the half-period histograms. Due to the larger synchrony index value of the red half-period, the major suppression phase from the original full-period histogram is determined as the red triangle which is located in the middle of the period.

Finally, the period histograms generated by the bias-tone level at or above the bias-tone alone excitation threshold were classified as "Excitation" and accordingly excluded from the suppression data pool. For the period histograms from the example fiber in Fig. 2.7, the period histograms at 110 and 120 dB SPL were excluded from the suppression data pool.

The analysis procedures described above are illustrated on the example fiber as shown in Fig. 2.9. The suppression phase determined by the first and the second harmonic are noted by a blue and a red inverted triangle respectively at 90 and 100 dB SPL of the bias-tone level respectively. In this example, the major suppression phase would be determined by the first harmonic phase at the bias-tone level of 90 dB SPL. Further, note the drastic shift in the shape of the period histogram at 110 dB SPL and 120 dB SPL to a shape resembling the period histograms associated with bias-tone excitation.

Fig. 2.10 shows the level functions of the spike rate, synchrony index and vector phase data for the first and second harmonic. Note that the firing rate starts to decrease at the suppression threshold at 90 dB SPL and bounces back up at the excitation threshold of 110 dB SPL. From the level function of the synchrony index, note the sharp increase of the synchrony index prior to reaching the suppression thresholds.

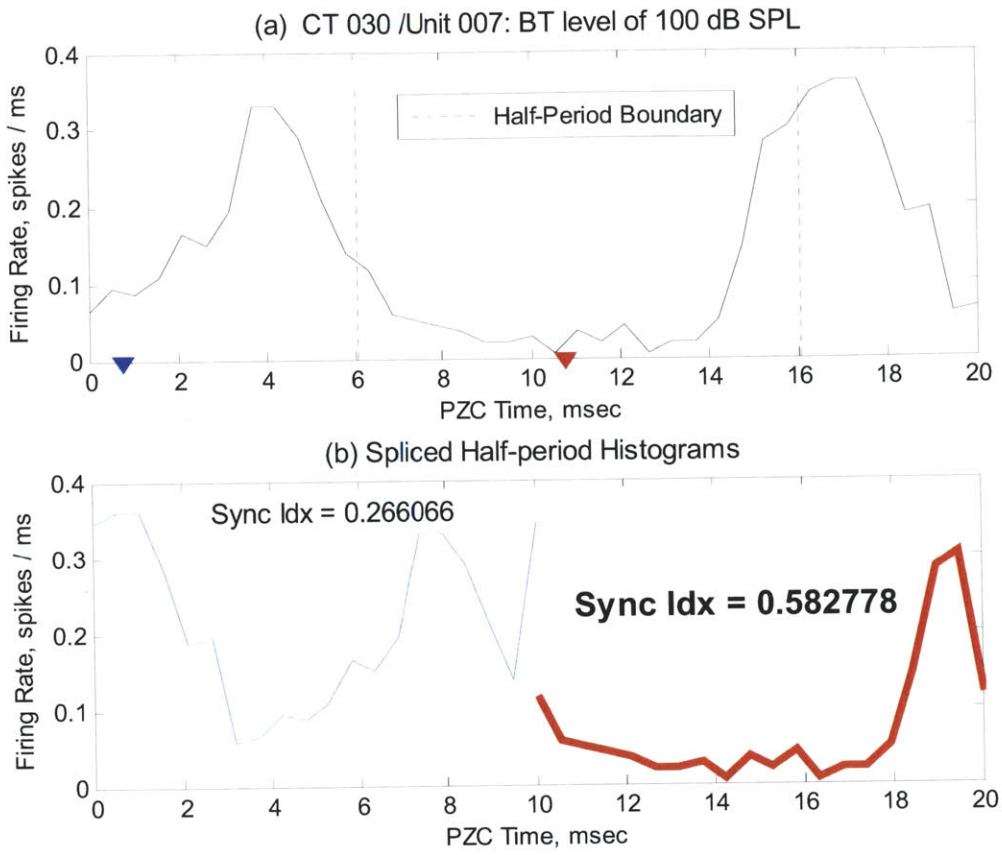

Fig. 2.8. Illustration of the "Half-period Analysis": method to determine the major suppression phase from a period histogram with a significant second harmonic component. The data came from the bias-tone-period histogram at 100 dB SPL from Fig. 2.7. *Top:* the two suppression phases based on the second harmonic phase are shown as blue & red inverted triangle. Half-period boundaries of equal width are formed around these two suppression phases in order to splice out the two half-period histograms. *Bottom:* the two half-period histograms & their first harmonic synchrony index are shown. The suppression phase noted with red has higher half-period synchrony index, and consequently, it is determined as the major suppression phase.

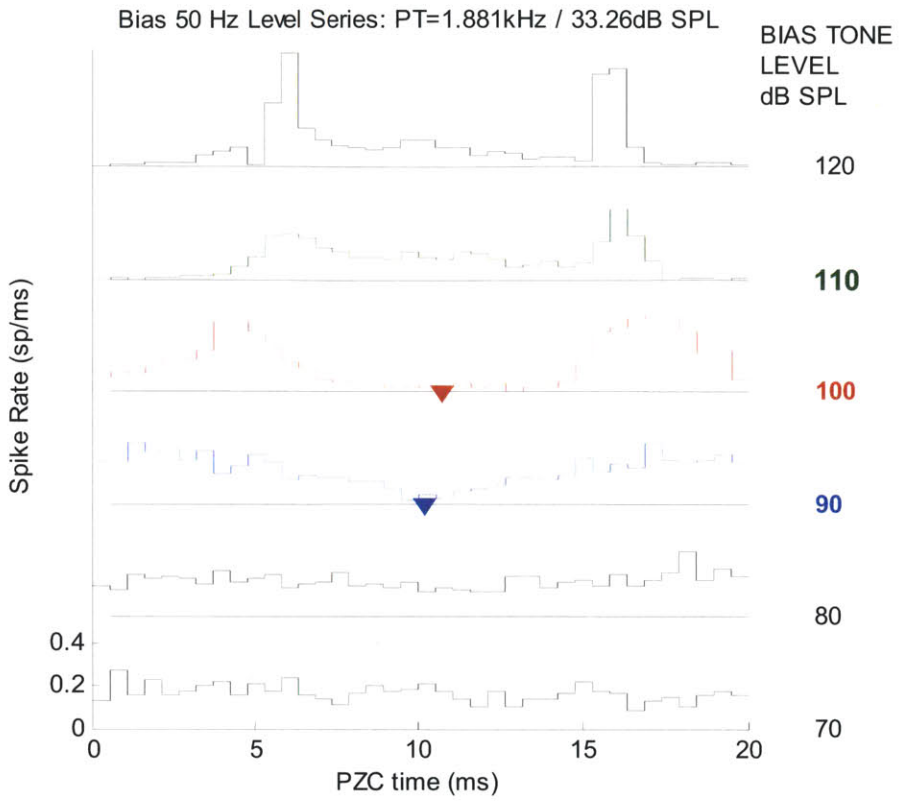

Fig. 2.9. The suppression phase analysis on the bias-tone-period histogram of the example fiber. The suppression threshold based on phase estimate error bound was met at 90 & 100 dB SPL for the first and second harmonic respectively. The suppression phases are noted with an inverted triangle on the period histogram. In this example, the major suppression phase would be determined by the first harmonic phase at the bias-tone level of 90 dB SPL. Further, note the drastic shift in the shape of the period histogram at 110 dB SPL & 120 dB SPL. Recall from Fig. 2.4. that the excitation threshold was reached at 110 dB SPL, which indicates that the spike pattern at 110 & 120 dB SPL are mainly due to the bias-tone excitation pattern.

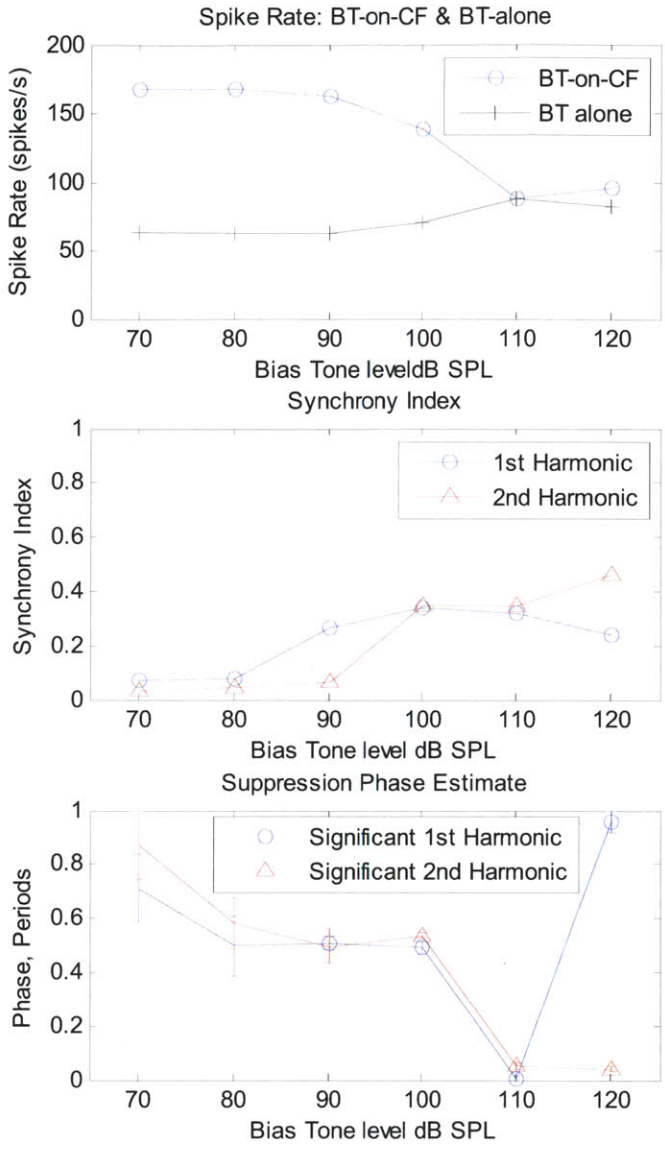

Fig. 2.10. The detailed data analysis on the bias-tone level functions on the suppression effects on CF-tone responses from the example fiber. *Top*: the rate-level function for the run with the bias-tone alone and for the bias on the probe tone run. Note that the firing rate starts to decrease at the suppression threshold of 90 dB SPL and bounces back up at the excitation threshold of 110 dB SPL. *Middle*: bias-tone level function of the synchrony index for 1st & 2nd harmonic. Note the sharp increase of the synchrony indices at the suppression thresholds. *Bottom*: level function of the suppression phase estimates for 1st & 2nd harmonic with their standard error. The data points meeting the error bound are noted with markers labeled as "Significant 1st Harmonic" and "Significant 2nd Harmonic". The 1st & 2nd harmonic suppression thresholds are met at 90 & 100 dB SPL respectively.

F. Experimental Paradigm for Bias-tone Effects on Clicks

The Click Stimulus

The click stimulus was generated by the 1-inch condenser earphone driven by 100 μsec duration rectangular pulses. Click intensities are expressed as peak-equivalent SPL (pSPL) which corresponds to the SPL of a tone stimulus with the same peak pressure generated by clicks as measured at the tympanic membrane. The click levels were calibrated to compensate for the square law non-linearity of the earphone.

Stimulus Paradigm and Data Collection

Click level series over the range of 30 dB pSPL to 115 dB pSPL were run in order to determine the click response threshold level. Each trial with the duration of 20 ms consists of a series of 10 ms alternating click polarity presentation, and the total of 100 such trials were averaged. The click level series from the example fiber, CT030_U007, is shown in Fig. 2.11 where the rarefaction click responses are plotted upward and the condensation click responses are plotted downward at each click intensity level. For this fiber, 60 dB pSPL of rarefaction click, which was ~20dB re. click threshold, was selected for the subsequent runs for bias-tone effects on low-level click responses.

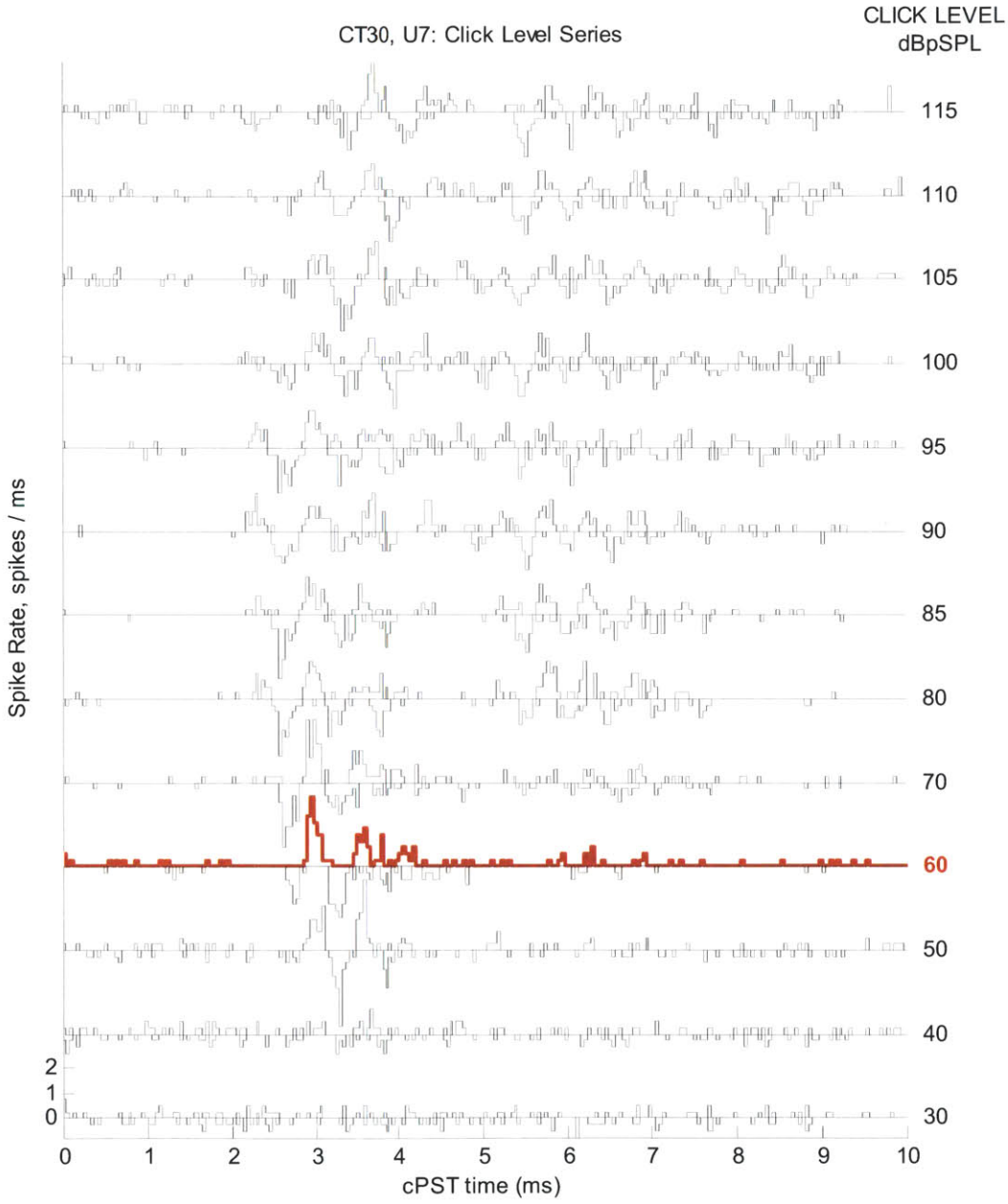

Fig. 2.11. Compound PST of the click level series for the example fiber. Responses to rarefaction and condensation clicks at each level are combined into a single plot by plotting the rarefaction click responses upward and the condensation click responses downward. The zero time reference of the plot is the burst time of the electrical pulse driving the earphone. The click intensity level selected for the subsequent bias-tone effect runs is indicated in red.

The acoustic stimulus paradigm for the bias-tone effects on click responses

Clicks with the duration of 100 μsec were repeated at 18 ms intervals throughout the trial period of 2160 ms. The ON stimulus period for the 50 Hz bias-tone extended from 90 ms to 1990 ms. This allows the analysis time duration for biased click responses from 90 ms to 1890 ms as shown in Fig. 2.12. The time window from 1998 ms to 2160 ms allows measurement of the firing rate invoked by clicks only. The phase slip between the click repetition interval of 18 ms and the bias-tone-period of 20 ms allowed presentation of a click stimulus at 10 equally spaced phases over the click-bias period of 180 ms as also noted in Fig. 2.12.

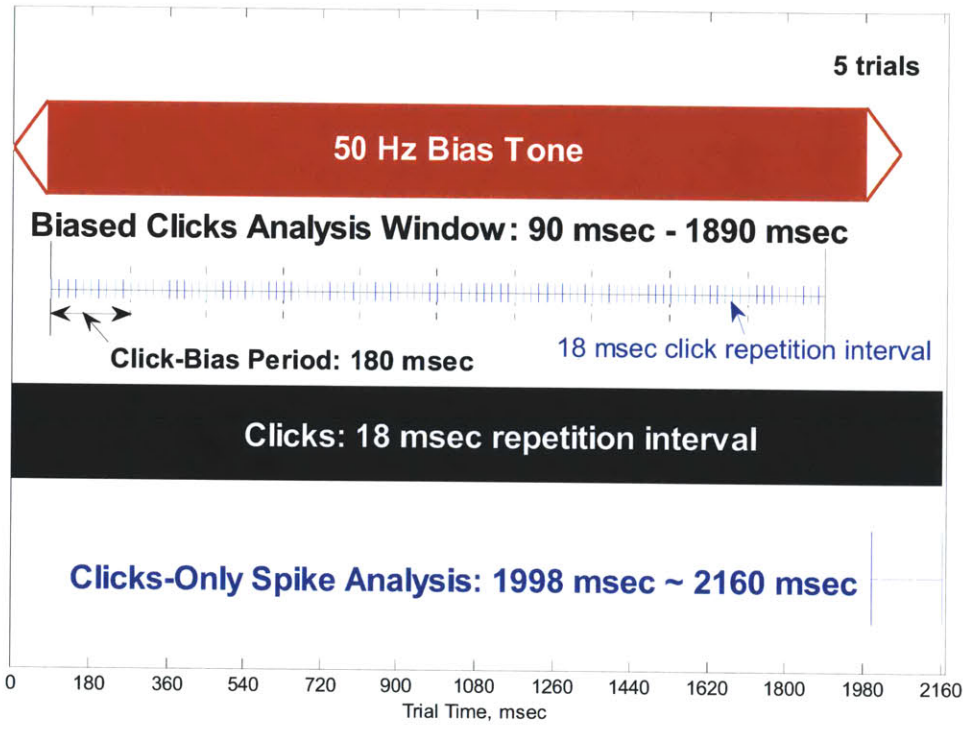

Fig. 2.12. The acoustic stimulus paradigm for the bias-tone effects on click responses. Clicks with the duration of 100 usec were repeated at 18 ms interval throughout the trial period of 2160 ms. The ON stimulus period for the 50 Hz bias-tone extended from 90 ms to 1990 ms with tapering windows of duration 80 ms surrounding the stimulus duration. This allows the analysis period for biased click responses to be from 90 ms to 1890 ms, and the analysis for clicks only response to be from 1998 ms to 2160 ms..

Spike records from the "Biased Clicks Analysis Period" with the duration of 1800 ms were binned re. 180 ms click-bias period. Five of such trials are averaged to produce the click-bias period histogram as shown in Fig. 2.13. The zero phase references of the 50 Hz bias-tone-period are indicated by red lines and the zero phase references for click repetition interval are noted by black dashed lines.

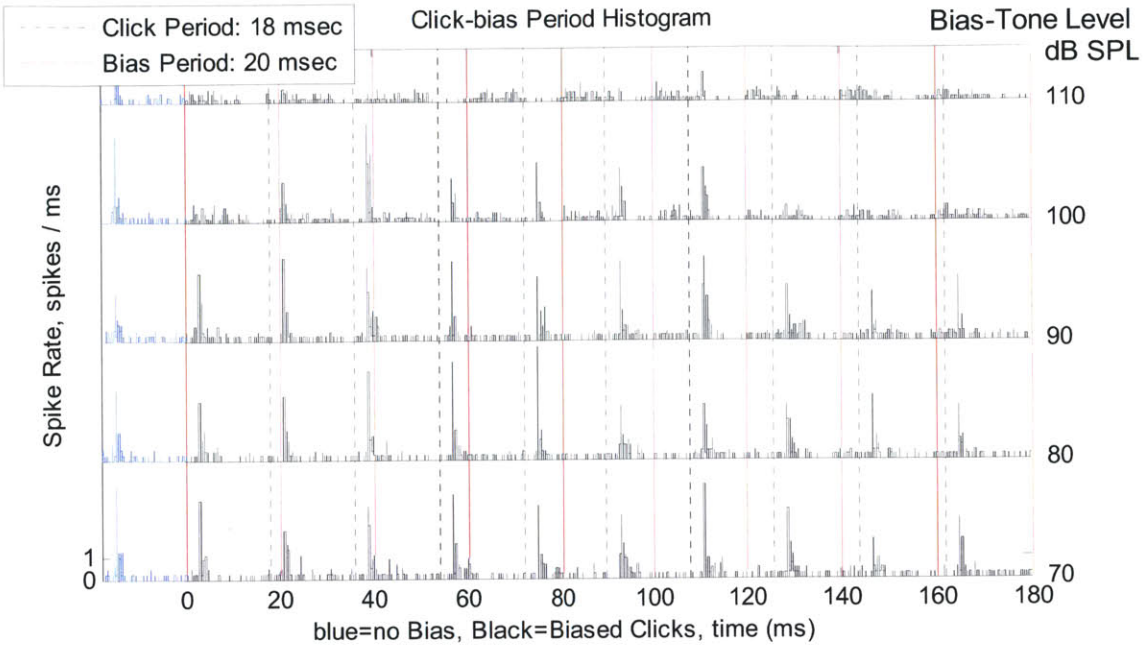

Fig. 2.13. Bias level series of click-bias period histograms: the phase slip between the click repetition, 18 ms, and bias-tone-period, 20 ms, allows click bursts at 10 phase locations within the bias-tone-period over the 180 ms of click-bias-tone-period. The data came from the example fiber. The zero phase reference of the bias-tone-period is indicated by red solid lines, and the zero phase references for click repetition interval are noted by black dashed lines. The time of click responses slips against the bias-tone-period reference. The averaged click responses from the clicks-only period are plotted far left in blue.

Time Windowed Period Histogram Analysis

We are interested in analyzing the bias-tone effects on individual peaks of the click response. Therefore, the click response components of interest span over small time windows with the duration of 1 - 1.5 ms. Therefore, period histograms over a particular time window component need to be constructed from the averaged firing rate over a particular post-click-time window from each of the 10 bias-tone phase samples of the click response. Consequently, the resulting period histogram would consist of 10 data points with the time bin width of one tenth of the bias-tone-period or 2 ms in this study.

Further, the phase delay associated with the time window needs to be accounted for in constructing the time-windowed period histogram and calculation of the suppression phase. For example, the first peak of the low-level click response of the example fiber spanned over the time window from 2.7 ms to 3.3 ms as shown in Fig. 2.16. The mid-point of the time window which is at 3.0 ms in this case is considered as the delay of the time window to be compensated for. Since the delay of 3.0 ms corresponds to 1.5 of the time bin width of the bias-tone-period histogram, the period histograms are built with the delay of one time bin, and the fractional residue of 0.5 time bin or 0.05 period is accounted for by adding it to the phase of the harmonic components.

An example of the time windowed period histogram is illustrated with the analysis over the time window of 0 - 1 ms at 60 dB pSPL shown in Fig. 2.14. Since this time window precedes the click response

latency, the resulting time windowed period histogram should be similar to the period histogram generated by a level series of 50 Hz bias-tone alone. For this time window with its center at 0.5 ms, the delay of the time window is accounted for by adding the phase offset of 0.025 period to the harmonic phase estimates resulting from the time windowed period histogram.

Fig. 2.15 compares the bias-tone-only firing pattern against the bias-tone-period histogram from the pre-click-latency portion of the bias-tone on click runs which are shown on the left and middle plot respectively. As expected, the two level series of period histograms showed similar progression of pattern over the bias-tone level. Specifically, similar phase of excitation with the peak splitting phenomenon was seen from the two sets of histograms at 100 and 110 dB SPL of the bias-tone. Note that the peak splitting phenomenon at 100 and 110 dB SPL captured by the two runs showed some difference in details for two reasons. Firstly, the bias-tone alone paradigm used much finer time bin width of 0.2 ms in its period histograms compared to the bias-tone on click paradigm. Specifically, for the analysis window of 0 – 1 ms, the period histograms for the bias-tone on clicks were built with samples of firing rates at 2 ms intervals with each sample calculated as the average firing rate over the time window duration of 1 ms. Secondly, as can be seen from the difference in their rate-level function, the AN fiber was at different states of adaptation which could affect the details of the peak splitting phenomenon.

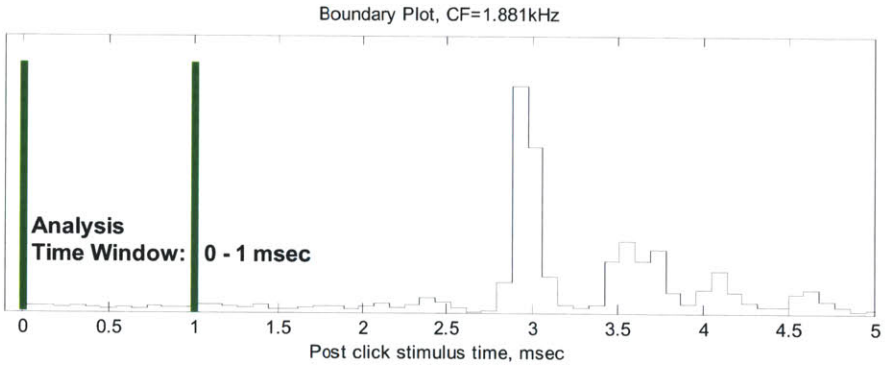

Fig. 2.14. Analysis time window prior to the click response latency, 0 – 1 ms: period histogram analysis over this time interval is expected show similar pattern as the period histogram generated the bias-tone only level series.

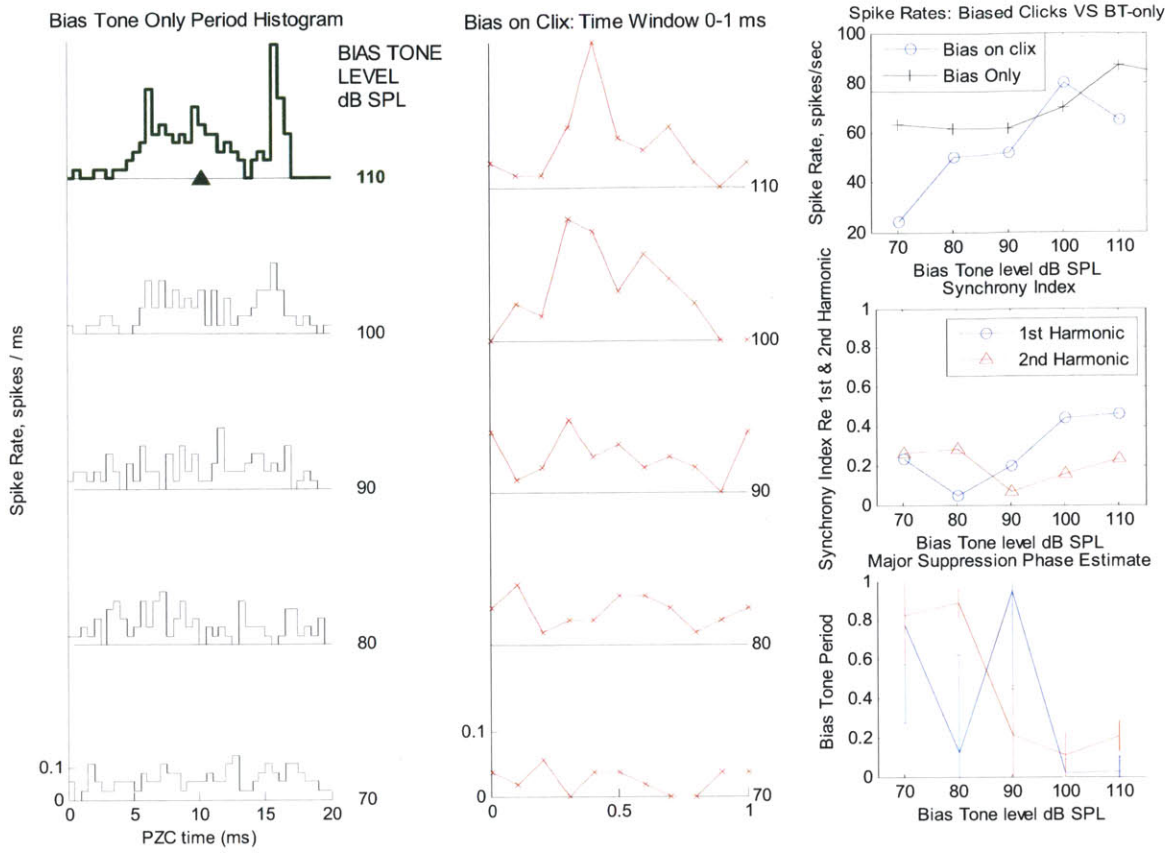

Fig. 2.15. Comparison of the BT-only firing pattern VS pre-click-latency portion of the Bias-tone on click runs: *Left:* period histogram from the bias-tone only level series; *Middle*: period histogram from the bias-tone on clicks over the time window of 0-1 ms prior to the click response latency. *Right*: Firing rate, synchrony index & suppression in the top-down order for the bias on click response. The firing rate for the bias-tone only and bias on click runs started off at different levels due to differences in their adaptation states but converged for the bias-tone levels of 90 dB SPL & above. At 100 and 110 dB SPL, period histograms from both runs showed similar excitation patterns with the peak splitting phenomenon. Note that there were some differences in details of peak splitting between the two runs. These differences can be explained by the difference in the time resolution of the period histograms of the two runs. Refer to the main text for details.

As for the low-level click response of the example fiber, the time windowed period histogram analysis was done over the first peak at 60 dB pSPL located at the time window from 2.7 ms to 3.3 ms as shown in Fig. 2.16. The detailed analysis in Fig. 2.17 shows that the suppression threshold of the second harmonic was reached at the bias-tone level of 100 dB SPL. The half-period histogram analysis was applied to locate the major suppression phase which was similar to that of low-level CF-tone response from Fig. 2.9.

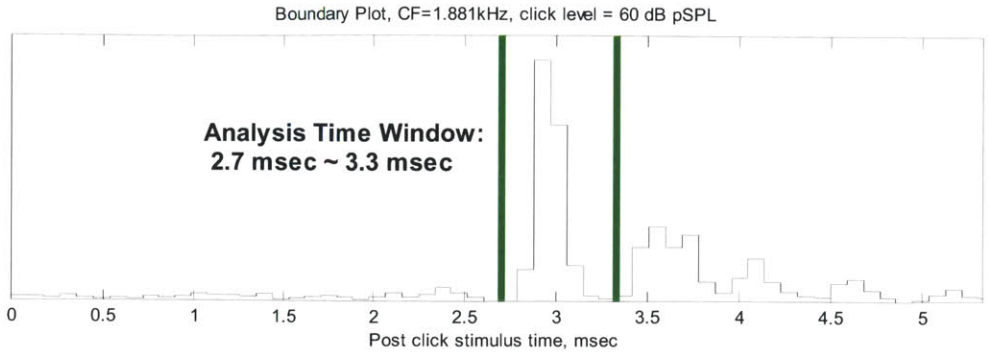

Fig. 2.16. Analysis time window, 2.7 ms - 3.3 ms, for the low-level click response from the same fiber, which includes the first prominent rarefaction peak.

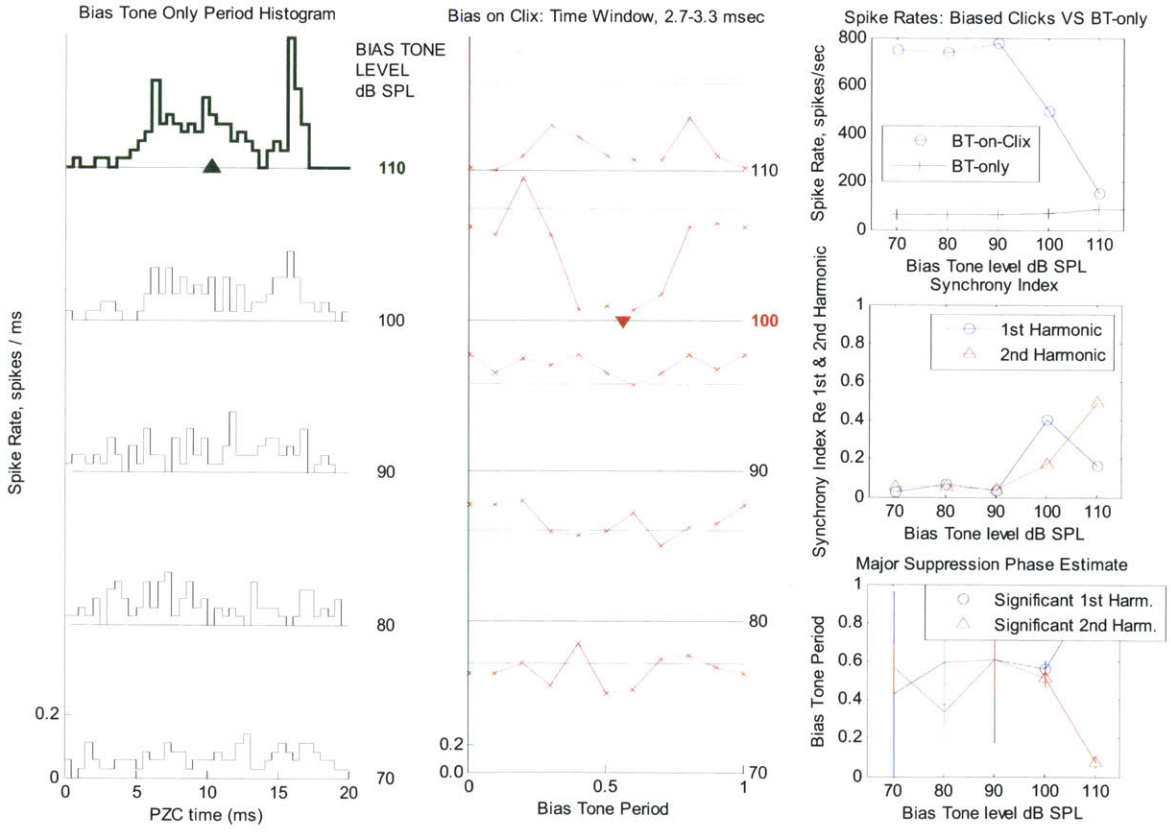

Fig. 2.17. Period histogram of the bias-tone alone level series along with the analysis of the bias-tone suppression effect on the low-level click response: *Left:* analysis of the bias-tone alone excitation pattern from Fig. 2.4 where the excitation threshold was reached at 110 dB SPL with the excitation phase noted with a green triangle; *Middle*: Bias-tone level series of the period histograms of the bias-tone effects on low-level click responses: the baseline firing rates without the bias-tone are noted with dashed blue lines, and the firing rates with the bias-tone on are plotted in red. Note that suppression threshold was reached at 100 dB SPL with the major suppression phase noted with a red inverted triangle; *Right:* detailed analysis on the bias-tone effects: the rate-level function with & without the bias-tone, level function of the synchrony index for the 1st & 2nd

harmonic and the suppression phase estimates for the 1st & 2nd harmonic are shown in the top-down order. Note the significant shifts in the all three metrics at the threshold of suppression. Specifically, the rates were suppressed, synchrony indices rose, and the error on the suppression phase estimates dropped within the suppression threshold.

III. Results

A. Phase of Excitation by 50 Hz Bias-tone Alone and Phase of Suppression on Low-level CF-tone Responses

The phase of excitation of AN fibers in response to 50 Hz bias-tone throughout the entire range of CF is plotted in Fig. 2.18. Note that the zero phase reference of the plots was the cosine phase of the 50 Hz earphone drive signal. Also plotted in Fig. 2.18 is the phase of major suppression on low-level CF-tone responses at the suppression threshold level. As mentioned previously, the standard error on all phase estimates was within ±20°which is noted on the plot as the blue error bar.

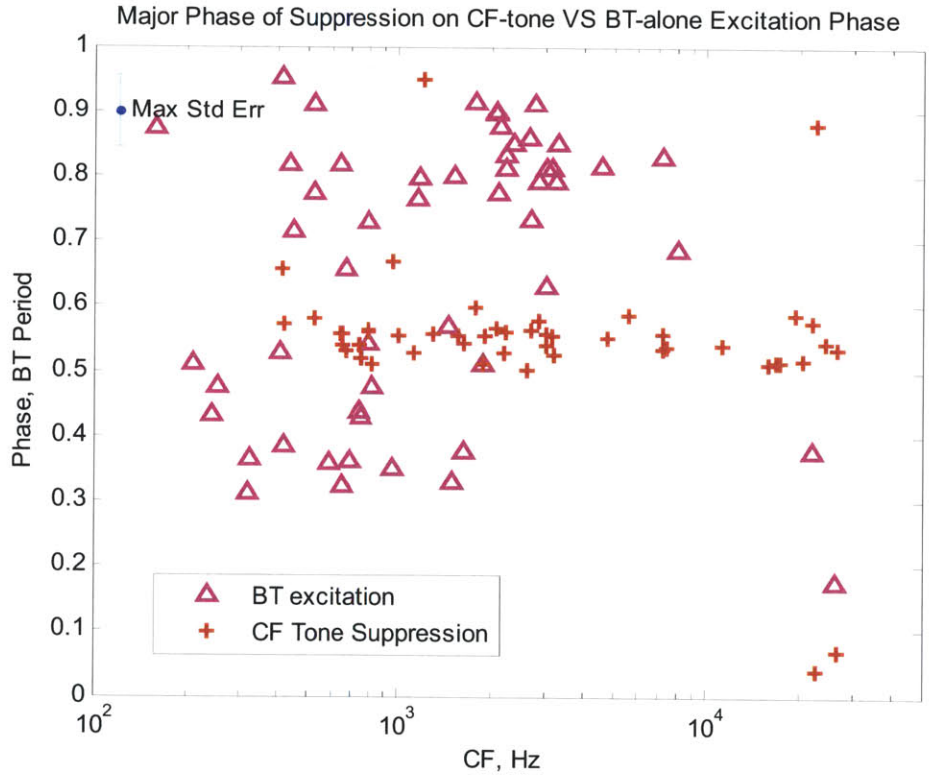

Fig. 2.18. Plot of the phase of excitation from the "bias-tone only" runs and the major suppression phase from the "bias-tone on CF-tone" responses. Note that the excitation phases form two clusters separated by about ½ cycle, and the phase of suppression on the CF-tone response lies approximately in the middle separated by about ¼ cycle from the phase of excitation. Similar results have been reported in previous studies [Cai & Geisler, 1992a].

The two data groups formed distinctly separate clusters. The data for the major suppression phase on the low-level CF-tone responses were located tightly around the phase of 0.55 T within ± one standard error where T denotes a period of the bias-tone. In contrast, there was significantly wider spread in the phase of excitation in response to 50 Hz bias-tone. Further, the pattern of data scatter for the phase of excitation by 50 Hz bias-tone changed sharply across the CF boundary of about 2 kHz as

shown in Fig. 2.19 where the histogram of the fiber count across the excitation phase are plotted first for fibers with CF < 2 kHz in Fig. 2.19(a) and for the fibers with CF ≥ 2 kHz in Fig. 2.19(b). For fibers with CF > 2 kHz, the phase of excitation data formed a single mode around 0.8 period whereas for CF < 2 kHz, the data were widely distributed with two main modes at 0.35 and 0.8 period which are approximately half a cycle apart. This bimodal distribution of the excitation phase for CF < 2 kHz can be explained by examining the details of the period histograms generated by 50 Hz bias-tone alone level series as shown in Fig. 2.4 and Fig. 2.20 where two peaks at about the opposite phases emerge from the period histogram at high levels of the bias-tone. Specifically, the typical pattern found throughout the animals showed a wider peak at about phase of 0.35 T as well as a sharper peak at the opposite phase. Depending on the relative size of the two peaks, the excitation phase was determined as the middle of the peaks as in Fig. 2.4, the earlier peak in Fig 2.20(a), and the later peak as in Fig. 2.20(b). As mentioned earlier in methods section, similar results have been reported in previous work on cats AN fibers below 2 kHz as the "peak splitting" phenomenon [Cai & Geisler, 1996; Johnson, 1980; Kiang, 1984; Kiang, 1990].

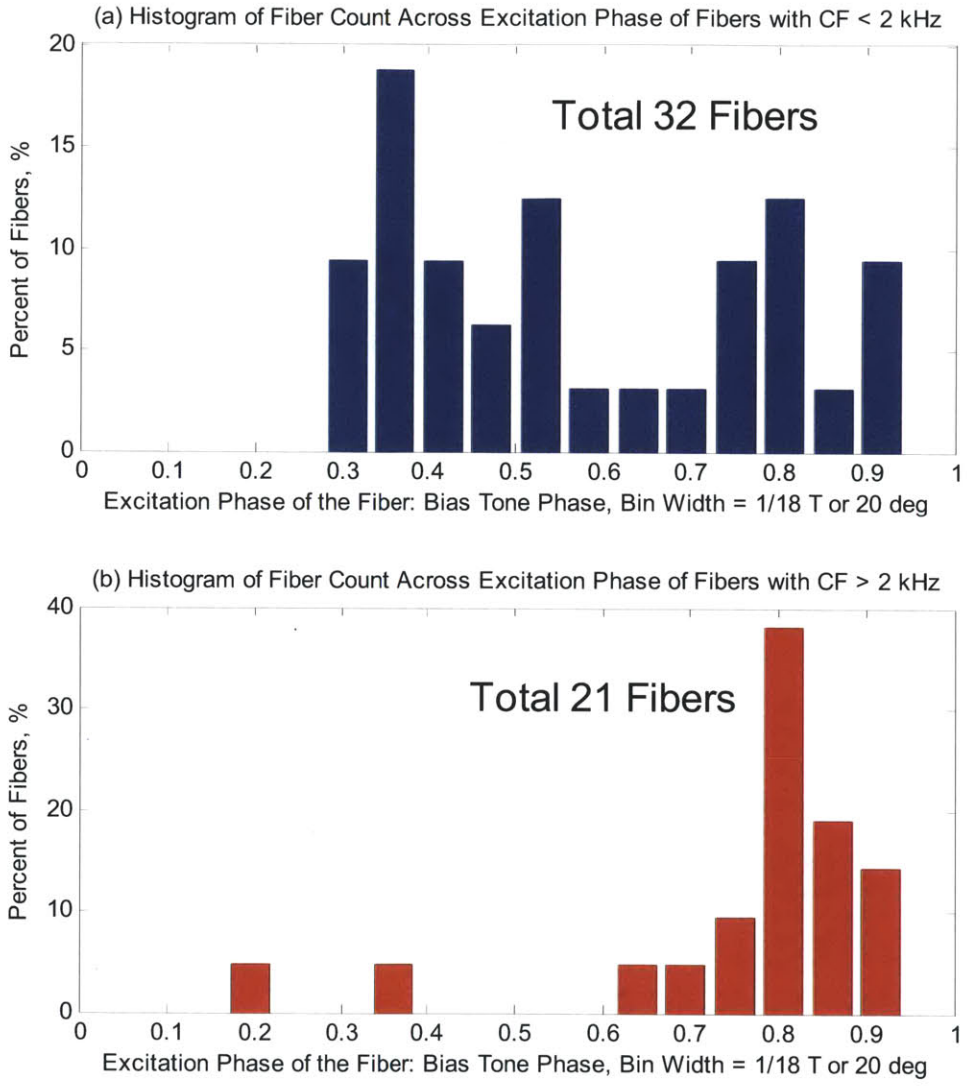

Fig. 2.19. Histogram of the AN fiber count across the phase of excitation of the AN fibers in response to 50 Hz bias-tone presented alone. As shown in Fig. 2.18, the distribution drastically changes across the CF of about 2 kHz. (a) The histogram for fibers with CF < 2 kHz shows three modes at ~0.35 T, 0.53 T & 0.8 T where T denotes a period of the bias-tone; (b) The histogram for fibers with CF >= 2 kHz shows a single prominent mode at 0.8T.

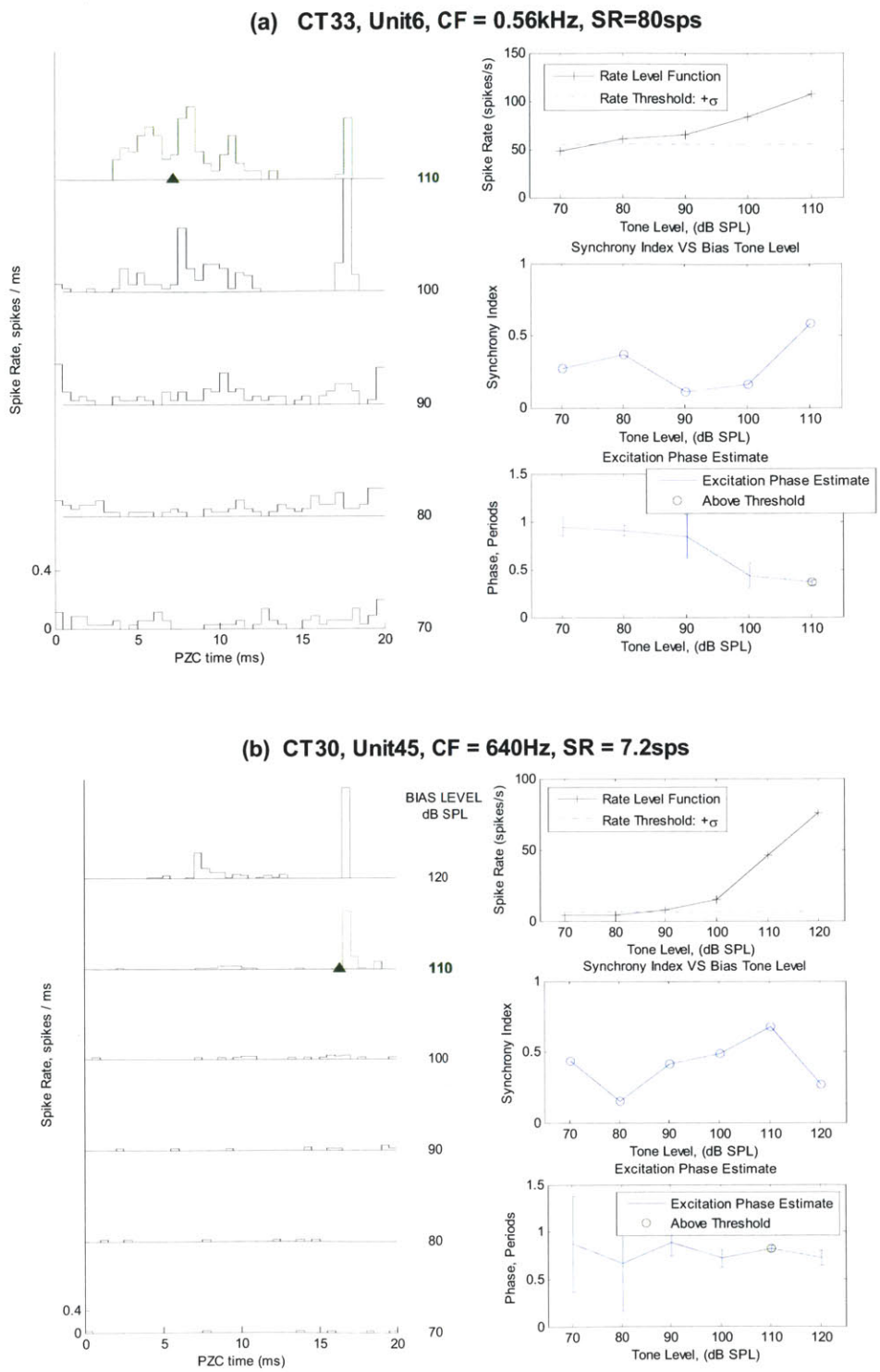

Fig. 2.20. Bias-tone alone excitation pattern for CF < 2 kHz displaying the peak splitting phenomenon. Two main excitation peaks emerge at about half a cycle apart. Depending on the relative size of the two modes, the first harmonic based vector phase estimate can select either the wider peak as in (a) or the narrower peak as in (b).

B. Suppression Effects on Low-level CF-tone Responses and Low-level Click Responses by 50 Hz Bias-tone

Fig. 2.21 shows the major suppression phase on low-level click responses by 50 Hz bias-tone together with the major suppression phase on low-level CF-tone responses at the threshold of suppression throughout the CF of the AN fiber. Most of the data points from both groups were located closely together within a band of ± one standard error which strongly indicates the similarity of the two data groups. Note, however, this comparison extends only up to 7 kHz due to the absence of the data for the low-level clicks above this frequency.

As for the CF dependency of the suppression phase, for both low-level click and tone responses there was a slight negative slope with increase of CF with the magnitude less than 0.1 period per decade of CF. Again, the zero phase reference for all data points is cosine phase of the 50 Hz electrical drive signal to the earphone.

Fig. 2.22 compares the 50 Hz bias-tone level at the threshold of suppression on the low-level CF-tone responses & low-level click responses. Fig. 2.22(a) shows the distributions of the fiber count over the suppression threshold. The mode of the distribution for the CF-tone responses was ~10 dB lower than that of the low-level clicks. Fig. 2.22(b) displays the suppression thresholds over the CF of the fiber. Up to the CF of ~10 kHz, the suppression threshold for both types of responses remained relatively flat over the CF with ~10 dB higher threshold for the low-level clicks. For CFs higher than 10 kHz, the suppression threshold for low-level CF responses rose steeply at the rate of ~10 dB per octave. Note that for the low-level click responses from the AN fibers with CF higher than 10 kHz, the suppression threshold was not reached within the maximum level of the 50 Hz bias-tone applied in the trial which varied from 100 dB SPL to 120 dB SPL. In the next section, the bias-tone effects on low-level click responses from this region of CF which remained sub-threshold are examined in details with two example AN fibers with CF of 17.28 kHz and 20.4 kHz.

Fig. 2.23 plots the ratio of 2^{nd} harmonic VS 1^{st} harmonic synchrony index at the suppression threshold by the 50 Hz bias-tone for the CF-tone responses and low-level click responses. A higher value of this ratio indicates stronger presence of the minor suppression phase at the threshold level of suppression thereby indicating more symmetrical location of the operating point of OHC mechano-electrical transduction function across the two saturation plateaus. The data for both response types showed an upward trend with increase of CF indicating stronger presence of the minor suppression phase at the threshold level of suppression for AN fibers with higher CFs and accordingly a more symmetrical location of the OHC operating point.

The degree of symmetry of the location of the operating point within the OHC mechano-electrical transduction function was examined by another metric, "Half-period Symmetry Index", which tries to quantify the ratio of modulation depth of the minor VS major suppression phase at the threshold of suppression. The range of this ratio is from 0 to 1, and as it approaches 1, it indicates more symmetrical depth of modulation between the two suppression phases thereby more symmetric location of the operating point of the OHC transduction function. For this purpose, the "Half-period Synchrony Analysis" method described in the methods section which was used to disambiguate the major

suppression phase from period histograms with two oppositely located suppression phases was adapted. Specifically, for period histograms which meet the suppression threshold criteria of the second harmonic, the ratio of the minor VS major suppression phase was calculated as a part of the analysis procedure to determine the major suppression phase. For period histograms which met the suppression threshold criteria for the first harmonic, the "Half-period Synchrony Analysis" procedure was carried out with the suppression phase based on the first harmonic phase estimate. The "half-period symmetry index" at suppression threshold for low-level CF-tone and low-level click responses are plotted over the CF of the fiber in Fig. 2.24. Note that the dashed line at the index value of 0.5 indicates the ratio of 1 to 2 in the half-period synchrony index. Note that most of the data points were located below the reference level of 0.5 except for the data group for CF-tone responses with CF > 10 kHz indicating more symmetric shape of suppression pattern at threshold for this data group as found in the other metrics, i.e., the ratio of second harmonic VS first harmonic synchrony index in Fig. 2.23.

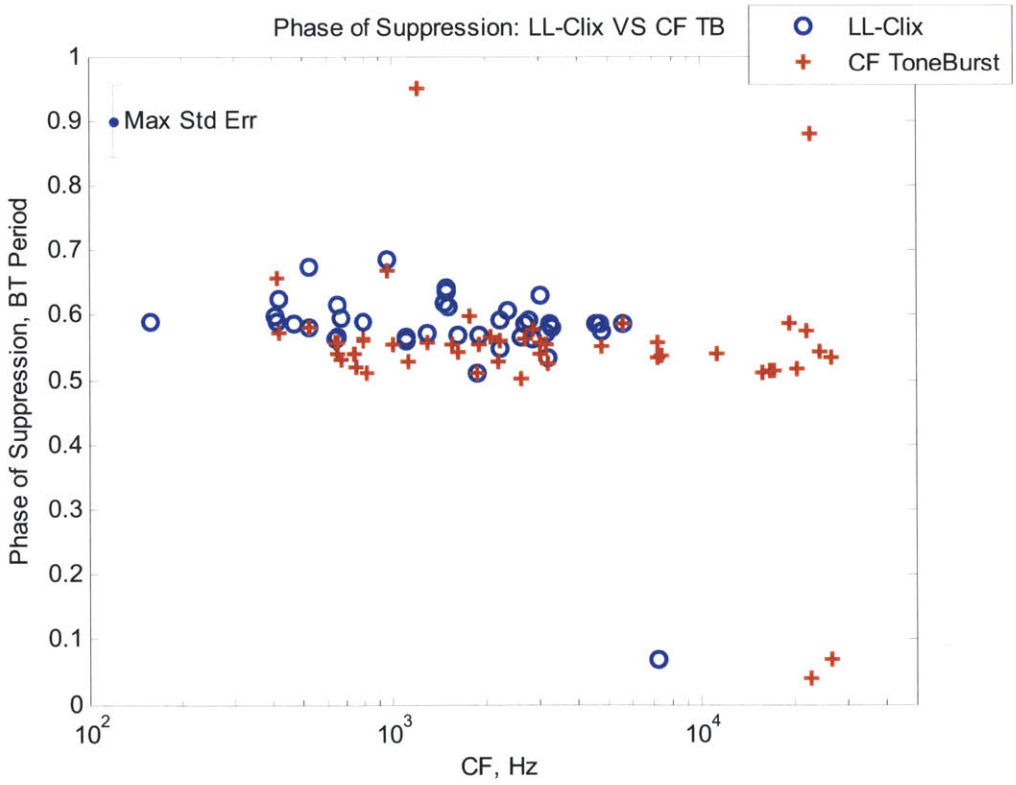

Fig. 2.21. The major suppression phase for the CF-tone response & low-level clicks are plotted together. Most data points fell within ± standard error (S.E). Note that both data groups showed a slight negative slope across increase of CF with the magnitude less than ~0.1 period / decade of CF. Similar results have been reported in Fig. 4A of [Cai and Geisler, 1996a]

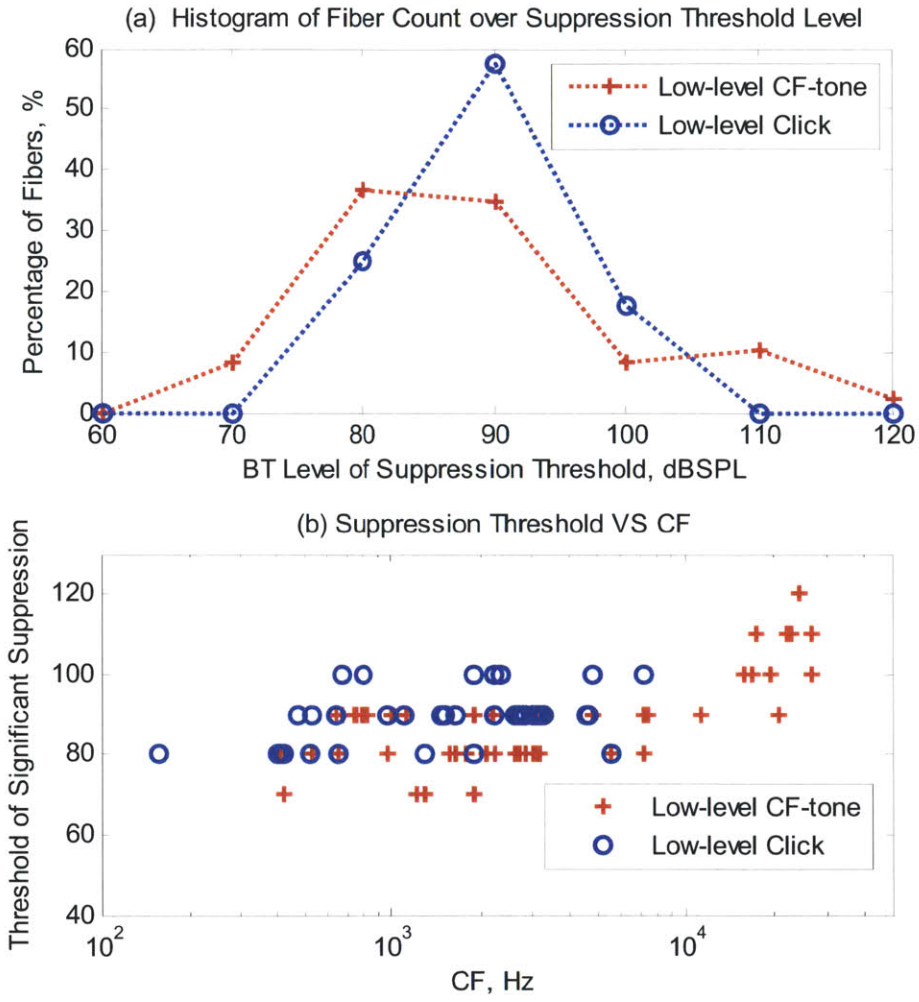

Fig. 2.22. The threshold of suppression on the CF-tone response and low-level click response: (a) Histogram of the fiber count over the suppression threshold; (b) the plot of the suppression thresholds over CF. The total fiber counts were 45 & 39 for the CF-tone & low-level clicks respectively. Both data showed that the threshold on the CF-tone responses was 5 - 10 dB lower than that of the low-level click response throughout CFs.

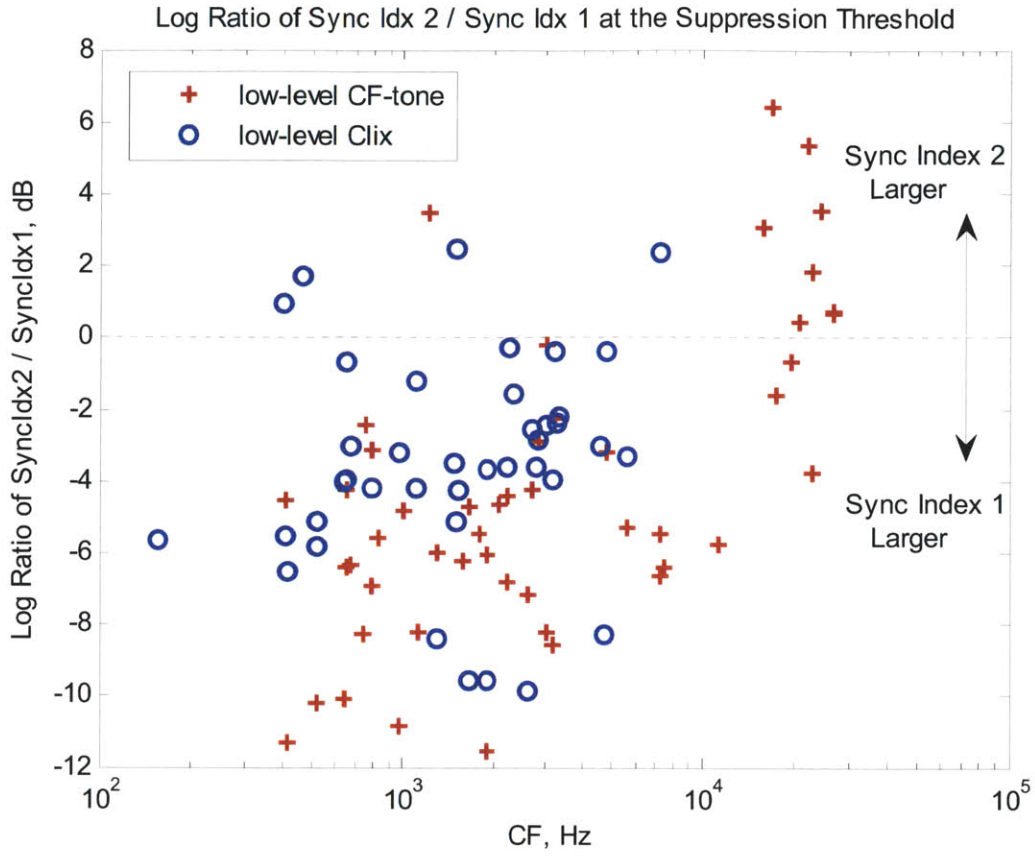

Fig. 2.23. Plot of the ratio of 2nd over 1st harmonic synchrony index at the suppression threshold VS CF of the fiber. Lower value of the ratio indicates more asymmetry in the suppression pattern between the two suppression dips; therefore, lower value of this ratio indicates more asymmetrical location of the operating point on the OHC mechano-electric transduction function. The data for the low-level clicks are about 10 dB higher than that of the CF-tone.

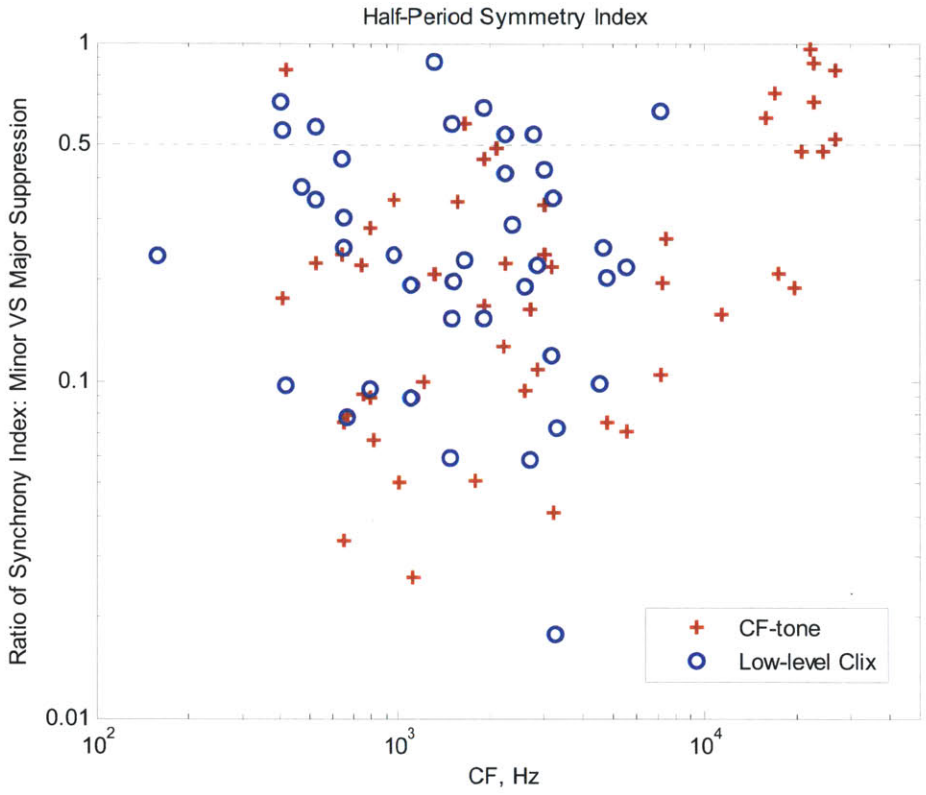

Fig. 2.24. Half-period Symmetry Index: is the ratio of the first harmonic synchrony index from the two "Half-period histograms" which tries to quantify the degree of symmetry in the modulation depth between the two major and minor suppression phases. Specifically, the "Half-Period Analysis Method" shown in Fig. 2.6 has been adapted for this purpose. The range of this ratio is from 0 to 1 where 1 indicates perfectly matched modulation depth between the major and minor suppression phase. Refer to the main text for details. Note the reference value of 0.5 which indicates the 1 to 2 ratio of modulation index between the two suppression phases. Most of the data points are located below this value except for the data group for CF-tone response with CF > 20 kHz. Note that similar trend was seen from the Fig. 2.23.

C. Example Results of the 50 Hz Bias-tone Suppression Effects on Low-level CF-tone and click responses

In order to aid the reader to appreciate how well the data from individual fibers fit with the data shown in the previous plots, this section documents the typical suppression patterns of low-level click and tone responses from individual fibers. Examples are presented from 8 normal AN fibers taken from 7 animals over the entire range of CFs. At least one example is shown for each of six bands with octave spacing starting at a band of CF < 700 Hz and ending with a band of CF > 11 kHz. For each example, the AN fiber is identified by its animal and unit number. Each example has three sets of plots. The first set shows, subplot (a) the threshold tuning curve (TC), and subplot (b) compound PST histograms of the responses to the click level series. The click level selected for the bias-tone studies is indicated in red. The second set of plots shows, subplot (c) at left, the 50 Hz bias-tone-level-series period histograms from the bias-tone only responses, the (d) in the middle, the bias-tone-level-series period histograms from the responses to bias-tones plus low-level clicks, and subplot (e) at right, the detailed analysis of

the suppression effects on the low-level click responses. The third set of plots shows, at left, subplot (f) bias-tone-level-series period histograms of the responses to bias-tones plus low-level CF-tone responses, and at right, subplot (g) the detailed analysis the suppression effects on the low-level CF-tone response are shown and compared to the suppression effects on the low-level click responses.

Example Result in Fig. 2.25: CT028, U009, CF=0.52 kHz, SR=85 sps

The data from this fiber show the typical pattern from the CF region below 1 kHz. The bias-tone only excitation threshold was met at 100 dB SPL with the excitation phase detected at the narrower peak in the period histogram as shown in Fig. 2.25(c). The suppression threshold on the low-level click and CF-tone responses was reached at 90 and 80 dB SPL as shown in Fig. 2.25(d) and Fig. 2.25(f) respectively. The minor suppression phase is not visible because the second harmonic suppression criterion was not met below the excitation threshold.

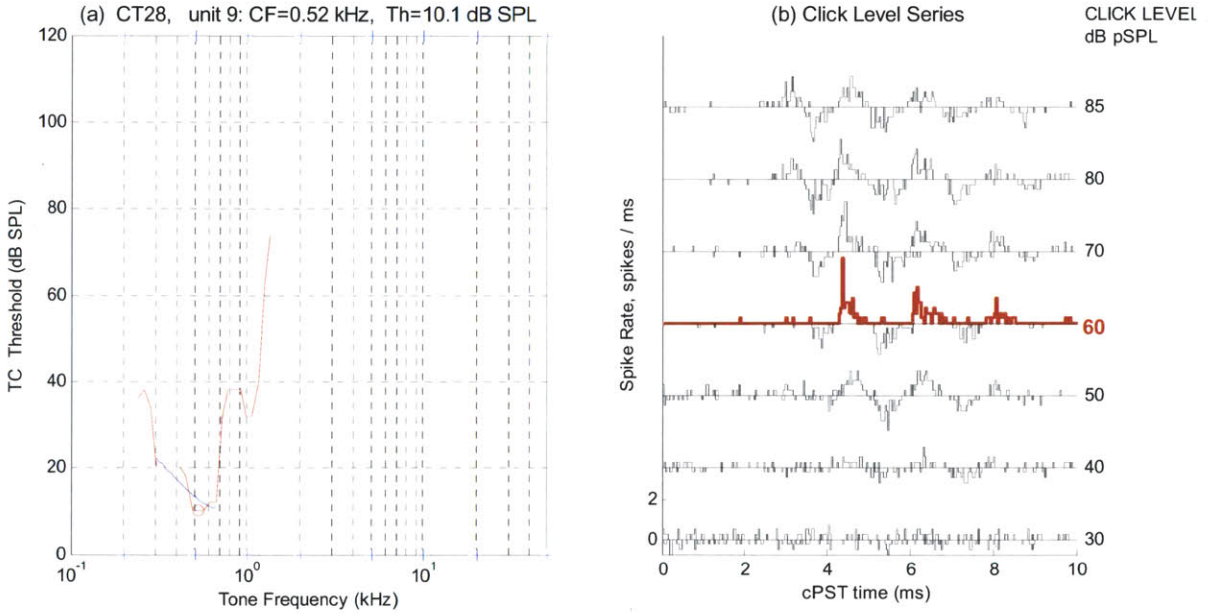

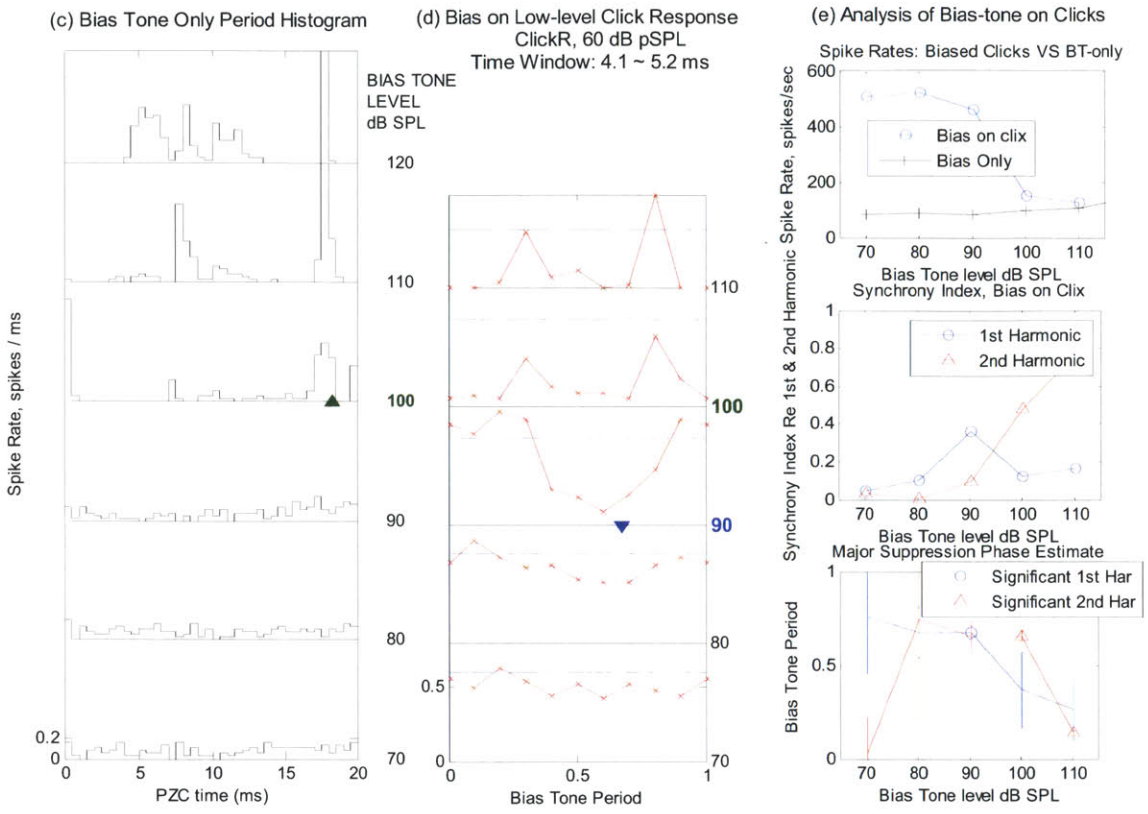
(c) Bias Tone Only Period Histogram
Spike Rate, spikes / ms
PZC time (ms)
(d) Bias on Low-level Click Response
ClickR, 60 dB pSPL
Time Window: 4.1 ~ 5.2 ms
BIAS TONE LEVEL dB SPL
Bias Tone Period
(e) Analysis of Bias-tone on Clicks
Spike Rates: Biased Clicks VS BT-only
Bias on clix
Bias Only
Bias Tone level dB SPL
Synchrony Index, Bias on Clix
1st Harmonic
2nd Harmonic
Synchrony Index Re 1st & 2nd Harmonic Spike Rate, spikes/sec
Major Suppression Phase Estimate
Significant 1st Har
Significant 2nd Har
Bias Tone Period

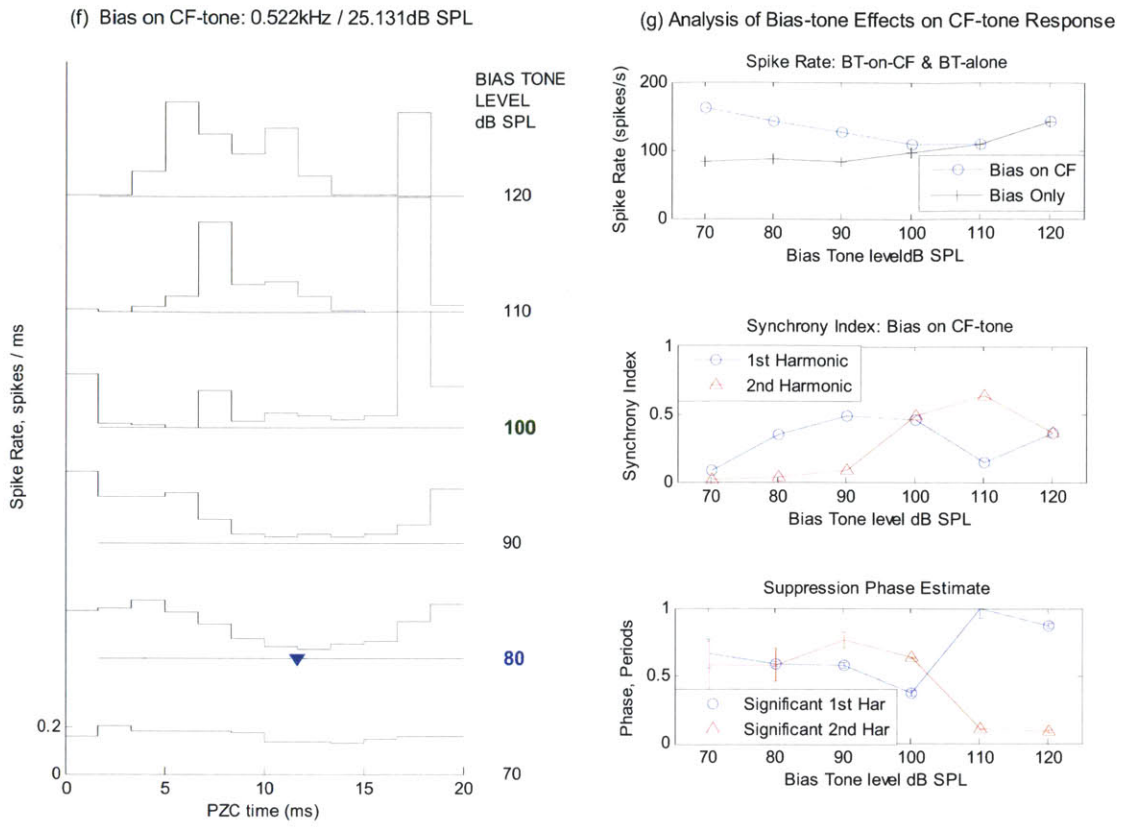

Fig. 2.25. Example Result: (a) Tuning Curve, CF=0.522kHz and SR= 85 sps; (b) Click Level Series, rarefaction click (ClickR) at 60 dB pSPL selected for bias-tone effects; (c) Bias-tone (BT) only level series, excitation threshold reached at 100 dB SPL. Excitation threshold level is indicated in green, and the excitation phase is indicated by a green triangle; (d) Bias-tone level-series on click response, ClickR at 60 dB pSPL, Time window 4.1 – 5.2 ms. The suppression threshold and the suppression phase of the 1st harmonic is indicated in blue; (e) Detailed analysis of the bias-tone effects on click response, Bias-tone level functions of firing rate, synchrony indices and phase of major suppression for the 1st and 2nd harmonic in the top-bottom order; (f) Bias-tone level-series on CF-tone response: suppression threshold for 1st harmonic was reached at 80 dB SPL. The major suppression phase of the low-level click and CF-tone responses was found at similar location approximately in the middle of the period; (g) Detailed analysis of the bias-tone effects on CF-tone response, Bias-tone level functions of firing rate, synchrony indices and phase of major suppression for the 1st and 2nd harmonic in the top-bottom order

Example Result in Fig. 2.26: CT025, U107, CF=0.96 kHz, SR= 84.5 sps

This fiber is another typical example from the CF region below 1 kHz. The bias-tone only excitation threshold was met at 120 dB SPL with the excitation phase detected at the broader peak in the period histogram. The suppression threshold on the low-level click and CF-tone responses were reached at 90 and 80 dB SPL respectively at a similar phase location. The minor suppression phase was not visible from the period histogram.

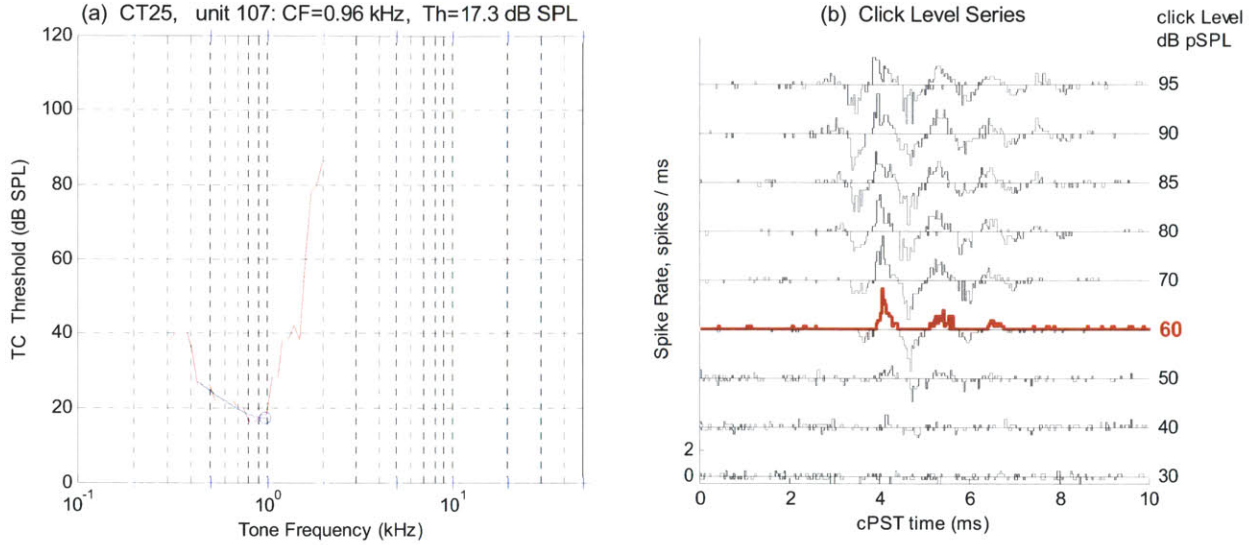

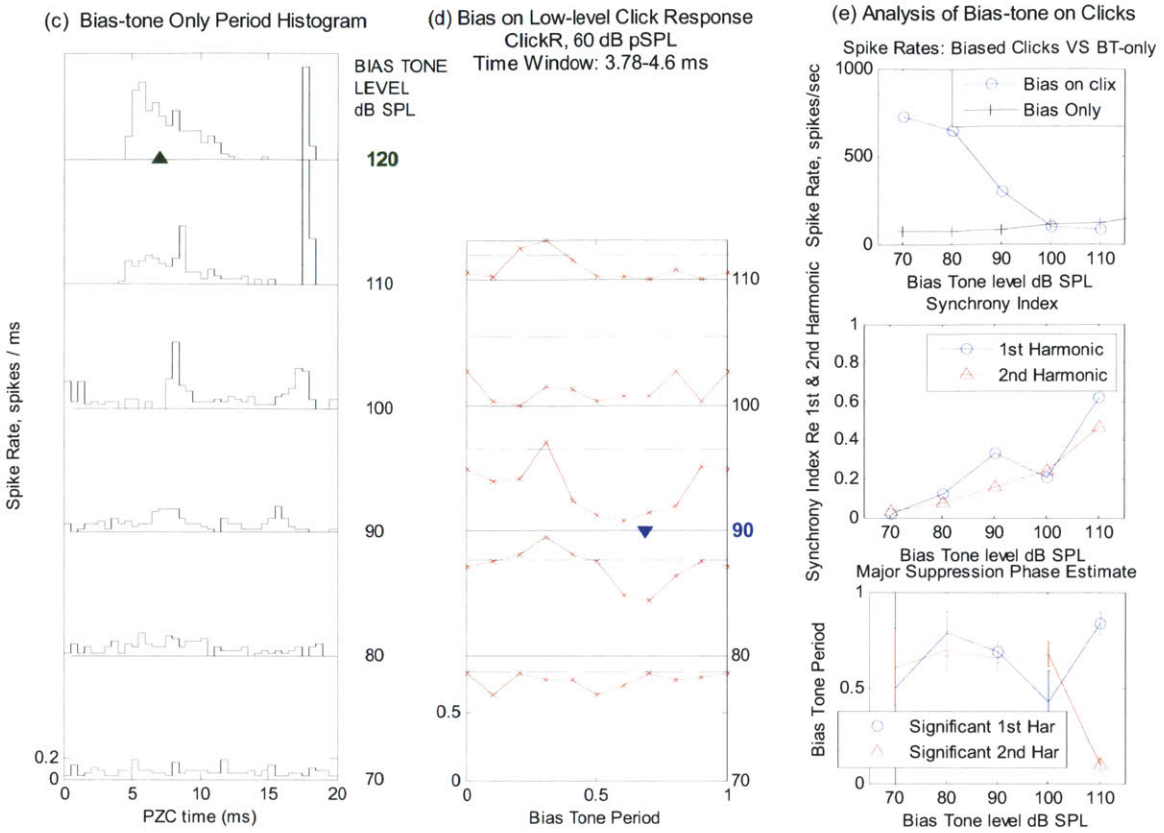
(c) Bias-tone Only Period Histogram
BIAS TONE LEVEL dB SPL
120
110
100
90
80
70
Spike Rate, spikes / ms
PZC time (ms)
(d) Bias on Low-level Click Response
ClickR, 60 dB pSPL
Time Window: 3.78-4.6 ms
Bias Tone Period
(e) Analysis of Bias-tone on Clicks
Spike Rates: Biased Clicks VS BT-only
Bias on clix
Bias Only
Spike Rate, spikes/sec
Bias Tone level dB SPL
Synchrony Index
1st Harmonic
2nd Harmonic
Synchrony Index Re 1st & 2nd Harmonic
Bias Tone level dB SPL
Major Suppression Phase Estimate
Significant 1st Har
Significant 2nd Har
Bias Tone Period
Bias Tone level dB SPL

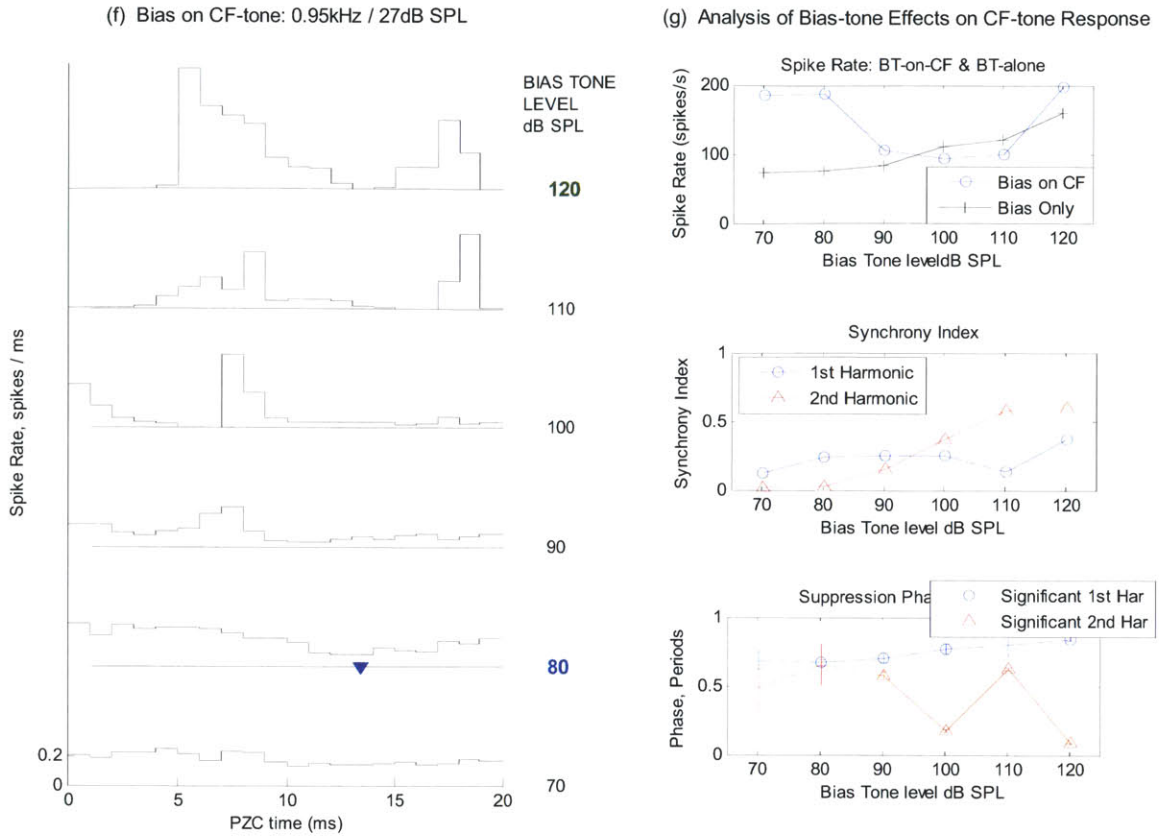

Fig. 2.26. Example Result: (a) Tuning Curve, CF=0.96 kHz and SR= 84.5 sps; (b) Click Level Series, ClickR at 60 dB pSPL selected for bias-tone effects; (c) Bias-tone (BT) only level series, excitation threshold reached at 120 dB SPL. Excitation threshold level is indicated in green, and the excitation phase is indicated by a green triangle; (d) Bias-tone level-series on click response, ClickR at 60 dB pSPL, Time window 3,78 – 4.6 ms. The suppression threshold and the suppression phase of the 1st harmonic is indicated in blue; (e) Detailed analysis of the bias-tone effects on click response, Bias-tone level functions of firing rate, synchrony indices and phase of major suppression for the 1st and 2nd harmonic in the top-bottom order; (f) Bias-tone level-series on CF-tone response: suppression threshold for 1st harmonic was reached at 80 dB SPL. The major suppression phase of the low-level click and CF-tone responses was found at similar location approximately in the middle of the period; (g) Detailed analysis of the bias-tone effects on CF-tone response, Bias-tone level functions of firing rate, synchrony indices and phase of major suppression for the 1st and 2nd harmonic in the top-bottom order

Example Result in Fig. 2.27 : CT033, U014, CF= 1.29 kHz, SR= 0.1 sps

This is a low-SR fiber with its CF just above 1 kHz. The bias-tone only level series did not show much excitation. The suppression threshold for 1st harmonic criterion was reached at 80 and 70 SPL of the bias-tone for the low-level click and CF-tone responses respectively. Further, at the bias-tone level of 10 dB above the 1st harmonic suppression threshold, the minor suppression phase was noticeable from both period histograms. For the case of the click response, because the bias-tone at 90 dB SPL led to almost complete suppression, the criterion for the second harmonic was not met.

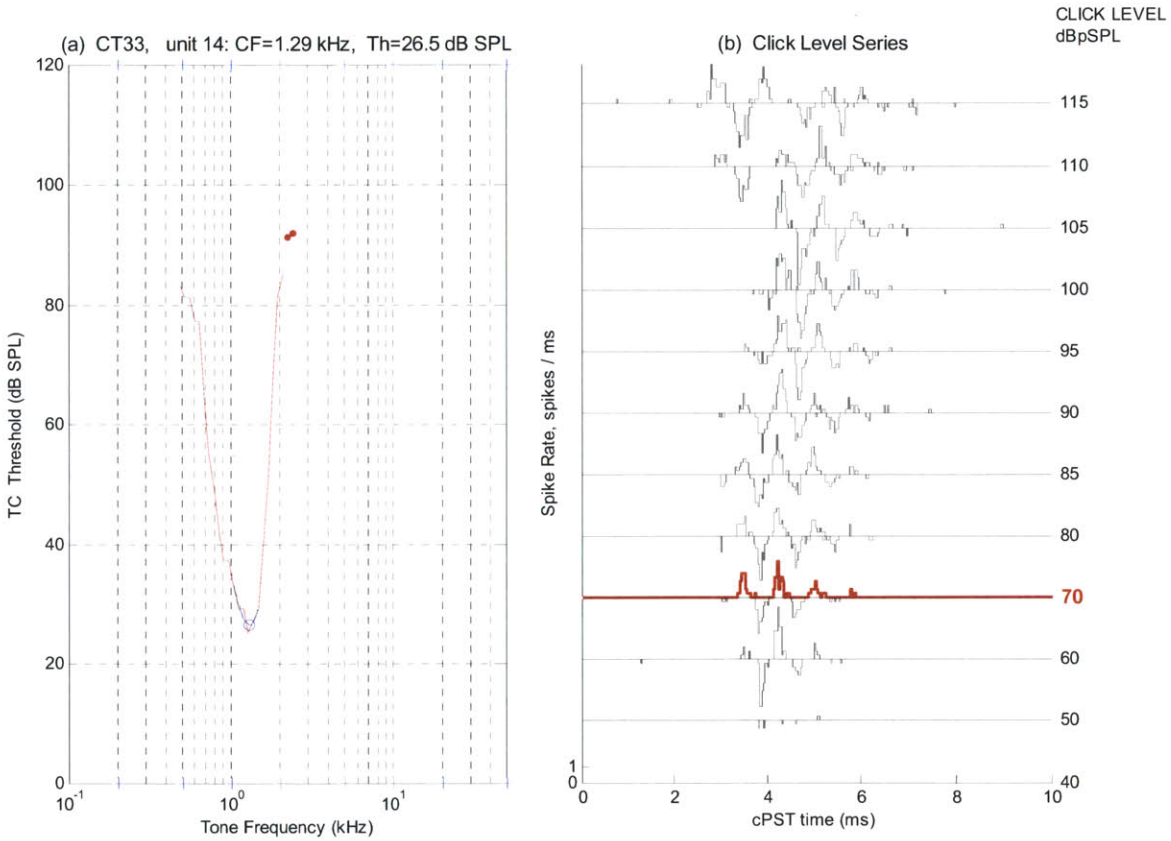

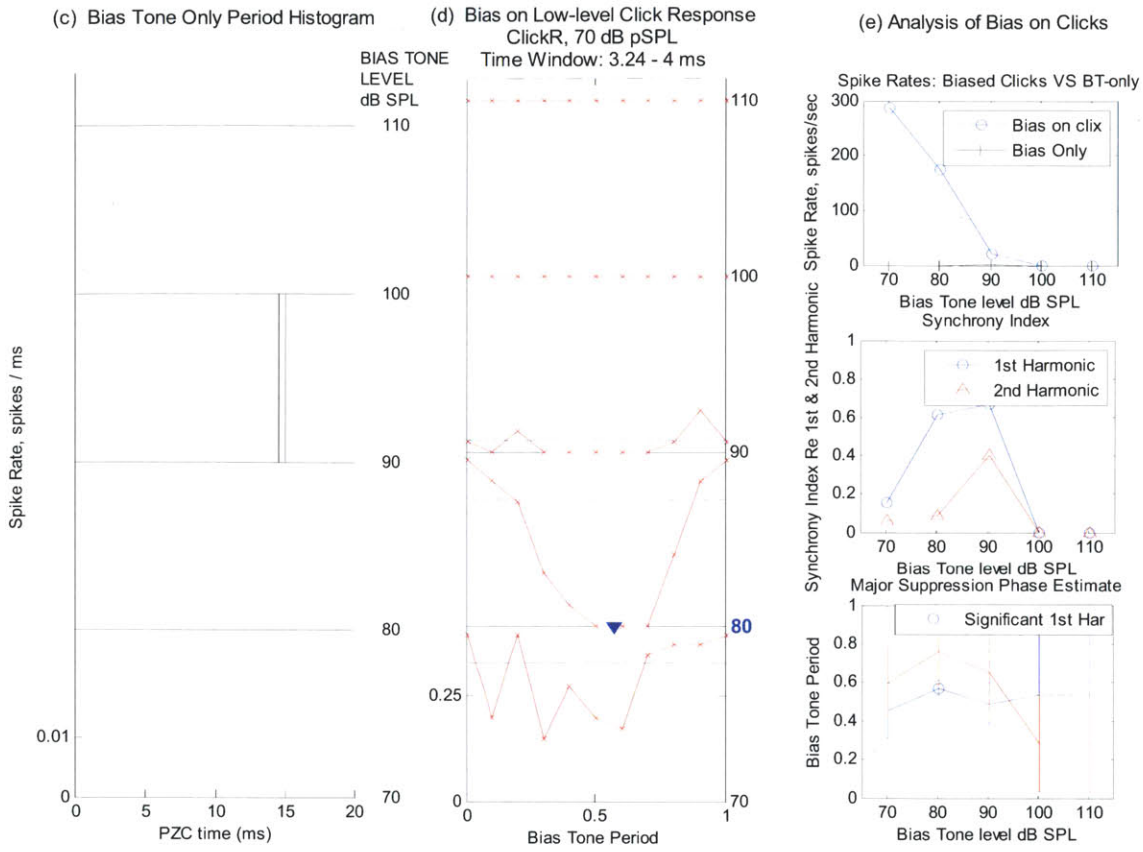
(c) Bias Tone Only Period Histogram
(d) Bias on Low-level Click Response
ClickR, 70 dB pSPL
Time Window: 3.24 - 4 ms
(e) Analysis of Bias on Clicks
BIAS TONE LEVEL dB SPL
Spike Rate, spikes / ms
PZC time (ms)
Bias Tone Period
Spike Rates: Biased Clicks VS BT-only
Bias on clix
Bias Only
Spike Rate, spikes/sec
Bias Tone level dB SPL
Synchrony Index
1st Harmonic
2nd Harmonic
Synchrony Index Re 1st & 2nd Harmonic
Major Suppression Phase Estimate
Significant 1st Har
Bias Tone Period

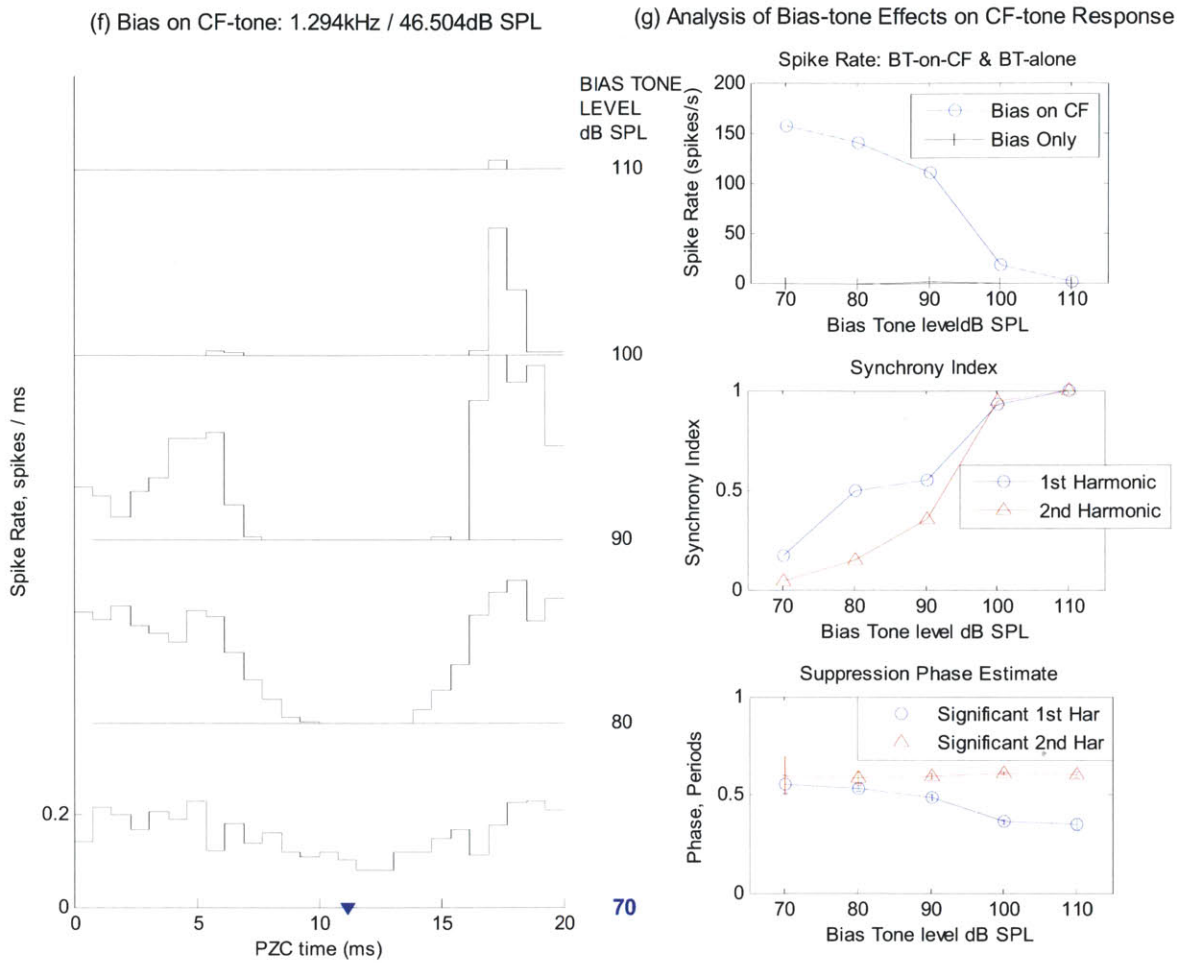

Fig. 2.27. Example Result: (a) Tuning Curve, CF=1.29 kHz and SR= 0.1 sps; (b) Click Level Series, ClickR at 70 dB pSPL selected for bias-tone effects; (c) Bias-tone (BT) only level series: excitation threshold was not reached within the maximum level of the bias-tone stimulus, 120 dB SPL; (d) Bias-tone level-series on click response, ClickR at 70 dB pSPL, Time window 3.24 - 4 ms. The suppression threshold and the suppression phase of the 1st harmonic is indicated in blue; (e) Detailed analysis of the bias-tone effects on click response, Bias-tone level functions of firing rate, synchrony indices and phase of major suppression for the 1st and 2nd harmonic in the top-bottom order; (f) Bias-tone level-series on CF-tone response: suppression threshold for 1st harmonic was reached at 70 dB SPL. The major suppression phase of the low-level click and CF-tone responses was found at similar location approximately in the middle of the period; (g) Detailed analysis of the bias-tone effects on CF-tone response, Bias-tone level functions of firing rate, synchrony indices and phase of major suppression for the 1st and 2nd harmonic in the top-bottom order

Example Result in Fig. 2.28: CT031, U079, CF= 2.8 kHz, SR= 14 sps

This fiber is a typical example from the CF region of 2-4 kHz. From the bias-tone-only period histograms, the peak splitting was not present in contrast to fibers with lower CFs although the narrow peak remained at about the same phase as in fibers with lower CFs. The suppression threshold for second harmonic was reached at 90 and 80 dB SPL for the low-level click and CF-tone responses respectively.

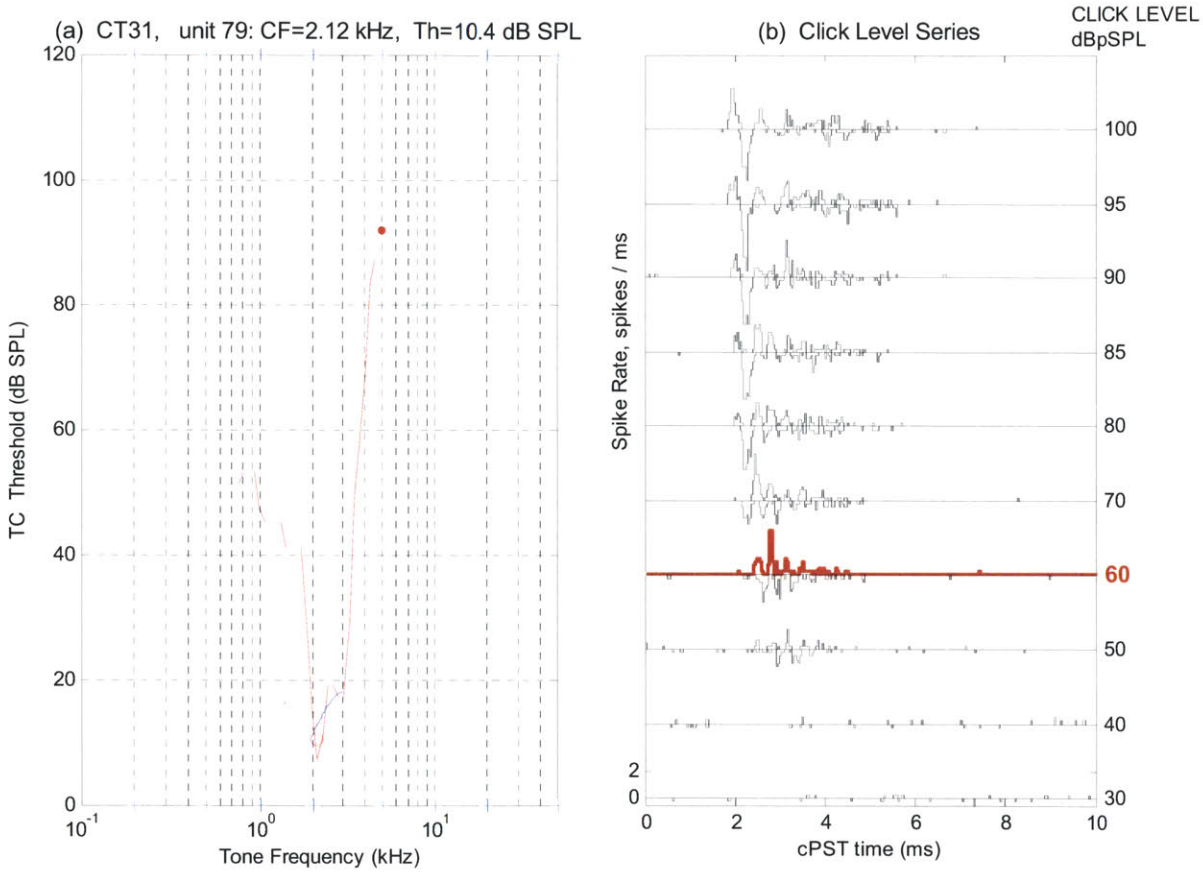

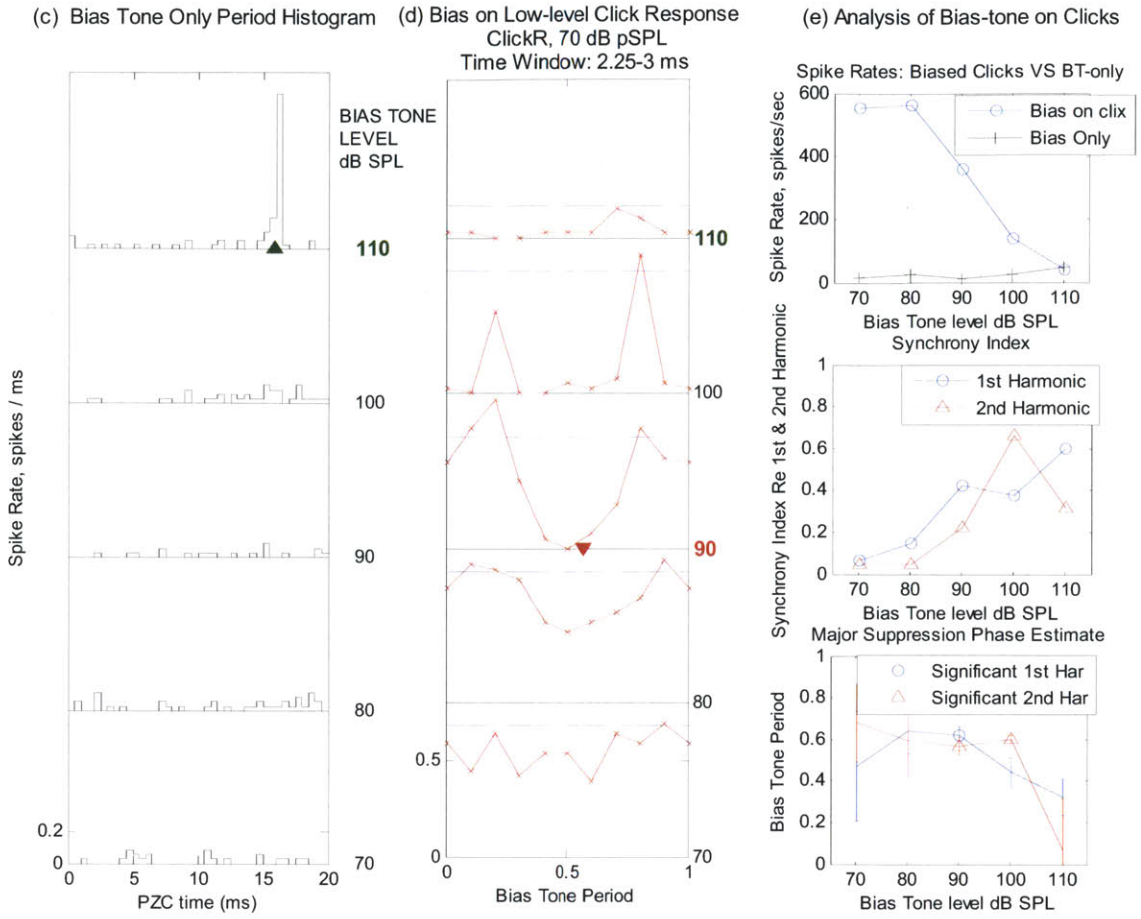
(c) Bias Tone Only Period Histogram
(d) Bias on Low-level Click Response
ClickR, 70 dB pSPL
Time Window: 2.25-3 ms
(e) Analysis of Bias-tone on Clicks
BIAS TONE LEVEL dB SPL
110
100
90
80
70
Spike Rate, spikes / ms
PZC time (ms)
Bias Tone Period
Spike Rates: Biased Clicks VS BT-only
Spike Rate, spikes/sec
Bias on clix
Bias Only
Bias Tone level dB SPL
Synchrony Index
Synchrony Index Re 1st & 2nd Harmonic
1st Harmonic
2nd Harmonic
Major Suppression Phase Estimate
Bias Tone Period
Significant 1st Har
Significant 2nd Har

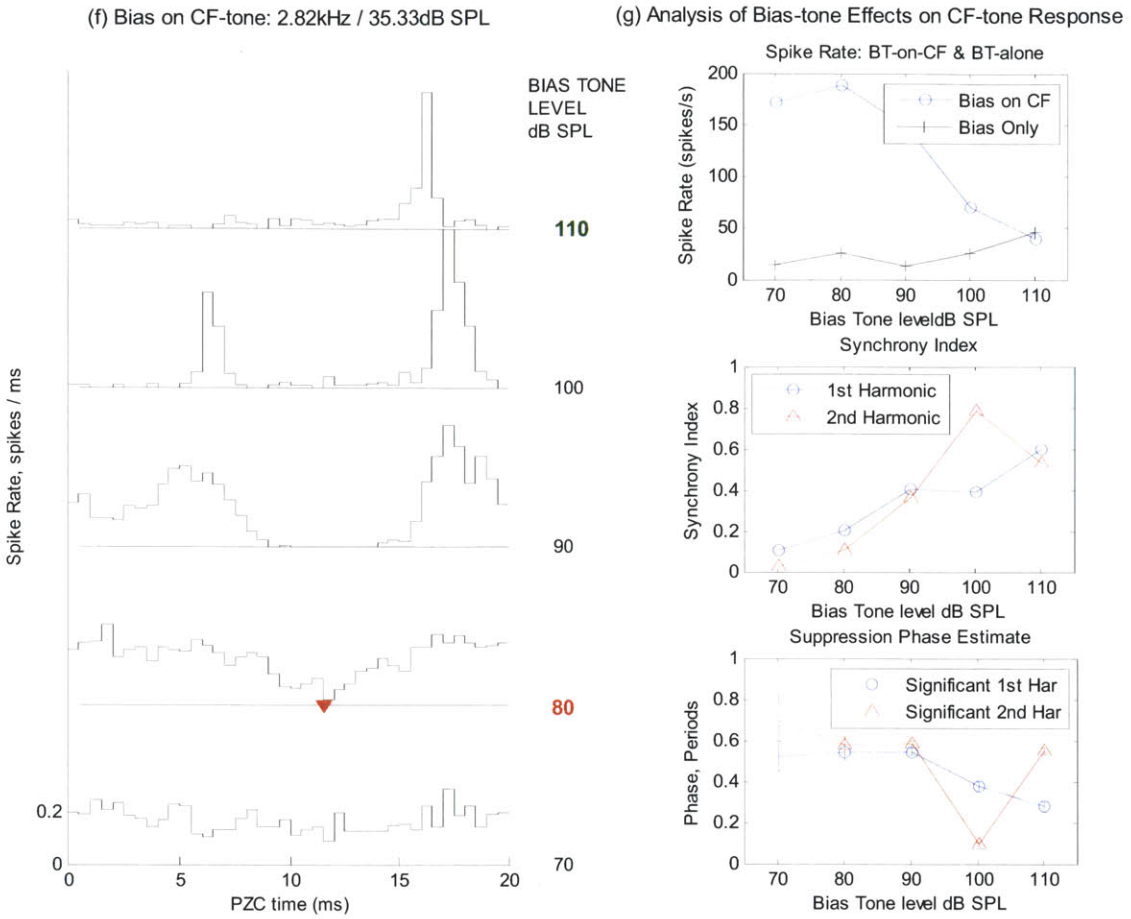

Fig. 2.28. Example Result: (a) Tuning Curve, CF=2.8 kHz and SR= 14 sps; (b) Click Level Series, ClickR at 60 dB pSPL selected for bias-tone effects; (c) Bias-tone (BT) only level series: peak splitting was not present. Only the narrow peak was excited at 110 dB SPL; (d) Bias-tone level-series on click response, ClickR at 60 dB pSPL, Time window 2.25 - 3 ms. The suppression threshold was met at 90 dB SPL for the 2nd harmonic. The suppression threshold and phase of the 2nd harmonic are indicated in red; (e) Detailed analysis of the bias-tone effects on click response, Bias-tone level functions of firing rate, synchrony indices and phase of major suppression for the 1st and 2nd harmonic in the top-bottom order; (f) Bias-tone level-series on CF-tone response: suppression threshold for 2nd harmonic was reached at 80 dB SPL. The major suppression phase of the low-level click and CF-tone responses was found at similar location approximately in the middle of the period; (g) Detailed analysis of the bias-tone effects on CF-tone response, Bias-tone level functions of firing rate, synchrony indices and phase of major suppression for the 1st and 2nd harmonic in the top-bottom order

Example Result in Fig. 2.29: CT031, U055, CF= 5.55 kHz, SR= 50 sps

Both the TC and the click level series show the typical characteristics of a high-CF fiber. Specifically, the TC shows a broad low-frequency tail, and the low-level click responses show the amplitude envelope only with no phase-locking to the CF-tone. From the bias-tone only period histograms, the peak splitting was not visible, and the narrow peak remained at about the same phase as in fibers with lower CFs. The suppression threshold was reached at 80 dB SPL with the first and second harmonic criterion for click and CF-tone response respectively. The suppression pattern on the low-level CF-tone responses showed more prominent minor suppression phase.

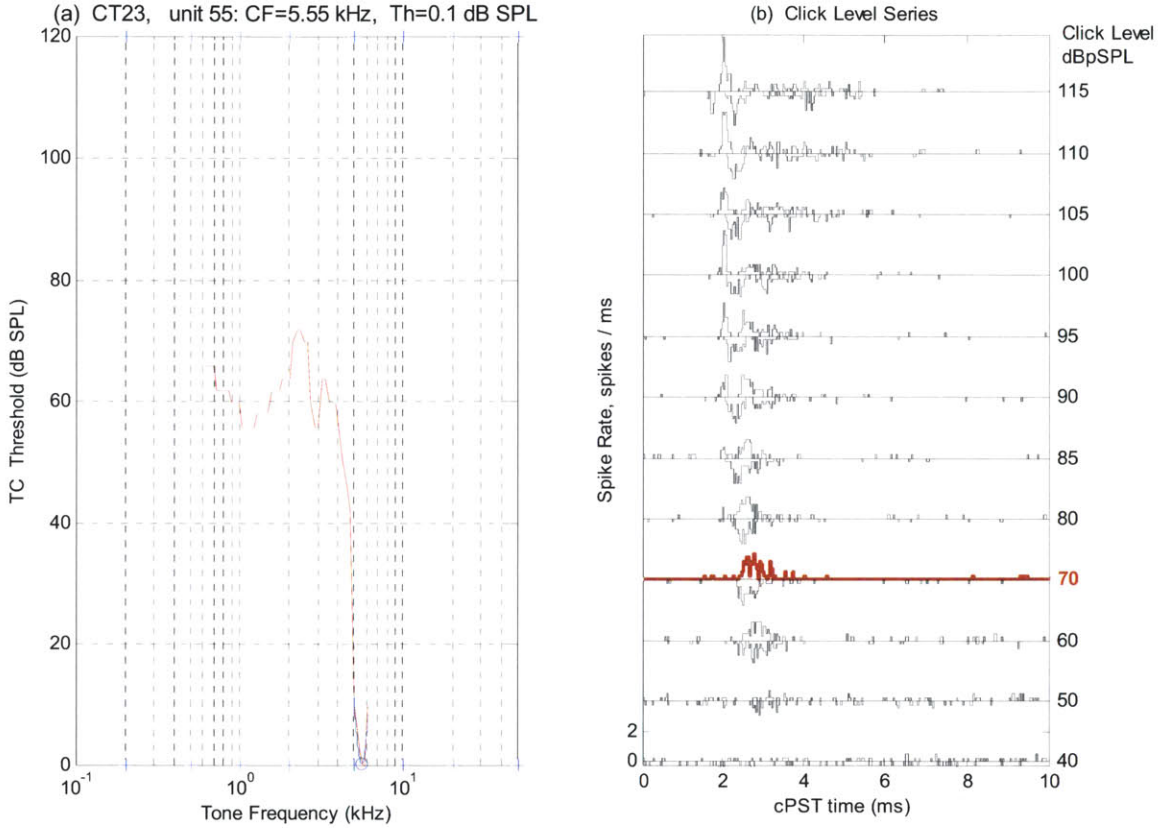

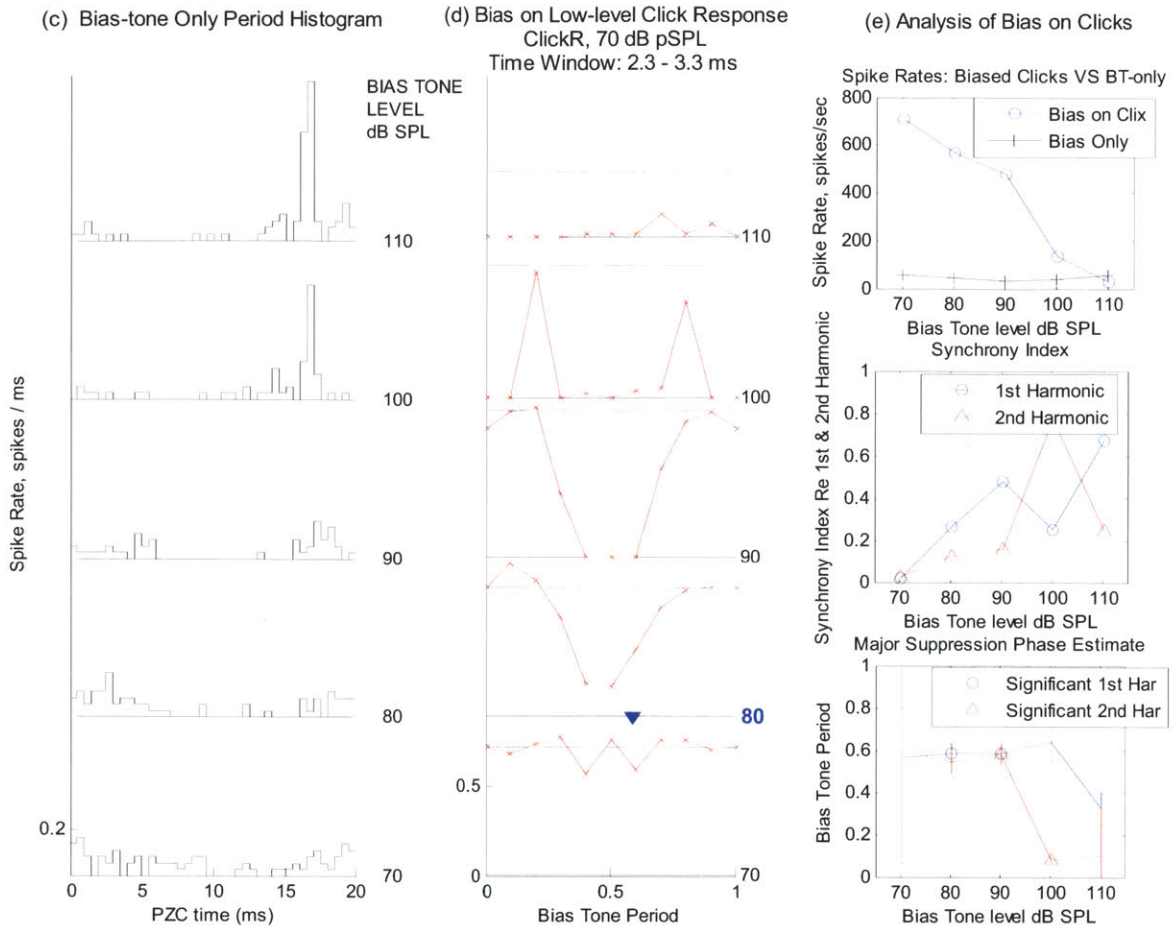
(c) Bias-tone Only Period Histogram
BIAS TONE LEVEL dB SPL
110
100
90
80
70
Spike Rate, spikes / ms
0.2
0
5
10
15
20
PZC time (ms)
(d) Bias on Low-level Click Response
ClickR, 70 dB pSPL
Time Window: 2.3 - 3.3 ms
110
100
90
80
70
0.5
0
0.5
1
Bias Tone Period
(e) Analysis of Bias on Clicks
Spike Rates: Biased Clicks VS BT-only
Bias on Clix
Bias Only
Spike Rate, spikes/sec
800
600
400
200
0
70
80
90
100
110
Bias Tone level dB SPL
Synchrony Index
1st Harmonic
2nd Harmonic
Synchrony Index Re 1st & 2nd Harmonic
1
0.8
0.6
0.4
0.2
0
70
80
90
100
110
Bias Tone level dB SPL
Major Suppression Phase Estimate
Significant 1st Har
Significant 2nd Har
Bias Tone Period
1
0.8
0.6
0.4
0.2
0
70
80
90
100
110
Bias Tone level dB SPL

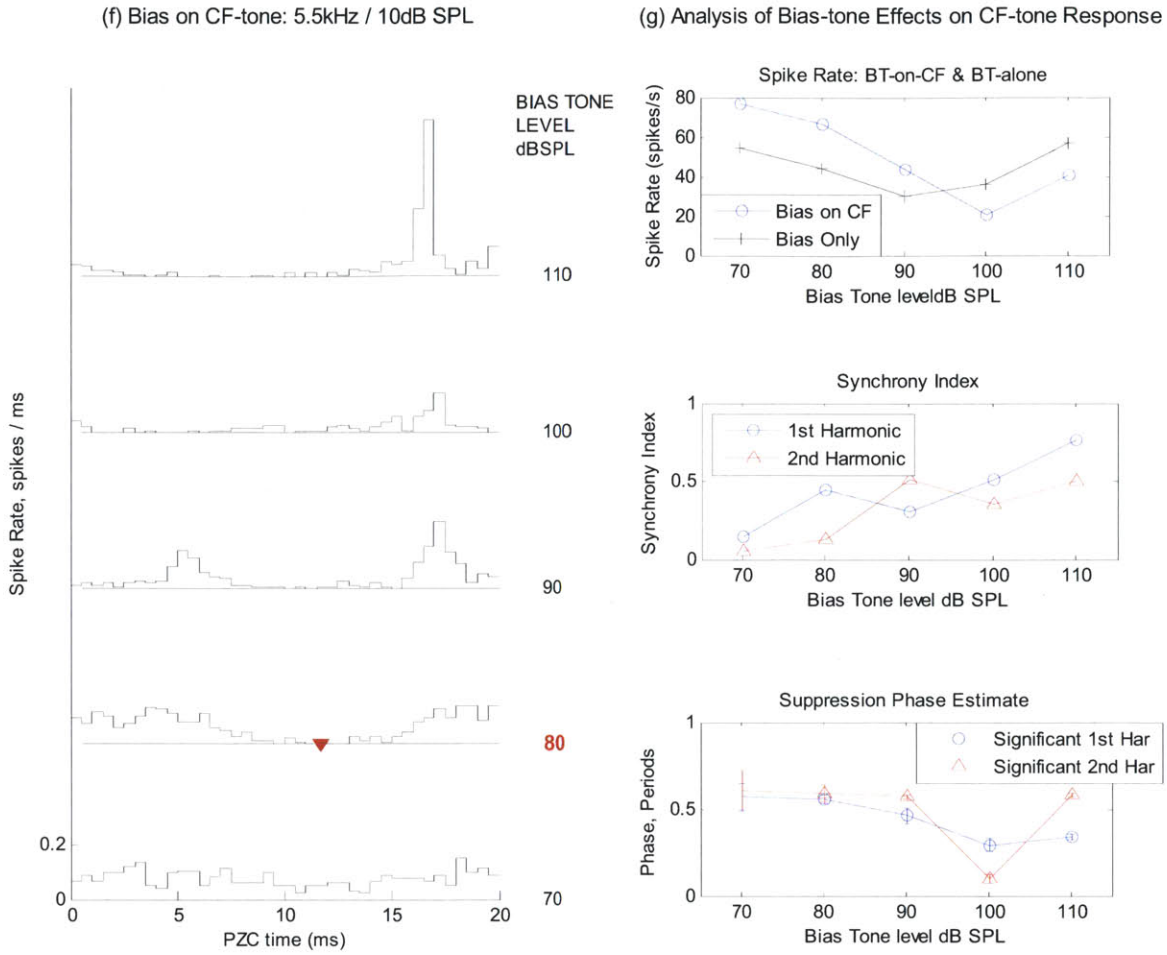

Fig. 2.29. Example Result: (a) Tuning Curve, CF=5.55 kHz and SR= 50 sps; (b) Click Level Series, ClickR at 70 dB pSPL selected for bias-tone effects; (c) Bias-tone (BT) only level series: peak splitting was not present. Only the narrow peak appeared at 100 dB SPL, but the rate threshold was note met; (d) Bias-tone level-series on click response, ClickR at 70 dB pSPL, Time window 2.3 – 3.3 ms. The suppression threshold was met at 80 dB SPL with the first harmonic; (e) Detailed analysis of the bias-tone effects on click response, Bias-tone level functions of firing rate, synchrony indices and phase of major suppression for the 1st and 2nd harmonic in the top-bottom order; (f) Bias-tone level-series on CF-tone response: suppression threshold for 2nd harmonic was reached at 80 dB SPL. The suppression pattern on CF-tone responses showed a more symmetrical shape; (g) Detailed analysis of the bias-tone effects on CF-tone response, Bias-tone level functions of firing rate, synchrony indices and phase of major suppression for the 1st and 2nd harmonic in the top-bottom order

Example Result in Fig. 2.30: CT023, U066, CF= 7.16 kHz, SR= 80 sps

This is the AN fiber with the highest CF from which the bias-tone effects on low-level click responses met the suppression threshold criteria. Both the TC and the click level series show the typical characteristics of a high-CF fiber; the TC shows a broad low-frequency tail, and the low-level click responses no longer is phased locked to the CF of the fiber but shows the amplitude envelope only. From the bias-tone only period histograms, the peak splitting is not visible, and the narrow peak remains at about the same phase as in fibers with lower CFs. The suppression threshold for the second harmonic was reached at 100 dB SPL and 90 dB SPL for low-level click and CF-tone and responses respectively. Note that for this fiber, the suppression phase for the low-level click responses was detected at the opposite phase to the main data group. However, also note that at 10 dB below the threshold at 90 dB SPL, the actual major suppression phase emerges at the typical location, but fell below the criterion. Therefore, the suppression pattern for this fiber was not actually different from other fibers in this CF region.

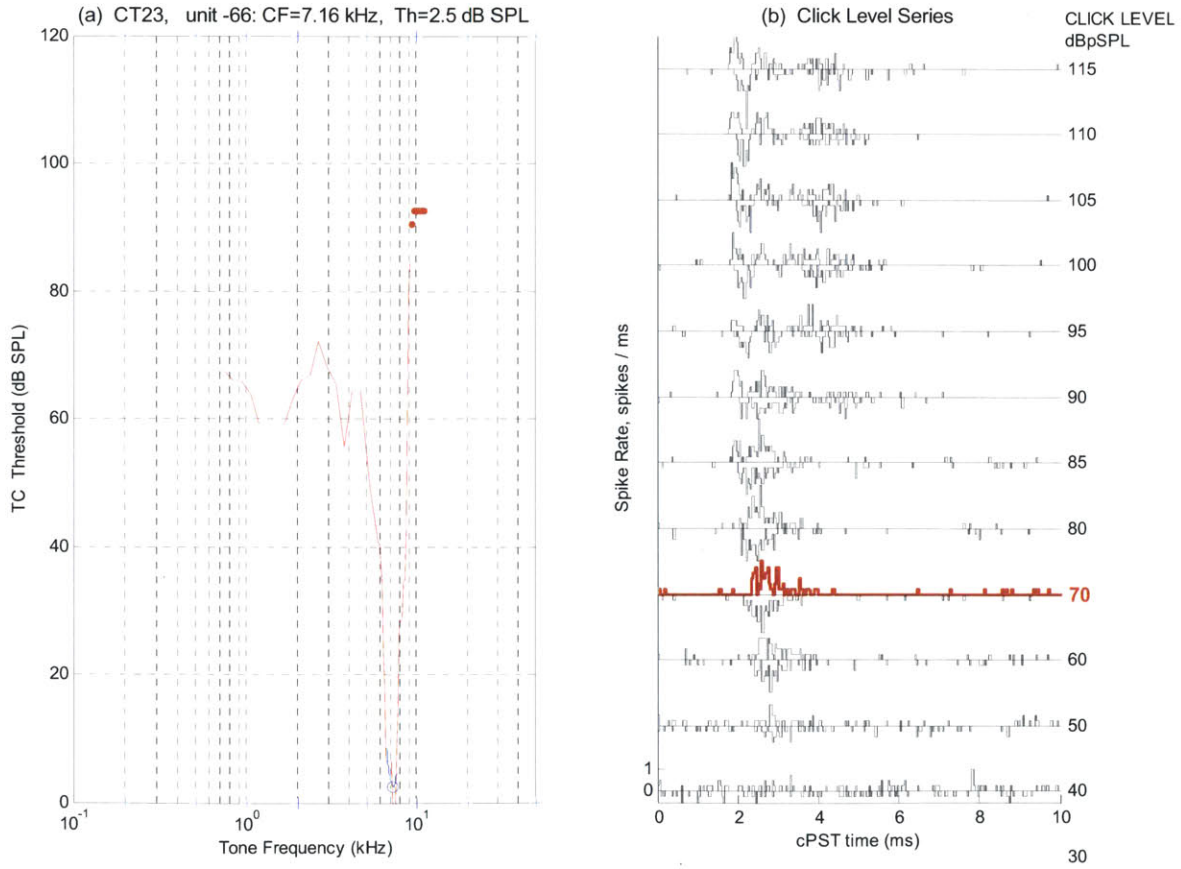

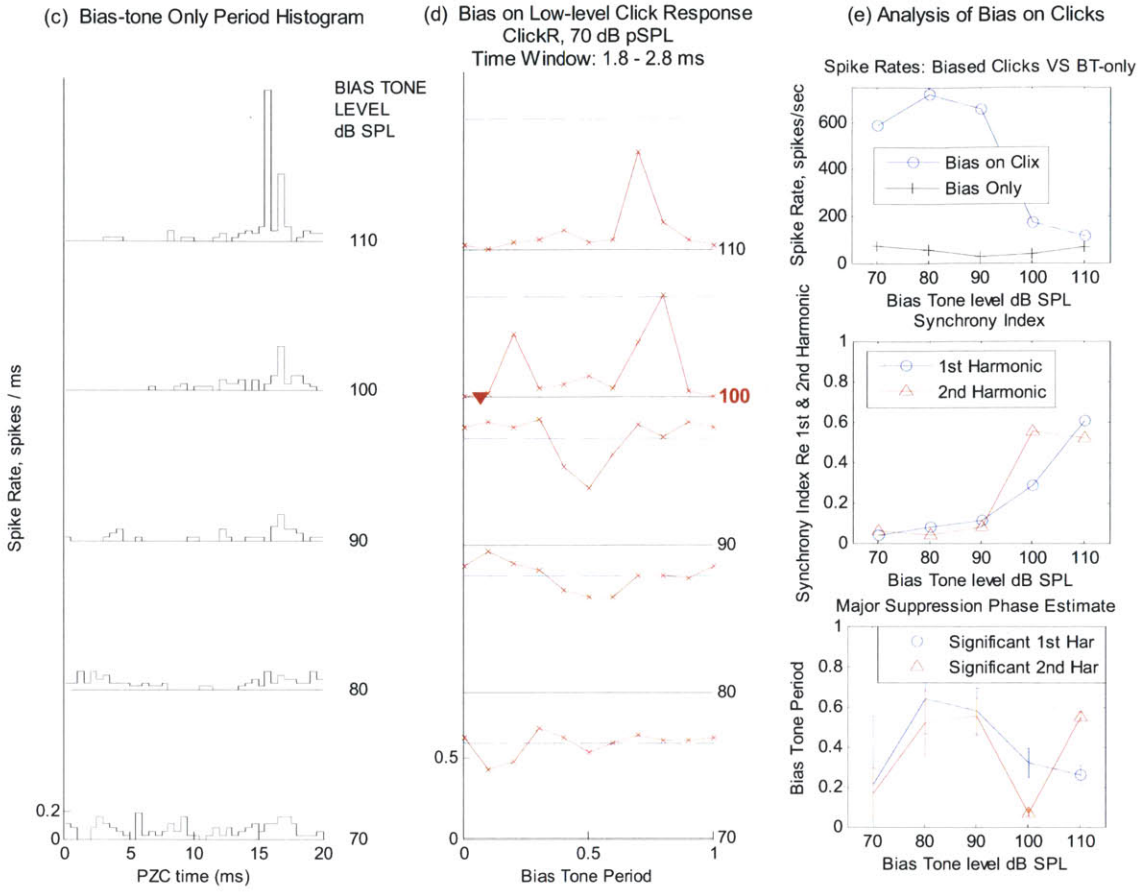
(c) Bias-tone Only Period Histogram
BIAS TONE LEVEL dB SPL
110
100
90
80
70
Spike Rate, spikes / ms
PZC time (ms)
(d) Bias on Low-level Click Response
ClickR, 70 dB pSPL
Time Window: 1.8 - 2.8 ms
Bias Tone Period
(e) Analysis of Bias on Clicks
Spike Rates: Biased Clicks VS BT-only
Spike Rate, spikes/sec
Bias on Clix
Bias Only
Bias Tone level dB SPL
Synchrony Index
Synchrony Index Re 1st & 2nd Harmonic
1st Harmonic
2nd Harmonic
Major Suppression Phase Estimate
Bias Tone Period
Significant 1st Har
Significant 2nd Har

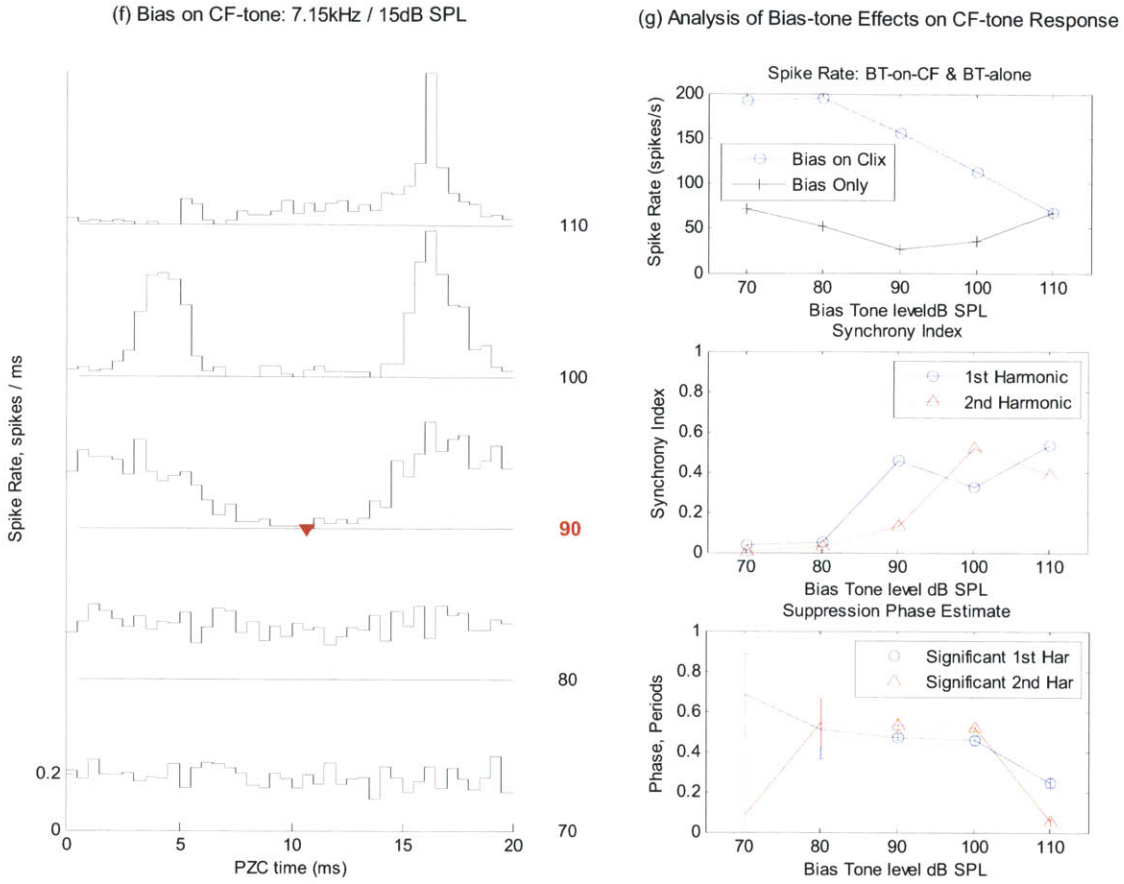

Fig. 2.30. Example Result: Example Result: (a) Tuning Curve, CF= 7.16 kHz and SR= 80 sps; (b) Click Level Series, ClickR at 70 dB pSPL selected for bias-tone effects; (c) Bias-tone (BT) only level series: peak splitting was not present. Only the narrow peak appeared at ~110 dB SPL, but the rate threshold was note met; (d) Bias-tone level-series on click response, ClickR at 70 dB pSPL, Time window 1.8 – 2.8 ms. The suppression threshold was met at 100 dB SPL with the second harmonic. The major suppression phase was opposite of the typical value; however, at 10 dB the threshold, the actual major suppression phase can be seen in the typical location. Therefore, the actual suppression characteristic of this fiber was not different from the typical pattern; (e) Detailed analysis of the bias-tone effects on click response, Bias-tone level functions of firing rate, synchrony indices and phase of major suppression for the 1st and 2nd harmonic in the top-bottom order; (f) Bias-tone level-series on CF-tone response: suppression threshold for 2nd harmonic was reached at 90 dB SPL. The suppression pattern on CF-tone responses showed a more symmetrical shape; (g) Detailed analysis of the bias-tone effects on CF-tone response, Bias-tone level functions of firing rate, synchrony indices and phase of major suppression for the 1st and 2nd harmonic in the top-bottom order.

Example Result in Fig. 2.31: CT030, U001, CF= 17.28 kHz, SR= 70 sps

This is one of the fibers with CF > 10 kHz from which the suppression threshold was not reached for the low-level click responses but found on low-level CF-tone responses at 110 dB SPL. Note that the maximum bias-tone level applied for the low-level click responses was 110 dB SPL which was 10 dB lower than on low-level CF response. Further note that the level function of the first harmonic synchrony index for the bias-tone effects on clicks began to show an upward trend at 110 dB SPL. Based on these data, the suppression threshold on the low-level clicks could have been slightly above the maximum level applied in this recording.

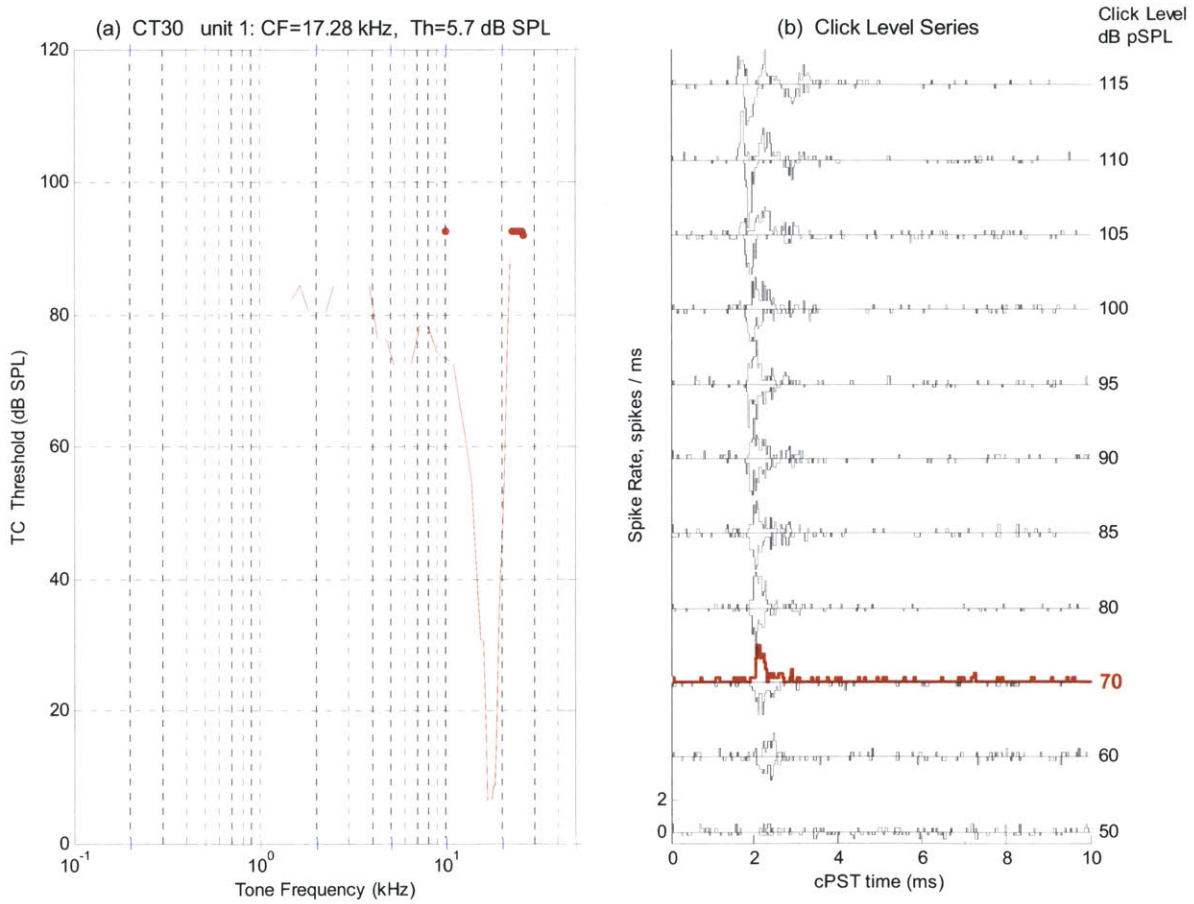

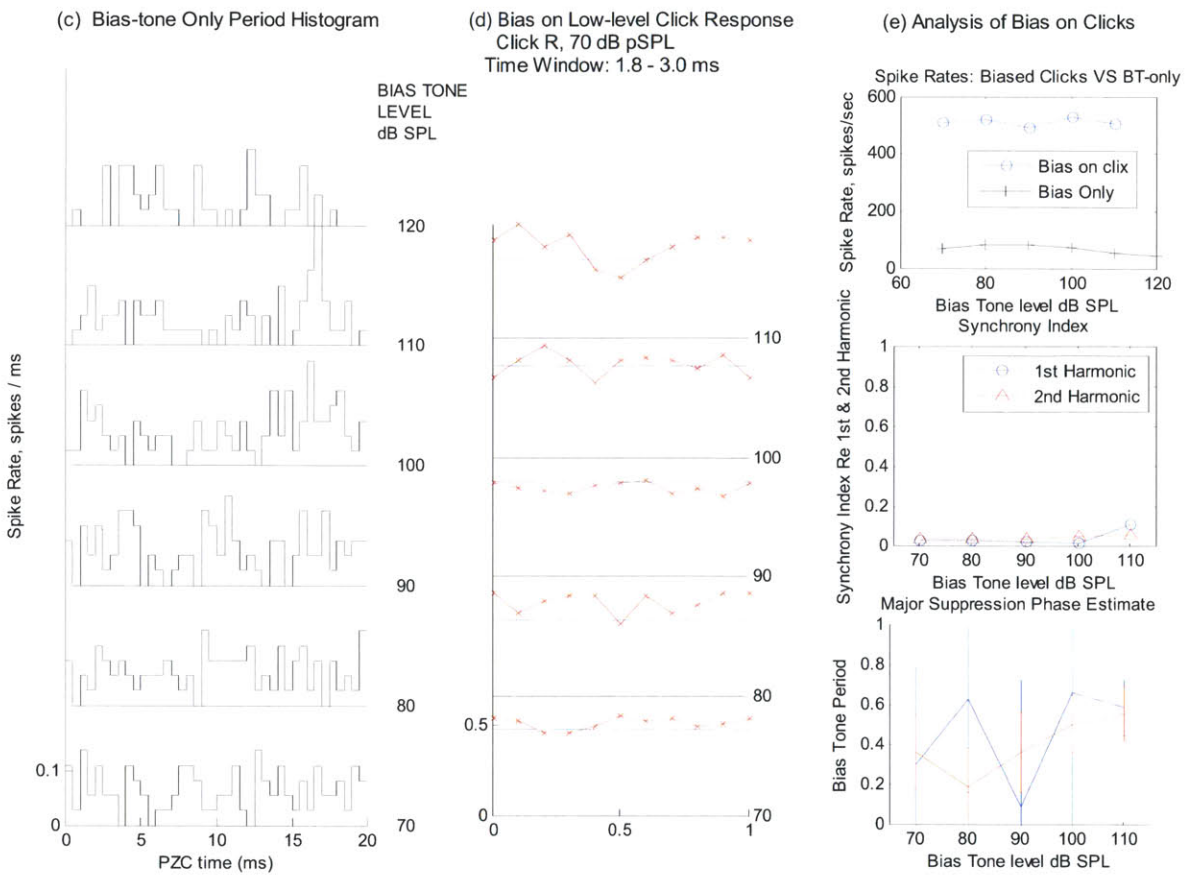
(c) Bias-tone Only Period Histogram
(d) Bias on Low-level Click Response
Click R, 70 dB pSPL
Time Window: 1.8 - 3.0 ms
(e) Analysis of Bias on Clicks
BIAS TONE LEVEL dB SPL
120
110
100
90
80
70
Spike Rate, spikes / ms
0.1
0
0
5
10
15
20
PZC time (ms)
0.5
0
0.5
1
Spike Rates: Biased Clicks VS BT-only
Spike Rate, spikes/sec
600
400
200
0
Bias on clix
Bias Only
60
80
100
120
Bias Tone level dB SPL
Synchrony Index
Synchrony Index Re 1st & 2nd Harmonic
1
0.8
0.6
0.4
0.2
0
1st Harmonic
2nd Harmonic
70
80
90
100
110
Bias Tone level dB SPL
Major Suppression Phase Estimate
Bias Tone Period
1
0.8
0.6
0.4
0.2
0
70
80
90
100
110
Bias Tone level dB SPL

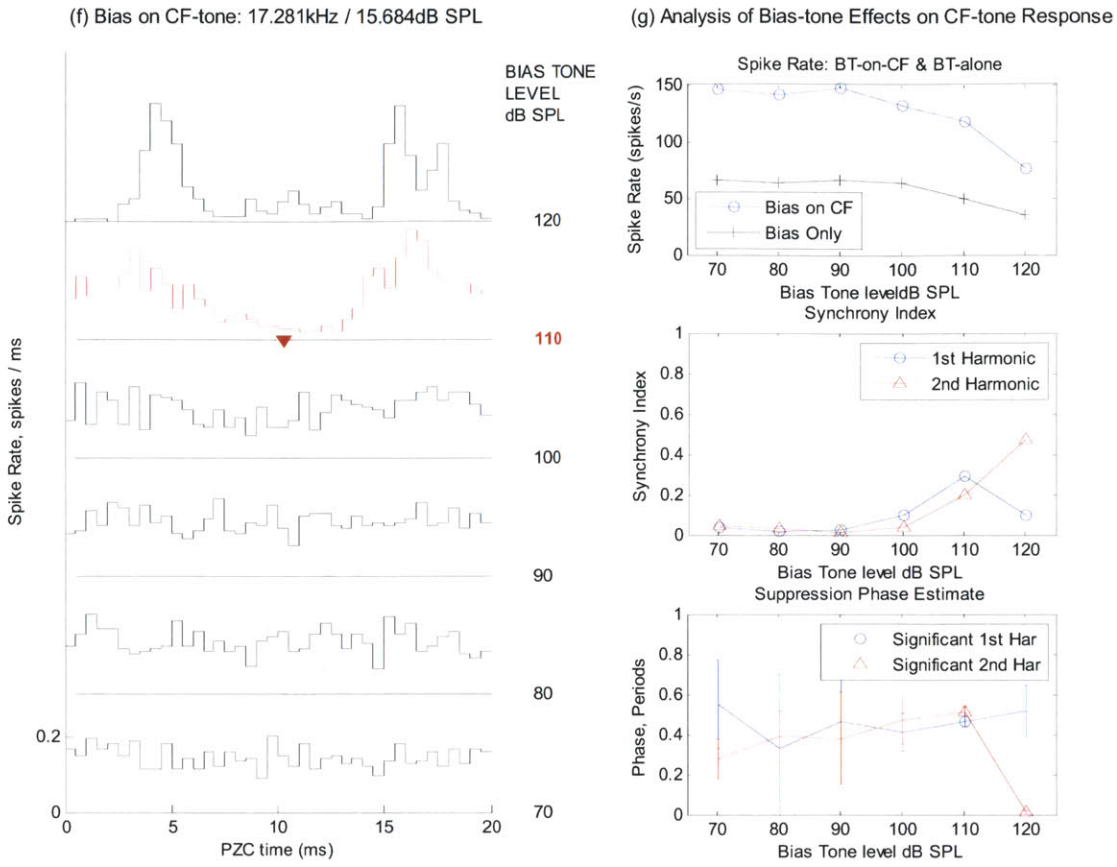

Fig. 2.31. Example Result: (a) Tuning Curve, CF= 17.28 kHz and SR= 70 sps; (b) Click Level Series, ClickR at 70 dB pSPL selected for bias-tone effects; (c) Bias-tone (BT) only level series: excitation threshold was not met; (d) Bias-tone level-series on click response, ClickR at 70 dB pSPL, Time window 1.8 – 3.0 ms. The suppression threshold was not reached within the maximum bias-tone level applied, 110 dB SPL; (e) Detailed analysis of the bias-tone effects on click response, Bias-tone level functions of firing rate, synchrony indices and phase of major suppression for the 1st and 2nd harmonic in the top-bottom order; (f) Bias-tone level-series on CF-tone response: suppression threshold for 2nd harmonic was reached at 100 dB SPL. The suppression pattern on CF-tone responses showed a more symmetrical shape; (g) Detailed analysis of the bias-tone effects on CF-tone response, Bias-tone level functions of firing rate, synchrony indices and phase of major suppression for the 1st and 2nd harmonic in the top-bottom order.

Example Result in Fig. 2.32: CT022, U013, CF= 20.4 kHz, SR= 107.6 sps

This is one of the fibers with CF > 10kHz from which the suppression threshold was not reached for the low-level click responses but found on low-level CF-tone responses at 90 dB SPL. Note that the maximum bias-tone level applied for suppression studies in this recording was 100 dB SPL. Further note that the level functions of the synchrony indices for the bias-tone effects on click responses began to show an upward trend at 90 dB SPL. Based on these, the suppression threshold on the low-level clicks may have been above the maximum level applied in this recording.

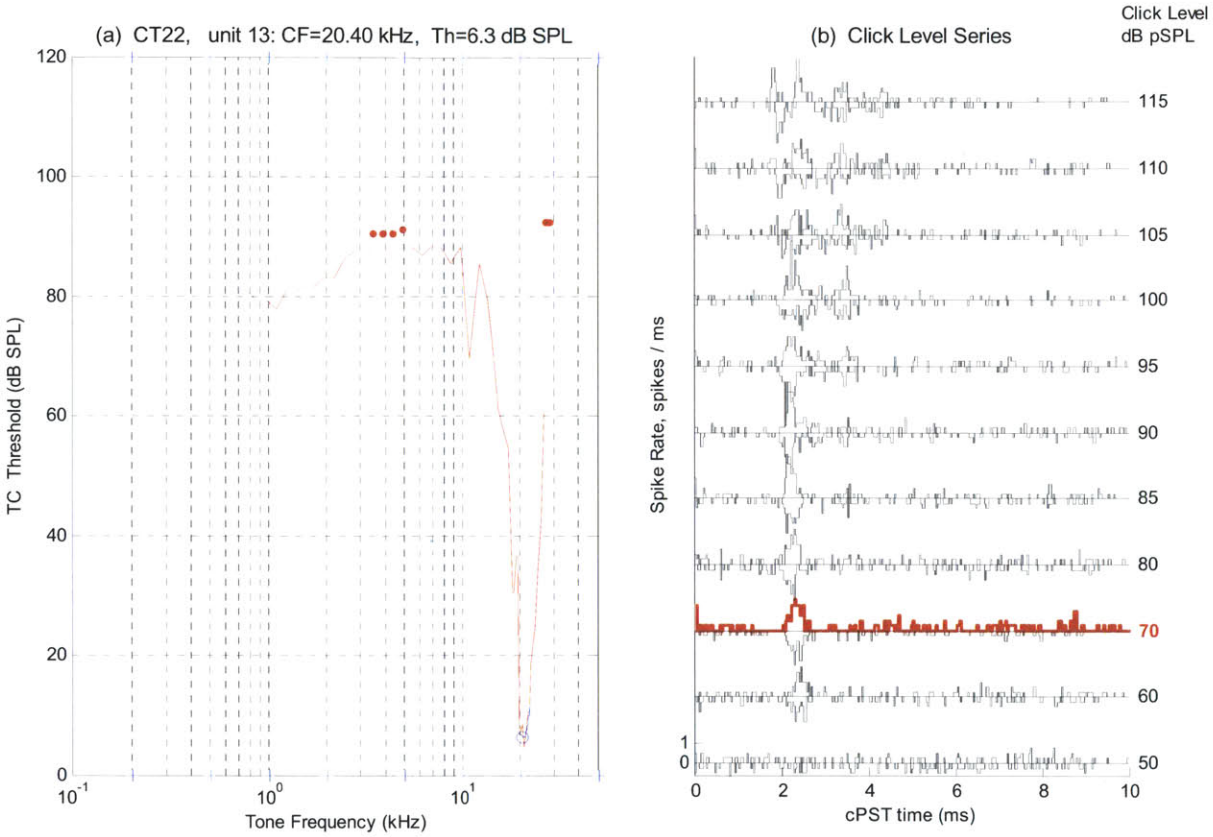

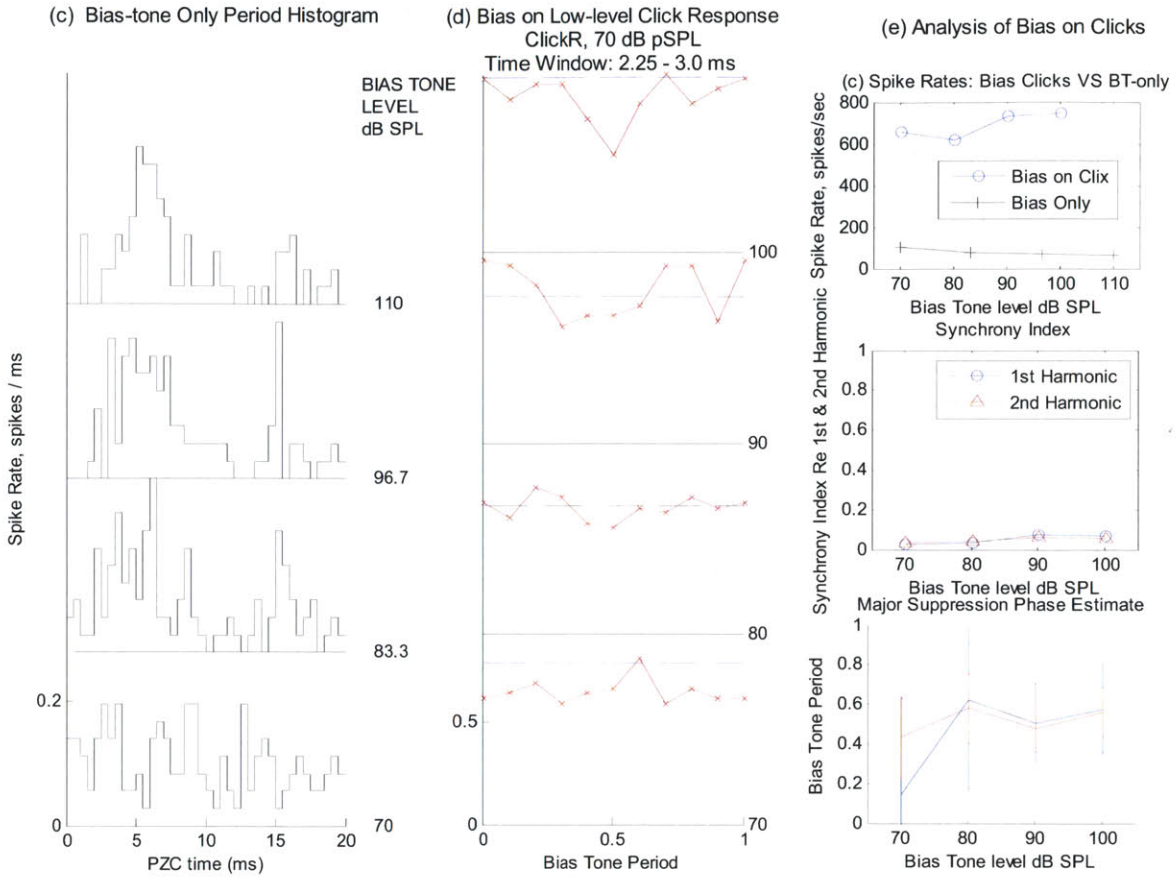
(c) Bias-tone Only Period Histogram
BIAS TONE LEVEL dB SPL
110
96.7
83.3
70
Spike Rate, spikes / ms
PZC time (ms)
(d) Bias on Low-level Click Response
ClickR, 70 dB pSPL
Time Window: 2.25 - 3.0 ms
100
90
80
70
Bias Tone Period
(e) Analysis of Bias on Clicks
(c) Spike Rates: Bias Clicks VS BT-only
Bias on Clix
Bias Only
Spike Rate, spikes/sec
Bias Tone level dB SPL
Synchrony Index
1st Harmonic
2nd Harmonic
Synchrony Index Re 1st & 2nd Harmonic
Bias Tone level dB SPL
Major Suppression Phase Estimate
Bias Tone Period
Bias Tone level dB SPL

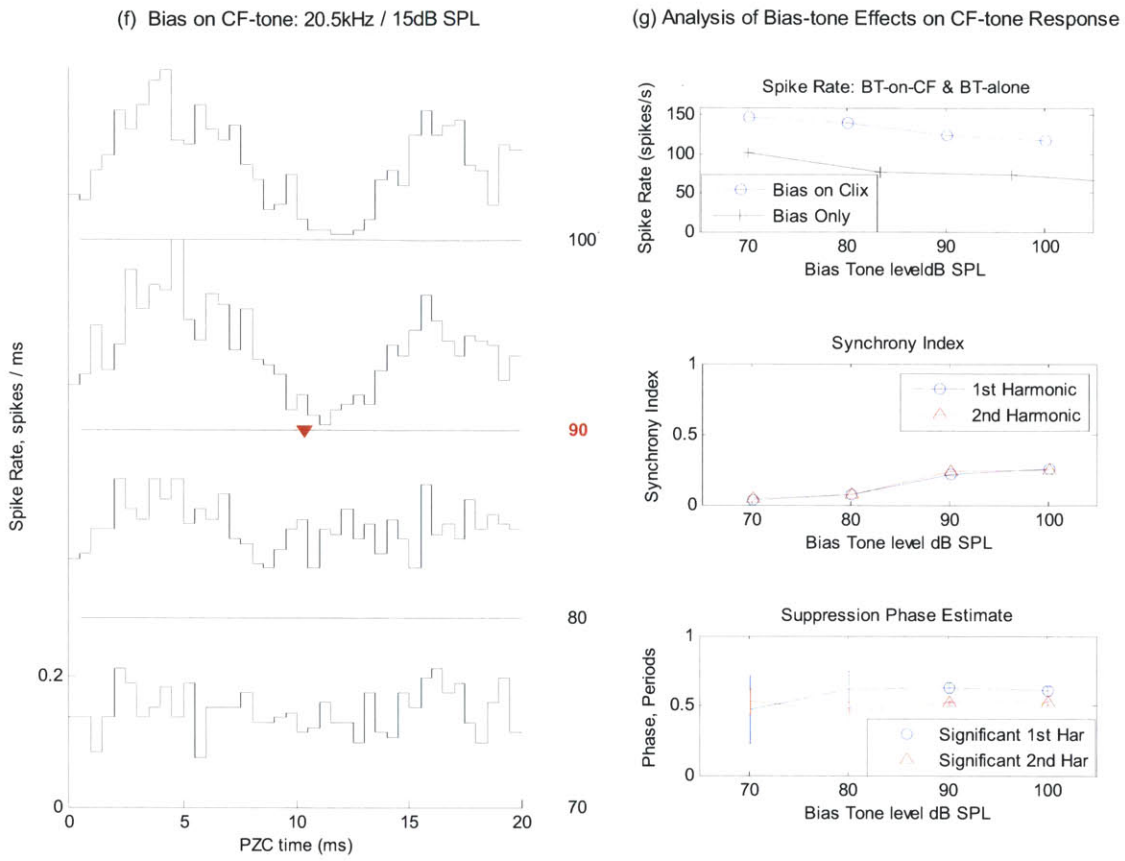

Fig. 2.32. Example Result: (a) Tuning Curve, CF= 20.4 kHz and SR= 107.6 sps; (b) Click Level Series, ClickR at 70 dB pSPL selected for bias-tone effects; (c) Bias-tone (BT) only level series: excitation threshold was not met; (d) Bias-tone level-series on click response, ClickR at 70 dB pSPL, Time window 2.25 – 3.0 ms. The suppression threshold was not reached within the maximum bias-tone level applied, 100 dB SPL; (e) Detailed analysis of the bias-tone effects on click response, Bias-tone level functions of firing rate, synchrony indices and phase of major suppression for the 1st and 2nd harmonic in the top-bottom order; (f) Bias-tone level-series on CF-tone response: suppression threshold for 2nd harmonic was reached at 90 dB SPL. The suppression pattern on CF-tone responses showed a more symmetrical shape; (g) Detailed analysis of the bias-tone effects on CF-tone response, Bias-tone level functions of firing rate, synchrony indices and phase of major suppression for the 1st and 2nd harmonic in the top-bottom order.

IV. Discussion

A. The Suppression Effects on AN Firing Reported in This Study Were Primarily Due to Stimulation of OHCs rather than Direct Stimulation of IHC Stereocilia by the 50 Hz Bias-tone

Although 50 Hz bias-tone used in this study is expected to stimulate the OHC stereocilia with higher amplitude than the IHC stereocilia [Russell and Sellick, 1983], it has been found in this study and elsewhere [Sellick et al, 1982; Patuzzi et al, 1984a; Cai and Geisler, 1996a] that AN responses to bias-tone level series with bias-tone alone do show both firing rate elevation and phasic modulation of period histograms at high enough levels of bias-tone. Consequently, it would be necessary to examine whether the results reported in this study as suppressive effects on OHC transduction function were not significantly affected by direct stimulation of the IHC stereocilia by the bias-tone.

In order to detect results with potential effects of direct stimulation of IHC stereocilia by the bias-tone, the excitation threshold level on AN firing by the bias-tone alone was measured from the AN response to bias-level series of bias-tone alone from each AN fiber. Then, the results from the bias-tone level series on either low-level CF-tone or click responses were not included in the data pool for suppression effects if the bias-tone level of the suppression data exceeded the excitation threshold.

The criteria to determine the excitation threshold of a AN fiber required firing rate elevation by one standard deviation and the standard error on the vector phase of firing to be within ±20°. Now, it would be necessary to examine whether the criteria applied on the reported results were appropriate. In order to examine the impact of the excitation threshold criteria on the suppression data, several iterations of data analysis were done with varying degrees of criteria around the values applied on the reported results. For example, the rate criteria with smaller increment such as ½ of standard deviation and the phase criteria with larger error bound such as ±30° are expected to lower the threshold of excitation by the bias-tone alone whereas a larger increment of firing rate such as two standard deviation and lower error bound on phase such as 10° would elevate the excitation threshold. Series of plots of the excitation phase and the major suppression phase on CF-tone and click response as shown in Fig. 2.18 and Fig. 2.21 with varying criteria on the excitation threshold did not show significant shifts in the results other than the number and scatter of data points around the same trend as shown in Fig. 2.18 and Fig. 2.21. Considering these, the suppression Effects on AN Firing reported in this study were concluded to be primarily due to stimulation of OHCs rather than direct stimulation of IHC stereocilia by the 50 Hz bias-tone

B. Comparison to Previous Studies on Low-frequency Bias-tone Effects on AN Responses to Low-level CF-tone

The previous study which is the most comparable to the results reported here for the bias-tone effects on low-level CF-tone responses comes from [Cai and Geisler, 1996a]. In their study, the temporal aspects of the suppressive effects of a low-frequency bias-tone on low-level CF-tone responses from cats AN fibers over the entire range of CFs were reported. Specifically, their results covered the bias-tone frequency of 50 Hz and comparison of the major suppression phase on the low-level CF-tone responses with the phase of excitation by the 50 Hz bias-tone alone as reported in this study. Overall, the results reported here were quite similar to the comparable results from [Cai and Geisler, 1996a] with no major discrepancies.

As reported in Fig 4.A and Fig. 5.A of [Cai and Geisler, 1996a] and in Fig. 2.18 of this study, the phase of major suppression by 50 Hz bias-tone on low-level CF-tone responses formed a smooth curve without significant discontinuities over the CFs of the AN fibers with a similar slope of ~-0.1 period of the 50 Hz bias-tone per decade of CF. Further, both studies showed that the major suppression phase was located ~1/4 cycle away from the phase of excitation by the bias-tone alone. Also both studies found that for the bias-tone frequency of 50 Hz, the phase of excitation by the bias-tone alone varied over the range of ~1/2 cycle for fibers with CF < ~2 kHz due to the peak-splitting phenomenon whereby a wide and a narrow peak separated by about ~1/2 cycle developed. For CF > 2 kHz, only the narrow peak was visible from the excitation pattern by the bias-tone alone, and with reference to the phase of the narrow peak, the major suppression phase was located with ~1/4 period lead as found by both studies. Further, similar results of ~1/4 lead of the suppression phase on AN responses to low-level CF-tone in relation to the phase of excitation by the bias-tone alone have been found from low-frequency bias-tone studies on guinea pigs and chinchillas [Sellick et al, 1982; Temchin et al, 1997]. Note that the results on chinchillas' AN were obtained with the bias-tone frequency of 50 Hz as done in this study [Temchin et al, 1997] while the studies on AN fibers from guinea pigs were done with a similar frequency of 40 Hz [Sellick et al, 1982].

Despite the agreement among various studies on the relationship between the major suppression phase and the phase of excitation, relating the major suppression phase to the phase of BM vibration resulted in conflicting reports on cats [Cai and Geisler, 1996a; Rhode and Cooper, 1993]. Studies on low-frequency bias-tone effects on cats' BM vibration to low-level CF-tone by Rhode and Cooper reported that the major suppression phase corresponded to the phase of peak displacement of BM toward ST as found in both BM and AN studies on guinea pigs and chinchillas [Sellick et al, 1982; Patuzzi and Sellick, 1984b; Geisler and Nuttall, 1997; Temchin et al, 1997]. However, the studies on the bias-tone effects on cats' AN responses in [Cai and Geisler, 1996a] reported that the major suppression phase corresponded to the phase of peak displacement of BM toward SV which is opposite phase to the finding from studies on cats BM vibration. In [Cai and Geisler, 1996a], the phase of BM vibration corresponding to the phase of period histogram of AN firing was estimated from the gross potential recorded from the electrode placed near the round window. According to their estimate of the phase of BM vibration, the phase of excitation by the 50 Hz bias-tone as well as the major suppression phase were opposite to the results on guinea pigs [Sellick et al, 1982]. Consequently, if the BM phase estimates used in [Cai and Geisler, 1996a] were erroneous such that the phase of excitation actually corresponded to the phase of peak velocity of BM toward SV as found in other species, the major suppression phase would indeed correspond to the phase of peak displacement of BM toward ST which would be consistent with the studies on BM vibration measurements by Rhode and Cooper and also with the AN and BM studies on guinea pigs and chinchillas.

C. Comparison of the Bias-tone Suppression Patterns on Low-level CF -tone VS Low-level Click Responses Indicates that OHC Mechano-electrical Transduction Function Is Similarly Involved in Generating Low-level CF-tone Response and Low-level Click Response of Cats AN Fibers

It has long been known that AN responses to low-level CF-tone are the tone response counterpart of low-level click responses [Kiang et al, 1965; Lin and Guinan, 2000]. Further, this relationship has been refined into the hypothesis that AN responses to low-level CF-tone and clicks are driven by a common mechanism whereby the OHC mechano-electric transduction is involved in similar ways [Guinan et al, 2005].

In order to test this hypothesis, the suppressive effects of 50 Hz bias-tone level series on AN responses to low-level CF-tone and clicks were analyzed to compare the shape of the OHC transduction function behind the two response types. Specifically, the major suppression phase and the degree of symmetry between the major and minor suppression phase at the suppression threshold were determined as shown in Fig. 2.21, Fig. 2.23 and Fig. 2.24.

Overall, comparison of the suppressive effects on low-level CF-tone VS low-level click responses in Fig. 2.21, Fig. 2.23 and Fig. 2.24 indicates that OHCs were involved in generating the low-level CF-tone and click responses with similar shape of mechano-electrical transduction function for AN fibers with CF up to ~10 kHz. The strongest evidence for this conclusion comes from Fig. 2.21 where the major suppression phase of the low-level CF-tone and click response were located mostly within the bound of one standard error from each other. As for the symmetry of the operating point of the OHC transduction function, most of the data points of the half-period symmetry index for CF < 10 kHz for both low-level CF-tone and click response were located below the value of 1/2 as shown in Fig. 2.24 indicating a significantly asymmetric location of the operating point of the OHC transduction function resembling the model of Fig. 2.1(b) rather than Fig. 2.1(a). As for any CF dependent trend in the symmetry of the operating point, the trend of increasingly symmetrical location of the operating point of OHC transduction function at higher CF was seen from the data for low-level CF-tone responses as shown in Fig. 2.23 and Fig. 2.24 while such a trend was less evident from the data for low-level click responses. Similar results have been reported in [Cai and Geisler, 1996a] for bias-tone suppression effects on low-level CF-tone responses from cats AN fibers where the OHC transduction function was found to change from the asymmetrical shape resembling Fig. 2.1(a) to the more symmetrical type in Fig. 2.1(b) at higher CFs particularly for AN fibers with CF > 2 kHz.

Note that the conclusion of similarity in the OHC transduction function behind response generation of the low-level CF-tone and click responses applies up to CFs of ~10 kHz. For AN fibers with CF > 10 kHz, the effects of 50 Hz bias-tone on low-level clicks remained below the suppression threshold for all four of the fibers from which data were collected. In contrast, for low-level-CF tone responses, the major suppression phase continued with a similar trend from the lower CF region for 12 of 16 fibers from which data were collected. This raises several questions: a) What were the details in the suppression data from the four fibers from which the bias-tone experiments on low-level click responses were carried out?; b) Do the detailed results indicate any limitations in the experimental methods for bias-tone effects on low-level click response study on these four fibers?; c) Are the details from these

four fibers compelling enough to conclude that the OHC transduction function worked differently in generating the low-level click response compared to low-level CF-tone responses for CFs > 10 kHz?

The detailed data from two of the four fibers with CF of 17.28 kHz and 20.4 kHz in Fig. 2.31 and Fig. 2.32 were discussed in the Results section. For those two fibers, the level series of the synchrony index and shape of the period histograms indicated that suppression was building up at a similar phase as the major suppression phase of CF-tone response but failed to reach the suppression threshold criteria within the maximum level of the bias-tone applied during the experiment.

The plot of the suppression threshold of low-level CF-tone and low-level click response over the CF in Fig. 4.22 shows that for up to ~10 kHz, the suppression threshold for low-level click response were ~10 dB higher than that of the low-level CF-tone response. For CF > 10 kHz, the suppression threshold on low-level CF-tone response rose sharply and reached the maximum limit of the bias-tone level, 120 dB SPL. Consequently, if the trend of ~10 dB higher suppression threshold on low-level click response compared to the low-level CF-tone responses continued for CF > 10 kHz, the projected values of suppression threshold on low-level click responses would reach or exceed the maximum limit of 120 dB SPL. Therefore, these data suggest that the sub-threshold result on the bias-tone effects on low-level click responses were likely due to limitation in the maximum level of the bias-tone in the experiment. Consequently, they do not suggest that OHC transduction mechanism worked differently in generating the low-level CF-tone VS low-level click responses for CF > 10 kHz. As for the higher level of suppression threshold on low-level click responses by ~10 dB over that of the CF-tone responses, they cannot be interpreted directly as indications for stronger involvement of OHC transduction function in generation of CF-tone responses over the click responses since suppression thresholds on AN responses by a low-frequency bias-tone have been found to depend on the relative intensity of the probe stimuli over the AN response thresholds [Patuzzi et al, 1984a; Cai and Geisler, 1996a]. In this study, only rough attempts were made in trying to match the relative intensity between the CF-tone and click stimuli over their respective threshold levels by applying each stimulus type at ~10-20 dB above the respective threshold.

Another experimental methodological factor behind the sub-threshold results on low-level click response for CF > 10 kHz could be with the parameters of the click stimulus. The pulse duration was 100 μsec with the approximate bandwidth of ~10 kHz beyond which the spectrum shows roll-off, ripples and zeros. Therefore, for fibers with CF > 10 kHz, the click stimulus would contain higher energy in the tail frequency region of the fiber's tuning curve compared to the CF region. Consequently, low-level click response evoked by such click stimuli from AN fibers with CF > 10 kHz might contain significant off-CF component as well as the CF component. This potential mix of CF and off-CF component in the low-level click response from AN fibers can lead to elevation of the suppression threshold by low-frequency bias-tone.

In conclusion, it can be seen from the results of this study that the suppression patterns on AN responses to low-level CF-tone and low-level click responses by a low-frequency bias-tone are similar despite the cochlear non-linearities in the AN response generation mechanisms. Therefore, the results from this study support the hypothesis that AN responses to both low-level CF-tone and clicks share a common drive mechanism to the IHCs based on the BM-based cochlear amplifier.

V. References

Cai Y, Geisler CD. (1996) Temporal patterns of the responses of auditory-nerve fibers to low-frequency tones. Hear Res. 1996 Jul;96(1-2):83-93.

Cai Y, Geisler CD (1996a) Suppression in auditory-nerve fibers of cats using low-side suppressors. I. Temporal aspects. Hear Res. 1996 Jul;96(1-2):94-112

Cai Y, Geisler CD (1996c) Suppression in auditory-nerve fibers of cats using low-side suppressors. III. Model results. Hear Res. 1996 Jul;96(1-2):126-40.

Cody AR, Russell IJ. (1987) The response of hair cells in the basal turn of the guinea-pig cochlea to tones. J Physiol. 1987 Feb;383:551-69.

Cooper NP. (1996) Two-tone suppression in cochlear mechanics. J Neurophysiol. 1997 Jul;78(1):261-70.

Dallos P. (1985), Membrane potential and response changes in mammalian cochlear hair cells during intracellular recording. J Neurosci. 1985 Jun;5(6):1609-15.

Geisler CD, Nuttall AL. (1997). Two-tone suppression of basilar membrane vibrations in the base of the guinea pig cochlea using "low-side" suppressors. J Acoust Soc Am. 1997 Jul;102(1):430-40.

Goldberg, J. M., and Brown, P. B. (1969). "Response of binaural neurons of dog superior olivary complex to dichotictonal stimuli: some physiological mechanisms Of sound localization, "J. Neurophysiol. 32, 613-636.

Guinan JJ Jr, Lin T, Cheng H. (2005) Medial-olivocochlear-efferent inhibition of the first peak of auditory-nerve responses: evidence for a new motion within the cochlea. J Acoust Soc Am. 2005 Oct;118(4):2421-33

Guinan J.J., Jr. (2009). Bias-tone effects on auditory-nerve responses reveal three mechanical drives, two dependent on outer-hair-cell motility and one passive. Asso. Res. Otolaryngol. Abstr 33, #1109.

Johnson DH. (1980) The relationship between spike rate and synchrony in responses of auditory-nerve fibers to single tones. J Acoust Soc Am. 1980 Oct;68(4):1115-22.

Kiang NYS, Watanabe T, Thomas EC, Clark LF (1965) Discharge Patterns of Single Fibers in the Cat's Auditory Nerve (MIT, Cambridge, MA)

Kiang NYS (1984) Peripheral Neural Processing of Auditory Information, Handbook of Physiology, The Nervous System III, Chapter 15

Kiang NY. (1990) Curious oddments of auditory-nerve studies. Hear Res. 1990 Nov;49(1-3):1-16.

Liberman MC, Kiang NY (1984) Single-neuron labeling and chronic cochlear pathology. IV. Stereocilia damage and alterations in rate- and phase-level functions. Hear Res. 1984 Oct;16(1):75-90

Lin T, Guinan JJ Jr. (2000) Auditory-nerve-fiber responses to high-level clicks: interference patterns indicate that excitation is due to the combination of multiple drives. J Acoust Soc Am. 2000 May;107(5 Pt 1):2615-30

Lin T, Guinan JJ Jr. (2004) Time-frequency analysis of auditory-nerve-fiber and basilar-membrane click responses reveal glide irregularities and non-characteristic-frequency skirts. J Acoust Soc Am. 2004 Jul;116(1):405-16.

Mardia KV (2000) Directional Statistics (Wiley, London)

Patuzzi R, Sellick PM, Johnstone BM (1984a) The modulation of the sensitivity of the mammalian cochlea by low-frequency tones. I. Primary afferent activity. Hear Res. 1984 Jan;13(1):1-8

Patuzzi R, Sellick PM, Johnstone BM (1984b) The modulation of the sensitivity of the mammalian cochlea by low-frequency tones. II. Inner hair cell receptor potentials. Hear Res. 1984 Jan;13(1):9-18

Patuzzi R, Sellick PM, Johnstone BM (1984c) The modulation of the sensitivity of the mammalian cochlea by low-frequency tones. III. Basilar membrane motion. Hear Res. 1984 Jan;13(1):19-27

Patuzzi RB, Yates GK, Johnstone BM. (1989) Outer hair cell receptor current and sensorineural hearing loss. Hear Res. 1989 Oct;42(1):47-72. Review.

Rhode WS, Cooper NP. (1993) Two-tone suppression and distortion production on the basilar membrane in the hook region of cat and guinea pig cochleae. Hear Res. 1993 Mar;66(1):31-45.

Robles L, Ruggero MA. Mechanics of the mammalian cochlea. Physiol Rev. 2001 Jul;81(3):1305-52. Review

Ruggero MA, Robles L, Rich NC (1992) Two-tone suppression in the basilar membrane of the cochlea: mechanical basis of auditory-nerve rate suppression. J Neurophysiol. 1992 Oct;68(4):1087-99

Russell IJ, Sellick PM. (1983) Low-frequency characteristics of intracellularly recorded receptor potentials in guinea-pig cochlear hair cells. J Physiol. 1983 May;338:179-206.

Russell IJ, Cody AR, Richardson GP (1986) The responses of inner and outer hair cells in the basal turn of the guinea-pig cochlea and in the mouse cochlea grown in vitro. Hear Res. 1986;22:199-216.

Sachs MB, Hubbard AE. (1981) Responses of auditory-nerve fibers to characteristic-frequency tones and low-frequency suppressors. Hear Res. 1981 Jul;4(3-4):309-24.

Santos-Sacchi J. (1993) Harmonics of outer hair cell motility. Biophys J. 1993 Nov;65(5):2217-27.

Schoonhoven R, Keijzer J, Versnel H, Prijs VF (1994) A dual filter model describing single-fiber responses to clicks in the normal and noise-damaged cochlea. J Acoust Soc Am. 1994 Apr;95(4):2104-21

Sellick PM, Patuzzi R, Johnstone (1982) BM Modulation of responses of spiral ganglion cells in the guinea pig cochlea by low-frequency sound. Hear Res. 1982 Jul;7(2):199-221

Stankovic KM, Guinan JJ Jr. (1999) Medial efferent effects on auditory-nerve responses to tail-frequency tones. I. Rate reduction. J Acoust Soc Am. 1999 Aug;106(2):857-69

Stankovic KM, Guinan JJ Jr. (2000) Medial efferent effects on auditory-nerve responses to tail-frequency tones II: alteration of phase. J Acoust Soc Am. 2000 Aug;108(2):664-78.

Temchin AN, Rich NC, Ruggero MA. (1997) Low-frequency suppression of auditory nerve responses to characteristic frequency tones. Hear Res. 1997 Nov;113(1-2):29-56.

Chapter 3 . Bias-tone Effects on AN Responses to Low-level and Mid-to-high-level Clicks

I. Introduction

Analysis of auditory nerve (AN) responses to clicks, (i.e., the acoustic realization of an impulse), can reveal the resonant properties of the mechanical drive behind the deflections of inner hair cell (IHC) stereocilia. Particularly, recent studies on AN responses to click level series have shown that the mechanical drive to the IHCs at mid-to-high-levels of clicks (60 – 100 dB SPL) are far more complex than at low-level clicks. The mechanical drive behind the AN responses to low-level clicks can be adequately explained through a single resonant response from the basilar membrane (BM) at the characteristic frequency (CF) of the AN fiber [Kiang et al, 1965]. In contrast, AN responses to mid-to-high-level clicks exhibit interactions of multiple resonances and potentially multiple drive mechanisms to the IHC stereocilia [Lin and Guinan, 2000; Lin and Guinan, 2004; Guinan et al, 2005; Guinan, 2009].

From the complex response characteristics of AN responses to mid-to-high-level clicks, it is of particular interest to investigate the role of outer hair cells (OHC). OHCs have been found to be directly responsible for the high sensitivity and sharp frequency tuning associated with the low-level click and low-level CF-tone responses [Liberman and Kiang, 1984; Schoonhoven et al, 1994]. Now it is widely accepted that the theory of the OHC-based "cochlear amplifier" provides adequate explanations to the mechanism behind the generation of the AN responses to low-level CF-tone and low-level clicks [Ruggero, 2001]. The critical part of the "cochlear amplifier" lies at the mechanical feedback between the BM and OHCs whereby the stereocilia of OHCs transduce the BM vibration to OHC transmembrane receptor voltage which returns as changes to the BM movement through the electromotility of the OHCs [Ruggero, 2001]. Up until recently, the prevailing view on the role of OHCs has been mainly on response generation of low-level click and CF-tone responses. However, OHCs have also been found to be involved in generating the initial peaks of AN responses to mid-to-high-levels of clicks [Guinan et al, 2005].

The role of OHCs in generating AN responses to mid-to-high-level clicks has been investigated by studying the effects of electrical stimulation of medial olivocochlear (MOC) efferent fibers on AN responses to click level series [Guinan, et al, 2005]. Through the efferent synapse on OHCs, electrical stimulation of MOC efferents has been found to inhibit electromotility of OHCs thereby inhibiting AN responses driven by electromotility of OHCs such as AN responses to low-level clicks [Guinan, 1996]. The studies have revealed that both the initial peaks of AN responses at mid-high click levels and the entire responses at low-levels of clicks are inhibited by stimulation of MOC efferents [Guinan, et al, 2005]. The inhibitory effects at mid-to-high-levels of clicks were particularly strong on the initial peaks of the AN response from fibers with the characteristic frequency (CF) below ~4 kHz while the later peaks following the inhibited initial peaks were largely unaffected [Guinan, et al, 2005]. These results hold particular significance since they show that the role of OHC electromotility in AN response generation is not limited to low-levels of clicks and tones as previously thought. Further, they show that the AN responses to mid-to-high-levels of clicks consist

of multiple distinct time segments which start with the initial peaks where the OHC electromotility is strongly involved and followed by the later peaks which are not as significantly affected by OHC electromotility.

Fig. 3.1 shows the compound post-stimulus histogram (cPST) of a cat's AN responses to click level series with alternating click polarity where the rarefaction click responses are plotted upward and the condensation click responses are plotted downward at each click level. The data came from a low-CF fiber, CT023_U051, with CF = 1.5 kHz and SR = 45 spikes / s. The click intensity ranged from 30 dB pSPL to 115 pSPL where click intensities are expressed as peak-equivalent SPL (pSPL) which corresponds to the SPL of a tone stimulus with the same peak pressure generated by clicks as measured near the tympanic membrane. The click response threshold of this fiber was ~40 dB pSPL, and the click responses at levels within ~20-30 dB from the threshold correspond to "low-level" click response region where OHC electromotility is strongly involved in response generation [Guinan et al, 2005]. At 80 dB pSPL, an initial peak termed as auditory nerve initial peak (ANIP) due to rarefaction clicks emerges ahead of the bulk of the responses that can also be seen at lower levels of clicks. The ANIP response has been found to be strongly inhibited by MOC efferent stimulation [Guinan et al, 2005]. Further, the second peak following ANIP, termed auditory nerve second peak (ANSP), which corresponds to the initial peak of condensation click response at the same level, has also been found to be inhibited by MOC efferent stimulation but by less than the ANIP inhibition. Within ~20-30 dB of click intensities above the threshold of ANIP, which is ~70 dB pSPL for this fiber, MOC efferent stimulation inhibited ANIP and ANSP with significantly stronger inhibitory effect on ANIP compared to ANSP while the later peaks following ANIP and ANSP were largely unaffected.

The MOC efferent studies on AN responses to clicks have shown that OHC electromotility is unexpectedly involved in response generation of ANIP and ANSP which are invoked by click levels well above the click response threshold. A question which naturally follows these findings is whether the detailed mechanism whereby OHC electromotility is coupled to AN firing of ANIP and ANSP might be somehow different from the mechanism at has been found to be the key mechanism. A part of the answer to this question comes from [Guinan and Cooper, 2008] which reported the effects of MOC efferent stimulation on BM responses from the basal region of guinea pig's cochlea to click level series. Unlike the AN responses to mid-to-high-levels of clicks from the apical region of cats, the initial peaks of the BM response to mid-to-high-levels of clicks were unaffected by MOC efferent stimulation. Based on these findings, it has been hypothesized that the response generation mechanism for ANIP and ANSP involves OHC electromotility as with the "cochlear amplifier"; however, the coupling mechanism to IHC stereocilia must be an unknown mechanism which is different from the BM based cochlear amplifier at low-level of clicks [Guinan et al, 2005; Guinan, 2009]. Specifically, in [Guinan et al, 2005; Guinan, 2009] squeezing and bulging of the subtectorial space driven by the electromotility of OHCs has been proposed as a potential explanation [Nowotny & Gummer, 2006]. In their studies, it has been found that contraction and elongation of OHCs brought on by their electromotility caused bulging and squeezing of the subtectorial space above the IHC stereocilia thereby resulting in fluid flow deflecting the stereocilia

of IHC with a sufficient magnitude to stimulate AN firing at frequencies up to 3 kHz [Nowotny & Gummer, 2006]. A schematized diagram of the Organ of Corti is shown in Fig. 3.3 for reference.

The objective of this study is to test the above hypothesis that the mechanism of OHC involvement in generating ANIP and ANSP responses from cat AN fibers with CF < 4 kHz at mid-to-high-levels of clicks is somehow different from the OHC mechanism behind AN response generation at low-levels of clicks. The experimental approach toward this objective is through comparison of suppressive effects by a low-frequency bias-tone on the three click response components, low-level clicks, ANIP and ANSP, from cat AN fibers.

A low-frequency tone such as 50 Hz with high enough amplitude but still under the neural threshold level has been known to suppress the firing pattern of AN invoked by a second higher frequency probe tone with a temporal pattern of suppression which is synchronized with the low-frequency bias-tone [Ruggero et al, 1992]. Typically the suppressive effects at low bias-tone levels start with a single suppression phase re. the bias-tone-period which deepens with increasing bias-tone level, and often progress to two suppression phases located at the opposite phases of the bias-tone-period [Patuzzi et al, 1984a].

The mechanism behind this typical suppression pattern has been found on the saturating non-linearity of the mechano-electric transduction function of OHCs which converts deflections of OHC stereocilia into transmembrane current [Robles and Ruggero, 2001]. In-vivo measurements of the OHC receptor potential in response to low-frequency acoustic tone stimuli from guinea pigs have shown that the mechano-electric transduction function can be generally described as a curve with saturating non-linearity at both ends of the output [Dallos, 1985; Russell et al, 1986]. Further, it has been found that the sharpness of saturation and the location of the transduction operating point on the curve depend on the CF location within the cochlea [Dallos, 1985; Russell et al, 1986]. A schematized version of the transduction function from the basal region of guinea pig cochlea as reported in Fig. 1 of [Russell et al, 1986] is shown in Fig 3.2(a) where the operating point is located approximately in the middle of the two saturation plateaus. Also, a schematized version of the transduction function from the apical region of guinea pig cochlea as reported in Fig. 10 of [Dallos, 1985] is shown in Fig 3.2(b) where the operating point is located closer to the hyperpolarizing saturation plateau.

The shape of the nonlinear transduction function of the OHCs is strikingly well reflected in the two tone interactions between a low-level probe tone and a second low-frequency bias-tone in the BM movement, hair cell receptor voltage as well as firing patterns from AN fibers [Ruggero et al, 1992; Patuzzi et al, 1984b; Cai and Geisler, 1996c]. A low-frequency bias-tone with high enough amplitude sinusoidally deflects the OHC stereocilia over a wide range such that the operating point of the mechano-electric transduction function traverses through the two saturating end regions during each cycle of the low-frequency bias-tone. Therefore, the gain of the OHC mechanoelectric transduction function and AN responses driven by it are suppressed as the operating point of the OHC transduction passes through the two saturating regions. Further, depending on the location of the operating point of the OHC transduction function at the particular place within the cochlea, one

of the suppression phases emerges at a lower level of the bias-tone with a larger depth of modulation [Cai and Geisler, 1996a; Cai and Geisler, 1996c].

Suppression effects on AN responses to a low-level CF-tone by a low-frequency bias-tone are illustrated through the AN firing pattern evoked by a low-level CF-tone at 1.6 kHz and a 50 Hz bias-tone recorded from a cat AN fiber with a CF of 1.63 kHz. Fig. 3.4 shows the bias-tone level series of bias-tone-period histograms which were constructed by binning the spike records relative to the period of the bias-tone. At the bias-tone level of 80 dB SPL, the firing rate in response to the low-level probe tone begins to be suppressed approximately in the middle of the period which is noted as the "major suppression phase". Then, at 90dB SPL the major suppression phase deepens to complete suppression, and a "minor suppression phase" develops at the opposite phase location. These suppression phases would correspond to the phase of the deflections of the OHC stereocilia into the two saturation plateaus brought on by the 50 Hz bias-tone.

Analysis of the period histograms of the suppression effects produced by a low-frequency bias-tone on AN response has served as an important investigative tool which revealed subtle differences in the OHC transduction function from the basal VS apical region of the cochlea [Cai and Geisler, 1996c]. Specifically, analysis of the suppression pattern on low-level CF-tone response recorded from basal AN fibers of cats has shown that the operating point of the OHC transduction function in response to the low-level CF-tone of the fiber is significantly more symmetric across the saturating ends than from apical fibers [Cai and Geisler, 1996c] as seen by the more symmetrical presence of the major and minor suppression phases at the basal region.

Further, previous studies have shown that the phase of suppression can be related to the phase of BM deflection thereby linking the phase of OHC stereocilia deflections brought on by the low-frequency bias-tone with the phase of BM displacement [Patuzzi et al, 1984a; Temchin et al, 1997; Geisler and Nuttall, 1997]. Specifically, by relating the phase of major suppression with the phase of cochlear microphonic and the phase of excitation by the bias-tone alone, it has been shown that the phase of major suppression on low-level CF-tone responses corresponds to the phase of maximum displacement of the BM toward the scala tympani (ST) in guinea pigs and chinchillas [Patuzzi et al, 1984a; Temchin et al, 1997; Geisler and Nuttall, 1997]. These aspects of the suppressive effects of a low-frequency bias-tone on AN firing are expected to provide insights on the following key questions of this study:

a. Are there significant differences in the low-frequency bias-tone induced suppression patterns on AN response to low-level clicks, ANIP and ANSP thereby indicating significant differences in the shape of the mechanoelectric transduction function expressed in the AN response generation mechanism behind the three click response components: low-level, ANIP and ANSP?

b. Are there any significant differences in the strength of involvement of the OHC mechanoelctric transduction function in the AN response generation mechanism behind the three click response components as indicated by the differences in the threshold of suppression on the click response components?

c. If there are differences from the question a and b, do they lie mainly in low-level click responses VS ANIP and ANSP in agreement with the predictions of the hypothesis that the mechanism of OHC involvement in generating ANIP and ANSP responses from cat AN fibers with CF < 4 kHz at mid-to-high-levels of clicks is somehow different from the OHC mechanism behind AN response generation at low-levels of clicks?

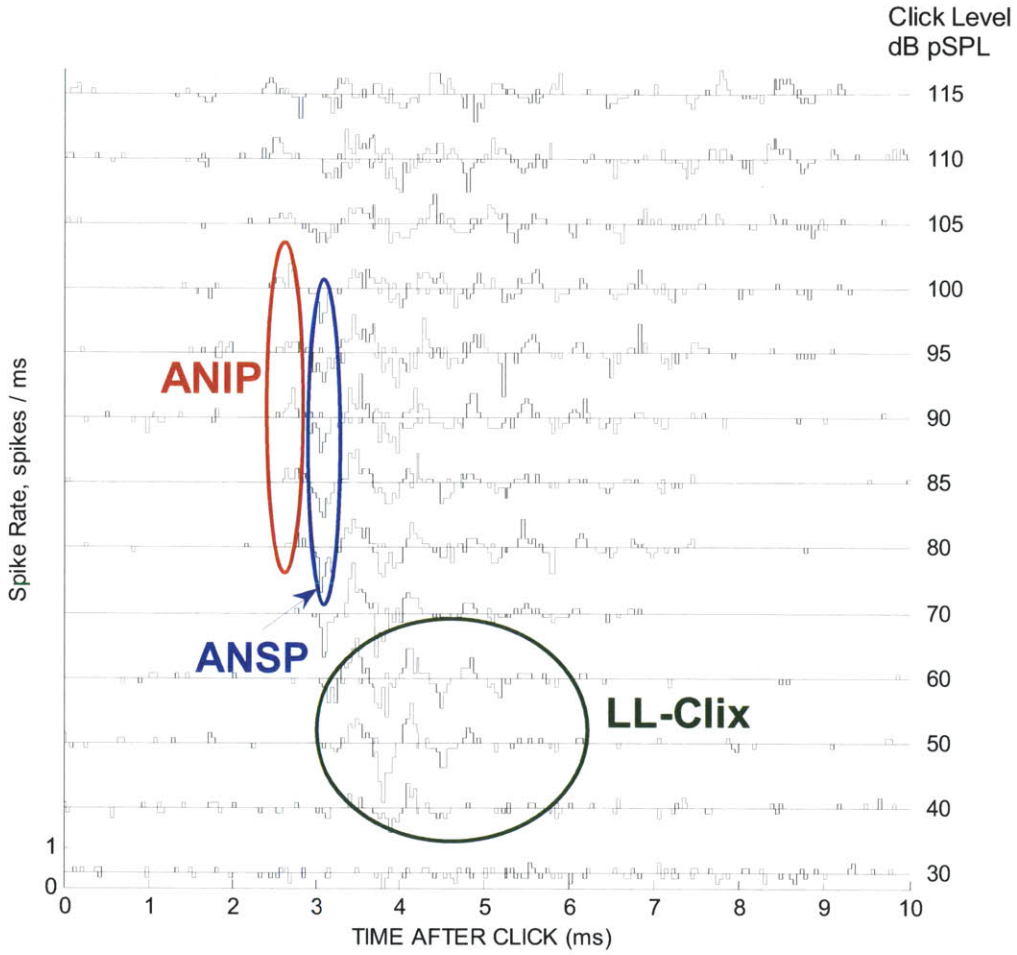

Fig. 3.1 Cat auditory nerve (AN) compound-PST (cPST) histogram showing responses to clicks at different sound levels. A cPST histogram plots responses to rarefaction clicks up and to condensation clicks down. ANIP = AN initial peak, ANSP = AN second peak, Rare = rarefaction click, Cond = condensation click. CF = 1.5 kHz. SR=45 sps

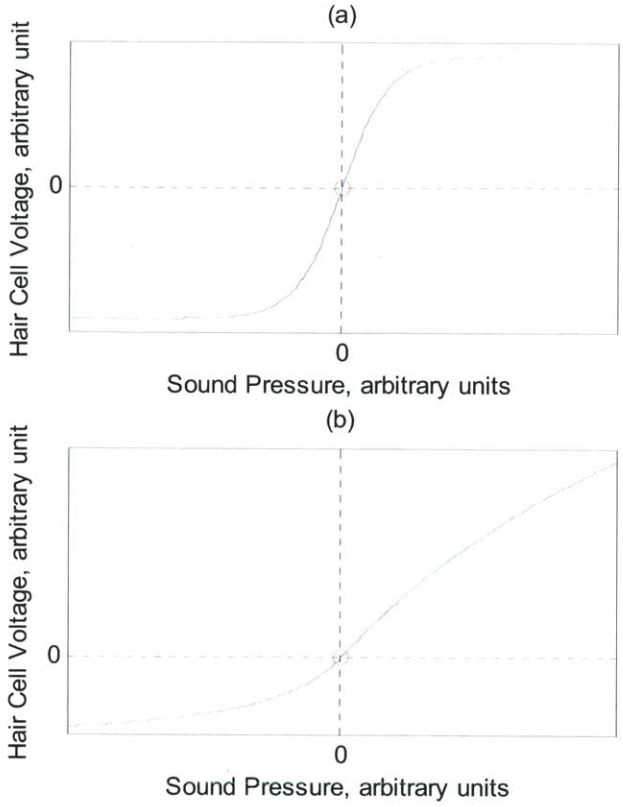

Fig. 3.2 Models of the mechano-electric transduction function of outer hair cells (OHC): the output shows saturating non-linearity at either ends of the input. The positive sound pressure indicates rarefaction. The gain of the cochlear amplifier has been linked to the slope of the transduction function at a particular operating point which is indicated by a red dot in the above plots. The operating point at rest has been found to lie at varying degree of asymmetry across the two saturating ends. (a) a schematized version of the OHC mechano-electric transduction function from the basal region of guinea pigs; (b) a schematized version of the OHC mechano-electric transduction function from the apical region of guinea pigs

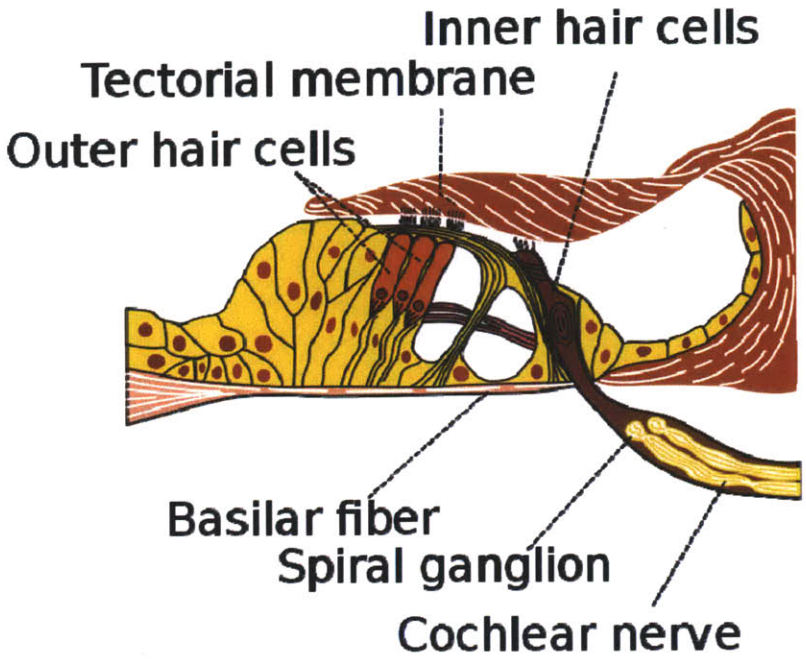

Fig. 3.3 Schematic diagram of the Organ of Corti, the sensory organ within the cochlea. The stereocilia of outer hair cells (OHCs) are embedded into the overlying tectorial membrane whereas the stereocilia of inner hair cells (IHCs) are free-standing within the endolymphatic fluid. Consequently, low-frequency transverse vibrations with frequency below ~100Hz on the Organ of Corti deflect the OHC stereocilia with significantly larger amplitude than the IHC stereocilia.

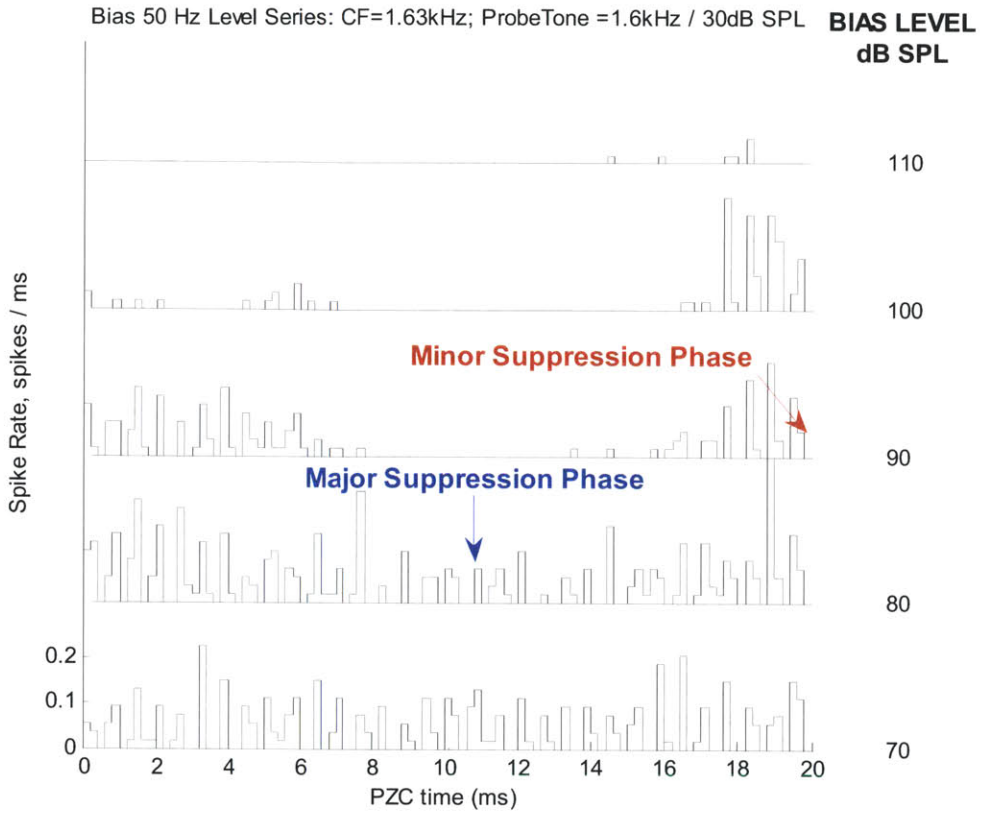

Fig. 3.4 Typical pattern of bias-tone suppression effects on low-level CF-tone responses over a bias-tone level series: bias-tone, 50Hz, level series, 70-110 dB SPL, was presented together with a low-level CF-tone stimulus. The CF of the fiber was 1.63 kHz. The probe tone was 1.6 kHz at 6 dB above threshold. The spikes were binned re. the bias-tone-period to form a bias-tone-period histogram. The bias-tone level series of the histograms are shown as vertically stacked plots with the corresponding bias-tone level indicated to the right of each histogram. The scale of the firing rate indicated for the bottom histogram applies to all the plots. Within the bias-tone-period histogram, the spikes are phase-locked to the probe tone frequency. At the bias-tone level of 80 dB SPL, the firing rate is suppressed in the middle of the period histogram, and at 90 dB SPL, the suppression depth in the middle of the period deepens significantly, and a second suppression phase develops at the opposite phase.

II. Methods

The experiments were done on cats at the Eaton-Peabody Laboratory (EPL) of Auditory Physiology. All experiments were conducted in compliance with protocols approved by the Committee on Animal Care at the Massachusetts Eye and Ear Infirmary.

A. Animal Preparations

23 healthy cats free from ear infections have been used for these experiments. The experimental methods for animal handling, surgical approach to the AN, and methods for recording from AN fibers of cats were as described in [Kiang et al, 1965; Stankovic & Guinan, 1999]. The methods for monitoring the health of hearing during experiments were as described in [Stankovic & Guinan, 1999].

All experiments were acute and began with anaesthetizing the cat with intra-peritoneal (IP) injection of Nembutal in Urethane with the dosage of 150 mg per kg body weight of the animal. Booster injection of the same initial mixture with 1/10 of the initial dose was delivered to maintain the level of the anesthesia. Throughout the duration of the experiment, the depth of anesthesia was monitored based on toe-pinch reflex, heart rate and breathing rate which determined the timing and amounts of the booster injections. The animal's temperature was monitored & maintained at 38 deg C with a rectal thermometer & a heating pad. Experiments typically lasted for 40 to 48 hours during which lactated ringers were dripped into a leg vein through a catheter.

After the initial anesthesia, the bulla cavities of both ears were exposed to reveal the round window. Posterior craniotomy followed by aspiration and retraction of the cerebellar tissues were performed to expose the auditory nerve.

B. Acoustic Setup

All experiments were done inside a double-walled, reduced-reflection chamber. Sound stimuli were delivered with an acoustic assembly consisting of two earphones and a microphone with a probe tube. A DT48 dynamic earphone, capable of high output at low-frequency, was used to generate the low-frequency bias-tone, and all other stimulus types including clicks were generated by the 1-inch condenser earphone [Bruel & Kjaer (B&K) 4145]. The magnitude and phase of the frequency response of the microphone plus probe tube combination were calibrated over the frequency band 0.02–45 kHz using a reference microphone in a calibration set up to measure the sound pressure near the tip of the probe tube. During the experiment, the assembly was placed inside the external meatus so that the probe-tube tip was a few millimeters away from the eardrum. Then, the magnitude and phase of the frequency response of the earphones were calibrated over the frequency band 0.02–40 kHz using the calibrated microphone plus probe tube.

Throughout all experiments, the frequency of the bias-tone was fixed at 50Hz which was selected because a low-frequency tone below 200-600 Hz can more selectively deflect the OHC stereocilia compared to the IHC stereocilia [Russell and Sellick, 1983].

C. Data Collection

A silver electrode was inserted through the bulla opening and placed near the round window to measure the cochlear compound action potentials (CAP). An automated tone-pip audiogram was measured over the frequency range from 0.5kHz to 32kHz at an octave interval with the criterion of 10

μV pp of the CAP. Tone pip audiograms were run periodically every hour or so, and also after a series of good data in order to ensure good health of the cochlea associated with the collected data.

A glass micropipette electrode filled with 3 M KCL electrolyte with 10 -20 MΩ impedance was driven through the exposed view of the auditory nerve by a remotely controlled microdrive until isolating an AN fiber using a wideband noise burst search stimulus. Spike timings were detected with the resolution of 10 μsec.

Upon isolating a unit, a threshold tuning curve (TC) was measured, the CF of the fiber was determined, and the spontaneous rate (SR) of the fiber was measured from the 20 sec duration recording of spontaneous firing. Then, responses to alternate-polarity click level series were recorded in order to determine the threshold level for low-level click response and ANIP. From fibers with CF < 4 kHz where cycle-by-cycle phase locking is evident from the click responses, the threshold level of ANIP was determined from the click-level series by identifying the initial half-cycle emerging ahead of the latency of low-level click response. Previous studies have shown that ANIP and ANSP are typically triggered by rarefaction and condensation clicks respectively at click levels of ~30 – 40 dB higher than the low-level click response threshold [Guinan et al, 2005]. Then, the following three types of 50Hz bias-tone paradigms were run:

- Bias-tone only paradigm
- Bias-tone effects on low-level click response: Rarefaction clicks at 10 – 20 dB above the threshold level were presented. Since the polarity of the click stimulus is not crucial for low-level click response studies, for most fibers only the rarefaction click stimulus was presented.
- Bias-tone effects on ANIP and ANSP: this procedure was limited to fibers with CF < 4 kHz where the threshold of ANIP could be determined. Clicks were presented at 10 – 20 dB above the threshold of ANIP.

Throughout the runs, the quality of spike triggering was monitored and adjusted. Only recordings with near perfect triggering with no extra or missed triggers were selected for this thesis. The methods for the above experimental paradigms are described in detail with actual data from the example fiber, CT023_U051, with its CF at 1.5 kHz & SR of 45.2 sps.

D. Bias-tone Only Paradigm: Excitation Threshold & Phase

Acoustic Stimulus and Data Collection

The objective of this paradigm was to measure the neural excitation threshold & phase of excitation of the fiber invoked by 50Hz bias-tone. A randomized level series of the 50Hz bias-tone over the range from 70 dB SPL to 120 dB SPL was presented. A single trial period was 500 ms with approximately 50% stimulus ON duty cycle. The spike records during the analysis time window of 200 ms duration from the stimulus ON period were binned re. the bias-tone-period in order to form a level series of the bias-tone-period histogram of the spike records. Averaged results from 8 of such trials were used to compute the level series of period histograms. The zero phase reference is the cosine phase of the earphone drive signal. Fig. 3.5 shows the 50Hz bias-tone level series of period histograms from the example fiber.

Data Analysis

The rate-level function was calculated from the level series of spike records, and the rate threshold was determined with the criterion of one standard deviation, σ, above the baseline rate. The baseline rate was determined as the spike rate at the minimum level of the bias-tone level series which was 60-70 dB SPL. The bias-tone level function of the spike rates including the baseline rate were calculated from the total spike collection time of 1600 ms averaged from 8 trials of 200 ms in each trial. Note that the baseline rate was not the spontaneous rate of the fiber. However, none of the recorded fibers showed a significant upward slope from their rate-level function at the baseline level. The standard deviation was estimated as the square root of the baseline rate under the assumption of Poisson random process behind the spikes.

Vector phase analysis was used to estimate the phase of excitation and synchrony index [Goldberg and Brown, 1969; Johnson, 1980]. Briefly, each spike is represented as a unit vector with its phase as the phase of occurrence of the spike within the period. The magnitude and phase of the average vector representation of all the spikes are the synchrony index and vector phase respectively. Mathematically the average vector corresponds to the first harmonic component of the Fourier series of the period histogram normalized by the total spike count [Goldberg and Brown, 1969].

Further, statistical significance of the phase estimates were evaluated through the standard error of the vector phase estimates. The mathematical model for standard error of the phase estimate, $S.E.\phi$, is described in [Mardia, 2000], and it had been previously applied in AN spike data analysis [Stankovic & Guinan, 2000].

The excitation threshold of the bias-alone alone response was met when both the rate threshold of the bias-tone alone response was met, and the standard error on the phase estimate dropped to be within 20° ($-20° \leq S.E.\phi \leq 20°$). This criterion allows statistically significant differentiation of the phase data points that are separated by at least 40°.

The bias-tone level series of the period histogram from the example fiber in response to 50 Hz bias-tone only are shown in Fig. 3.5 with the detailed data analysis in Fig. 3.6 where the bias-tone level function of the spike rate, synchrony index and estimate of the excitation phase are displayed in the top-down order.

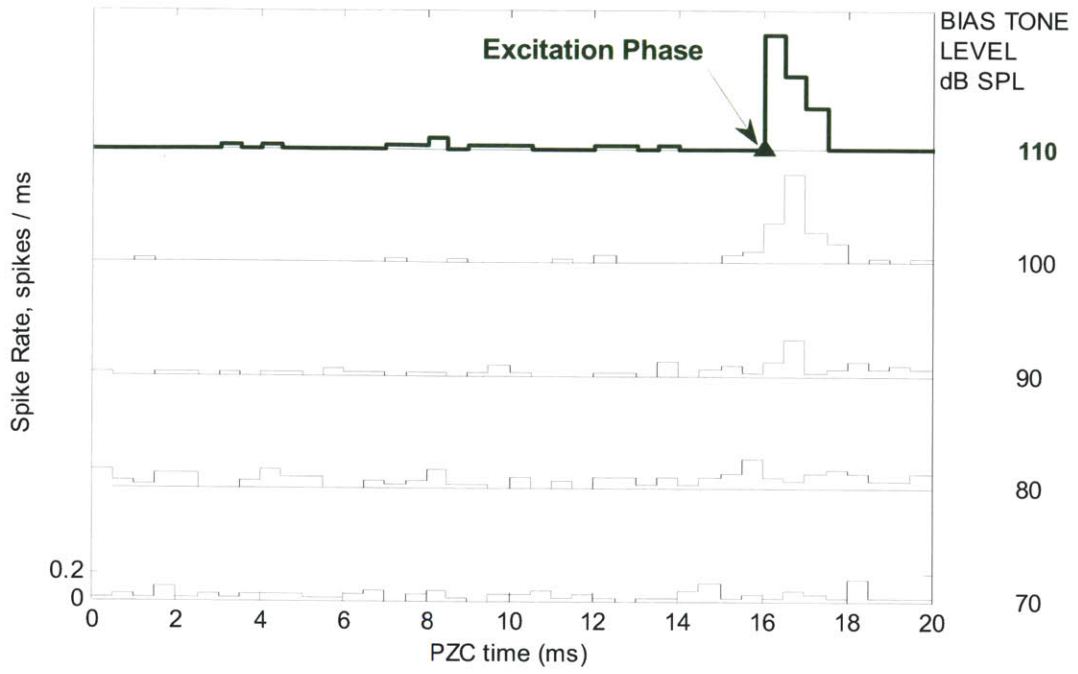

Fig. 3.5 Bias-tone level series of the 50 Hz bias-tone-period histogram of the example fiber, CT023_U051, CF=1.5 kHz & SR=45.2 sps. The excitation threshold level was determined as 110 dB SPL with the excitation phase noted on the period histogram.

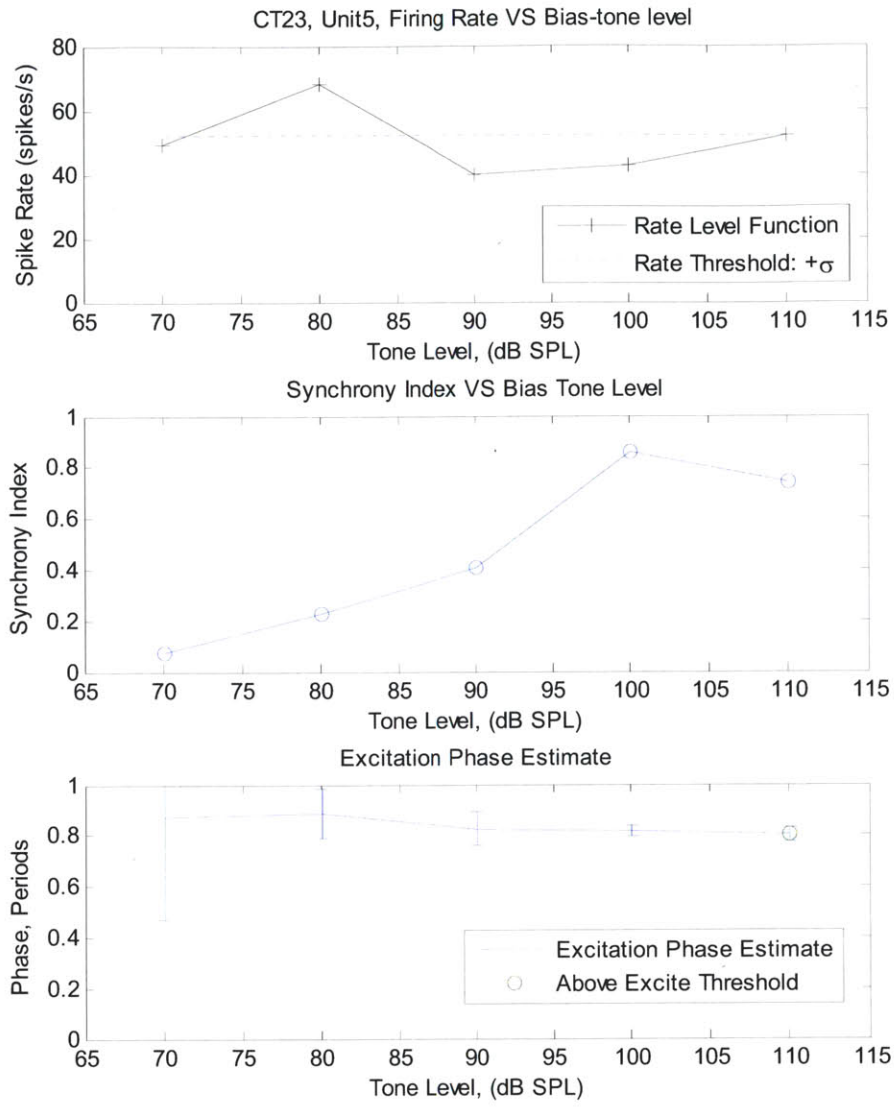

Fig. 3.6 Detailed data analysis metrics to determine bias-tone only response threshold & response phase. *Top*: Rate-level function from which the rate-threshold is determined when the spike rate exceeds one standard deviation above the average; *Middle*: Level function of the synchrony index; *Bottom*: the excitation phase estimates with their standard error. The excitation phase & its standard error were determined by the vector phase method. The excitation threshold is met when both the rate threshold is met and also when the standard error on the phase estimate drops within 20°. In this example, the excitation criteria were met at 110 dB SPL.

E. Experimental Paradigm for Bias-tone Effects on Clicks

The Click Stimulus

The click stimulus was generated by the 1-inch condenser earphone driven by 100 μsec duration rectangular pulses. Click intensities are expressed as peak-equivalent SPL (pSPL) which corresponds to the SPL of a tone stimulus with the same peak pressure generated by clicks as measured at the tympanic membrane. The click levels were calibrated to compensate for the square law non-linearity of the earphone.

Stimulus Paradigm and Data Collection

Click level series over the range of 30 dB pSPL to 115 dB pSPL were run in order to determine the response threshold of low-level click response and ANIP. Each trial with the duration of 20 ms consisted of a series of 10 ms alternate click polarity presentation, and the total of 100 such trials were averaged. The click level series from the example fiber, CT023_U051, is shown in Fig. 3.1 where the rarefaction click responses are plotted upward and the condensation click responses are plotted downward at each click intensity level. For this fiber, 60 dB pSPL of rarefaction click, which is approximately 20dB re. click threshold, was selected for the subsequent runs for bias-tone effects on low-level click responses. The response threshold of ANIP was ~80 dB pSPL; therefore, 90 dB pSPL of rarefaction and condensation clicks were used for bias-tone studies on ANIP and ANSP respectively.

The acoustic stimulus paradigm for the bias-tone effects on click responses

Clicks at a fixed level and polarity with the duration of 100 μsec were repeated at 18 ms intervals throughout the trial period of 2160 ms. The ON stimulus period for the 50Hz bias-tone extended from 90 ms to 1990 ms. This allows the analysis time duration for biased click responses to be from 90 ms to 1890 ms as shown in Fig. 3.7. The time window from 1998 ms to 2160 ms allows measurement of the firing rate invoked by clicks only. The phase slip between the click repetition interval of 18 ms and the bias-tone-period of 20 ms allows presentation of a click stimulus at 10 equally spaced phases over the click-bias period of 180 ms as also noted in Fig. 3.7.

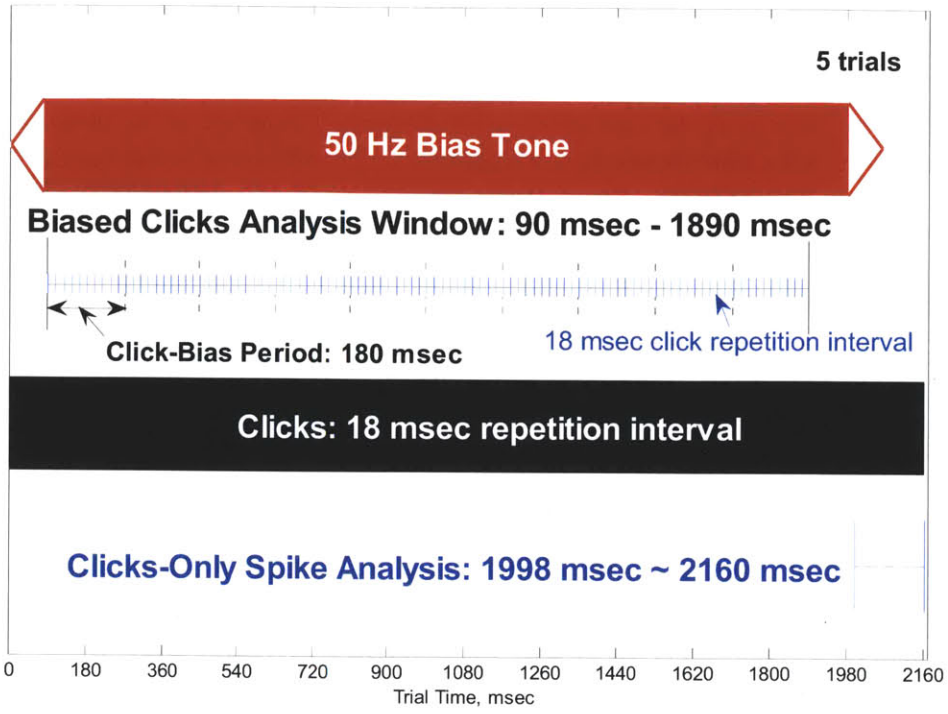

Fig. 3.7 The acoustic stimulus paradigm for the bias-tone effects on click responses. Clicks with the duration of 100 usec were repeated at 18 ms interval throughout the trial period of 2160 ms. The ON stimulus period for the 50 Hz bias-tone extended from 90 ms to 1990 ms with tapering windows of duration 80 ms surrounding the stimulus duration. This allows the analysis period for biased click responses to be from 90 ms to 1890 ms, and the analysis for clicks only response to be from 1998 ms to 2160 ms.

Spike records from the Biased Clicks Analysis Period with the duration of 1800 ms were binned re. 180 ms click-bias period. Five of such trials were averaged to produce the click-bias period histogram as shown in Fig. 3.8. The zero phase reference of the 50Hz bias-tone-period is indicated by red lines and the zero phase references for click repetition interval are noted by black dashed lines.

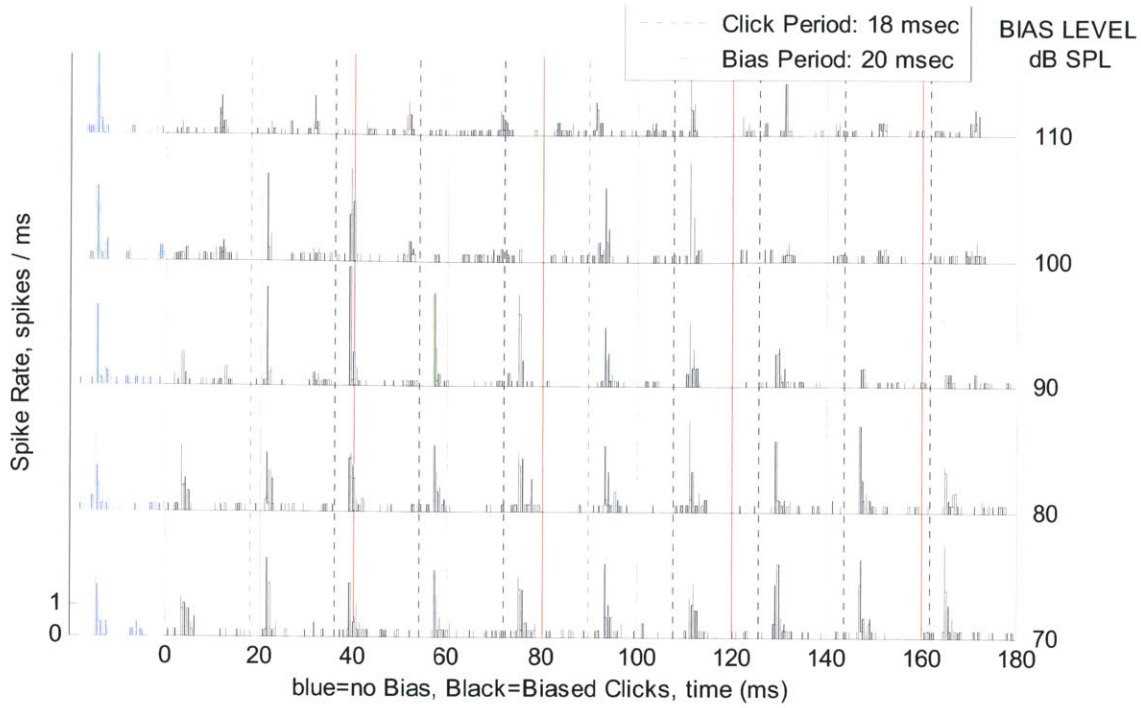

Fig. 3.8 Bias level series of click-bias period histograms: the phase slip between the click repetition, 18 ms, and bias-tone-period, 20 ms, allows click bursts at 10 phase locations within the bias-tone-period over the 180 ms of click-bias-tone-period. The data came from the example fiber. The zero phase reference of the bias-tone-period is indicated by red solid lines, and the zero phase references for click repetition interval are noted by black dashed lines. The time of click responses slips against the bias-tone-period reference. The averaged click responses from the clicks-only period are plotted far left in blue.

Time Windowed Bias-tone-period Histograms

We are interested in analyzing the bias-tone effects on individual peaks of the click response. The click response components of interest span over small time windows with durations of 1 - 1.5 ms. Therefore, period histograms over a particular time window component need to be constructed from the averaged firing rate over a particular post-click-time window from each of the 10 bias-tone phase samples of the click response. Consequently, the resulting period histogram would consist of 10 data points with the time bin width of one tenth of the bias-tone-period or 2 ms in this study.

Further, the phase delay associated with the time window needs to be accounted for in constructing the time-windowed period histogram and calculation of the suppression phase. For example, the first peak of the low-level click response of the example fiber spanned over the time window from 3.15 ms to 3.85 ms as noted as "Time Window B" in Fig. 3.9. The mid-point of the time window which is at 3.5 ms in this case is the delay to be compensated for. Since the delay of 3.5 ms corresponds to 1.75 of the time bin width of the bias-tone-period histogram, the period histograms are built with the delay of one time bin, and the fractional residue of 0.75 time bin or 0.075 period needs to be accounted for by adding it to the estimates of the phase of suppression of the period histogram.

The bias-tone level series of the time-windowed bias-tone-period histograms for the "Time Window B" from Fig. 3.9 which corresponds to the first peak of low-level click response of the example fiber is shown in Fig. 3.10. As in this example, the analysis window for low-level click response covered the first peak with the width of the window set to 1 – 1.5 ms for the data in this thesis. The blue dashed line in each of the stacked plots notes the average firing rate within the time window without the bias-tone, and the red plot shows the firing rate with the bias-tone presented the level noted on the right side of each plot. At 90 dB SPL of the bias-tone, the major suppression phase developed approximately in the middle of the period. At the next level of 100 dB SPL, the minor suppression phase also appeared at ~1/2 cycle away from the major suppression phase. Then, at 110 dB SPL the shape of the period histogram drastically shifted to resemble the bias-tone only excitation pattern at 110 dB SPL shown in Fig. 3.5. The major suppression phase at 100 and 110 dB SPL determined by the analysis method for suppression effects on period histograms are noted by a blue and red inverted triangle respectively. The details of the analysis method for suppression effects on period histograms are presented in the next section.

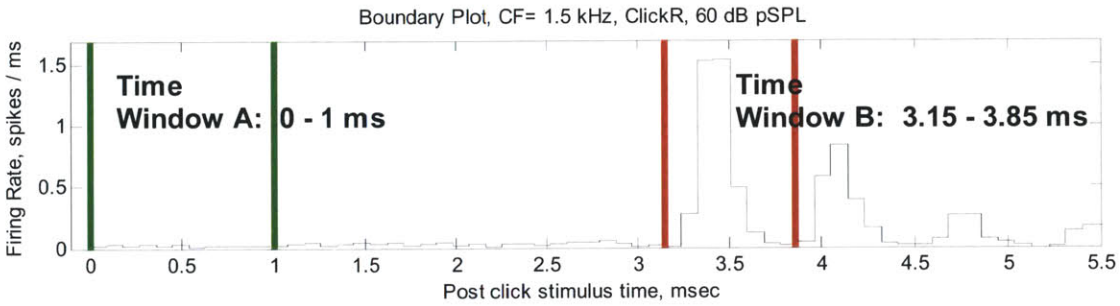

Fig. 3.9 Time windows for computing bias-tone effects on click responses: Time Window A) analysis time window prior to the click response latency, 0 – 1 ms: the bias-tone level series of the period histogram over this time window is expected show similar pattern as the period histogram generated the bias-tone only level series; Time Window B) analysis time window for low-level click response

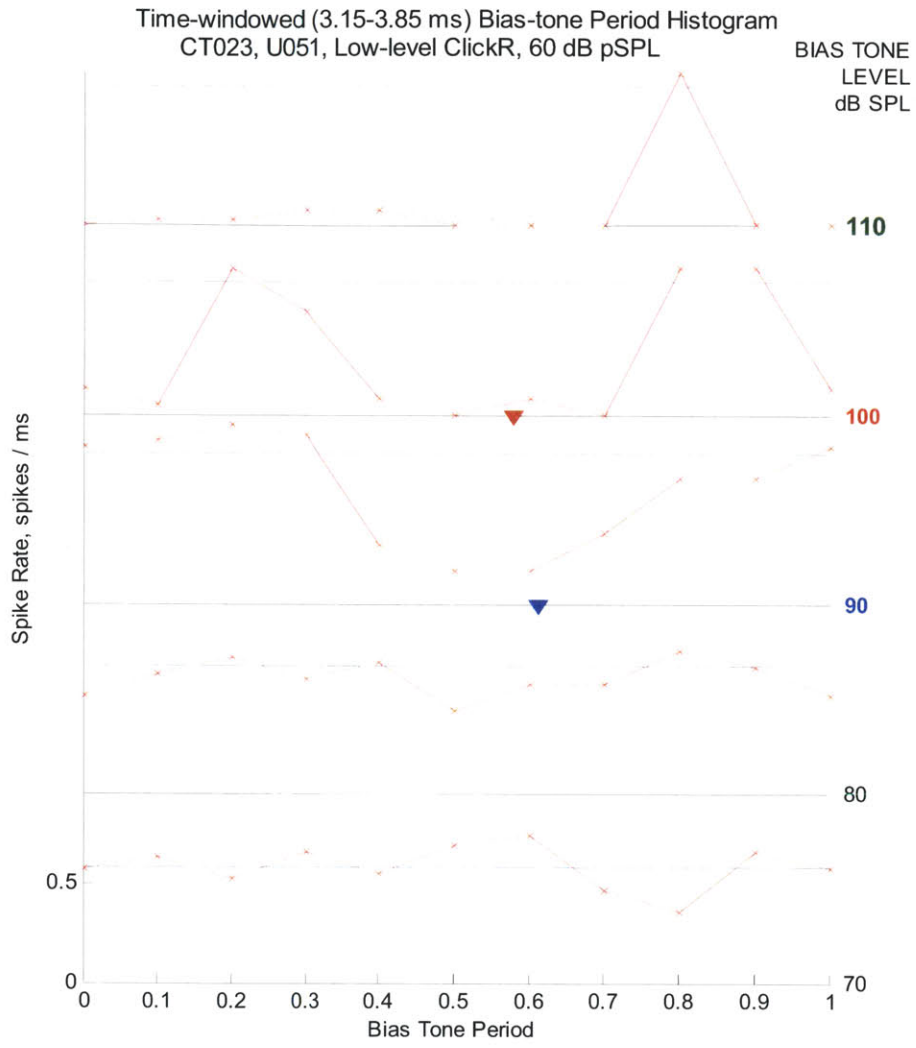

Fig. 3.10 Bias-tone level series of the time-windowed (3.15 – 3.85 ms) period histogram over the first peak of low-level click response of the example fiber: the click parameters were 60 dB pSPL, rarefaction. The blue dashed lines in each of the stacked plot represent the average firing rate over the time window without the bias-tone. Note that the major suppression phase emerged at 90 dB SPL of the bias-tone in the middle of the period which further developed to major and minor suppression phase separated by ~1/2 cycle at 100 dB SPL. The major suppression phase determined by the quantitative analysis method at 100 and 110 dB SPL are noted by a blue and a red inverted triangle. The details of the analysis method for suppression effects in period-histograms are presented in the next section. Also note the drastic shift in the shape of the period histogram at 110 dB SPL. Recall from Fig. 3.6 that the excitation threshold was reached at 110 dB SPL which indicates that the spike pattern at this level was due to excitation by the bias-tone.

Another example of time windowed bias-tone-period histogram is given with the "Time Window A" shown in Fig. 3.9 which ranges from 0 – 1 ms which precedes the click response latency; therefore, the bias-tone level series of the resulting histograms is expected to show similar pattern as the period histograms generated by a level series of 50 Hz bias-tone alone.

Fig. 3.11 compares the bias-tone-only firing pattern VS the bias-tone-period histogram from the pre-click-latency portion of the bias-tone on click runs which are shown in Fig. 3.11(a) and Fig. 3.11(b) respectively. As expected, the two sets of period histograms showed similar progressions of patterns over the bias-tone levels. Specifically, there were similar phases of excitation at 100 and 110 dB SPL of the bias-tone. Note that the rate-level functions started at different values but began to converge for bias-tone levels > 90 dB SPL. This can be attributed to the differences in the adaptation state of the fiber caused by the differences in the stimulus paradigms.

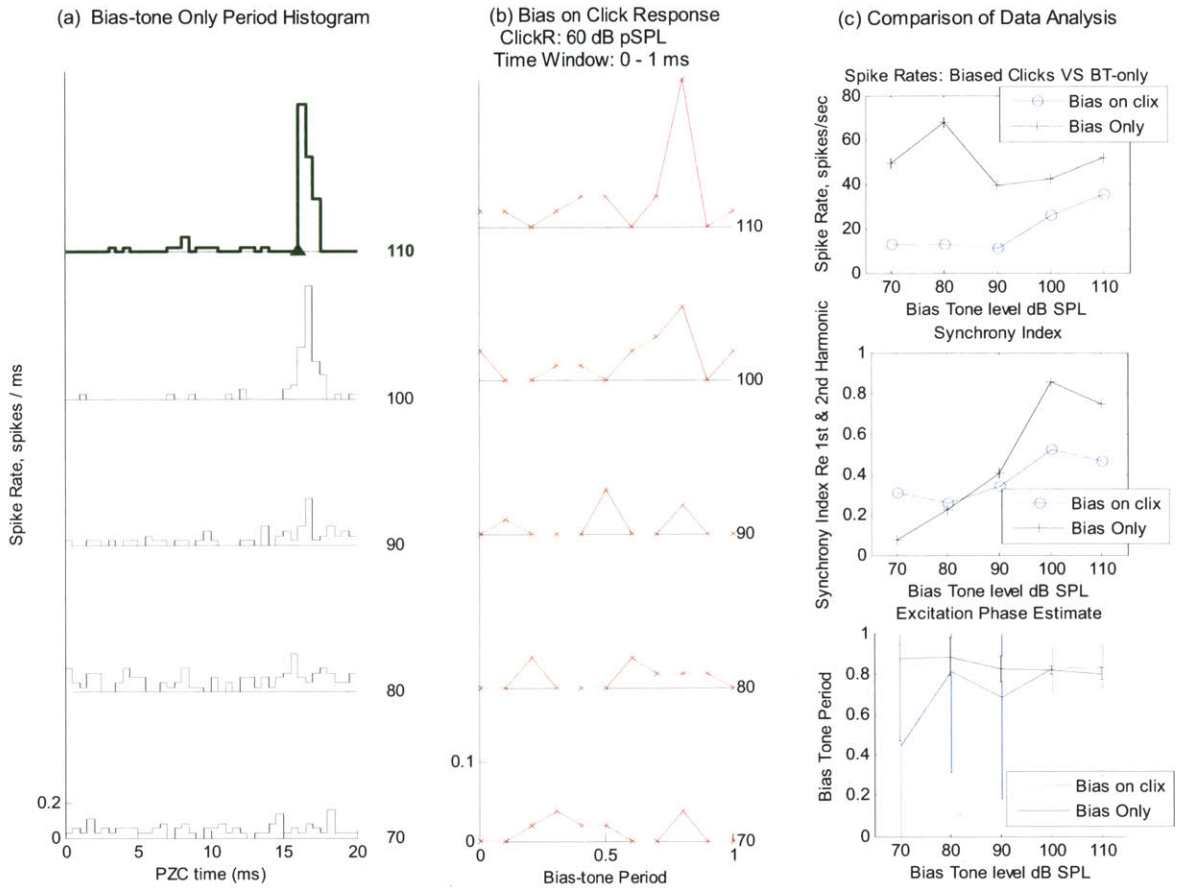

Fig. 3.11 Comparison of the BT-only firing pattern VS pre-click-latency portion of the bias-tone on click runs: (a) period histogram from the bias-tone only level series; (b) period histogram from the bias-tone on clicks over the time window of 0-1 ms prior to the click response latency; (c) Firing rate, synchrony index & estimate of excitation phase in the top-down order for Bias-on Clix VS Bias-tone only. The firing rate for the bias-tone only and bias on click runs started off at different levels due to differences in their adaptation states but started to converge for the bias-tone levels of 100 dB SPL & above. At 100 and 110 dB SPL, period histograms from both runs showed similar excitation patterns with very close values of the excitation phase estimates.

Analysis of Bias-tone-period Histograms for Suppression Effects

Previous studies have shown that that the suppression effects by a low-frequency bias-tone predominantly result in either a single major suppression phase or two suppression phases at opposite phase locations [Patuzzi et al, 1984a; Cai & Geisler, 1996a; Temchin et al, 1997].

Detecting a period histogram with a single major suppression phase was done through the vector phase analysis for the first harmonic component. Specifically, significant suppression was detected when the standard error on phase estimate, $S.E.\phi$, for the first harmonic dropped below 20° ($-20° \leq S.E.\phi \leq 20°$).

Period histograms with two peaks at opposite phase locations can also be analyzed with the same basic framework of directional statistical analysis by examining the synchrony index, vector phase and the standard error on the phase estimate with respect to the second harmonic component of the period histogram [Mardia, 2000]. As with the first harmonic, maximum criterion of 40° on the standard error on phase for the second harmonic component, $S.E.\phi_2$, was applied to detect a period histogram with two suppression phases at opposite phase locations; $-40° \leq S.E.\phi_2 \leq 40°$. Since the span of 40° of second harmonic phase is equivalent to 20° of the first harmonic phase, equivalent detection criteria were applied to both the first and second harmonic.

Since the second harmonic phase points to two suppression phases within the period histogram separated by half a cycle, it was necessary to disambiguate the major suppression phase between the two. The analysis procedure for this problem termed as "Half-period Synchrony Analysis" was based on the observation that the major suppression phase typically has a higher level of synchrony compared to the minor suppression phase. The analysis procedure first cuts the original period histogram into two half-period histograms of equal-length around the two suppression phase locations. The resultant two half-period histograms would have a single major suppression phase in each, and the depth of suppression in each were calculated as the synchrony index for the first harmonic of each half-period. Finally, the major suppression phase from the original full-period histogram was determined as the suppression phase with higher level of half-period synchrony index. This procedure is illustrated in Fig. 3.12 with the period histogram at the bias-tone level of 100 dB SPL from the example fiber. In Fig. 3.12(a) the two suppression phase locations determined by the second harmonic phase are marked with a blue & red inverted triangle. The resulting two half-period histograms are shown in Fig. 3.12(b). Note that the half-period histogram centered at the blue triangle starts with the wrapped around data from the time window from 18 ms to 20 ms. The synchrony index for the first harmonic of each of the half-period is shown in the half-period histograms. Due to the larger synchrony index value of the red half-period, the major suppression phase from the original full-period histogram at 100 dB SPL of the bias-tone was determined as the red triangle located in the middle of the period which was similar to the major suppression phase at 10 dB below from Fig. 3.10.

Finally, the period histograms generated by the bias-tone level at or above the bias-tone alone excitation threshold were classified as "Excitation" and accordingly excluded from the suppression data pool. For the period histograms from the example fiber in Fig. 3.10, the period histograms at 110 dB SPL noted in green was not included in the suppression data pool.

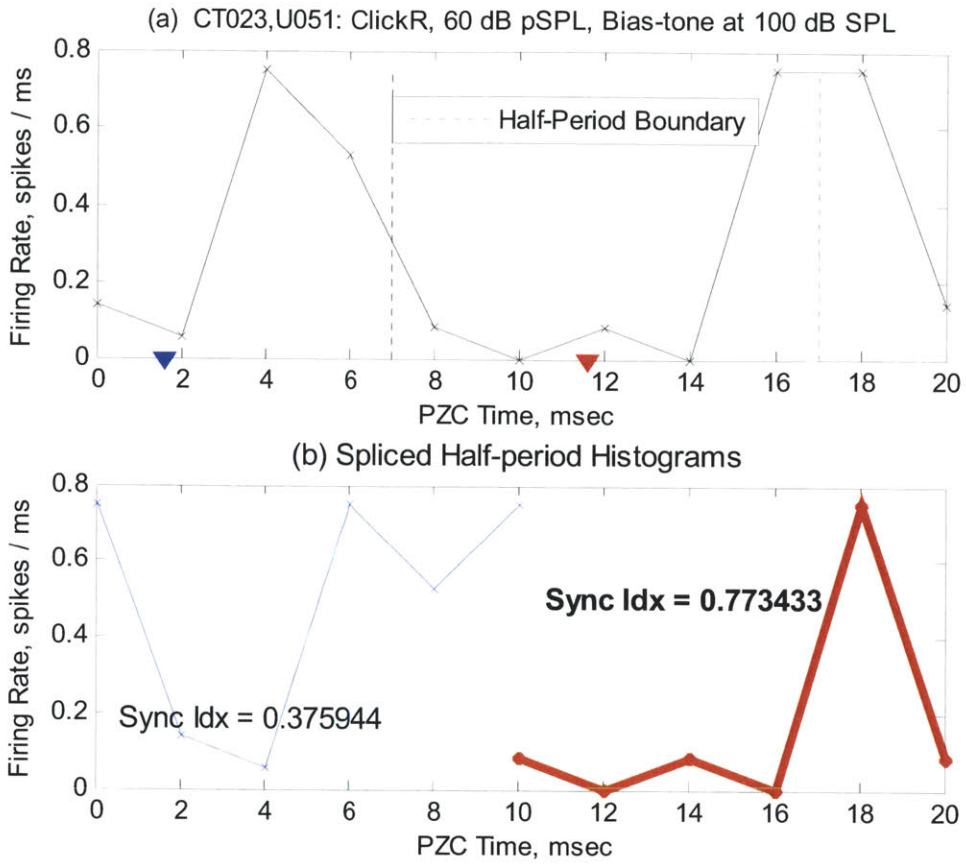

Fig. 3.12 Illustration of the "Half-period Analysis": method to determine the major suppression phase from a period histogram with a significant second harmonic component. The data came from the bias-tone-period histogram at 100 dB SPL from Fig. 3.10. (a) the two suppression phases based on the second harmonic phase are shown as blue & red inverted triangle. Half-period boundaries of equal width are formed around these two suppression phases in order to splice out the two half-period histograms; (b) the two half-period histograms & their first harmonic synchrony index are shown. The suppression phase noted in red has higher half-period synchrony index; therefore, it was determined as the major suppression phase.

The results of the analysis procedures described above on the period histograms in Fig. 3.10 are shown in Fig. 3.13 which includes the level functions of the spike rate, synchrony index and vector phase data for the first and second harmonic in the top-down order. Note that all three metrics started to show significant changes at the suppression threshold which was 90 dB SPL. Specifically, the firing rate started to decline, the synchrony index of the first harmonic started to rise, and the standard error on the suppression phase dropped sharply at 90 dB SPL.

The time-windowed period histogram analysis procedures have been applied on the ANIP and ANSP component of the click response generated by rarefaction and condensation click at 90 dB SPL respectively from the example fiber. Their time windows are shown in Fig. 3.14, and the analysis results are shown in Fig. 3.15 and Fig. 3.16 for ANIP and ANSP respectively. Note that the analysis time windows were determined visually to cover the first peak from the click response at the respective

polarity of click. Also, the width of the time window was limited to the maximum of 1 – 1.5 ms. Fig. 3.15 shows the suppression threshold on the ANIP response was reached at the bias-tone level of 100 dB SPL with the second harmonic criterion. Note that the major suppression phase was approximately opposite to that of low-level click response in Fig. 3.10. As for ANSP, Fig. 3.11 shows that the major suppression phase was found at a similar location as ANIP at the bias-tone level which was 10 dB higher than the case of ANIP. Note, however, that the suppression data on ANSP at the bias-tone level of 110 dB SPL were not included in the suppression data pool since the suppression threshold was not below the excitation threshold from the bias-tone alone run.

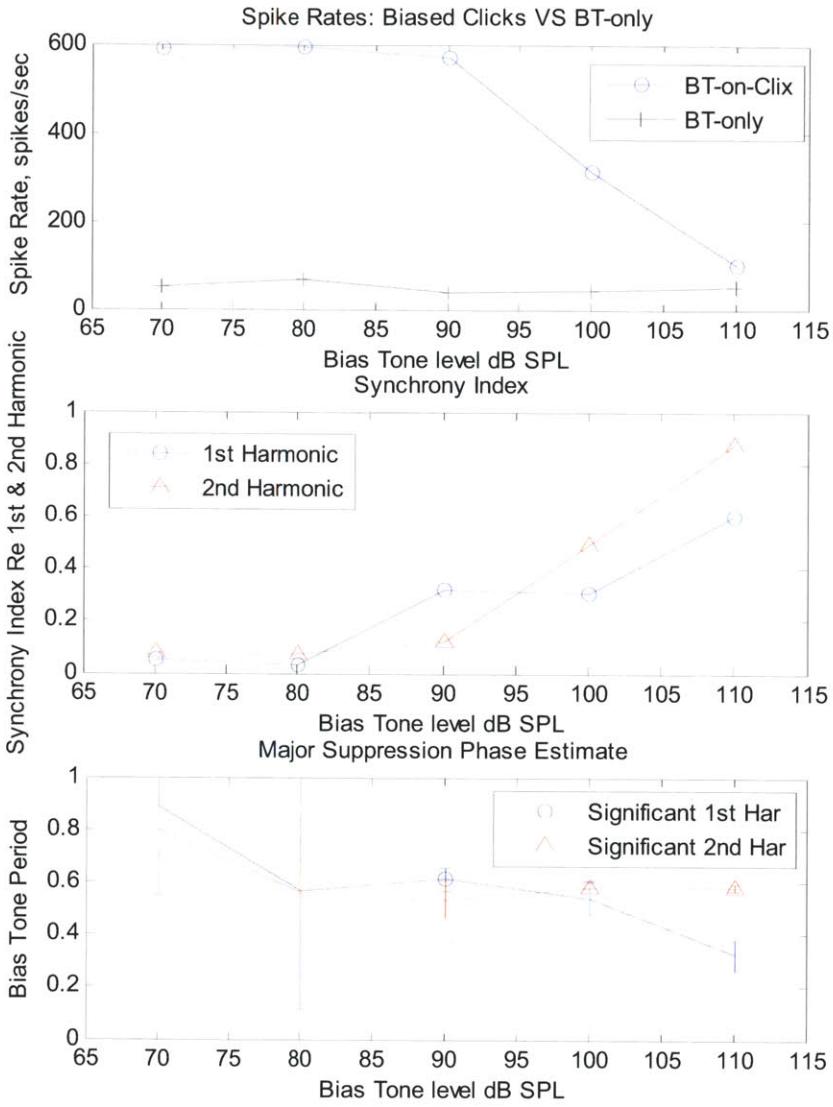

Fig. 3.13 Detailed data analysis on the bias-tone effects on the first peak of low-level click response from the example fiber: the period histograms are shown in Fig. 3.10. *Top:* the rate-level function from the bias on clicks and bias-tone alone runs. Note that the firing rate started to decrease at the suppression threshold of 90 dB SPL and closely approached the rate from the bias-tone only run at 110 dB SPL, which was the excitation threshold; *Middle*: bias-tone level function of the synchrony index for 1st & 2nd harmonic. Note the sharp increase of the synchrony indices at the suppression thresholds. *Bottom*: level function of the suppression phase estimates for 1st & 2nd harmonic with their standard error. The data points meeting the error bound are noted with symbols labeled as "Significant 1st Harmonic" and "Significant 2nd Harmonic". The 1st & 2nd harmonic suppression thresholds were met at 90 & 100 dB SPL respectively.

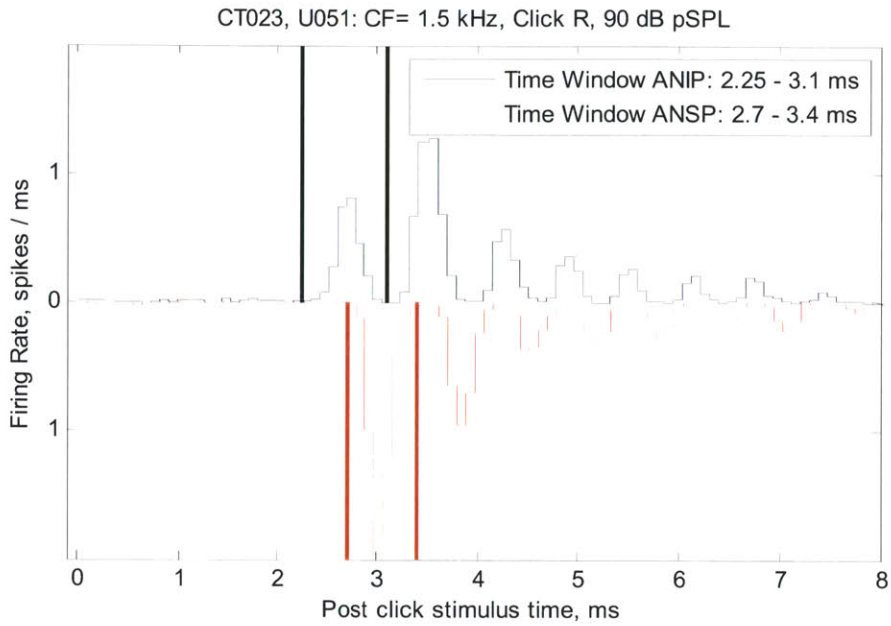

Fig. 3.14 Analysis Time Window for ANIP and ANSP at the click level of 90 dB SPL from the example fiber: ANIP and ANSP were generated by rarefaction and condensation click at 90 dB pSPL respectively.

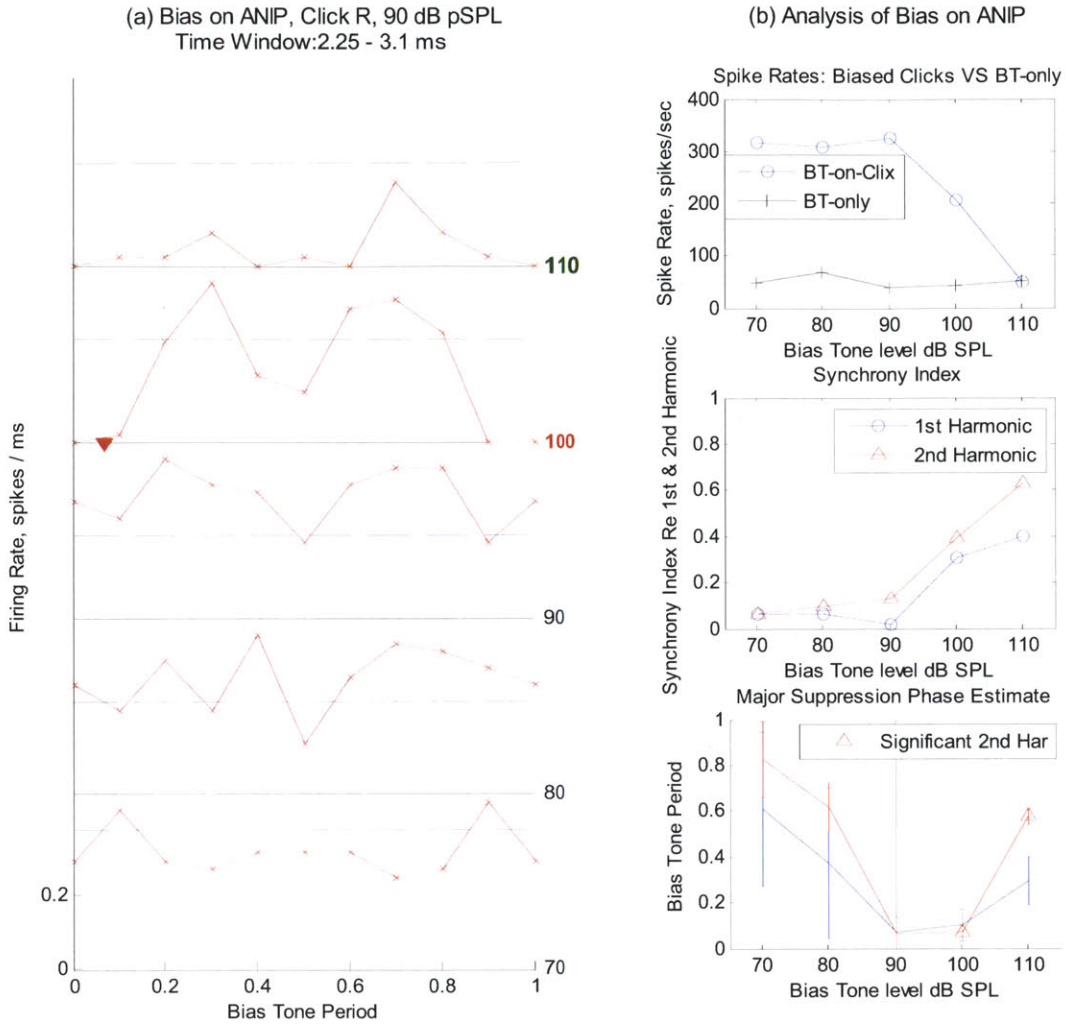

Fig. 3.15 Time Windowed Period Histogram and Suppression Data Analysis on ANIP: Stimulated by 90 dB pSPL rarefaction click. Time Window: 2.25 – 3.1 ms. The suppression threshold was met with the second harmonic criterion at 100 dB SPL of the bias-tone. Note that the phase of major suppression was approximately opposite to that of low-level click response shown in Fig. 3.10.

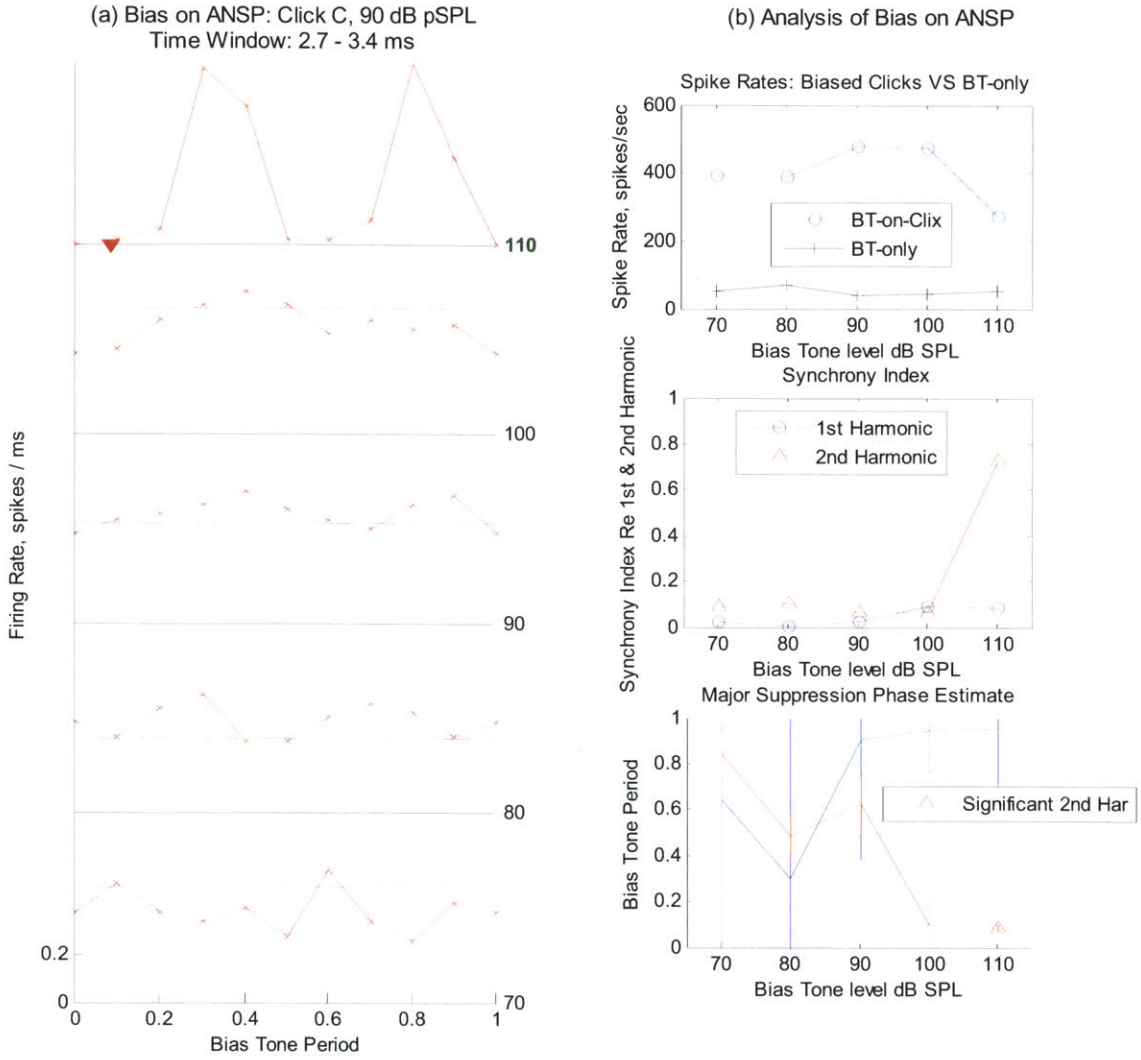

Fig. 3.16 Time Windowed Period Histogram and Suppression Data Analysis on ANSP: Stimulated by 90 dB pSPL condensation click. Time Window: 2.7 – 3.4 ms. The suppression threshold was met with the second harmonic criterion at 110 dB SPL of the bias-tone with the major suppression phase at a similar location as ANIP but opposite to that of low-level click response. Since the suppression threshold was reached at the same level of the bias-tone as the excitation threshold from the bias-tone only run, these data were not included in the suppression data pool as explained in detail in the main text.

III. Results

A. Phase of Excitation by 50 Hz Bias-tone Alone and Phase of Suppression on Low-level Click Responses

The phase of excitation of AN fibers in response to 50 Hz bias-tone throughout the entire range of CF is plotted in Fig. 3.17. Note that the zero phase reference of the plots was the cosine phase of the 50 Hz earphone drive signal. Also plotted in Fig. 3.17. is the phase of major suppression on low-level click responses at the suppression threshold level. As mentioned previously, the standard error on all phase estimates was within ±20°which is noted on the plot as the blue error bar.

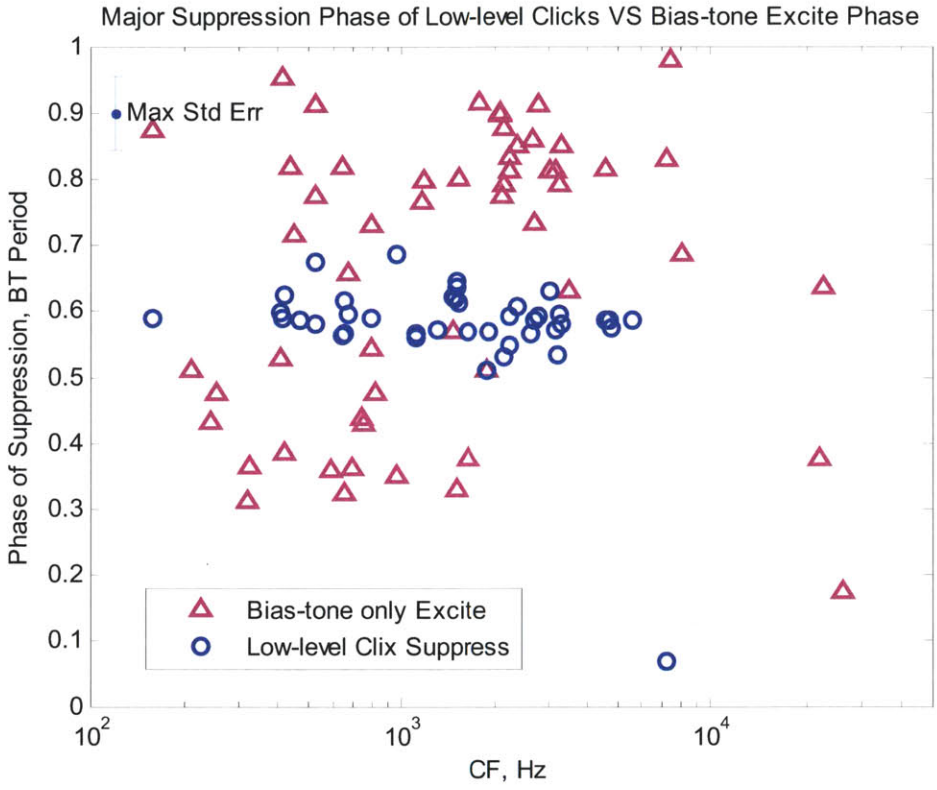

Fig. 3.17 Plot of the phase of excitation from the "bias-tone only" runs and the major suppression phase from the "bias-tone on low-level click" responses. Note that the excitation phases form two clusters separated by about ½ cycle, and the phase of suppression on low-level click response lies approximately in the middle separated by about ¼ cycle from the phase of excitation.

The two data groups formed distinctly separate clusters. The data for the major suppression phase on the low-level click responses were located tightly around the phase of 0.55 T within ± one standard error where T denotes a period of the bias-tone. In contrast, there was significantly wider spread in the phase of excitation in response to 50 Hz bias-tone. Further, the pattern of data scatter changed sharply across the CF boundary of about 2kHz as shown in Fig. 3.18 where the histogram of the fiber count across the excitation phase are plotted first for fibers with CF < 2 kHz in Fig. 3.18(a) and for the fibers with CF ≥ 2 kHz in Fig. 3.18(b). For fibers with CF > 2 kHz, the phase of excitation data formed

a single mode around 0.8 period whereas for CF < 2 kHz, the data were widely distributed with two main modes at 0.35 and 0.8 period which are approximately half a cycle apart. This bimodal distribution of the excitation phase for CF < 2 kHz can be explained by examining the details of the period histograms generated by 50 Hz bias-tone alone level series as shown in Fig. 3.19 where two peaks at about the opposite phases emerge from the period histogram at high levels of 50 Hz bias-tone. The typical pattern found throughout the animals showed a wider peak at about phase of 0.35 T as well as a sharper peak at the opposite phase. Depending on the relative size of the two peaks, the excitation phase was determined as either the earlier peak in Fig 3-19(a), the later peak as in Fig. 3.19(b) or the middle of the two peaks. As mentioned earlier in methods section, similar results have been reported in previous work on cats AN fibers below 2kHz as the "peak splitting" phenomenon [Cai & Geisler, 1996; Kiang & Moxon, 1972; Johnson, 1980; Kiang, 1984, 1990].

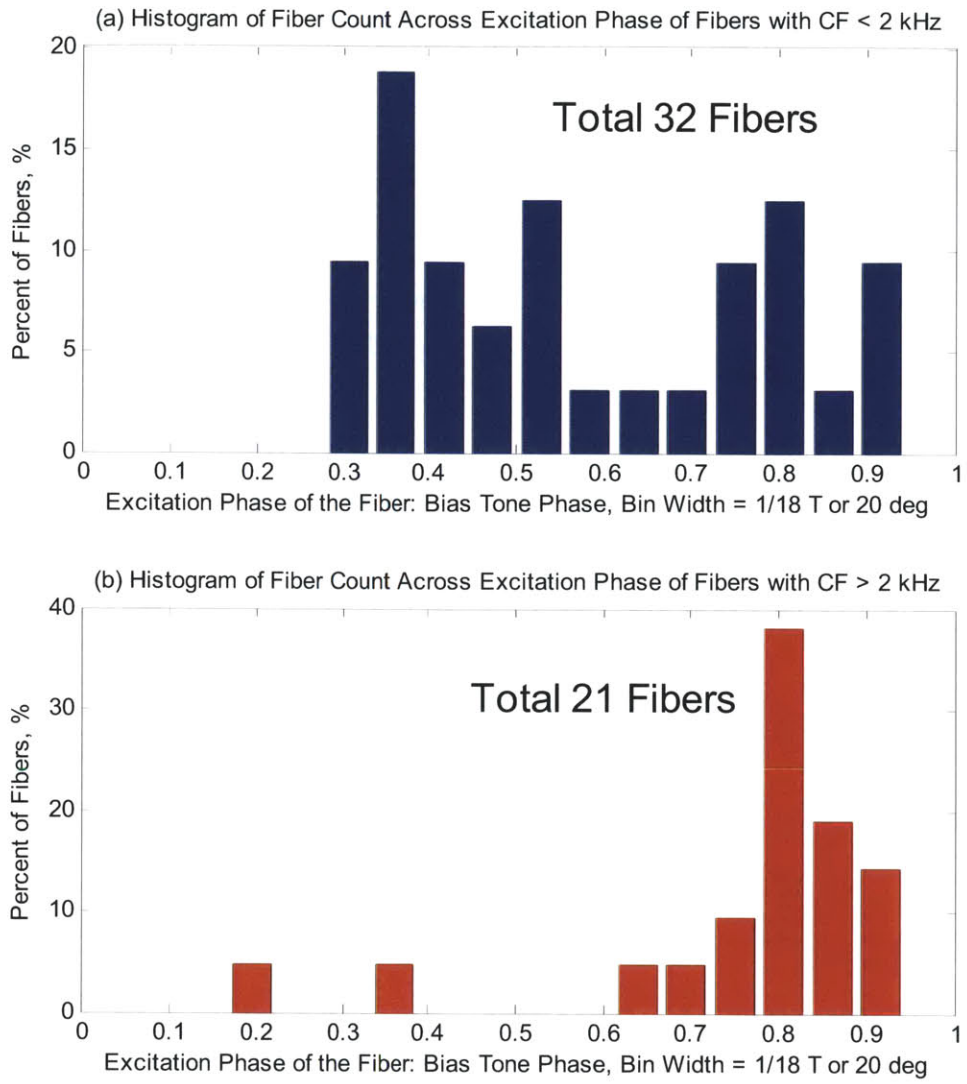

Fig. 3.18 Histogram of the AN fiber count across the phase of excitation of the AN fibers in response to 50 Hz bias-tone presented alone. As shown in Fig. 3.17, the distribution drastically changes across the CF of about 2 kHz. (a) The histogram for fibers with CF < 2 kHz shows three modes at ~0.35 T, 0.53 T & 0.8 T where T denotes a period of the bias-tone; (b) The histogram for fibers with CF >= 2kHz shows a single prominent mode at 0.8T.

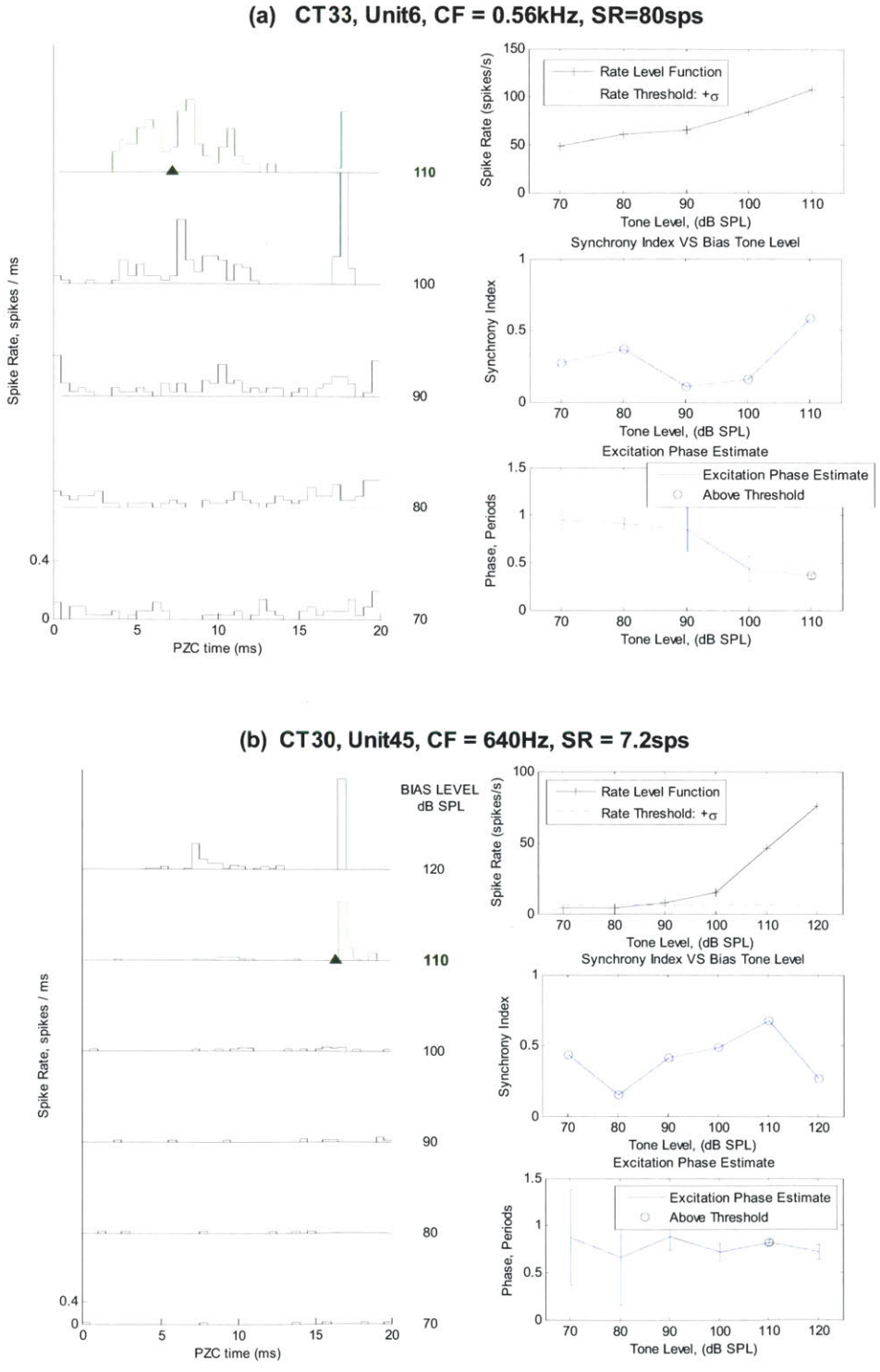

Fig. 3.19 Bias-tone alone excitation pattern for CF < 2 kHz displaying the peak splitting phenomenon. Two main excitation peaks emerge at about half a cycle apart. Depending on the relative size of the two modes, the first harmonic based vector phase estimate can select either the wider peak as in (a) or the narrower peak as in (b).

B. Suppression Effects by 50 Hz Bias-tone on Click Response Components: Low-level Click response, ANIP and ANSP

Overall, the effects of 50 Hz bias-tone level series on low-level clicks, ANIP and ANSP from most of the fibers with CF < 3 kHz in this study were qualitatively similar to the pattern exhibited by the example fiber in the method section, CT023_U051, CF=1.5 kHz & SR=45.2 sps.

Major Suppression Phase

The major suppression phase on ANIP and ANSP were quite similar to each other but opposite to that of low-level click responses as shown in Fig. 3.20. Specifically, the major suppression phase of ANIP and ANSP were located within one standard error of ±20 deg but at opposite phase from that of low-level click responses. Therefore, the difference in the major suppression phase of ANIP and ANSP VS low-level click responses is undoubtedly significant.

Note that data collection trials on ANIP and ANSP were limited to fibers with CF < 4 kHz where the phase-locked initial peak response could be identified. For low-level click responses, all fibers were included in the study. The fiber with the highest CF with supra-threshold suppression effects on ANIP or ANSP was CT026, U039, with the CF=2.585 kHz and SR=70 sps.

Bias-tone Level at the Threshold of Suppression

Fig. 3.21 compares the 50 Hz bias-tone level at the threshold of suppression on the low-level click responses, ANIP and ANSP. Fig. 3.21(a) shows the distributions of the fiber count over the suppression threshold. The mode of the distribution for low-level click responses was ~5 dB lower than that of ANIP. Further, the mode of the ANIP suppression threshold was ~5 dB lower than of ANSP. Fig. 3.21(b) displays the suppression thresholds over the CF of the fiber. Note that the difference in the threshold of suppression of ANIP and ANSP in comparison to low-level click responses was more notable for CF > 1 kHz, and the suppression threshold for ANIP and ANSP for fibers with CF > 2 kHz was approaching the maximum level of the bias-tone available. In the next section, the details of the suppression effects on the ANIP and ANSP responses from fibers with the CFs of 2.82 kHz and 3.23 kHz are analyzed to examine how the suppression effects on ANIP and ANSP were affected with increase of CF.

Degree of Symmetry between the Major and Minor Suppression Phase

Fig. 3.22 plots the ratio of 2^{nd} harmonic VS 1^{st} harmonic synchrony index at the threshold of suppression by the 50 Hz bias-tone for the CF-tone responses and low-level click responses. A higher value of this ratio indicates stronger presence of the minor suppression phase at the threshold level of suppression thereby indicating more symmetrical location of the operating point of OHC mechano-electrical transduction function across the two saturation plateaus. The data for ANIP and ANSP were ~5 - 10 dB higher than the low-level click responses

The degree of symmetry of the location of the operating point within the OHC mechano-electrical transduction function was examined by another metric, "Half-period Symmetry Index", which tries to quantify the ratio of modulation depth around the minor VS major suppression phase at the threshold of suppression. The range of this ratio is from 0 to 1, and as it approaches 1, it indicates more symmetrical depth of modulation between the two suppression phases thereby more symmetric

location of the operating point of the OHC transduction function. For this purpose, the "Half-period Synchrony Analysis" method described in the methods section which was used to disambiguate the major suppression phase from period histograms with two oppositely located suppression phases was adapted. Specifically, for period histograms which meet the suppression threshold criteria of the second harmonic, the ratio of the minor VS major suppression phase was calculated as a part of the analysis procedure to determine the major suppression phase. For period histograms which met the suppression threshold criteria for the first harmonic, the "Half-period Synchrony Analysis" procedure was carried out with the suppression phase based on the first harmonic phase estimate. The "half-period symmetry index" at suppression threshold for low-level click responses, ANIP and ANSP are plotted over the CF of the fiber in Fig. 3.23. Note that the dashed line at the index value of 0.5 indicates the ratio of 1 / 2 in the half-period synchrony index. Note that most of the data points for low-level click responses were located below the reference level of 0.5 whereas for ANIP and ANSP approximately half of their data points were located above 1/2 thereby indicating stronger presence of the minor suppression phase at the suppression threshold for ANIP and ANSP in comparison to low-level click responses. Note that similar trends were seen from the plots of the ratio of second VS first harmonic synchrony index in Fig. 3.22.

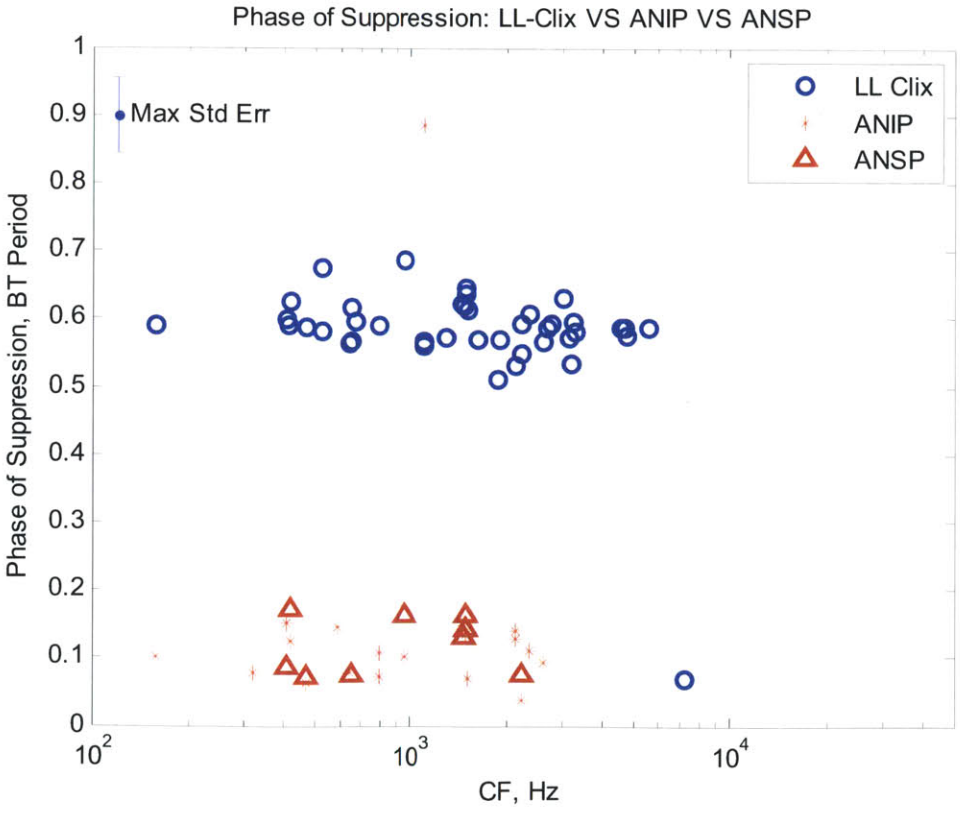

Fig. 3.20 Major suppression phase of the click response components, Low-level, ANIP and ANSP: major suppression phase for ANIP and ANSP were located closely together within the bounds of one standard error

over the CFs. The major suppression phase of low-level clicks was located ~1/2 cycle away from the data group for ANIP and ANSP.

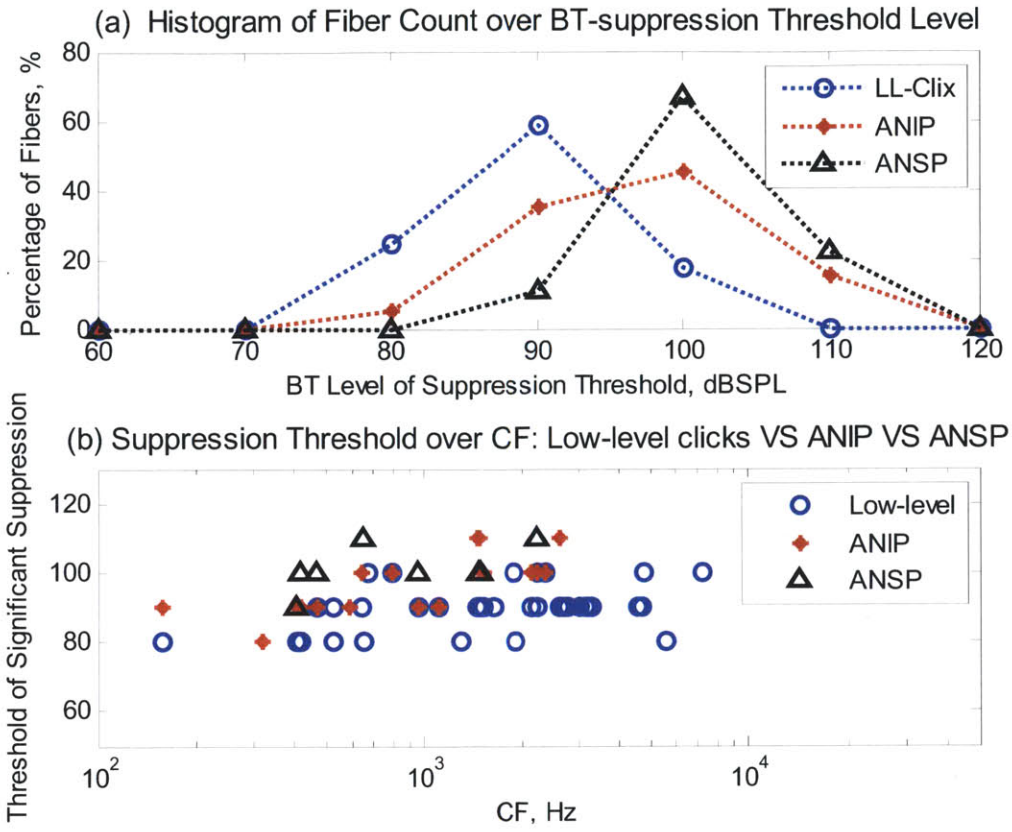

Fig. 3.21 The threshold of suppression of the click response components, low-level, ANIP and ANSP: (a) Histogram of the fiber count over the suppression threshold; (b) the plot of the suppression thresholds over CF. The fiber counts for low-level, ANIP and ANSP were 41, 20 and 9 respectively. Both data showed that the suppression threshold on low-level clicks was ~5-10 dB lower than that of ANIP or ANSP. Between ANIP and ANSP, suppression threshold on ANIP was ~5 dB lower than that of ANSP.

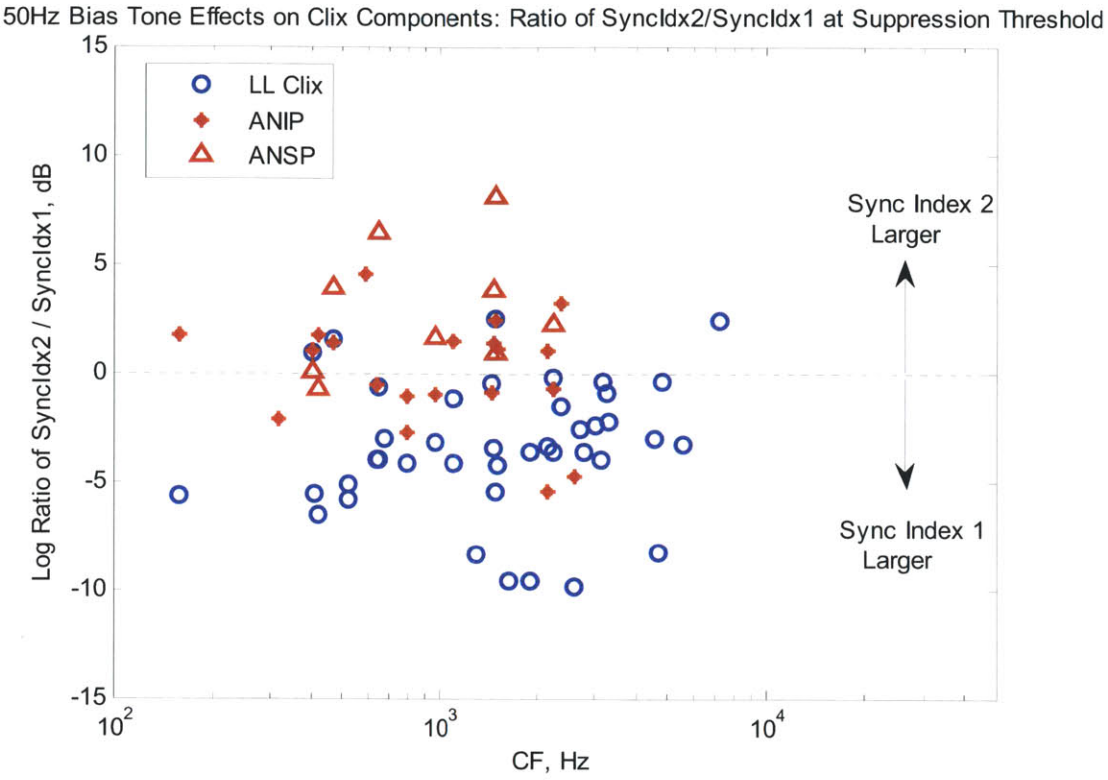

Fig. 3.22 Plot of the ratio of 2nd over 1st harmonic synchrony index at the suppression threshold for the click response components, low-level, ANIP and ANSP: Lower value of the ratio indicates more asymmetry in the suppression pattern between the two suppression dips; therefore, lower value of this ratio indicates more asymmetrical location of the operating point on the OHC mechano-electric transduction function. The data for ANIP and ANSP were 5~10 dB higher than the low-level click responses.

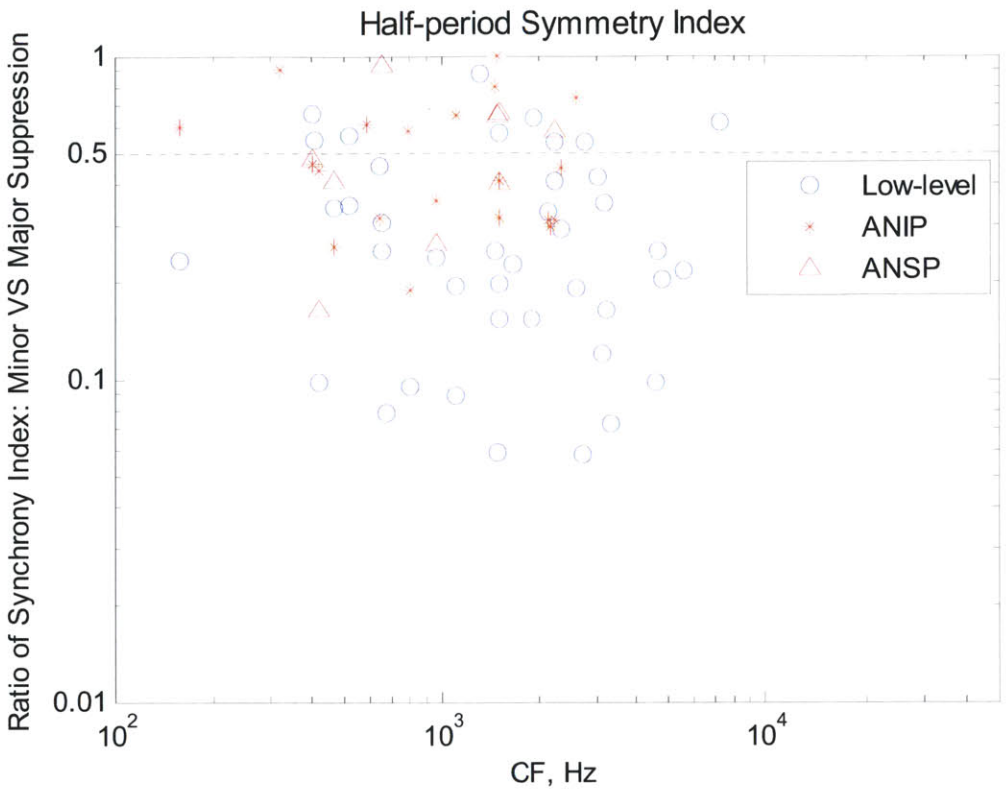

Fig. 3.23 Half-period Symmetry Index: is the ratio of the first harmonic synchrony index from the two "Half-period histograms" which tries to quantify the degree of symmetry in the modulation depth between the major and minor suppression phases. Specifically, the "Half-Period Analysis Method" shown in Fig. 3.12 has been adapted for this purpose. The range of this ratio is from 0 to 1 where 1 indicates perfectly matched modulation depth between the major and minor suppression phase. Refer to the main text for details. Note the reference value of 0.5 which indicates the 1 to 2 ratio of modulation index between the two suppression phases. Note that the percentage of data points above the reference value of 0.5 for ANIP and ANSP exceeded that of low-level clicks thereby indicating relatively more symmetrical shape of the operating point of OHC transduction function for ANIP and ANSP.

C. Example Results of the 50Hz Bias-tone Suppression Effects on Click Response Components: Low-level, ANIP and ANSP

In order to aid the reader to appreciate how well the data from individual fibers fit with the data shown in the previous plots, this section documents the typical suppression patterns of low-level click responses, ANIP and ANSP from individual fibers. Examples are presented from 6 normal AN fibers taken from 4 animals. At least one example is shown for each of 5 bands with octave spacing starting at a band of CF < 700 Hz and ending with the band, 5kHz < CF < 10 kHz. For each example, the AN fiber is identified by its animal and unit number. Each example has four sets of plots. The first set shows, subplot (a) the threshold tuning curve (TC), and subplot (b) compound PST histograms of the responses to the click level series. The click level selected for low-level click and ANIP response is indicated in blue and red respectively. The second set of plots shows, subplot (c) at left, the 50Hz bias-tone-level-series period histograms from the bias-tone only responses, subplot (d) in the middle, the bias-tone-level-series period histograms from the responses to bias-tones plus low-level clicks, and subplot (e) at right,

the detailed analysis of the suppression effects on the low-level click responses. The third set of plots shows, at left, subplot (f) bias-tone-level-series period histograms of the responses to bias-tones plus ANIP responses, and at right, subplot (g) the detailed analysis the suppression effects on the ANIP response are shown. Lastly, the fourth set of plots shows, at left, subplot (h) bias-tone-level-series period histograms of the responses to bias-tones plus ANSP responses, and at right, subplot (i) the detailed analysis the suppression effects on the ANSP response are shown.

Example Result in Fig. 3.24: CT026, U013, CF=0.47 kHz, SR=43.3 sps

The data from this fiber show the typical pattern from the CF region below 1 kHz. The suppression threshold on the low-level click, ANIP and ANSP was met at 90, 90 and 100 dB SPL of the bias-tone respectively. Around the suppression threshold level of each click response component, the average firing rate started to decline, and at around the threshold of excitation by the bias-tone alone, which was 110 dB SPL for this fiber, the firing rates started to plateau down at a rate similar to the rate by the bias-tone alone. Similar trends on rate suppression patterns over the bias-tone levels were found from all fibers which met the synchrony based suppression-threshold criterion. As for the major suppression phase, the suppression phase on low-level clicks was opposite to that of ANIP and ANSP as seen throughout CFs.

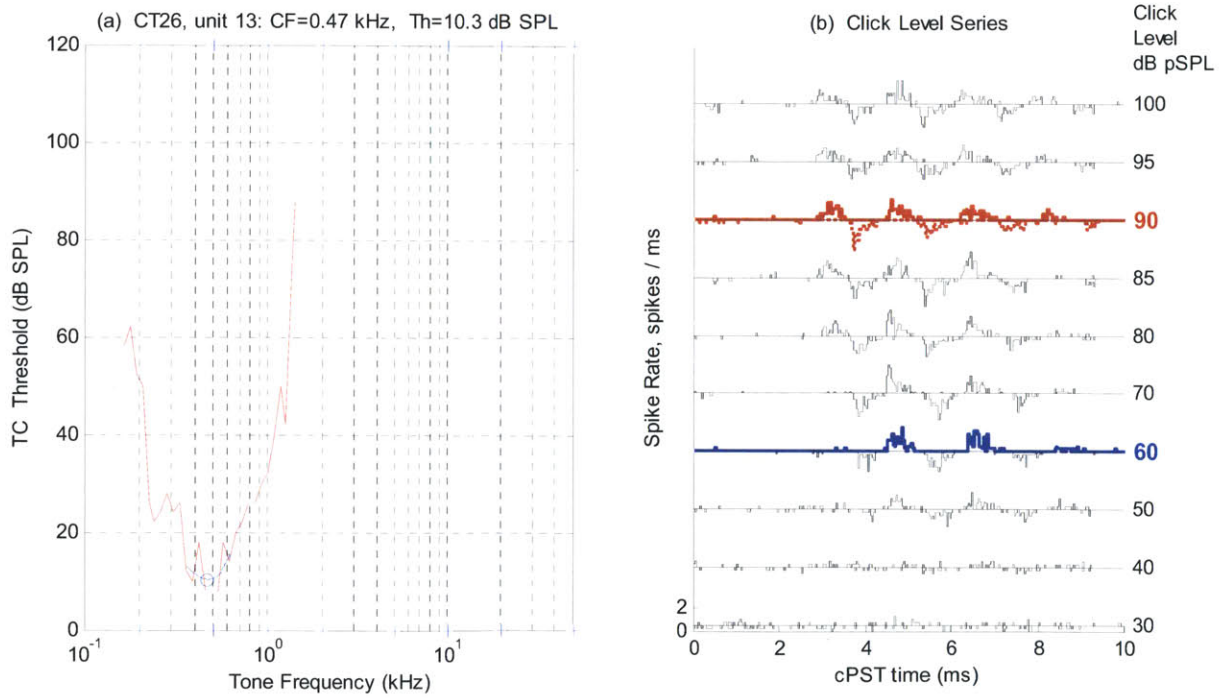

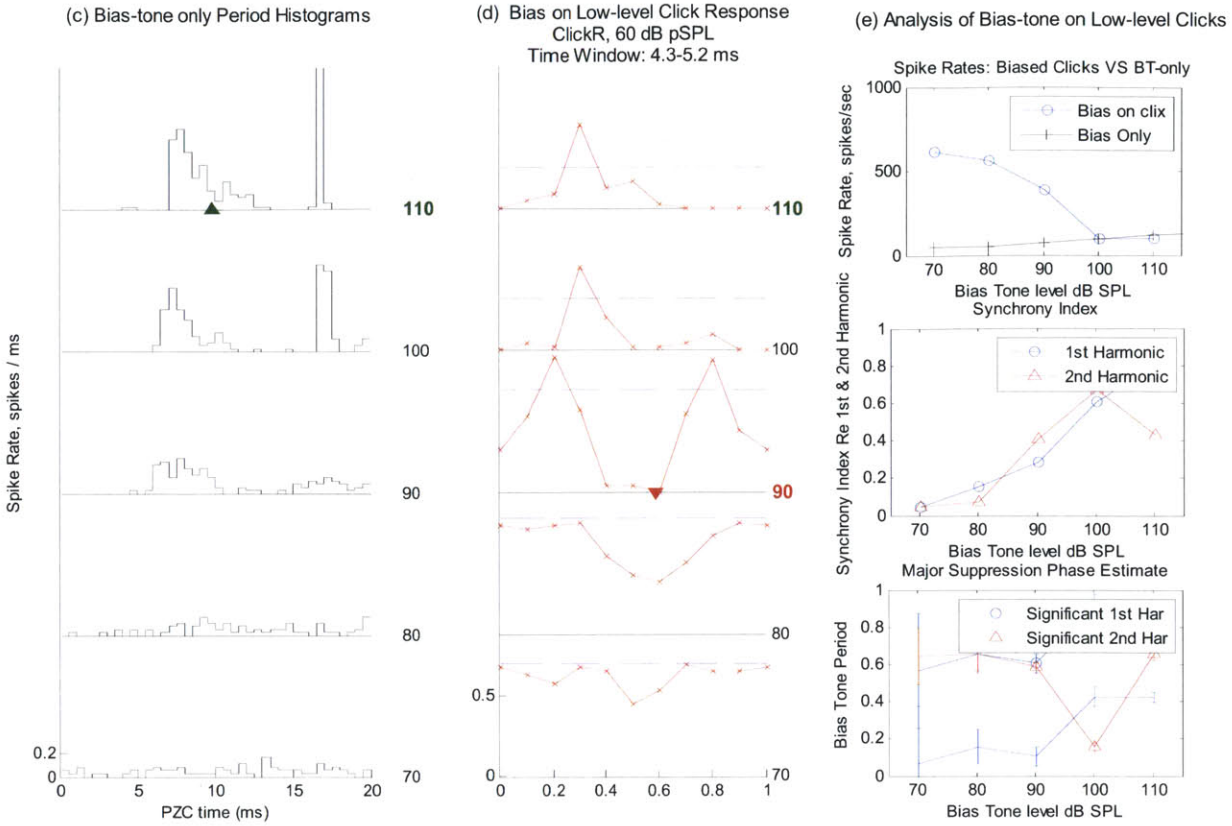
(c) Bias-tone only Period Histograms
Spike Rate, spikes / ms
110
100
90
80
70
0.2
0
0
5
10
15
20
PZC time (ms)
(d) Bias on Low-level Click Response
ClickR, 60 dB pSPL
Time Window: 4.3-5.2 ms
110
100
90
80
70
0.5
0
0
0.2
0.4
0.6
0.8
1
(e) Analysis of Bias-tone on Low-level Clicks
Spike Rates: Biased Clicks VS BT-only
Spike Rate, spikes/sec
1000
500
0
Bias on clix
Bias Only
70
80
90
100
110
Bias Tone level dB SPL
Synchrony Index
Synchrony Index Re 1st & 2nd Harmonic
1
0.8
0.6
0.4
0.2
0
1st Harmonic
2nd Harmonic
70
80
90
100
110
Bias Tone level dB SPL
Major Suppression Phase Estimate
Bias Tone Period
1
0.8
0.6
0.4
0.2
0
Significant 1st Har
Significant 2nd Har
70
80
90
100
110
Bias Tone level dB SPL

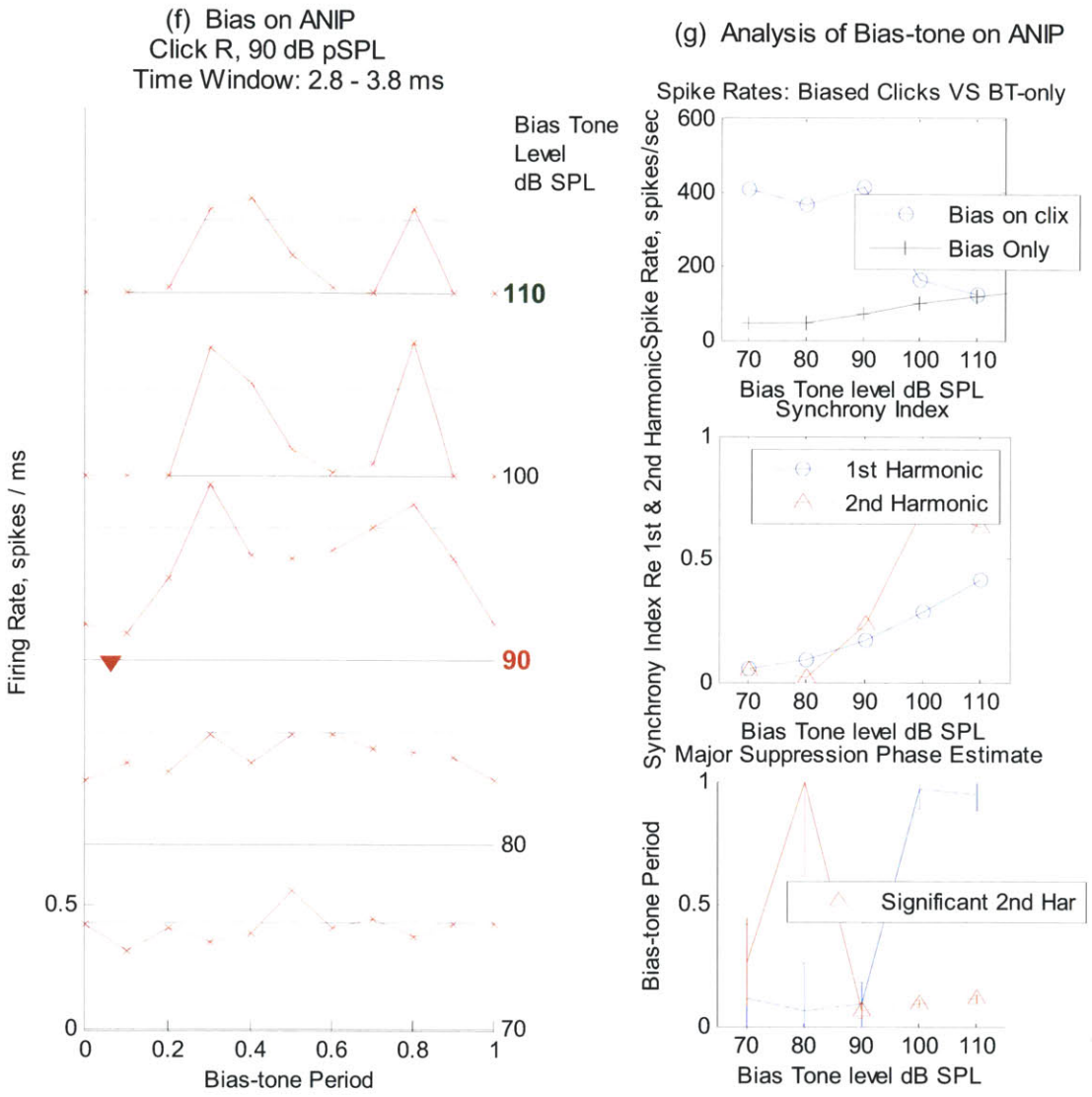
(f) Bias on ANIP
Click R, 90 dB pSPL
Time Window: 2.8 - 3.8 ms
Bias Tone Level dB SPL
110
100
90
80
70
Firing Rate, spikes / ms
0.5
0
0 0.2 0.4 0.6 0.8 1
Bias-tone Period
(g) Analysis of Bias-tone on ANIP
Spike Rates: Biased Clicks VS BT-only
Spike Rate, spikes/sec
600
400
200
0
Bias on clix
Bias Only
70 80 90 100 110
Bias Tone level dB SPL
Synchrony Index
Synchrony Index Re 1st & 2nd Harmonic
1
0.5
0
1st Harmonic
2nd Harmonic
70 80 90 100 110
Bias Tone level dB SPL
Major Suppression Phase Estimate
Bias-tone Period
1
0.5
0
Significant 2nd Har
70 80 90 100 110
Bias Tone level dB SPL

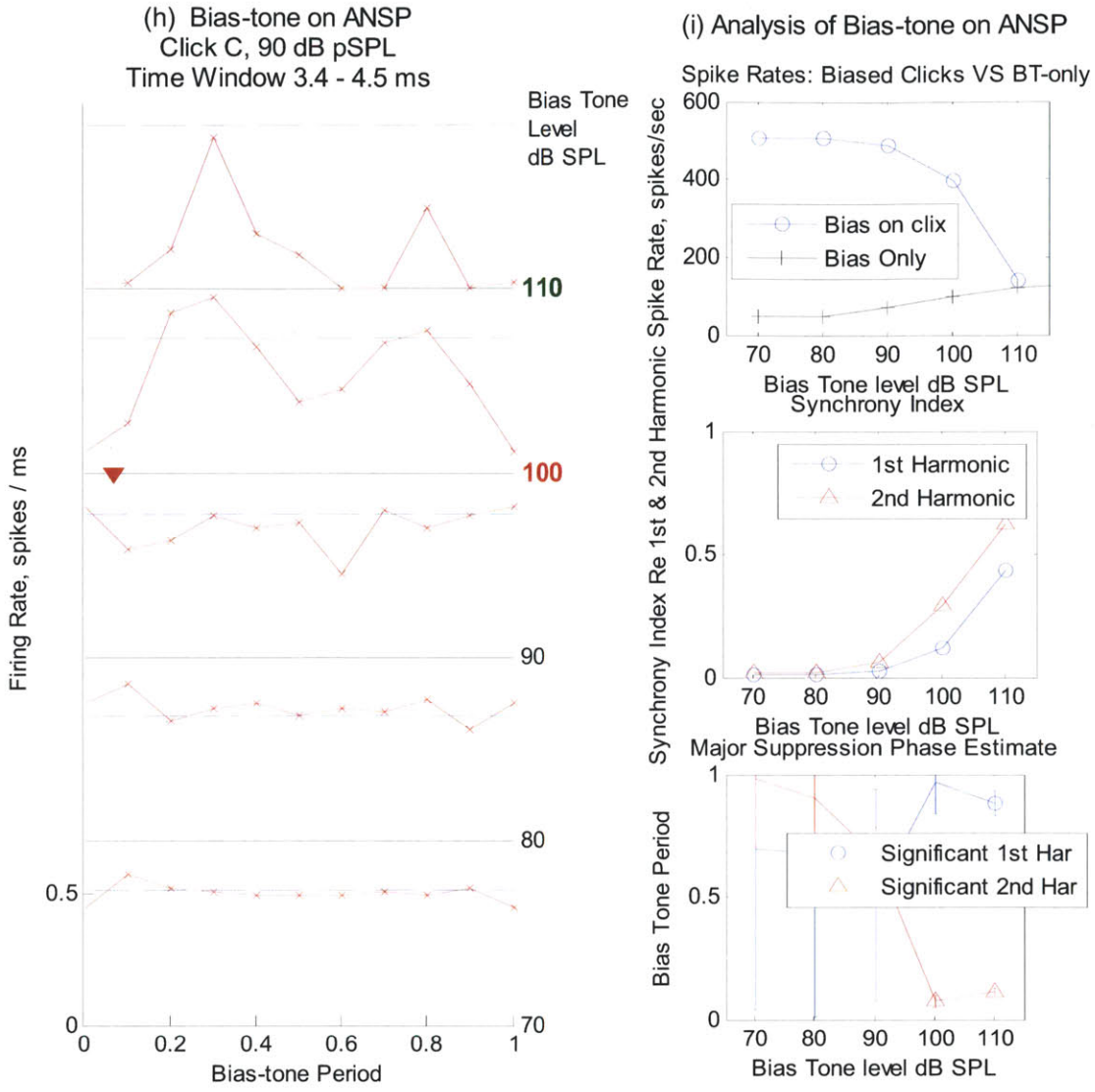

Fig. 3.24 Example Result: (a) Tuning Curve, CF=0.47kHz and SR= 43.3 sps; (b) Click Level Series: the click level selected for low-level click and ANIP/ANSP is noted in blue and red respectively. For all the data presented in this chapter, rarefaction click was used for low-level studies. For all the data on ANIP and ANSP in this chapter, ANIP was generated by rarefaction click, and ANSP was generated by a condensation click. The click response selected for ANSP is plotted in red dotted line; (c) Bias-tone (BT) only level series, excitation threshold reached at 110 dB SPL. Excitation threshold level is indicated in green, and the excitation phase is indicated by a green triangle; (d) Bias-tone level-series on low-level click response, ClickR(Rarefaction) at 60 dB pSPL, Time window 4.3 – 5.2 ms. The suppression threshold and the suppression phase of the 1st and 2nd harmonic is indicated in blue and red respectively; (e) Detailed analysis of the bias-tone effects on click response, Bias-tone level functions of firing rate, synchrony indices and phase of major suppression for the 1st and 2nd harmonic in the top-bottom order; (f) Bias-tone level-series on ANIP: suppression threshold for 2nd harmonic was reached at 90 dB SPL. Note that the major suppression phase on ANIP was opposite of the low-level click response; (g) Detailed analysis of the bias-tone effects on ANIP, Bias-tone level functions of firing rate, synchrony indices and phase of major suppression for the 1st and 2nd harmonic in the top-bottom order; h) Bias-tone level-series on

ANSP: suppression threshold for 2nd harmonic was reached at 100 dB SPL. Note that the major suppression phase on ANSP was similar to that of ANIP opposite of the low-level click response; (i) Detailed analysis of the bias-tone effects on ANIP, Bias-tone level functions of firing rate, synchrony indices and phase of major suppression for the 1st and 2nd harmonic in the top-bottom order;

Example Result in Fig. 3.25: CT025, U107, CF=0.96 kHz, SR=84.5 sps

This fiber is a typical example from the CF region centered at ~1 kHz. The bias-tone only excitation threshold was met at 120 dB SPL with the excitation phase detected at the broader peak in the period histogram. The suppression threshold on the low-level click, ANIP and ANSP was reached at 90, 90 and 100 dB SPL of the bias-tone respectively.

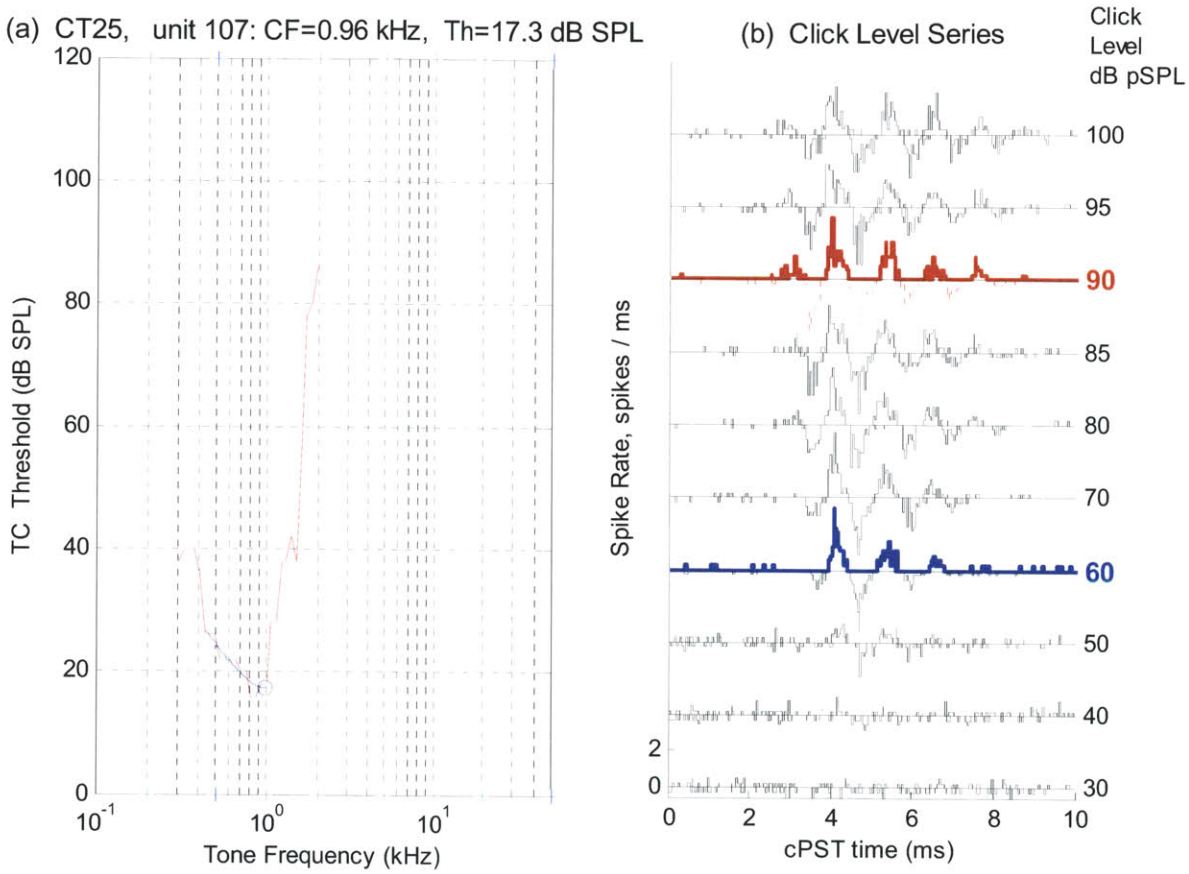

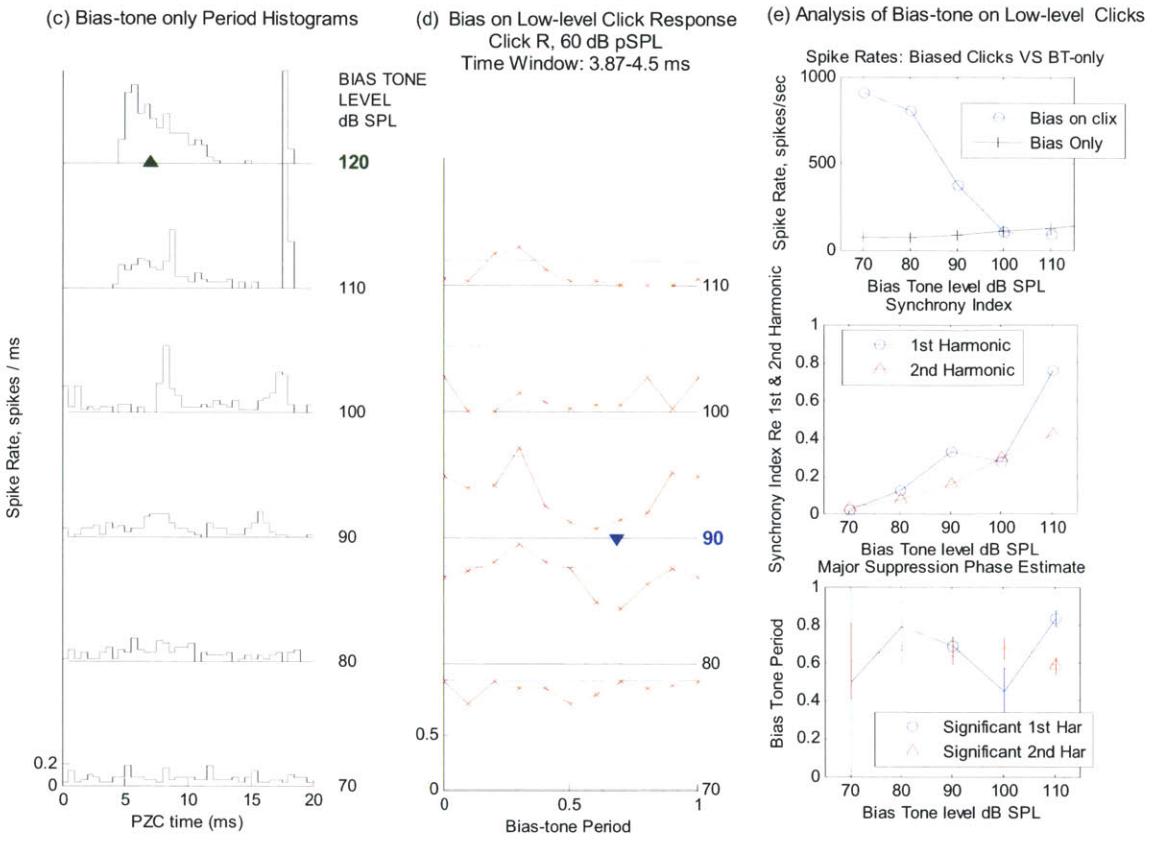
(c) Bias-tone only Period Histograms
BIAS TONE LEVEL dB SPL
120
110
100
90
80
70
Spike Rate, spikes / ms
PZC time (ms)
(d) Bias on Low-level Click Response
Click R, 60 dB pSPL
Time Window: 3.87-4.5 ms
Bias-tone Period
(e) Analysis of Bias-tone on Low-level Clicks
Spike Rates: Biased Clicks VS BT-only
Bias on clix
Bias Only
Spike Rate, spikes/sec
Bias Tone level dB SPL
Synchrony Index
1st Harmonic
2nd Harmonic
Synchrony Index Re 1st & 2nd Harmonic
Bias Tone level dB SPL
Major Suppression Phase Estimate
Significant 1st Har
Significant 2nd Har
Bias Tone Period
Bias Tone level dB SPL

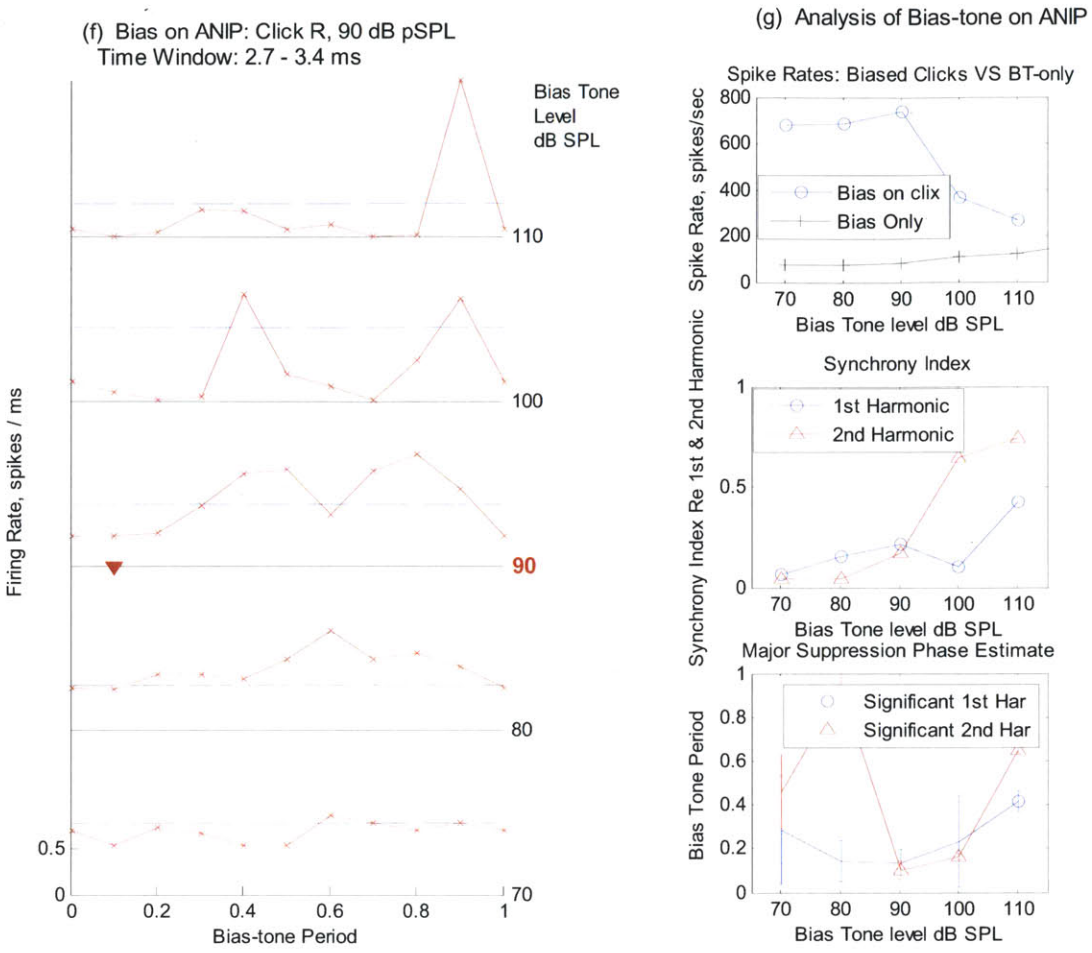
(f) Bias on ANIP: Click R, 90 dB pSPL
Time Window: 2.7 - 3.4 ms
Bias Tone Level dB SPL
110
100
90
80
70
Firing Rate, spikes / ms
0.5
0
0
0.2
0.4
0.6
0.8
1
Bias-tone Period
(g) Analysis of Bias-tone on ANIP
Spike Rates: Biased Clicks VS BT-only
Spike Rate, spikes/sec
800
600
400
200
0
Bias on clix
Bias Only
70
80
90
100
110
Bias Tone level dB SPL
Synchrony Index
Synchrony Index Re 1st & 2nd Harmonic
1
0.5
0
1st Harmonic
2nd Harmonic
70
80
90
100
110
Bias Tone level dB SPL
Major Suppression Phase Estimate
Bias Tone Period
1
0.8
0.6
0.4
0.2
0
Significant 1st Har
Significant 2nd Har
70
80
90
100
110
Bias Tone level dB SPL

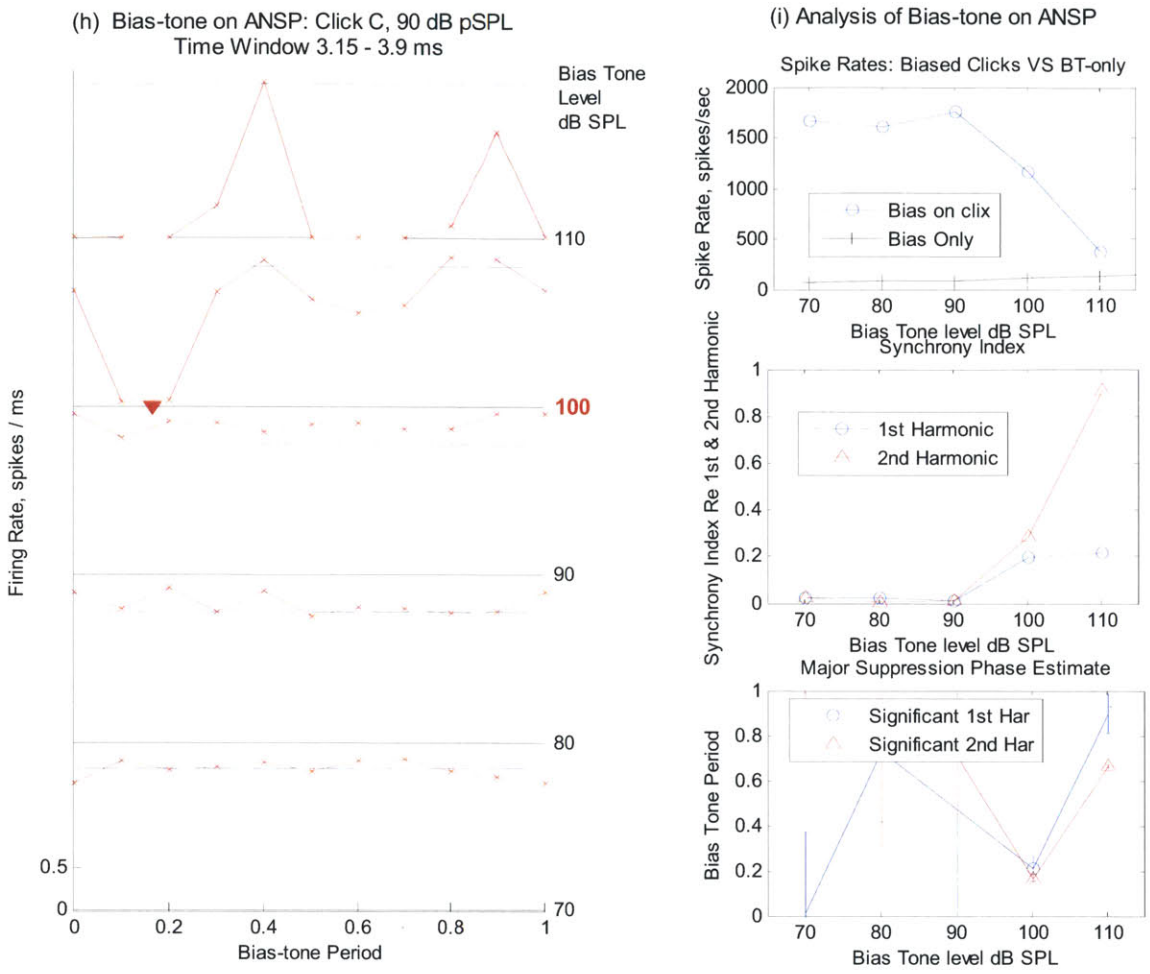

Fig. 3.25 Example Result: (a) Tuning Curve, CF=0.96 kHz and SR= 84.5 sps; (b) Click Level Series: the click level selected for low-level click and ANIP/ANSP is noted in blue and red respectively. For all the data presented in this chapter, rarefaction click was used for low-level studies. For all the data on ANIP and ANSP in this chapter, ANIP was generated by rarefaction click, and ANSP was generated by a condensation click. The click response selected for ANSP is plotted in red dotted line; (c) Bias-tone (BT) only level series, excitation threshold reached at 120 dB SPL. Excitation threshold level is indicated in green, and the excitation phase is indicated by a green triangle; (d) Bias-tone level-series on low-level click response, ClickR(Rarefaction) at 60 dB pSPL, Time window 3.87 – 4.5 ms. The suppression threshold and the suppression phase of the 1st and 2nd harmonic is indicated in blue and red respectively; (e) Detailed analysis of the bias-tone effects on click response, Bias-tone level functions of firing rate, synchrony indices and phase of major suppression for the 1st and 2nd harmonic in the top-bottom order; (f) Bias-tone level-series on ANIP: suppression threshold for 2nd harmonic was reached at 90 dB SPL. Note that the major suppression phase on ANIP was opposite of the low-level click response; (g) Detailed analysis of the bias-tone effects on ANIP, Bias-tone level functions of firing rate, synchrony indices and phase of major suppression for the 1st and 2nd harmonic in the top-bottom order; h) Bias-tone level-series on ANSP: suppression threshold for 2nd harmonic was reached at 100 dB SPL. Note that the major suppression phase on ANSP was similar to that of ANIP opposite of the low-level click response; (i) Detailed analysis of the bias-tone effects on ANIP, Bias-tone level functions of firing rate, synchrony indices and phase of major suppression for the 1st and 2nd harmonic in the top-bottom order;

Example Result in Fig. 3.26: CT025, U102, CF=1.49 kHz, SR=66 sps

This fiber is another example from the CF region, 1 kHz < CF < 2 kHz. The bias-tone only excitation threshold was met at 120 dB SPL with the excitation phase detected at the broader peak in the period histogram. The suppression threshold for ANIP and ANSP was 100 dB SPL with the major suppression phase opposite to that of low-level click response on which suppression threshold was reached at 90 dB SPL.

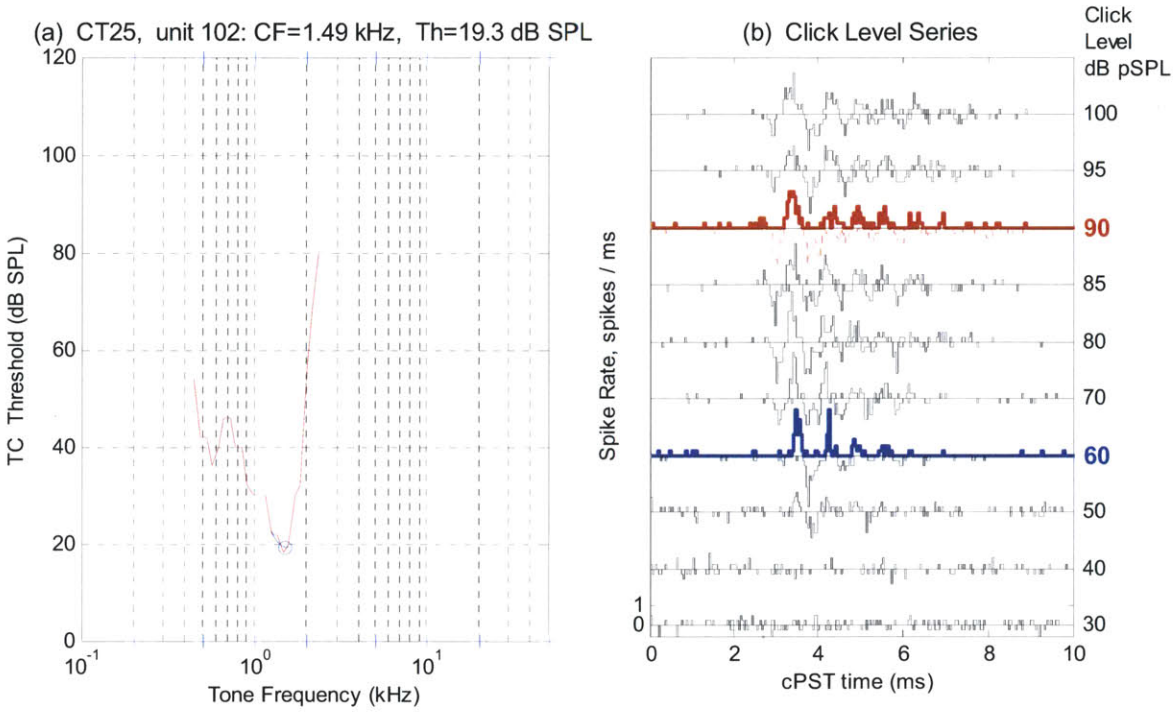

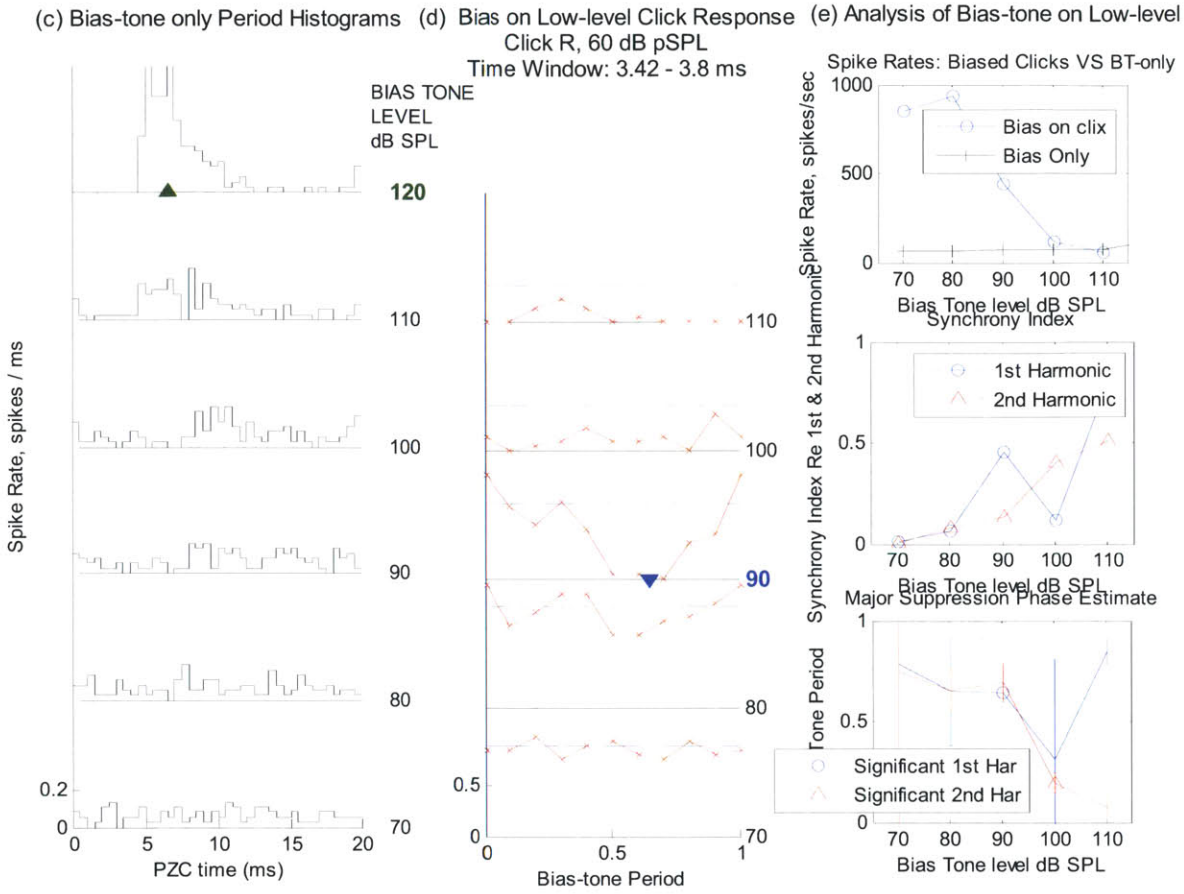
(c) Bias-tone only Period Histograms
(d) Bias on Low-level Click Response
Click R, 60 dB pSPL
Time Window: 3.42 - 3.8 ms
(e) Analysis of Bias-tone on Low-level
BIAS TONE
LEVEL
dB SPL
120
110
100
90
80
70
Spike Rate, spikes / ms
PZC time (ms)
Bias-tone Period
Spike Rates: Biased Clicks VS BT-only
Spike Rate, spikes/sec
Bias on clix
Bias Only
Bias Tone level dB SPL
Synchrony Index
Synchrony Index Re 1st & 2nd Harmonic
1st Harmonic
2nd Harmonic
Major Suppression Phase Estimate
Tone Period
Significant 1st Har
Significant 2nd Har

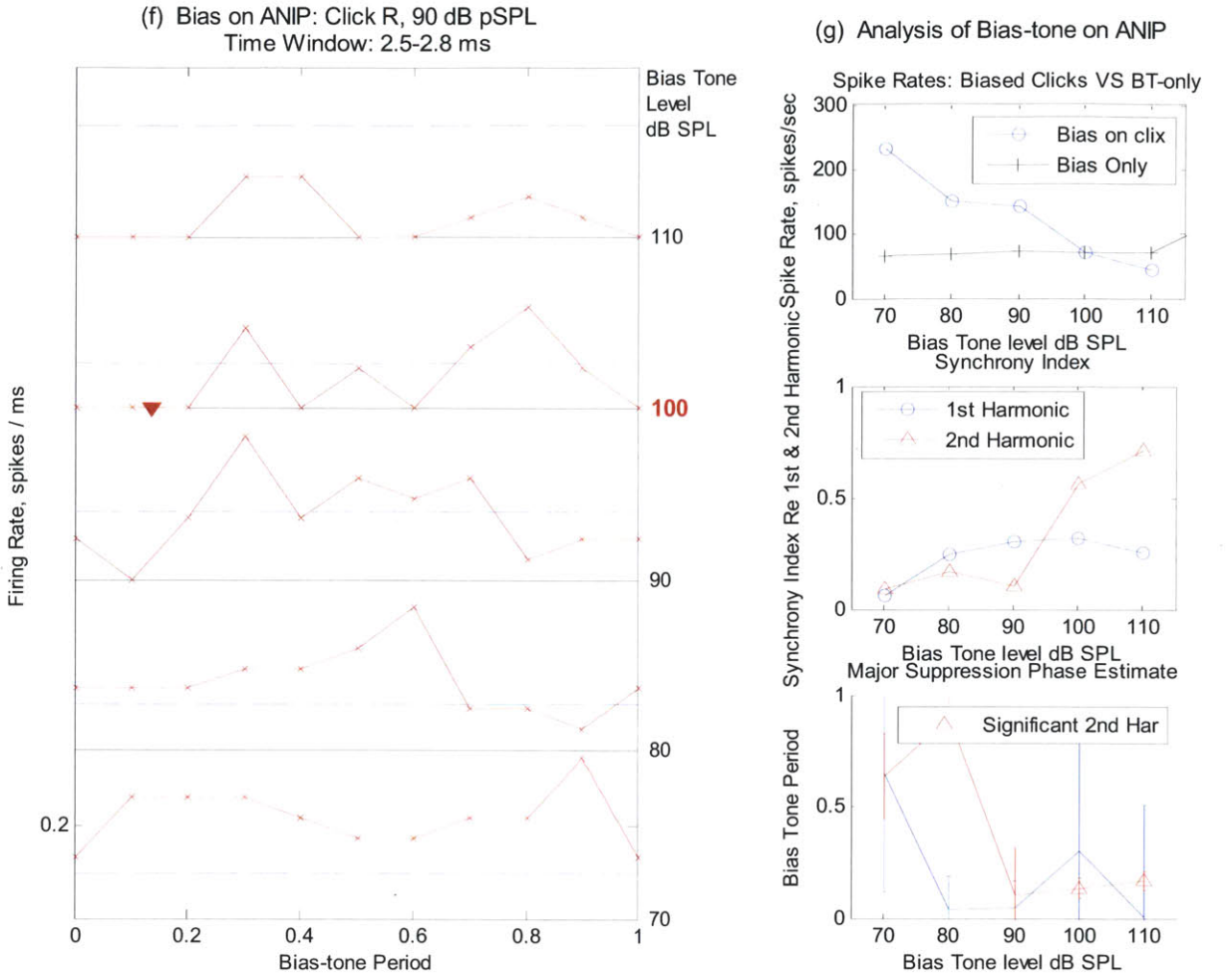
(f) Bias on ANIP: Click R, 90 dB pSPL
Time Window: 2.5-2.8 ms
Bias Tone Level dB SPL
110
100
90
80
70
Firing Rate, spikes / ms
0.2
0
0.2
0.4
0.6
0.8
1
Bias-tone Period
(g) Analysis of Bias-tone on ANIP
Spike Rates: Biased Clicks VS BT-only
Spike Rate, spikes/sec
300
200
100
0
Bias on clix
Bias Only
70
80
90
100
110
Bias Tone level dB SPL
Synchrony Index
Synchrony Index Re 1st & 2nd Harmonic
1
0.5
0
1st Harmonic
2nd Harmonic
Bias Tone level dB SPL
Major Suppression Phase Estimate
Bias Tone Period
Significant 2nd Har
Bias Tone level dB SPL

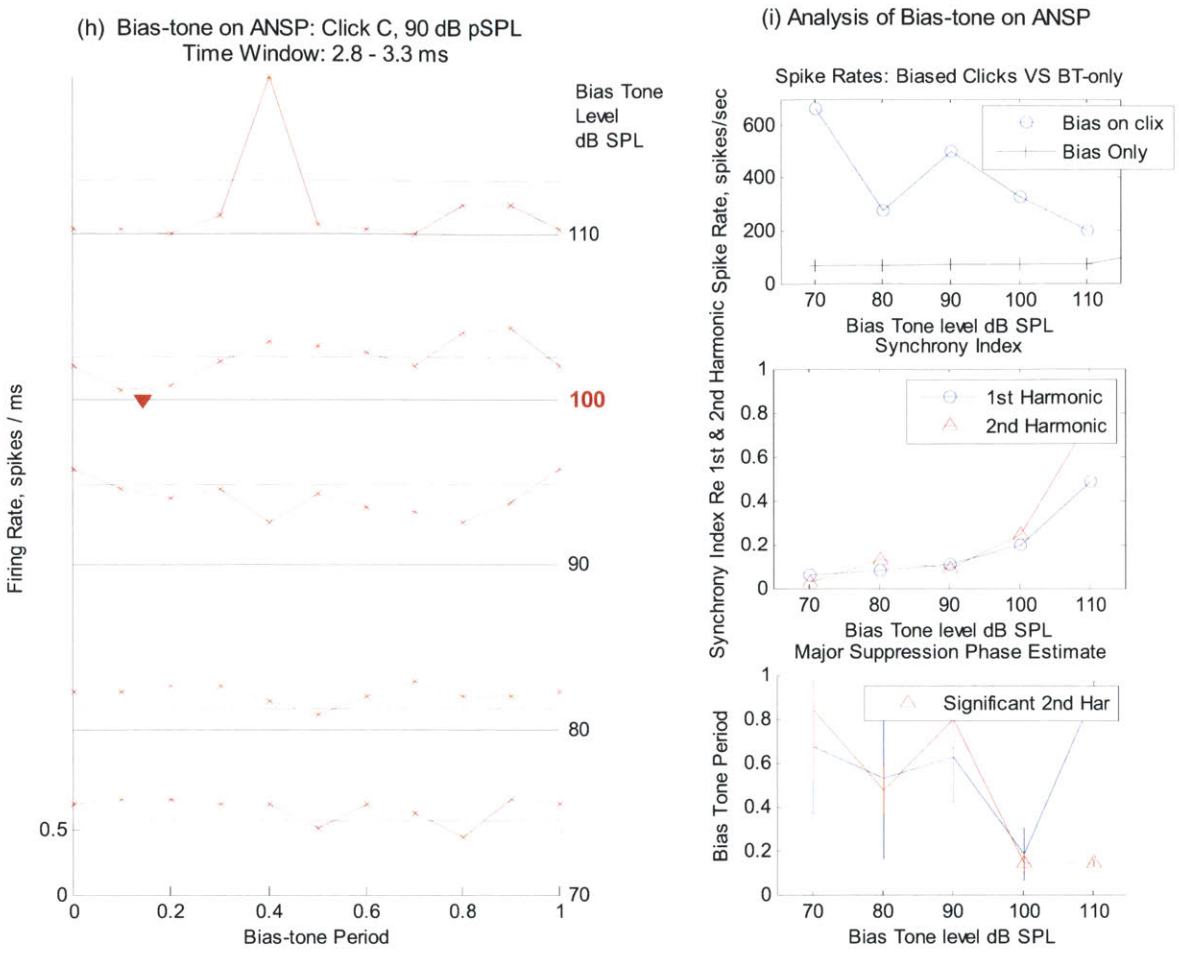

Fig. 3.26 Example Result: (a) Tuning Curve, CF=1.49 kHz and SR= 66 sps; (b) Click Level Series: the click level selected for low-level click and ANIP/ANSP is noted in blue and red respectively. For all the data presented in this chapter, rarefaction click was used for low-level studies. For all the data on ANIP and ANSP in this chapter, ANIP was generated by rarefaction click, and ANSP was generated by a condensation click. The click response selected for ANSP is plotted in red dotted line; (c) Bias-tone (BT) only level series, excitation threshold reached at 120 dB SPL. Excitation threshold level is indicated in green, and the excitation phase is indicated by a green triangle; (d) Bias-tone level-series on low-level click response. The suppression threshold and the suppression phase of the 1st and 2nd harmonic is indicated in blue and red respectively; (e) Detailed analysis of the bias-tone effects on click response, Bias-tone level functions of firing rate, synchrony indices and phase of major suppression for the 1st and 2nd harmonic in the top-bottom order; (f) Bias-tone level-series on ANIP: suppression threshold for 2nd harmonic was reached at 100 dB SPL. Note that the major suppression phase on ANIP was opposite of the low-level click response; (g) Detailed analysis of the bias-tone effects on ANIP, Bias-tone level functions of firing rate, synchrony indices and phase of major suppression for the 1st and 2nd harmonic in the top-bottom order; h) Bias-tone level-series on ANSP: suppression threshold for 2nd harmonic was reached at 100 dB SPL. Note that the major suppression phase on ANSP was similar to that of ANIP opposite of the low-level click response; (i) Detailed analysis of the bias-tone effects on ANIP, Bias-tone level functions of firing rate, synchrony indices and phase of major suppression for the 1st and 2nd harmonic in the top-bottom order.

Example Result in Fig. 3.27: CT031, U079, CF=2.12 kHz, SR=14 sps

This is a typical example fiber from the CF region, 2 kHz < CF < 3 kHz, which was the band with highest CF from which suppression thresholds were reached on ANIP and ANSP. Note from Fig. 3.21 that the suppression threshold on ANIP and ANSP began to rise sharply in this CF region.

The suppression thresholds on low-level click response, ANIP and ANSP was 90, 100 and 110 dB SPL respectively. The major suppression phase for ANIP and ANSP was again opposite to that of low-level click responses. Since the suppression threshold on ANSP at 110 dB SPL was not below the excitation threshold which was also 110 dB SPL, the ANSP data for this fiber were not included in the suppression data pool.

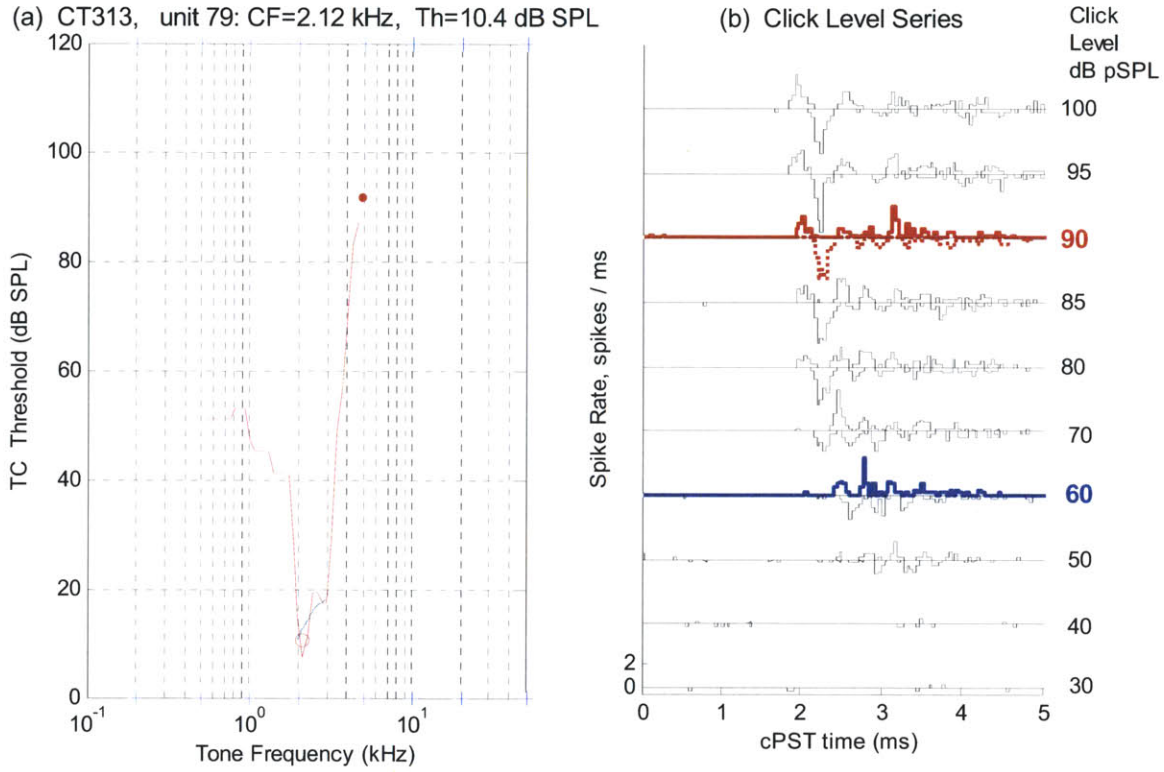

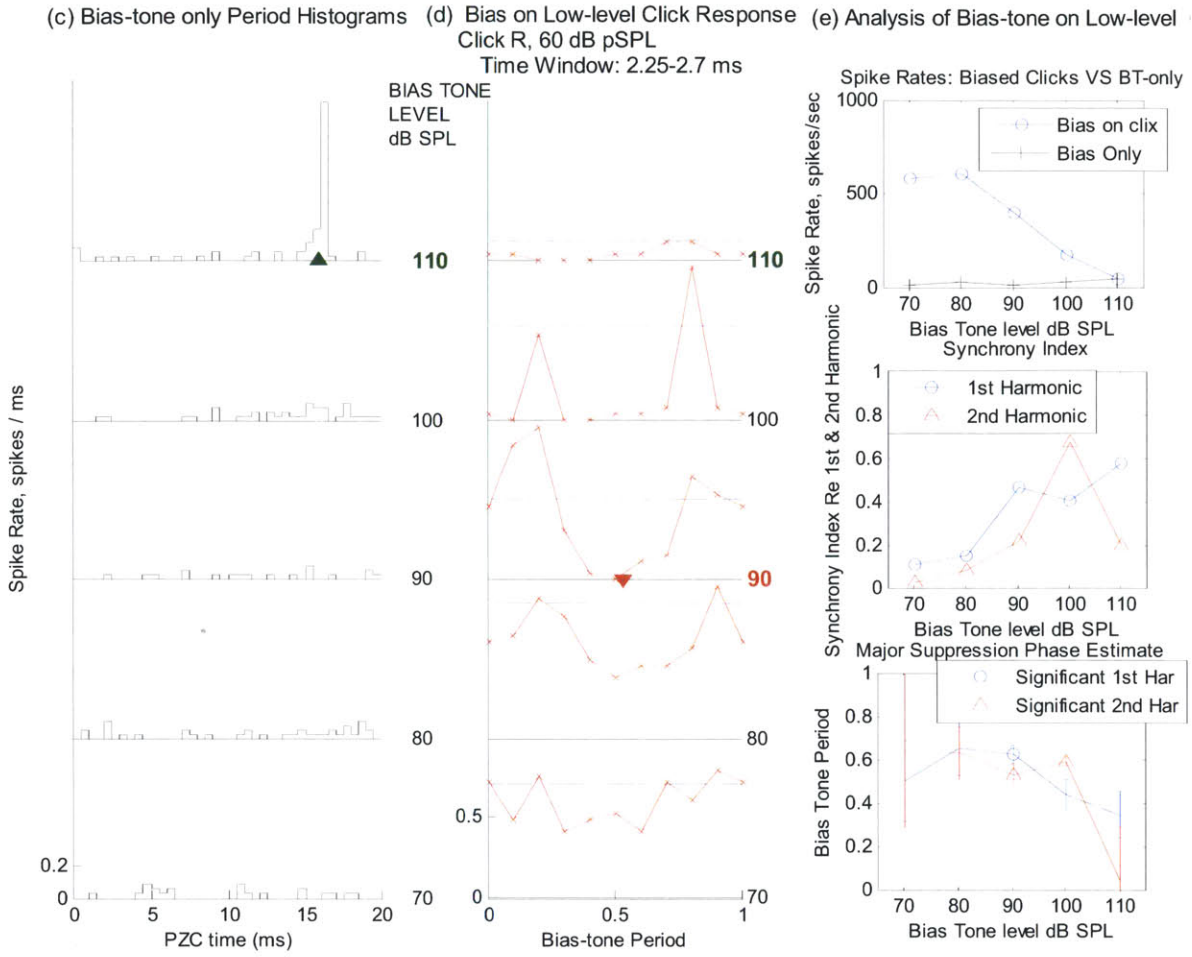
(c) Bias-tone only Period Histograms
(d) Bias on Low-level Click Response
Click R, 60 dB pSPL
Time Window: 2.25-2.7 ms
(e) Analysis of Bias-tone on Low-level
BIAS TONE
LEVEL
dB SPL
110
100
90
80
70
Spike Rate, spikes / ms
PZC time (ms)
Bias-tone Period
Spike Rates: Biased Clicks VS BT-only
Spike Rate, spikes/sec
Bias on clix
Bias Only
Bias Tone level dB SPL
Synchrony Index
Synchrony Index Re 1st & 2nd Harmonic
1st Harmonic
2nd Harmonic
Major Suppression Phase Estimate
Bias Tone Period
Significant 1st Har
Significant 2nd Har

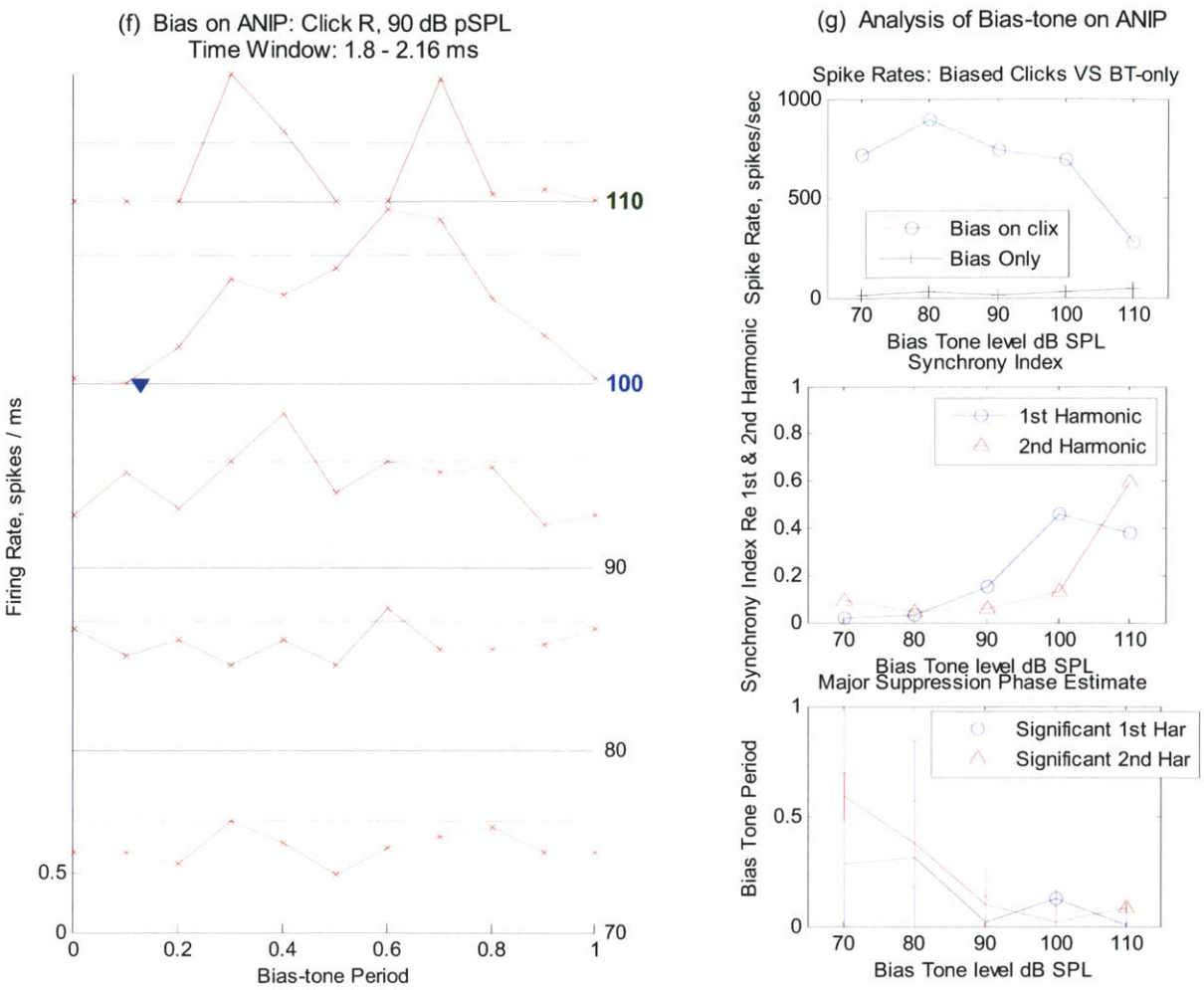
(f) Bias on ANIP: Click R, 90 dB pSPL
Time Window: 1.8 - 2.16 ms
Firing Rate, spikes / ms
Bias-tone Period
110
100
90
80
70
0.5
0
0.2
0.4
0.6
0.8
1
(g) Analysis of Bias-tone on ANIP
Spike Rates: Biased Clicks VS BT-only
Spike Rate, spikes/sec
1000
500
0
Bias on clix
Bias Only
70
80
90
100
110
Bias Tone level dB SPL
Synchrony Index
Synchrony Index Re 1st & 2nd Harmonic
1
0.8
0.6
0.4
0.2
0
1st Harmonic
2nd Harmonic
Bias Tone level dB SPL
Major Suppression Phase Estimate
Bias Tone Period
0.5
Significant 1st Har
Significant 2nd Har
Bias Tone level dB SPL

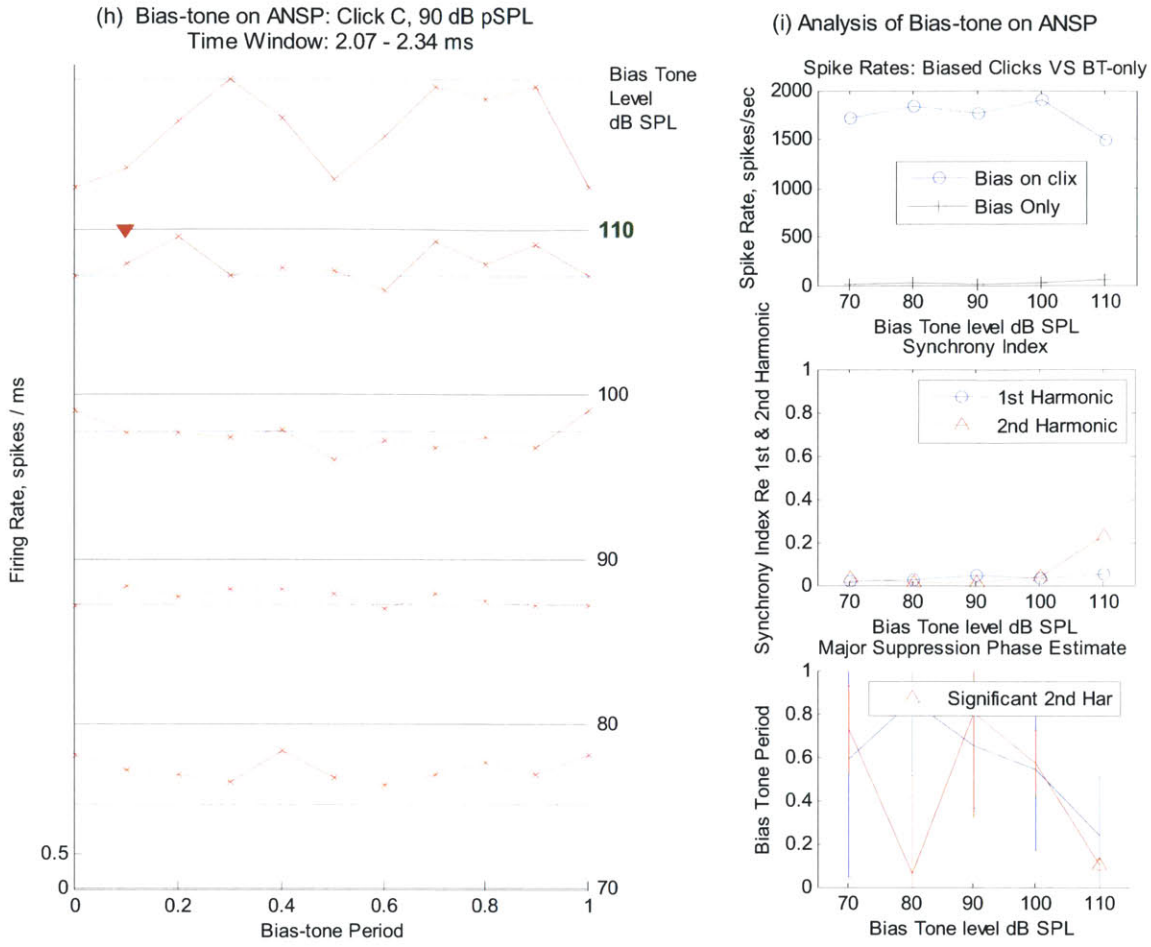

Fig. 3.27 Example Result: (a) Tuning Curve, CF=2.12 kHz and SR= 14 sps; (b) Click Level Series: the click level selected for low-level click and ANIP/ANSP is noted in blue and red respectively. For all the data presented in this chapter, rarefaction click was used for low-level studies. For all the data on ANIP and ANSP in this chapter, ANIP was generated by rarefaction click, and ANSP was generated by a condensation click. The click response selected for ANSP is plotted in red dotted line; (c) Bias-tone (BT) only level series, excitation threshold reached at 110 dB SPL. Excitation threshold level is indicated in green, and the excitation phase is indicated by a green triangle; (d) Bias-tone level-series on low-level click response. The suppression threshold and the suppression phase of the 1st and 2nd harmonic is indicated in blue and red respectively; (e) Detailed analysis of the bias-tone effects on click response, Bias-tone level functions of firing rate, synchrony indices and phase of major suppression for the 1st and 2nd harmonic in the top-bottom order; (f) Bias-tone level-series on ANIP: suppression threshold for 2nd harmonic was reached at 100 dB SPL. Note that the major suppression phase on ANIP was opposite of the low-level click response; (g) Detailed analysis of the bias-tone effects on ANIP, Bias-tone level functions of firing rate, synchrony indices and phase of major suppression for the 1st and 2nd harmonic in the top-bottom order; h) Bias-tone level-series on ANSP: suppression threshold for 2nd harmonic was reached at 100 dB SPL. Note that the major suppression phase on ANSP was similar to that of ANIP opposite of the low-level click response; (i) Detailed analysis of the bias-tone effects on ANIP, Bias-tone level functions of firing rate, synchrony indices and phase of major suppression for the 1st and 2nd harmonic in the top-bottom order.

Example Result in Fig. 3.28: CT031, U071, CF=3.228 kHz, SR=56.4 sps

For this fiber with CF of 3.23 kHz, the suppression threshold on low-level click response and ANIP was reached at 90 and 110 dB SPL while the threshold was not reached for ANSP within the maximum level of the bias-tone applied, which was 110 dB SPL.

The suppression pattern on low-level clicks and ANIP were similar to the other fibers with lower CFs except for the elevated threshold level. For ANIP at the bias-tone level of 100 dB SPL, the major suppression phase was visually identifiable at the typical location but was below the threshold criterion. At the next level of 110 dB SPL which met the threshold criterion, the analysis method, however, apparently selected the wrong phase as the major suppression phase. Since the excitation threshold was at 100 dB SPL which was exceeded by the suppression threshold on ANIP, the data for ANIP were not included in the suppression data pool. As for ANSP, signs of suppression were not visible from the period-histograms or the rate-level function.

These results suggest that as the CF of the fiber exceeded ~2 kHz, the threshold of suppression was elevated; however, the overall pattern of suppression remained qualitatively similar to the fibers with lower CFs.

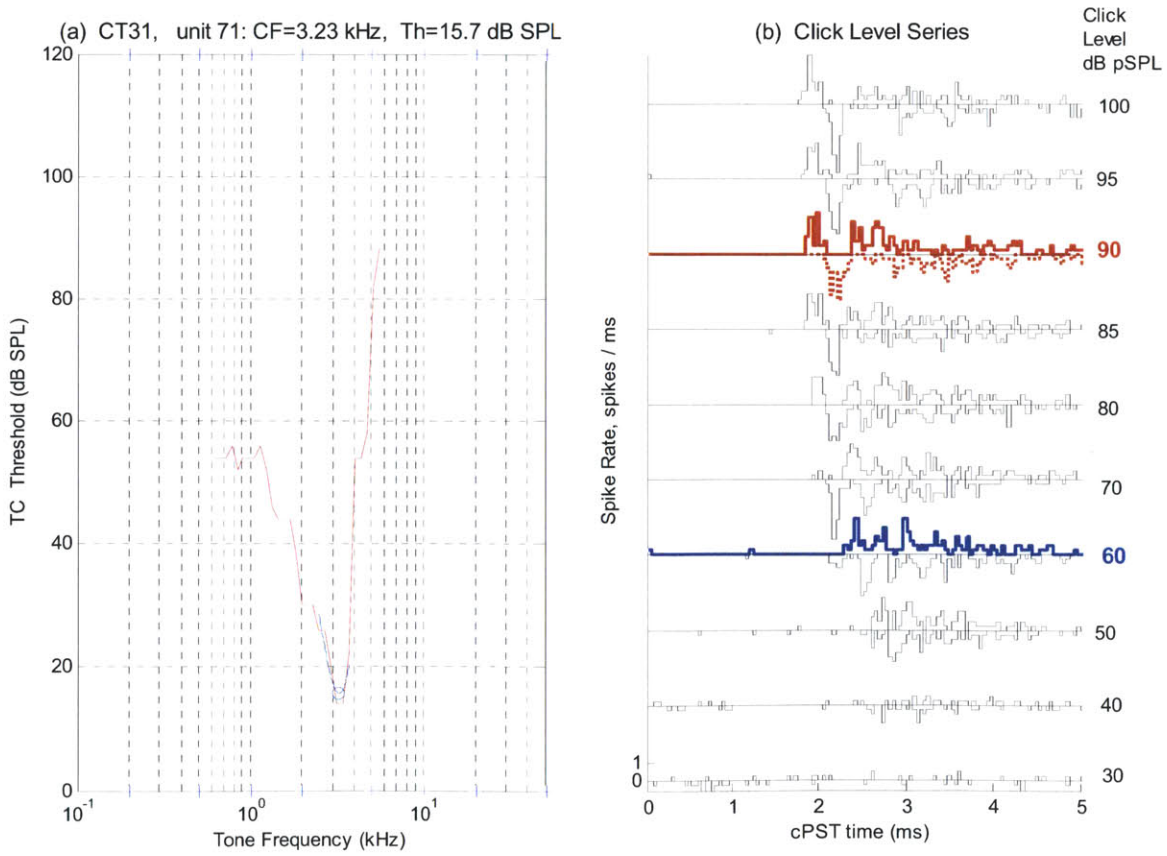

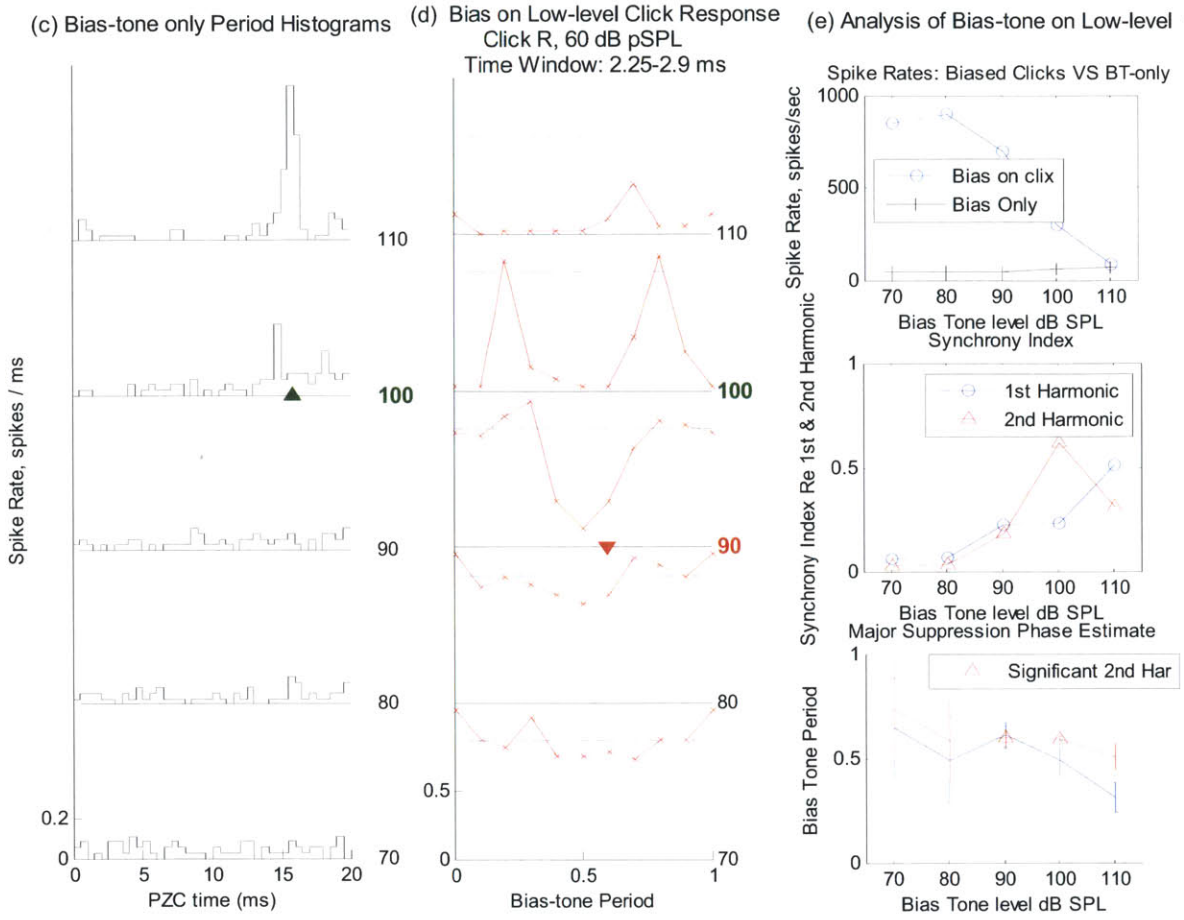
(c) Bias-tone only Period Histograms
Spike Rate, spikes / ms
110
100
90
80
70
0.2
0
0
5
10
15
20
PZC time (ms)
(d) Bias on Low-level Click Response
Click R, 60 dB pSPL
Time Window: 2.25-2.9 ms
110
100
90
80
70
0.5
0
0
0.5
1
Bias-tone Period
(e) Analysis of Bias-tone on Low-level
Spike Rates: Biased Clicks VS BT-only
Spike Rate, spikes/sec
1000
500
0
Bias on clix
Bias Only
70
80
90
100
110
Bias Tone level dB SPL
Synchrony Index
Synchrony Index Re 1st & 2nd Harmonic
1
0.5
0
1st Harmonic
2nd Harmonic
70
80
90
100
110
Bias Tone level dB SPL
Major Suppression Phase Estimate
Bias Tone Period
1
0.5
0
Significant 2nd Har
70
80
90
100
110
Bias Tone level dB SPL

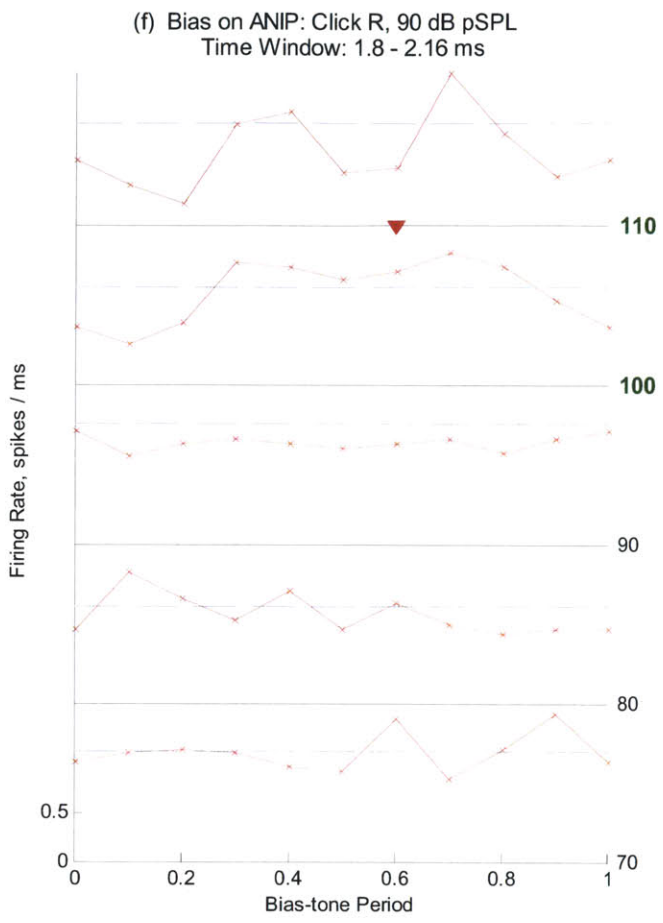
(f) Bias on ANIP: Click R, 90 dB pSPL
Time Window: 1.8 - 2.16 ms
Firing Rate, spikes / ms
110
100
90
80
70
0.5
0
0
0.2
0.4
0.6
0.8
1
Bias-tone Period

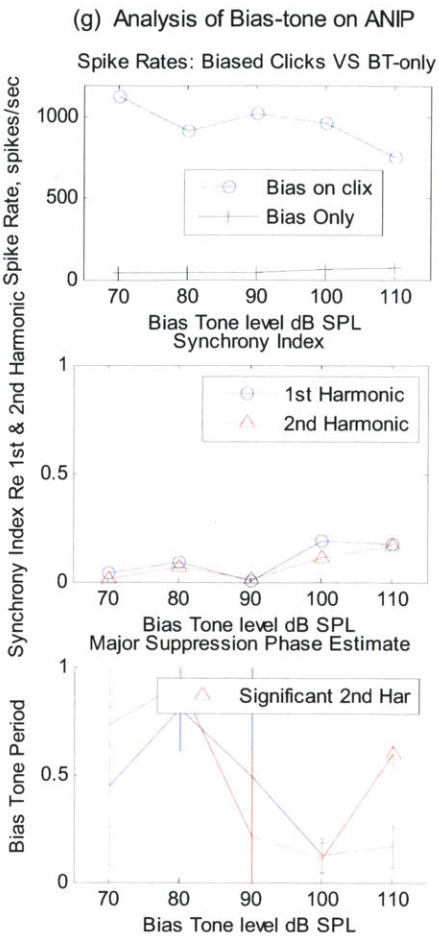
(g) Analysis of Bias-tone on ANIP
Spike Rates: Biased Clicks VS BT-only
Spike Rate, spikes/sec
1000
500
0
Bias on clix
Bias Only
70
80
90
100
110
Bias Tone level dB SPL
Synchrony Index
Synchrony Index Re 1st & 2nd Harmonic
1
0.5
0
1st Harmonic
2nd Harmonic
70
80
90
100
110
Bias Tone level dB SPL
Major Suppression Phase Estimate
Bias Tone Period
1
0.5
0
Significant 2nd Har
70
80
90
100
110
Bias Tone level dB SPL

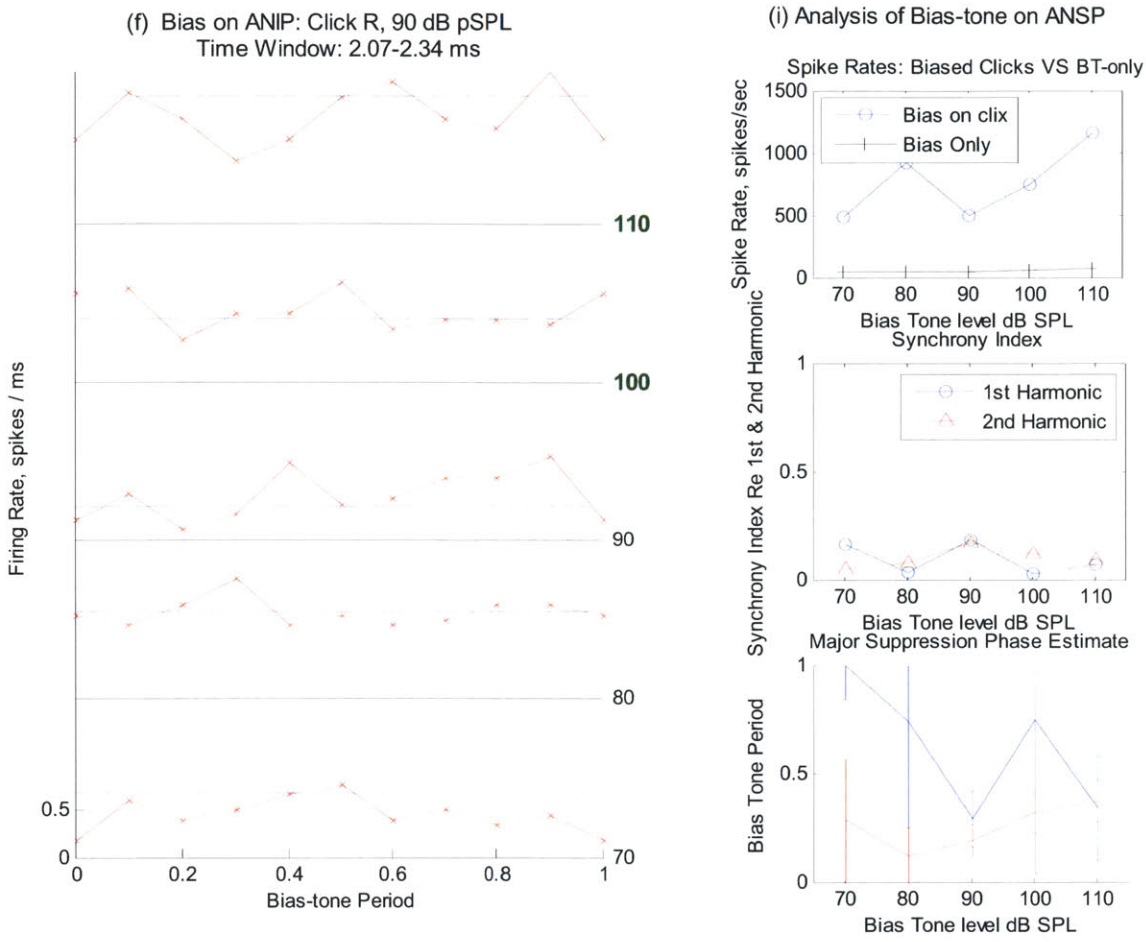

Fig. 3.28 Example Result: (a) Tuning Curve, CF=3.23 kHz and SR= 56.4 sps; (b) Click Level Series: the click level selected for low-level click and ANIP/ANSP is noted in blue and red respectively. For all the data presented in this chapter, rarefaction click was used for low-level studies. For all the data on ANIP and ANSP in this chapter, ANIP was generated by rarefaction click, and ANSP was generated by a condensation click. The click response selected for ANSP is plotted in red dotted line; (c) Bias-tone (BT) only level series, excitation threshold reached at 100 dB SPL. Excitation threshold level is indicated in green, and the excitation phase is indicated by a green triangle; (d) Bias-tone level-series on low-level click response. The suppression threshold and the suppression phase of the 1st and 2nd harmonic is indicated in blue and red respectively; (e) Detailed analysis of the bias-tone effects on click response, Bias-tone level functions of firing rate, synchrony indices and phase of major suppression for the 1st and 2nd harmonic in the top-bottom order; (f) Bias-tone level-series on ANIP: suppression threshold for 2nd harmonic was reached at 100 dB SPL. Note that the major suppression phase on ANIP was opposite of the low-level click response; (g) Detailed analysis of the bias-tone effects on ANIP, Bias-tone level functions of firing rate, synchrony indices and phase of major suppression for the 1st and 2nd harmonic in the top-bottom order; h) Bias-tone level-series on ANSP: suppression threshold for 2nd harmonic was reached at 100 dB SPL. Note that the major suppression phase on ANSP was similar to that of ANIP opposite of the low-level click response; (i) Detailed analysis of the bias-tone effects on ANIP, Bias-tone level functions of firing rate, synchrony indices and phase of major suppression for the 1st and 2nd harmonic in the top-bottom order.

Example Result in Fig. 3.29: CT023, U066, CF= 7.16 kHz, SR= 80 sps

On this fiber with the CF of 7.16 kHz, bias-tone studies were done on the low-level click responses only. Both the TC and the click level series show the typical characteristics of a high-CF fiber; the TC shows a broad low-frequency tail, and the low-level click responses no longer is phased locked to the CF of the fiber but shows the amplitude envelope only. From the bias-tone only period histograms, the peak splitting was not visible, and the narrow peak remained at about the same phase as in fibers with lower CFs.

The suppression threshold for the second harmonic was reached at 100 dB SPL for low-level click responses. Note that for this fiber, the suppression phase for the low-level click responses was detected at the opposite phase to the main data group. However, also note that at 10 dB below the threshold at 90 dB SPL, the actual major suppression phase emerges at the typical location, but fell below the criterion. Therefore, the suppression pattern for this fiber was not actually different from other fibers in this CF region.

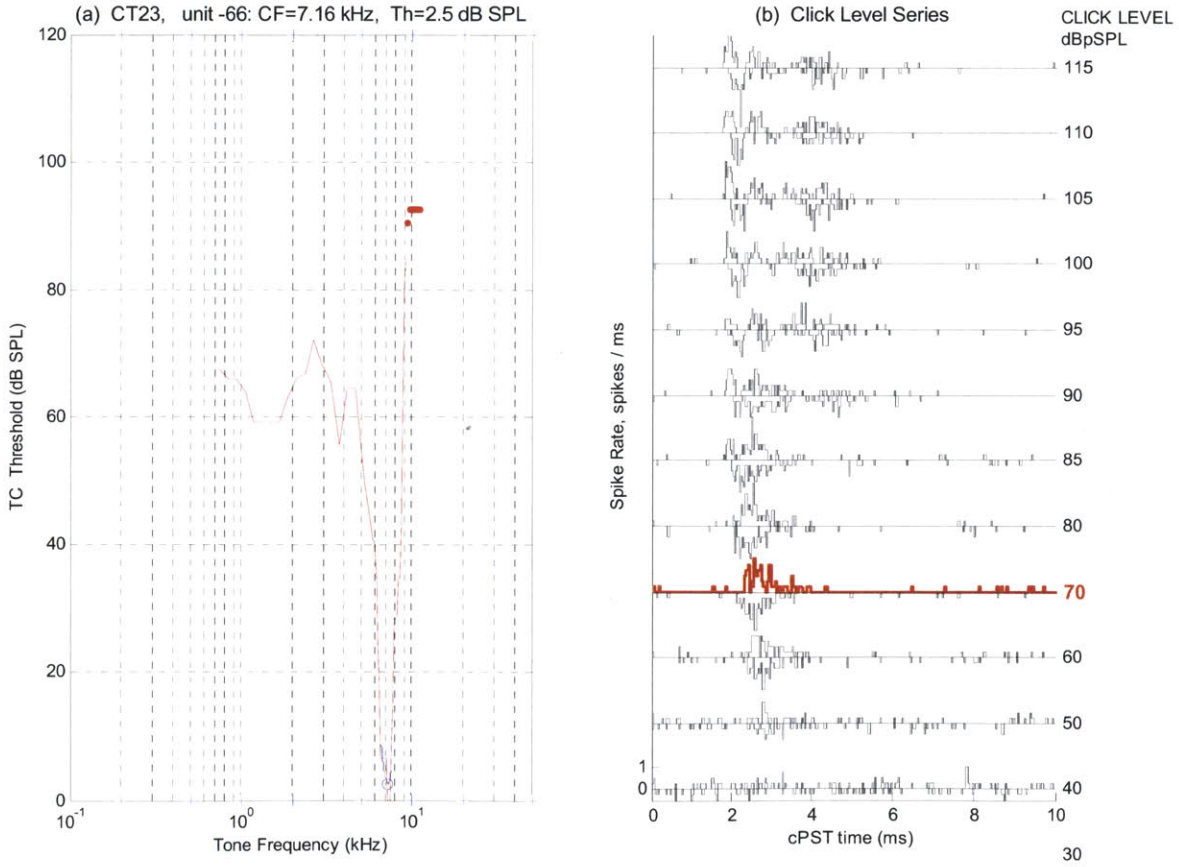

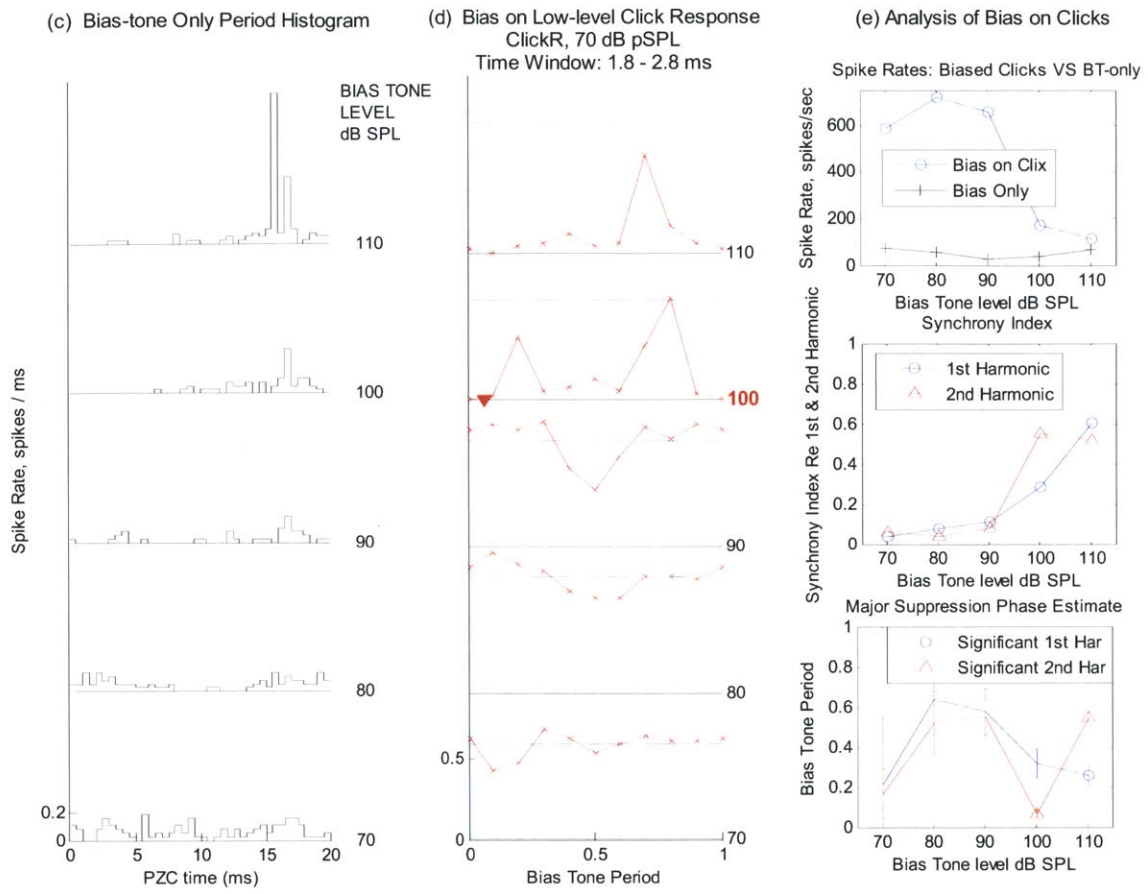

Fig. 3.29 Example Result: (a) Tuning Curve, CF= 7.16 kHz and SR= 80 sps; (b) Click Level Series, ClickR at 70 dB pSPL selected for bias-tone effects; (c) Bias-tone (BT) only level series: peak splitting was not present. Only the narrow peak appeared at ~110 dB SPL, but the rate threshold was note met; (d) Bias-tone level-series on click response, ClickR at 70 dB pSPL, Time window 1.8 – 2.8 ms. The suppression threshold was met at 100 dB SPL with the second harmonic. The major suppression phase was opposite of the typical value; however, at 10 dB the threshold, the actual major suppression phase can be seen in the typical location. Therefore, the actual suppression characteristic of this fiber was not different from the typical pattern; (e) Detailed analysis of the bias-tone effects on click response, Bias-tone level functions of firing rate, synchrony indices and phase of major suppression for the 1st and 2nd harmonic in the top-bottom order.

IV. Discussion

A. The Suppression Effects on AN Firing Reported in This Study Were Primarily Due to Stimulation of OHCs rather than Direct Stimulation of IHC Stereocilia by the 50 Hz Bias-tone

Although 50 Hz bias-tone used in this study is expected to stimulate the OHC stereocilia with higher amplitude than the IHC stereocilia [Russell and Sellick, 1983], it has been found in this study and elsewhere [Sellick et al, 1982; Patuzzi et al, 1984a; Cai and Geisler, 1996a] that AN responses to bias-tone level series with bias-tone alone do show both firing rate elevation and phasic modulation of period histograms at high enough levels of bias-tone. Consequently, it would be necessary to examine whether the results reported in this study as suppressive effects on OHC transduction function were not significantly affected by direct stimulation of the IHC stereocilia by the bias-tone.

In order to detect results with potential effects of direct stimulation of IHC stereocilia by the bias-tone, the excitation threshold level on AN firing by the bias-tone alone was measured from the AN response to level series of bias-tone alone from each AN fiber. Then, the results from the bias-tone level series on click responses at the bias-tone level at or above the excitation threshold were not included in the data pool for suppression effects.

The criteria to determine the excitation threshold of an AN fiber required firing rate elevation by a standard deviation and the standard error on the vector phase of firing to be within ±20°. Now, it would be necessary to examine whether the criteria applied on the reported results were appropriate. In order to examine the impact of the excitation threshold criteria on the suppression data, several iterations of data analysis were done with varying degrees of criteria around the values applied on the reported results. For example, the rate criteria with smaller increment such as ½ of standard deviation and the phase criteria with larger error bound such as ±30° are expected to lower the threshold of excitation by the bias-tone alone whereas a larger increment of firing rate such as two standard deviation and lower error bound on phase such as 10° would elevate the excitation threshold. Series of plots of the excitation phase by 50 Hz bias-tone alone and the major suppression phase on click response components as shown in Fig. 3.17 and Fig. 3.20 with varying criteria on the excitation threshold did not reveal significant shifts in the results other than the number and scatter of data points around the same trend. Considering these, the suppression Effects on AN Firing reported in this study were primarily due to stimulation of OHCs rather than direct stimulation of IHC stereocilia by the 50 Hz bias-tone.

B. The Suppression Data on Click Response Components from AN Fibers Show that the Non-linear Mechanoelectric Transduction Function of OHCs are Involved in Generating ANIP and ANSP as well as Low-level Click Responses

Qualitatively the suppression effects of 50 Hz bias-tones on the three click response components from AN fibers were similar to the widely reported results on the suppression effects on AN responses to low-level CF-tones [Patuzzi et al, 1984a; Cai and Geisler, 1996a]. As in the suppressive effects on low-level CF-tone responses, the suppressive patterns on AN responses to click components typically progressed from the appearance of a major suppression phase to two suppression phases at opposite phases at higher levels of the bias-tone.

Previous studies have shown that the mechanism behind these suppression patterns on low-level CF-tone responses is likely to be at the non-linear mechanoelectric transduction function of OHCs with saturating plateaus at either ends of the stereocilia deflection [Robles and Ruggero, 2001]. As for the non-linearity of OHCs in response generation of ANIP and ANSP, the possibility of the involvement of the stereocilia motility of OHCs rather than electromotility has been discussed in [Guinan et al, 2005]. Since the transduction function for force generation by OHCs through their stereocilia motility also involves saturating plateaus at either ends of stereocilia deflection [Fettiplace, 2006; Hudspeth, 2008], the possibility that the bias-tone suppression patterns found on ANIP and ANSP responses may be due to stereocilia motility cannot be completely ruled out. However, as argued in [Guinan et al, 2005] stereocilia motility is unlikely to be the drive mechanism behind ANIP and ANSP since stimulation of MOC efferents is expected to enhance stereocilia motility rather than inhibiting it since hyperpolarization of OHCs brought on by MOC efferent stimulation would result in increased influx of the Ca^{2+} ions which in turn is expected to increase OHC sterecilia motility. The suppression data on ANIP, ANSP and low-level click responses found in this study along with the inhibitive effects by MOC efferents [Guinan et al, 2005] strongly suggest that both the mechanoelectric transduction function and the elctromotility of OHCs are involved in generating ANIP and ANSP responses at mid-to-high-levels of clicks as well as low-level click responses from AN fibers.

C. Reversal of Major Suppression Phase between the Low-level Click Responses VS ANIP and ANSP at Mid-to-high-levels of Clicks

Although the overall pattern of suppressive effects by a low-frequency tone on AN responses to low-level clicks, ANIP and ANSP were similar whereby two suppression phases at opposite phases were found from all three click response types in this study, the phase of major suppression by 50 Hz bias-tone on low-level click responses was opposite to that on ANIP and ANSP as shown in Fig. 3.20 while the major suppression phase of ANIP and ANSP at mid-high click levels was quite similar to each other such that the data for ANIP and ANSP were located within one standard error of ± 20°. These data are in support of the hypothesis that the mechanism of OHC involvement in generating AN responses to low-level clicks VS ANIP and ANSP at mid-to-high-levels of clicks are somehow different [Guinan et al, 2005]. Further, similar to the stronger inhibitive effect on ANIP compared to ANSP by MOC efferent stimulation reported in [Guinan et al, 2005], the threshold of suppression on ANSP was ~5 dB higher than that of ANIP thereby supporting the hypothesis that ANSP may consist of offset envelope of ANIP response which is actively driven by OHCs through an unknown mechanism and the onset of another type of response with a longer latency than ANIP where OHCs are not actively involved in response generation [Guinan et al, 2005].

D. Previous Reports of Reversal of Major Suppression Phase by a Low-frequency Bias-tone on AN Responses

It is of interest to review previous reports of results which are similar to the key findings of this study, i.e., reversal of the major suppression phase of low-frequency bias-tone effects on AN responses in order to gather any insights that they may provide. From the suppression patterns on AN responses to low-level CF-tones by low-frequency bias-tones from cats, [Cai and Geisler, 1996a] reported a wide range of major suppression phase spanning 180° from the basal region of the cochlea with the CF of 8.1

kHz < CF < 13 kHz. Specifically, Fig. 10 of [Cai and Geisler, 1996a] shows fibers with opposite phase of major suppression phase along with fibers with very symmetrical depths of suppression. In the companion paper to [Cai and Geisler, 1996a], the mechanism behind the varying location of the major suppression phase among those individual fibers in the basal region was attributed to the varying location of the operating point of the mechanoelectric transduction function of OHCs operating behind the AN fibers [Cai and Geisler, 1996c]. Specifically, for the fibers with symmetrical shape of the suppression phases, the operating point of the OHC transduction function was attributed to a location symmetrical across the two saturation plateaus as in Fig. 3.2(a). For fibers with the major suppression phase which was similar to the apical fibers, the operating point was placed away from the depolarizing voltage plateau as in Fig. 3.30(a) while the fibers with reversal of the major suppression phase, the operating point of the OHC transduction function was placed away from the hyperpolarizing voltage plateau as in Fig. 3.30(b).

Although the stimulus paradigm and the CF region of the AN fibers in [Cai AND Geisler, 1996a] are different from this study, the cochlear mechanistic interpretations of reversal of the major suppression phase in [Cai and Geisler, 1996c] raises the following question on the results from this study: Was the operating point of the mechanoelectric transduction function of OHCs also shifted as described in [Cai and Geisler, 1996c] from low-levels of clicks to mid-to-high-levels of clicks coincident with the reversal of the major suppression phase on AN responses to low-level clicks VS ANIP and ANSP? Experimentally based answers to this question would require intracellular recordings of transduction voltage of the OHCs from the apex of the cochlea under the experimental paradigm of bias-tone on click response as done in this study. Such data are currently unavailable and expected to be difficult to obtain due to the challenges of maintaining the health of the cochlea during intracellular recordings from the apex of the cochlea [Dallos, 1986]. However, it would be desirable to review relevant studies from the past which have been primarily from the base of the cochlea for any insights that they might provide [Cody and Russell, 1985; Cody and Russell, 1987; Russell and Kössl, 1992].

E. Shift in the Operating Point of OHC Mechanoelectric Transduction Function Can be Seen From Shift in the DC Component of OHC Transduction Voltage

The transduction voltage response of OHCs to low-frequency tones have been found to show both AC and DC component [Cody and Russell, 1985; Dallos, 1986]. It is widely accepted that the DC component is generated by the non-linearity in the OHC transduction function, particularly by the asymmetry of the operating point from the saturation plateaus of the mechanoelectric transduction function of OHCs [Cody and Russell, 1985; Dallos, 1986]. Specifically, a positive DC component in the OHC transduction voltage has been associated with asymmetry similar to that of Fig. 3.30(a) where the operating point is away from the depolarizing voltage output as seen predominantly from the OHCs in the apex of the cochlea [Dallos, 1986]. Further, negative DC component from the OHC transduction voltage has also been found from the base of guinea pig cochlea [Cody and Russell, 1985; Cody and Russell, 1987] thereby supporting the theory proposed in [Cai and Geisler, 1996c] which links the reversal of the major suppression phase induced by a low-frequency bias-tone with a reversal of the asymmetry of the operating point of OHC transduction function over different regions of the cochlea. Furthermore, the DC component of the OHC transduction function from the base of the guinea pig

cochlea has been found to change over increasing levels of a low-frequency tone with frequencies in the range of 200 Hz – 600 Hz [Cody and Russell, 1985; Cody and Russell, 1987]. Specifically, at low and moderate levels of low-frequency tones, the DC component was negative thereby suggesting the shape of the underlying mechanoelectric transduction function similar to that of Fig. 3.30(b). At high levels of the tone stimulus above 90 dB SPL, the DC component was nulled out and came back with an inverted polarity of positive voltage over increasing levels of the tone [Cody and Russell, 1985; Cody and Russell, 1987] thereby suggesting a reversal in the asymmetry of the operating point of the OHC transduction function over the levels of the tone stimulus. These studies have shown that the asymmetry of the operating point of OHCs vary across the cochlea regions and also dynamically shift over the levels of sound stimulus at a given cochlea location thereby providing a level of support to the hypothesis that the reversal of the major suppression phase on AN responses to clicks from low-levels of clicks to mid-to-high-levels of clicks generating ANIP and ANSP as found in this study may be linked to shift in the operating point of the OHC transduction function over the levels of click stimulus.

Also in [Cody and Russell, 1987], the mechanism responsible for dynamic shift in the operating point of OHC transduction function over tone stimulus levels has been considered. It has been argued in [Cody and Russell, 1987] that the dynamic shift in the operating point of OHC transduction function is likely to be due to changes in the mechanical input to the OHC stereocilia over tone stimulus levels arising from micromechanical changes in the positions and motions of OHC stereocilia and tectorial membrane rather than due to non-linearity inherent in the OHCs since OHC transduction voltage measurements in vitro in response to direct mechanical stimulation of OHC stereocilia do not show any shift in the asymmetry in the operating point. The issue of potential changes in the cochlear mechanics linked with shift in the operating point of OHC transduction function over stimulus tone levels has been investigated in [Russell and Kössl, 1992] through recordings of the OHC receptor potential from the basal region of guinea pig cochlea under the paradigm of 100 Hz bias-tone presented together with a near-CF-tone [Russell and Kössl, 1992] as discussed in the next section.

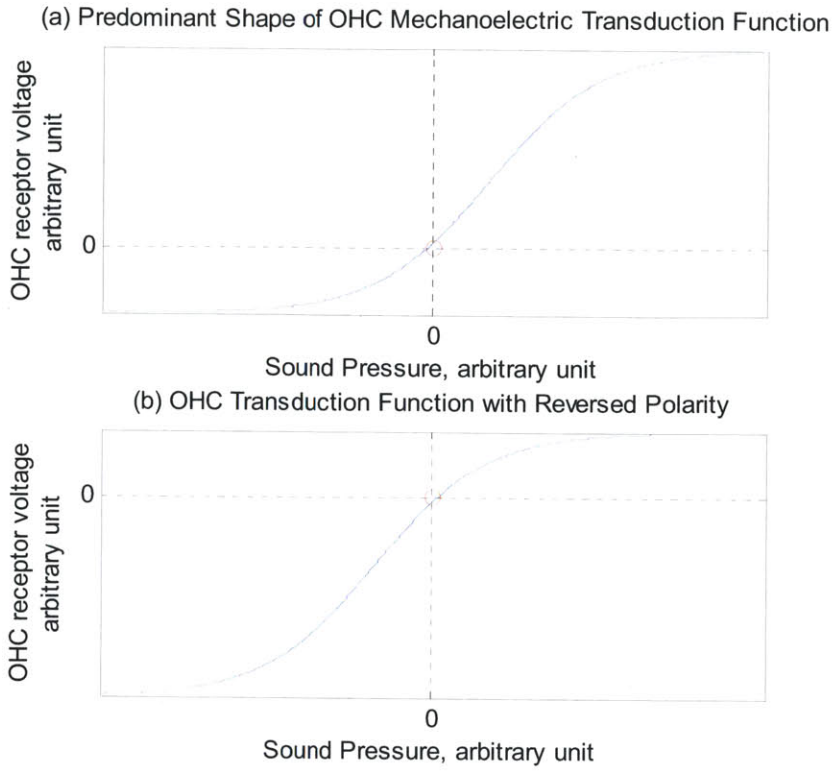

Fig. 3.30 Schematized version of non-linear mechanoelectric transduction function of OHCs: (a) the predominant shape where the operating point leads to depolarizing DC component in OHC receptor potentials; (b) hypothetical version of a OHC transduction function with polarity reversal. The location of the operating point leads to hyperpolarizing DC component in OHC receptor potential

F. Previous Reports of Changes in the Cochlear Mechanics Related to Shift in the Operating Point of Mechanoelectric Transduction Function of OHCs

A low-frequency bias-tone is known to suppress OHC and IHC receptor voltages as well as AN firings in response to low-level CF-tones with two suppression phases at opposite phases of the bias-tone at high enough levels [Pattuzi and Sellick, 1984]. In [Russell and Kössl, 1992], the effects of 100 Hz bias-tone at the fixed level of 80 dB SPL on the IHC and OHC receptor voltages of guinea pigs in response to tone stimulus near the CF (CF = 16 kHz) of the recording site were studied. The intensity of the near-CF-tone stimuli extended from 30 dB SPL to 105 dB SPL which went well above the saturation threshold of the OHC and IHC responses. As expected, at low-levels of the near-CF-tone stimuli, the bias-tone suppressed the OHC and IHC receptor potentials in response to the near-CF-tone. Also, as expected from the saturation of the "cochlear amplifier" at high-levels of the near-CF-tone stimuli, the suppression effects by the 100 Hz bias-tone on OHC and IHC receptor potentials in response to high-levels of near-CF-tone stimulus above ~70 dB SPL were negligible.

Along with these expected results on the suppressive effects on the near-CF tone component of the OHC responses, significant changes in the DC component of the OHC transduction function were seen across the saturation level of the near-CF-tone stimulus. Specifically, with the near-CF-tone stimuli with

frequencies of ~1/2 octave below the CF presented together with the bias-tone, the negative value of the DC component of the OHC transduction function measured at low levels of the near-CF tone was nulled out, and returned with a polarity reversal as a positive value over increasing levels above ~80 dB SPL of the near-CF tone. These results show that the near-CF tone component of OHC response which is driven by the "cochlear amplifier" was saturated over the level of the near-CF-tone where significant shift in the operating point of the OHC transduction function was observed. Furthermore, over this critical transition level of the near-CF tone, the phase of both 100 Hz bias-tone component and the near-CF-tone component went through a sharp reversal [Russell and Kössl, 1992]. These results show that significant changes in the cochlear mechanics, i.e., saturation of the cochlear amplifier and reversal of phase in both 100 Hz bias-tone and near-CF-tone response, occurred over the shift in the operating point of the OHC transduction function. As for the micromechanics behind the shift in the operating point of OHC transduction function and the concurrent changes in the cochlear mechanics listed above, changes in the dynamics of the feedback loop involving the TM-OHC-BM complex brought on by stimulus dependent changes in the rotational stiffness of OHC stereocilia or changes in the steady-state length of the OHCs due to non-linearity in the reverse transduction function of OHCs were proposed as potential explanations [Russell and Kössl, 1992].

Despite the differences in the species, stimulus paradigms and the CF region of recording in comparison to this study, the probe-stimulus level dependent shift in the operating point of OHC transduction function found from the base of the guinea pig cochlea in [Cody and Russell, 1987; Russell and Kössl, 1992] are of significance in interpreting the results in this study since it provides a solid framework to interpret the stimulus-level dependent reversal of the major suppression phase on AN responses from low-levels of clicks to mid-to-high-levels of clicks found in this study. Specifically, if the mechanism behind the reversal of the major suppression phase involves shift in the in the operating point of the OHC transduction function from low levels of stimulus to mid-to-high-levels of stimulus through similar mechanism as found and proposed in [Russell and Kössl, 1992], the reversal of the major suppression phase would indicate significant changes in the cochlear mechanics occurring together which includes saturation of the cochlear amplifier at mid-to-high-levels of clicks. This interpretation would be entirely consistent with the studies on MOC efferent effects on AN responses to click level series where the inhibitive effects on AN response to mid-to-high levels of clicks were limited to ANIP and ANSP which are thought to be driven by a mechanism which is different from the "cochlear amplifier" while the later peaks were not affected since the gain of the "cochlear amplifier" is significantly reduced at mid-to-high-levels of clicks. Therefore, this interpretation is in support of the hypothesis that ANIP and ANSP are driven by OHC electromotility through an unknown coupling mechanism to the IHCs which must be different from the BM-based cochlear amplifier [Guinan et al, 2005; Guinan, 2009].

V. References

Cai Y, Geisler CD (1996a) Suppression in auditory-nerve fibers of cats using low-side suppressors. I. Temporal aspects. Hear Res. 1996 Jul;96(1-2):94-112

Cai Y, Geisler CD (1996c) Suppression in auditory-nerve fibers of cats using low-side suppressors. III. Model results. Hear Res. 1996 Jul;96(1-2):126-40.

Cody AR, Russell IJ. (1985) Outer hair cells in the mammalian cochlea and noise-induced hearing loss. Nature. 1985 Jun 20-26;315(6021):662-5.

Cody AR, Russell IJ. (1987) The response of hair cells in the basal turn of the guinea-pig cochlea to tones. J Physiol. 1987 Feb;383:551-69.

Dallos P. (1985) Membrane potential and response changes in mammalian cochlear hair cells during intracellular recording. J Neurosci. 1985 Jun;5(6):1609-15.

Dallos P. (1986) Neurobiology of cochlear inner and outer hair cells: intracellular recordings. Hear Res. 1986;22:185-98.

Fettiplace R. (2006) Active hair bundle movements in auditory hair cells. J Physiol. 2006 Oct 1;576(Pt 1):29-36. Epub 2006 Aug 3. Review.

Geisler CD, Nuttall AL. (1997). Two-tone suppression of basilar membrane vibrations in the base of the guinea pig cochlea using "low-side" suppressors. J Acoust Soc Am. 1997 Jul;102(1):430-40.

Goldberg, J. M., and Brown, P. B. (1969). "Response of binaural neurons of dog superior olivary complex to dichotictonal stimuli: some physiological mechanisms Of sound localization, "J. Neurophysiol. 32, 613-636.

Guinan JJ Jr, Lin T, Cheng H. (2005) Medial-olivocochlear-efferent inhibition of the first peak of auditory-nerve responses: evidence for a new motion within the cochlea. J Acoust Soc Am. 2005 Oct;118(4):2421-33

Guinan JJ Jr, Cooper NP. (2008) Medial olivocochlear efferent inhibition of basilar-membrane responses to clicks: evidence for two modes of cochlear mechanical excitation. J Acoust Soc Am. 2008 Aug;124(2):1080-92.

Guinan J.J., Jr. (2009). Bias-tone effects on auditory-nerve responses reveal three mechanical drives, two dependent on outer-hair-cell motility and one passive. Asso. Res. Otolaryngol. Abstr 33, #1109.

Hudspeth AJ. (2008) Making an effort to listen: mechanical amplification in the ear. Neuron. 2008 Aug 28;59(4):530-45. Review.

Johnson DH. (1980) The relationship between spike rate and synchrony in responses of auditory-nerve fibers to single tones. J Acoust Soc Am. 1980 Oct;68(4):1115-22.

Kiang NYS, Watanabe T, Thomas EC, Clark LF (1965) Discharge Patterns of Single Fibers in the Cat's Auditory Nerve (MIT, Cambridge, MA)

Liberman MC, Kiang NY (1984) Single-neuron labeling and chronic cochlear pathology. IV. Stereocilia damage and alterations in rate- and phase-level functions. Hear Res. 1984 Oct;16(1):75-90

Lin T, Guinan JJ Jr. (2000) Auditory-nerve-fiber responses to high-level clicks: interference patterns indicate that excitation is due to the combination of multiple drives. J Acoust Soc Am. 2000 May;107(5 Pt 1):2615-30

Mardia KV (1972) Statistics of Directional Data (Academic Press, New York)

Nowotny M, Gummer AW (2006) Nanomechanics of the subtectorial space caused by electromechanics of cochlear outer hair cells. Proc Natl Acad Sci U S A. 2006 Feb 14;103(7):2120-5. Epub 2006 Feb 6

Patuzzi R, Sellick PM, Johnstone BM (1984a) The modulation of the sensitivity of the mammalian cochlea by low-frequency tones. I. Primary afferent activity. Hear Res. 1984 Jan;13(1):1-8

Patuzzi R, Sellick PM, Johnstone BM (1984b) The modulation of the sensitivity of the mammalian cochlea by low-frequency tones. II. Inner hair cell receptor potentials. Hear Res. 1984 Jan;13(1):9-18

Patuzzi R, Sellick PM, Johnstone BM (1984c) The modulation of the sensitivity of the mammalian cochlea by low-frequency tones. III. Basilar membrane motion. Hear Res. 1984 Jan;13(1):19-27

Patuzzi RB, Yates GK, Johnstone BM. (1989) Outer hair cell receptor current and sensorineural hearing loss. Hear Res. 1989 Oct;42(1):47-72. Review.

Robles L, Ruggero MA. Mechanics of the mammalian cochlea. Physiol Rev. 2001 Jul;81(3):1305-52. Review

Ruggero MA, Robles L, Rich NC (1992) Two-tone suppression in the basilar membrane of the cochlea: mechanical basis of auditory-nerve rate suppression. J Neurophysiol. 1992 Oct;68(4):1087-99

Russell IJ, Sellick PM. (1983) Low-frequency characteristics of intracellularly recorded receptor potentials in guinea-pig cochlear hair cells. J Physiol. 1983 May;338:179-206.

Russell IJ, Cody AR, Richardson GP (1986) The responses of inner and outer hair cells in the basal turn of the guinea-pig cochlea and in the mouse cochlea grown in vitro. Hear Res. 1986;22:199-216.

Russell IJ, Kössl M. (1992) Modulation of hair cell voltage responses to tones by low-frequency biasing of the basilar membrane in the guinea pig cochlea. J Neurosci. 1992 May;12(5):1587-601.

Santos-Sacchi J. (1993) Harmonics of outer hair cell motility. Biophys J. 1993 Nov;65(5):2217-27.

Schoonhoven R, Keijzer J, Versnel H, Prijs VF (1994) A dual filter model describing single-fiber responses to clicks in the normal and noise-damaged cochlea. J Acoust Soc Am. 1994 Apr;95(4):2104-21

Sellick PM, Patuzzi R, Johnstone (1982) BM Modulation of responses of spiral ganglion cells in the guinea pig cochlea by low-frequency sound. Hear Res. 1982 Jul;7(2):199-221

Stankovic KM, Guinan JJ Jr. (1999) Medial efferent effects on auditory-nerve responses to tail-frequency tones. I. Rate reduction. J Acoust Soc Am. 1999 Aug;106(2):857-69

Stankovic KM, Guinan JJ Jr. (2000) Medial efferent effects on auditory-nerve responses to tail-frequency tones II: alteration of phase. J Acoust Soc Am. 2000 Aug;108(2):664-78.

Temchin AN, Rich NC, Ruggero MA. (1997) Low-frequency suppression of auditory nerve responses to characteristic frequency tones. Hear Res. 1997 Nov;113(1-2):29-56.

Chapter 4 . Bias-tone Effects on Low-level CF-tone and Off-CF-tone Responses from Low-CF Fibers

I. Introduction

Cochlear mechanics in the apex has long been suggested to differ significantly from the base [Kiang, 1984; Liberman, 1984; Carney et al, 1999]. Supporting evidence for this notion comes from the discontinuities in the function of group delay VS frequency measurements from auditory nerve (ANs) responses to tones from low-CF fibers with CF < 4 kHz where a CF-centered region with longer group delay adjoins a "side-lobe" or "off-CF" region with shorter group delay [Pfeiffer & Molnar, 1980; Kiang, 1984]. For AN fibers with CF < 1 kHz from cats [Pfeiffer & Molnar, 1980; Kiang, 1984; Van der Heijden & Joris, 2006] and chinchillas [Temchin et al, 2009], the group delay VS frequency function constructed from AN responses to tones can be described as a composite of two regions where the shorter group delay is seen from stimulus tone frequencies above the CF of the fiber in comparison to the lower frequency region which extends slightly above the CF of the fiber. Further, similar discontinuities in the slope of the threshold tuning curves (TC) of AN fibers with CF < 1 kHz can be found whereby the sharply tuned tip region adjoins the broadly tuned "side-lobe" region with similar locations of the break frequencies in the group delay function and TC of the fiber [Kiang, 1984]. These characteristics of TC and group delay function of AN fibers with CF < 1 kHz are illustrated through an example in Fig. 4.1 for an AN fiber of a cat with CF = 0.4 kHz. Further, for AN fibers with 1 kHz < CF < 4 kHz, similar discontinuities can be found in the group delay function and TC of the fiber but at the frequency location of the shorter group delay region in the low-frequency-side of the CF in contrast to the fibers with CF < 1 kHz [Pfeiffer & Molnar, 1980; Kiang, 1984; Van der Heijden & Joris, 2006; Temchin et al, 2009]. These characteristics have been interpreted through the hypothesis that they are likely due to multiple sources driving the inner hair cells (IHCs) of low-CF fibers [Lin and Guinan, 2000; Guinan et al, 2005].

Recent work exploring the relationship between the group delay function of tone responses and the temporal trajectory of the instantaneous frequency (referred to as "frequency glide" in the cochlear mechanics literature) of impulse responses from ANs and basilar membrane (BM) vibrations allows some critical evaluation of the above hypothesis. Studies have found that the location of the frequency region with shorter group delay relative to the CF of the AN fiber in its tone responses is related to direction of the "frequency glide" in the click responses [Carney et al, 1999]. For low-CF fibers with CF < 1 kHz where the shorter group delay region is located in the upper-side frequencies re. the CF of the fiber, the instantaneous frequency of the click responses descends from above-CF frequencies settling down to the CF of the fiber. In contrast, for low-CF fibers with 1 kHz < CF < 4 kHz, where the shorter group delay region is located in the lower-side frequencies re. the CF of the fiber, the instantaneous frequency in the click responses ascends from below-CF frequencies leveling to the CF of the fiber [Carney et al, 1999; Temchin et al, 2009]. Measurements of group delay VS frequency and frequency glide of impulse responses from the basal region of BM with the characteristic place > 5 kHz of guinea pigs [deBoer and Nuttall, 1997] showed similar pattern of the group delay and frequency glide as found with the low-CF AN fibers with 1 kHz < CF < 4 kHz. These similarities in the BM measurement data from the basal region and the AN response characteristics for AN fibers with 1 kHz < CF < 4 kHz led to the view

whereby the mechanism behind the upward frequency glide and the discontinuities in the group delay found from AN fibers with CF > 1 kHz can be explained through the frequency dispersive wave propagation of BM rather than multiple sources driving the IHCs of AN fibers [Carney, 1999; Shera, 2001]. With this current view point, cochlear mechanics as seen from the basal region of the cochlea is thought to extend down to the CF of ~1.5 kHz where an upward frequency glide is seen from impulse responses, and in the frequency domain, the sharply tuned CF region is flanked by the broadly tuned low-frequency tail region with lower group delay [Shera, 2001]. Even with this view point, however, cochlear mechanics for the apical region with CF < 1 kHz, which is characterized by an upward frequency glide in the impulse response, remains unclear and thought to differ significantly from the base of the cochlea [Carney, 1999].

In exploring the cochlear mechanics in the apex of the cochlea, it is of particular interest to investigate the role of outer hair cells (OHC) in giving rise to the peculiar characteristics of the AN firing patterns from the apical fibers; for example, the role of OHCs in generating AN responses to the tones from the "off-CF" or "side-lobe" region with shorter group delay. OHCs have been found to be directly responsible for the high sensitivity and sharp frequency tuning associated with the low-level click and low-level CF tone responses [Liberman and Kiang, 1984; Schoonhoven et al, 1994]. Now it is widely accepted that the theory of the OHC based "cochlear amplifier" provides adequate explanations to the mechanism behind the generation of the AN responses to low-level CF tone and low-level clicks [Ruggero, 2001]. The critical part of the "cochlear amplifier" lies at the mechanical feedback between the BM and OHCs whereby the stereocilia of OHCs transduce the BM vibration to OHC transmembrane receptor voltage which returns as changes to the BM movement through the electromotility of the OHCs [Ruggero, 2001].

The role of OHCs in generating AN responses from the apical fibers to the tones from the CF and the "off-CF" or "side-lobe" frequency regions have been investigated by studying the effects of electrical stimulation of medial olivocochlear (MOC) efferent fibers on AN responses to tones [Gifford and Guinan, 1988c]. Through the efferent synapse on OHCs, electrical stimulation of MOC efferents has been found to inhibit electromotility of OHCs thereby inhibiting AN responses driven by electromotility of OHCs such as AN responses to low-level CF-tone responses [Guinan, 1996]. The studies have revealed that MOC efferent stimulation resulted in significant inhibition of AN responses to tones from the CF-centered tip region and also from the off-CF frequency region of apical fibers. One peculiar finding from this study was that for some fibers with CFs near 1 – 2 kHz, the inhibitory effects on the near-threshold level off-CF-tone responses were stronger than on the near-threshold level CF-tone responses thereby resulting in further sharpening of tuning rather than broadening of tuning due to MOC efferent stimulation as found from the rest of the fibers [Gifford and Guinan, 1988c]. The unexpected sharpening of tuning of a low-CF fiber resulting from stimulation of MOC efferent is illustrated through an example with a cat's AN fiber with CF = 0.8 kHz in Fig. 4.2. In a recent work [Guinan, 2009], these findings have been interpreted as an indication that the detailed mechanism of OHCs in generating the "off-CF" tone responses from these low-CF fibers may be distinct from the mechanism generating low-level CF-tone responses, i.e., the BM-based cochlear amplifier.

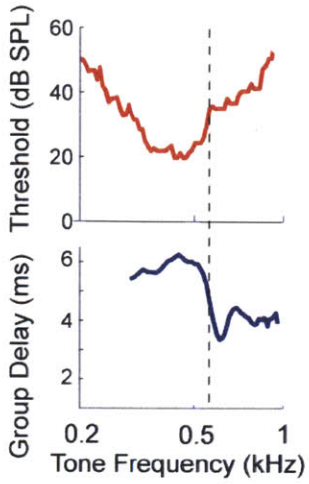

Fig. 4.1. Tuning Curve & Phase Response Plot of a Low CF=0.4kHz fiber. The phase response displayed as the group delay VS frequency plot shows two distinct regions where the delay group values for tone frequencies above the CF of the fiber are distinctly lower compared to the lower half of tone frequency. Note that the break-frequency in the group delay is aligned with the break-frequency in the neural threshold tuning curve demarking the side-lobe region. Courtesy of Prof. John J Guinan [Guinan, 2009]

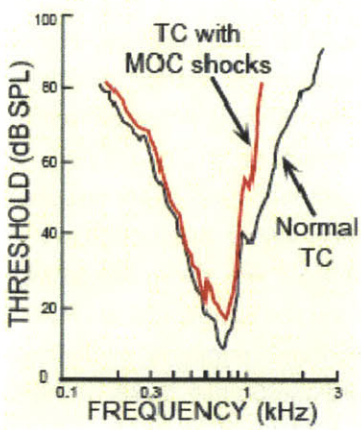

Fig. 4.2. MOC efferent stimulation inhibits the off-CF portion of responses more strongly from fibers with CF near 1 – 2 kHz thereby sharpening the tuning of the neural threshold TC. . Courtesy of Prof. John J Guinan [Guinan, 2009]

The objective of this study is further explorations on the possible differences in the OHC mechanism behind generation of AN responses from low-CF fibers with CF < 4 kHz to tones from the CF

VS the "off-CF" region of the fiber where shorter group delay values in comparison to the CF-tone region were reported in [Pfeiffer & Molnar, 1980; Kiang, 1984; Van der Heijden & Joris, 2006]. Specifically, the selection criteria for the "off-CF" tone frequency was for the selected frequency to be in the region with lower value of group delay in comparison to the CF region as reported in [Pfeiffer & Molnar, 1980; Kiang, 1984; Van der Heijden & Joris, 2006]. Rather than directly measuring the phase-frequency response from each fiber, determination of the "off-CF" region with shorter group delay for all fibers was based on the group delay measurements from low-CF fibers reported in [Pfeiffer & Molnar, 1980; Kiang, 1984; Van der Heijden & Joris, 2006; Temchin et al, 2009] where such "off-CF" region was found at either the low-frequency or high-frequency side of the CF for fibers with CF higher or lower than some break-frequency values respectively. Specifically, [Pfeiffer and Molnar, 1980] reported that the off-CF region with lower group delay could be found in the high-frequency side of the CF for fibers with CF < 1 kHz, and on the low-frequency side of the CF for fibers with CF > 1.2 kHz for cats AN fibers. Similar values of break-frequencies can be found elsewhere for cats AN [Van der Heijden & Joris, 2006; Carney et al, 1999] and for ANs of chinchillas [Temchin et al, 2009]. Accordingly, in this study a single break-frequency of 1.2 kHz was used whereby the "off-CF" tone frequency was selected from the high-side and low-side of the CF for fibers with CF ≤ 1.2 kHz and CF > 1.2 kHz respectively. Specifically, from either the low- or high-side of the CF as described above, the off-CF-tone frequency was selected with the spacing of 0.7 – 2 octave from the CF of the fiber. Note that the frequency spacing of the "off-CF" tone from the CF of the fiber was also based on the group delay measurements reported in [Van der Heijden & Joris, 2006; Temchin et al, 2009]. Specifically, [Temchin et al, 2009] reported that the lower-group delay region began at ~0.5 octave away from the CF of the fiber, and it can be seen from Figure 3 of [Van der Heijden & Joris, 2006] that the "off-CF" region with lower group delay can be found at ~0.7 – 1 octave from the CF of the fiber for the population of fibers in their study. In the remainder of this chapter, the terms "off-CF" are based on the above definitions.

As for the experimental approach toward exploring the role of OHC mechanism behind the AN responses to CF-tone VS off-CF tones, suppressive effects by a low-frequency bias-tone on AN responses to tones from the CF region VS the "off-CF" region were measured and compared.

A low-frequency tone such as 50 Hz with high enough amplitude but still under the neural threshold level has been known to suppress the firing pattern of AN invoked by a second higher frequency probe tone with a temporal pattern of suppression which is synchronized with the low-frequency bias-tone [Ruggero et al, 1992]. Typically the suppressive effects at low bias-tone levels start with a single suppression phase re. the bias-tone-period which deepens with increasing bias-tone level, and often progress to two suppression phases located at the opposite phases of the bias-tone-period [Patuzzi et al, 1984a].

The mechanism behind this typical suppression pattern has been found in the saturating non-linearity of the mechano-electric transduction function of OHCs which converts deflections of OHC stereocilia into transmembrane current [Robles and Ruggero, 2001]. In-vivo measurements of the OHC receptor potential in response to low-frequency acoustic tone stimuli from guinea pigs have shown that the mechano-electric transduction function can be generally described as a curve with saturating non-linearity at both ends of the output [Dallos, 1985; Russell et al, 1986]. Further, it has been found that

the sharpness of saturation and the location of the transduction operating point on the curve depend on the CF location within the cochlea [Dallos, 1985; Russell et al, 1986]. A schematized version of the transduction function from the basal region of guinea pig cochlea as reported in Fig. 1 of [Russell et al, 1986] is shown in Fig 4.3(a) where the operating point is located approximately in the middle of the two saturation plateaus. Also, a schematized version of the transduction function from the apical region of guinea pig cochlea as reported in Fig. 10 of [Dallos, 1985] is shown in Fig 4.3(b) where the operating point is located closer to the hyperpolarizing saturation plateau.

The shape of the nonlinear transduction function of the OHCs is strikingly well reflected in the two tone interactions between a low-level probe tone and a second low-frequency bias-tone in BM movement, hair cell receptor voltage and firing patterns from AN fibers [Ruggero et al, 1992; Patuzzi et al, 1984b; Cai and Geisler, 1996c]. A low-frequency bias-tone with high enough amplitude sinusoidally deflects the OHC stereocilia over a wide range such that the operating point of the mechano-electric transduction function traverses through the two saturating end regions during each cycle of the low-frequency bias-tone. Therefore, the gain of the OHC mechanoelectric transduction function and AN responses driven by it are suppressed as the operating point of the OHC transduction passes through the two saturating regions. Further, depending on the location of the operating point of the OHC transduction function at the particular place within the cochlea, one of the suppression phases emerges at a lower level of the bias-tone with a larger depth of modulation [Cai and Geisler, 1996a; Cai and Geisler, 1996c].

Suppression effects on AN responses to a low-level CF-tone by a low-frequency bias-tone are illustrated through the AN firing pattern evoked by a low-level CF-tone at 1.6 kHz and a 50 Hz bias-tone recorded from a cat AN fiber with a CF of 1.63 kHz. Fig. 4.5 shows the bias-tone level series of bias-tone-period histograms which were constructed by binning the spike records relative to the period of the bias-tone. At the bias-tone level of 80 dB SPL, the firing rate in response to the low-level probe tone begins to be suppressed approximately in the middle of the period which is noted as the "major suppression phase". Then, at 90dB SPL the major suppression phase deepens to complete suppression, and a "minor suppression phase" develops at the opposite phase location. These suppression phases would correspond to the phase of the deflections of the OHC stereocilia into the two saturation plateaus brought on by the 50Hz bias-tone.

Analysis of the period histograms of the suppression effects produced by a low-frequency bias-tone on AN responses has served as an important investigative tool which revealed subtle differences in the OHC transduction function from the basal VS apical region of the cochlea [Cai and Geisler, 1996c]. Specifically, analysis of the suppression pattern on low-level CF-tone response recorded from basal AN fibers of cats has shown that the operating point of the OHC transduction function in response to the low-level CF-tone of the fiber is significantly more symmetric across the saturating ends than the apical fibers [Cai and Geisler, 1996c] as seen by the more symmetrical presence of the major and minor suppression phases at the basal region.

Further, previous studies have shown that the phase of suppression can be related to the phase of BM deflection thereby linking the phase of OHC stereocilia deflections brought on by the low-

frequency bias-tone with the phase of BM displacement [Patuzzi et al, 1984a; Temchin et al, 1997; Geisler and Nuttall, 1997]. Specifically, by relating the phase of major suppression with the phase of cochlear microphonic and the phase of excitation by the bias-tone alone, it has been shown that the phase of major suppression on low-level CF-tone responses corresponds to the phase of maximum displacement of the BM toward the scala tympani (ST) in guinea pigs and chinchillas [Patuzzi et al, 1984a; Temchin et al, 1997; Geisler and Nuttall, 1997]. These aspects of the suppressive effects of a low-frequency bias-tone on AN firing are expected to provide insights on the following key questions of this study:

a. Are there significant differences in the low-frequency bias-tone induced suppression patterns on AN responses to CF-tone VS off-CF-tones from low-CF fibers with CF < 4 kHz thereby indicating significant differences in the shape of the mechanoelectric transduction function expressed in the mechanism behind generation of AN responses to CF-tones VS off-CF-tones?

b. Are there any significant differences in the strength of involvement of the OHC mechanoelctric transduction function in the AN response generation mechanism behind the CF-tone VS off-CF-tone response from low-CF fibers with CF < 4 kHz as indicated by the differences in the threshold of suppression on the CF-tone VS off-CF-tone responses?

c. Are there significant differences in the low-frequency bias-tone induced suppression patterns on AN responses to the off-CF-tone responses from the low-CF fibers with CF < 1kHz VS fibers with CF > 1 kHz? These two groups of low-CF fibers are distinct in terms of the direction of frequency glide in their impulse responses.

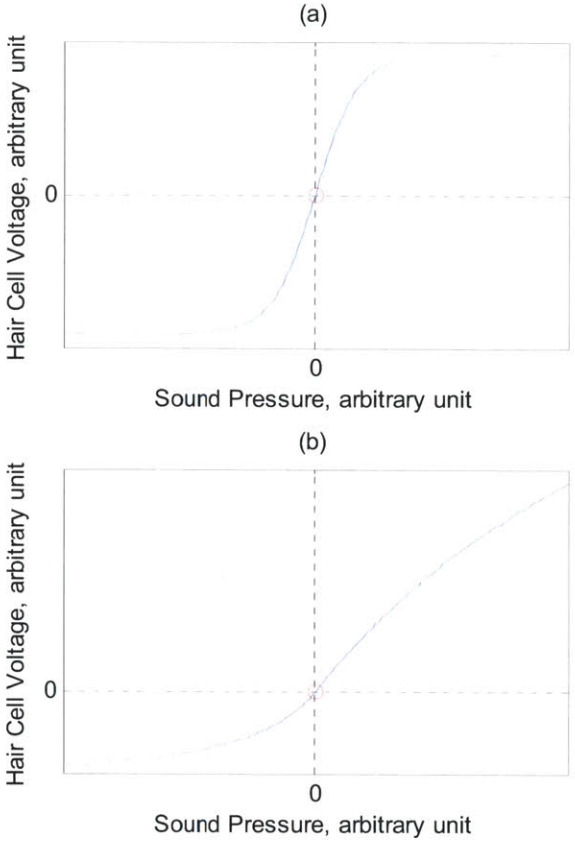

Fig. 4.3. Models of the mechano-electric transduction function of outer hair cells (OHC): they are with saturating non-linearity at either ends of the output. The positive sound pressure indicates rarefaction. The gain of the cochlear amplifier has been linked to the slope of the transduction function at a particular operating point which is indicated by a red dot in the above plots. The operating point has been found to lie at varying degree of asymmetry across the two saturating ends. (a) a schematized version of the OHC mechano-electric transduction function from the basal region of guinea pigs; (b) a schematized version of the OHC mechano-electric transduction function from the apical region of guinea pigs

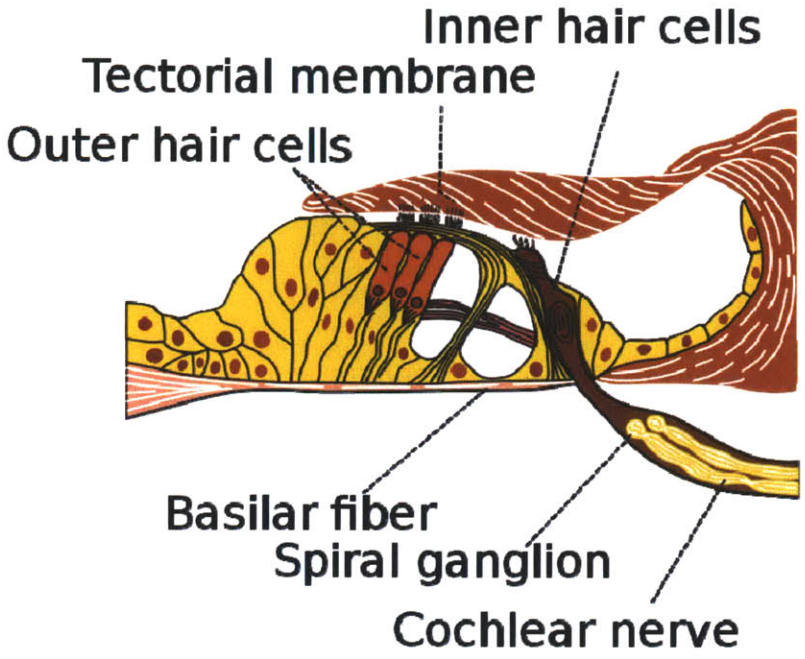

Fig. 4.4. Schematic diagram of the Organ of Corti, the sensory organ within the cochlea. The stereocilia of outer hair cells (OHCs) are embedded into the overlying tectorial membrane whereas the stereocilia of inner hair cells (IHCs) are free-standing within the endolymphatic fluid. Consequently, low-frequency transverse vibrations with frequency below ~100Hz on the Organ of Corti deflect the OHC stereocilia with significantly larger amplitude than the IHC stereocilia.

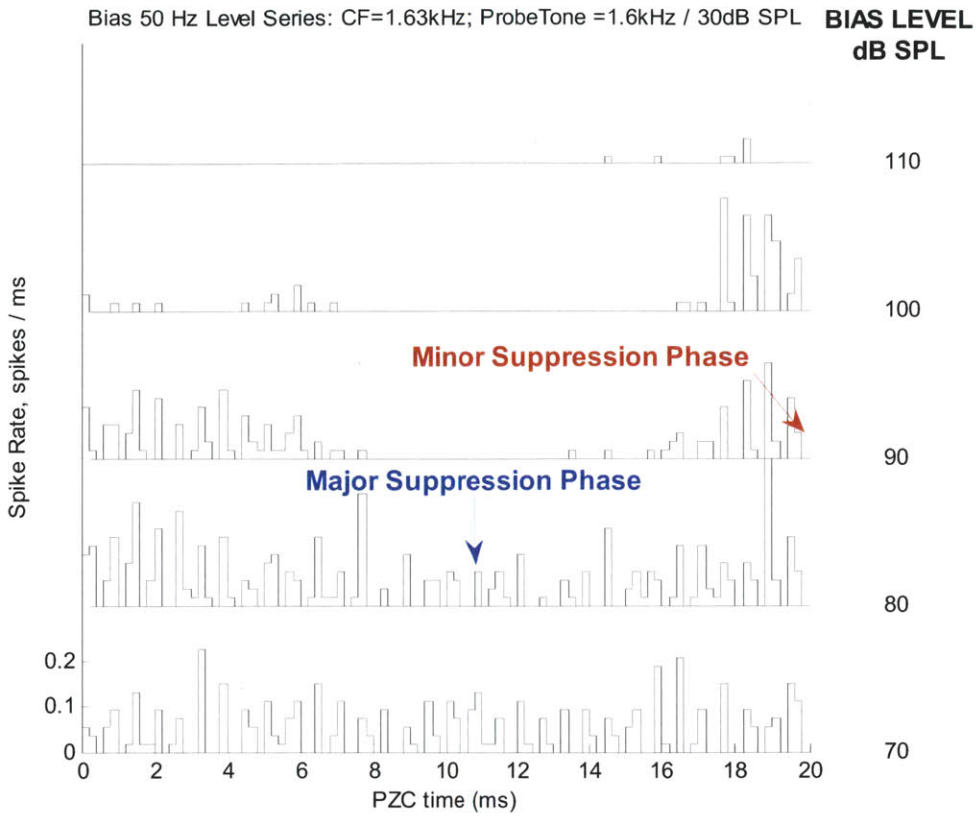

Fig. 4.5. Typical pattern of bias-tone suppression effects on low-level CF-tone responses over a bias-tone level series: a 50 Hz bias-tone at levels, 70-110 dB SPL, was presented together with a low-level CF-tone stimulus. The CF of the fiber was 1.63 kHz. The probe tone was 1.6 kHz at 6 dB above threshold. The spikes were binned re. the bias-tone-period to form bias-tone-period histograms. The bias-tone level series of these histograms are shown as vertically stacked plots with the corresponding bias-tone level indicated to the right of each histogram. The scale of the firing rate indicated for the bottom histogram applies to all the plots. Within each bias-tone-period histogram, the spikes were phase-locked to the probe tone frequency. At the bias-tone level of 80 dB SPL, the firing rate was suppressed in the middle of the period histogram, and at 90 dB SPL, the suppression depth in the middle of the period deepened significantly, and a second suppression phase developed at the opposite phase.

II. Methods

The experiments were done on cats at the Eaton-Peabody Laboratory (EPL) of Auditory Physiology. All experiments were conducted in compliance with protocols approved by the Committee on Animal Care at the Massachusetts Eye and Ear Infirmary.

A. Animal Preparations

23 healthy cats free from ear infections have been used for these experiments. The experimental methods for animal handling, surgical approach to the AN, and methods for recording from AN fibers of cats were as described in [Kiang et al, 1965; Stankovic & Guinan, 1999]. The methods for monitoring the health of hearing during experiments were as described in [Stankovic & Guinan, 1999].

All experiments were acute and began with anaesthetizing the cat with intra-peritoneal (IP) injection of Nembutal in Urethane with the dosage of 150 mg per kg body weight of the animal. Booster injection of the same initial mixture with 1/10 of the initial dose was delivered to maintain the level of the anesthesia. Throughout the duration of the experiment, the depth of anesthesia was monitored based on toe-pinch reflex, heart rate and breathing rate which determined the timing and amounts of the booster injections. The animal's temperature was monitored & maintained at 38 deg C with a rectal thermometer & a heating pad. Experiments typically lasted for 40 to 48 hours during which lactated ringers were dripped into a leg vein through a catheter.

After the initial anesthesia, the bulla cavities of both ears were exposed to reveal the round window. Posterior craniotomy followed by aspiration and retraction of the cerebellar tissues were performed to expose the auditory nerve.

B. Acoustic Setup

All experiments were done inside a double-walled, reduced-reflection chamber. Sound stimuli were delivered with an acoustic assembly consisting of two earphones and a microphone with a probe tube. A DT48 dynamic earphone, capable of high output at low-frequency, was used to generate the low-frequency bias-tone, and all other stimulus types including clicks were generated by the 1-inch condenser earphone [Bruel & Kjaer (B&K) 4145]. The magnitude and phase of the frequency response of the microphone plus probe tube combination were calibrated over the frequency band 0.02–45 kHz using a reference microphone in a calibration set up to measure the sound pressure near the tip of the probe tube. During the experiment, the assembly was placed inside the external meatus so that the probe-tube tip was a few millimeters away from the eardrum. Then, the magnitude and phase of the frequency response of the earphones were calibrated over the frequency band 0.02–40 kHz using the calibrated microphone plus probe tube.

Throughout all experiments, the frequency of the bias-tone was fixed at 50Hz which was selected because a low-frequency tone below 200-600 Hz can more selectively deflect the OHC stereocilia compared to the IHC stereocilia [Russell and Sellick, 1983].

C. Data Collection

A silver electrode was inserted through the bulla opening and placed near the round window to measure the cochlear compound action potentials (CAP). An automated tone-pip audiogram was measured over the frequency range from 0.5kHz to 32kHz at an octave interval with the criterion of 10

μV pp of the CAP. Tone pip audiograms were run periodically every hour or so, and also after a series of good data in order to ensure good health of the cochlea associated with the collected data.

A glass micropipette electrode filled with 3 M KCL electrolyte with 10 -20 MΩ impedance was driven through the exposed view of the auditory nerve by a remotely controlled microdrive until isolating an AN fiber using a wideband noise burst search stimulus. Spike timings were detected with the resolution of 10 μsec.

Upon isolating a unit, a threshold tuning curve (TC) was measured, the CF of the fiber was determined, and the spontaneous rate (SR) of the fiber was measured from a 20 sec duration recording of spontaneous firing. Upon locating a low-CF fiber with CF < 4 kHz, the following list of 50Hz bias-tone paradigms were run:

- Bias-tone alone paradigm
- Bias-tone effects on tone responses: low-level CF-tone and low-level off-CF-tone. The frequency of the off-CF tone was determined as follows.

Selection of the Off-CF tone for bias-tone effect study

The selection criterion for the off-CF tone was for the selected frequency to be in the region with lower value of group delay in comparison to the CF region as reported in [Pfeiffer & Molnar, 1980; Kiang, 1984; Van der Heijden & Joris, 2006]. Rather than directly measuring the phase-frequency response from each fiber, determination of the "off-CF" region with shorter group delay for all fibers was based on the group delay measurements from low-CF fibers reported in [Pfeiffer & Molnar, 1980; Kiang, 1984; Van der Heijden & Joris, 2006; Temchin et al, 2009] where such "off-CF" region was found at either the low-frequency or high-frequency side of the CF for fibers with CF higher or lower than some break-frequency values respectively. Specifically, [Pfeiffer and Molnar, 1980] reported that the off-CF region with lower group delay could be found in the high-frequency side of the CF for fibers with CF < 1 kHz, and on the low-frequency side of the CF for fibers with CF > 1.2 kHz for cats AN fibers. Similar values of break-frequencies can be found elsewhere for cats AN [Van der Heijden & Joris, 2006; Carney et al, 1999] and for ANs of chinchillas [Temchin et al, 2009]. Accordingly, in this study a single break-frequency of 1.2 kHz was used whereby the "off-CF" tone frequency was selected from the high-side and low-side of the CF for fibers with CF ≤ 1.2 kHz and CF > 1.2 kHz respectively. Specifically, from either the low- or high-side of the CF as described above, the off-CF-tone frequency was selected with the spacing of 0.7 – 2 octave from the CF of the fiber. Note that the frequency spacing of the "off-CF" tone from the CF of the fiber was also based on the group delay measurements reported in [Van der Heijden & Joris, 2006; Temchin et al, 2009]. Specifically, [Temchin et al, 2009] reported that the lower-group delay region began at ~0.5 octave away from the CF of the fiber, and it can be seen from Figure 3 of [Van der Heijden & Joris, 2006] that the "off-CF" region with lower group delay can be found at ~0.7 – 1 octave from the CF of the fiber for the population of fibers in their study.

Throughout the runs, the quality of spike triggering was monitored & adjusted, and data from recordings with near perfect triggering with no extra or missed triggers have been selected for this

thesis. The methods for the above experimental paradigms are described in detail with actual data from the example fiber, CT030_U007, with its CF at 1.88 kHz & SR of 87.2 sps in Fig. 4.6 – Fig. 4.15.

D. Bias-tone Only Paradigm: Excitation Threshold & Phase

Acoustic Stimulus and Data Collection

The objective of this paradigm was to measure the neural excitation threshold and phase of excitation of the fiber invoked by 50Hz bias-tone. A randomized level series of the 50Hz bias-tone over the range from 70 dB SPL to 120 dB SPL was presented. A single trial period was 500 ms with approximately 50% stimulus ON duty cycle. The spike records during the analysis time window of 200 ms duration from the stimulus ON period were binned re. the bias-tone-period in order to form a level series of bias-tone-period histogram of the spike records. Averaged results from 8 of such trials were used to compute the level series of period histograms. The zero phase reference is the cosine phase of the earphone drive signal. Fig. 4.6 shows the 50Hz bias-tone level series of period histograms from the example fiber.

Data Analysis

The rate-level function was calculated from the level series of spike records, and the rate threshold was determined with the criterion of one standard deviation, σ, above the baseline rate. The baseline rate was determined as the spike rate at the minimum level of the bias-tone level series which was 60-70 dB SPL. The bias-tone level function of the spike rates including the baseline rate were calculated from the total spike collection time of 1600 ms averaged from 8 trials of 200 ms in each trial. Note that the baseline rate was not the spontaneous rate of the fiber. However, none of the recorded fibers showed a significant upward slope from their rate-level function at the baseline level. The standard deviation was estimated as the square root of the baseline rate under the assumption of Poisson random process behind the spikes.

Vector phase analysis was used to estimate the phase of excitation and synchrony index [Goldberg and Brown, 1969; Johnson, 1980]. Briefly, each spike is represented as a unit vector with its phase as the phase of occurrence of the spike within the period. The magnitude and phase of the average vector representation of all the spikes are the synchrony index and vector phase respectively. Mathematically the average vector corresponds to the first harmonic component of the Fourier series of the period histogram normalized by the total spike count [Goldberg and Brown, 1969].

Further, statistical significance of the phase estimates were evaluated through the standard error of the vector phase estimates. The mathematical model for standard error of the phase estimate, $S.E.\phi$, is described in [Mardia, 2000], and it had been previously applied in AN spike data analysis [Stanknovic, 1998; Stankovic & Guinan, 1999b].

The excitation threshold of the bias-alone alone response was met when both the rate threshold of the bias-tone alone response was met, and the standard error on the phase estimate dropped to be within 20° ($-20° \leq S.E.\phi \leq 20°$). This criterion allows statistically significant differentiation of the phase data points that are separated by at least 40°.

The detailed analysis of the period histograms in Fig. 4.6 are shown in Fig. 4.7 where the bias-tone level function of the spike rate, synchrony index and estimate of the excitation phase are displayed in the top-down order. In this example, the excitation threshold was met at the bias-tone level of 110 dB SPL. Note that the shape of the histogram moves to a pattern with two modes separated by approximately half a cycle at 110 dB SPL. The vector phase estimate based on the first harmonic component estimated the mid-point of the two peaks as the excitation phase as noted in Fig. 4.6. This phenomenon known as "peak splitting" has been widely reported in previous work for AN response studies on cats particularly from low-CF fibers below 2 kHz in response to low-frequency tone below 200 Hz [Johnson, 1980; Kiang, 1984; Kiang, 1990; Cai & Geisler, 1996].

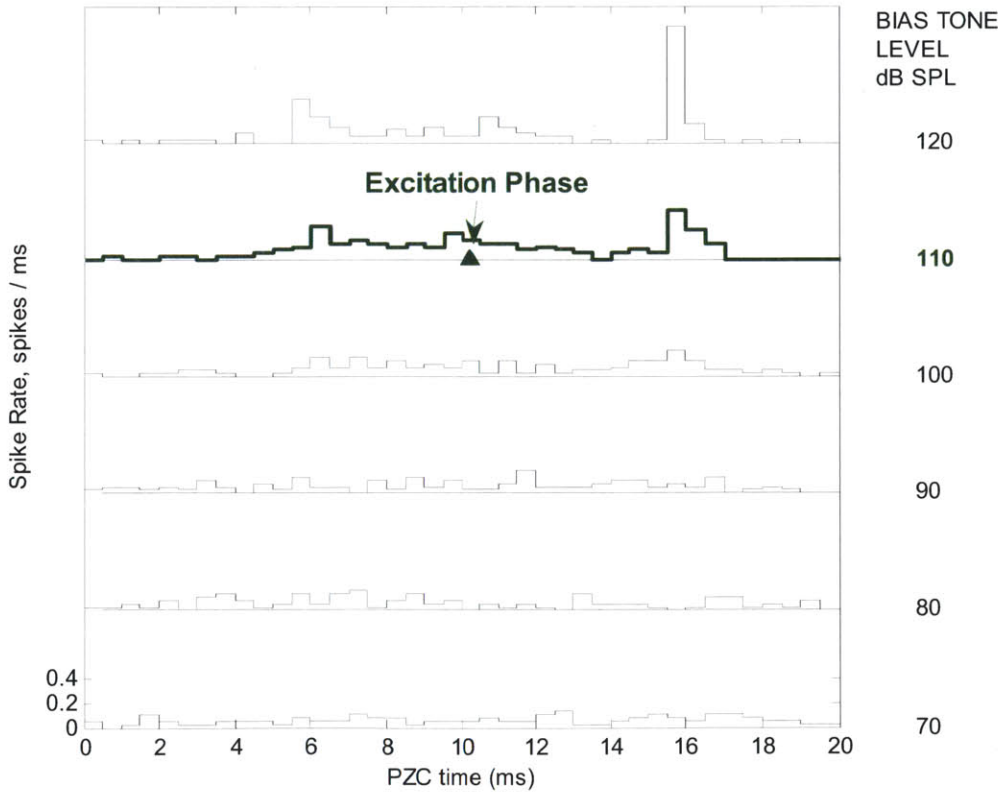

Fig. 4.6. Bias-tone level series of 50 Hz bias-tone-period histograms of the example fiber, CT030_U007, CF=1.88 kHz & SR=87.2 sps. The excitation threshold level was determined as 110 dB SPL with the excitation phase noted on the period histogram.

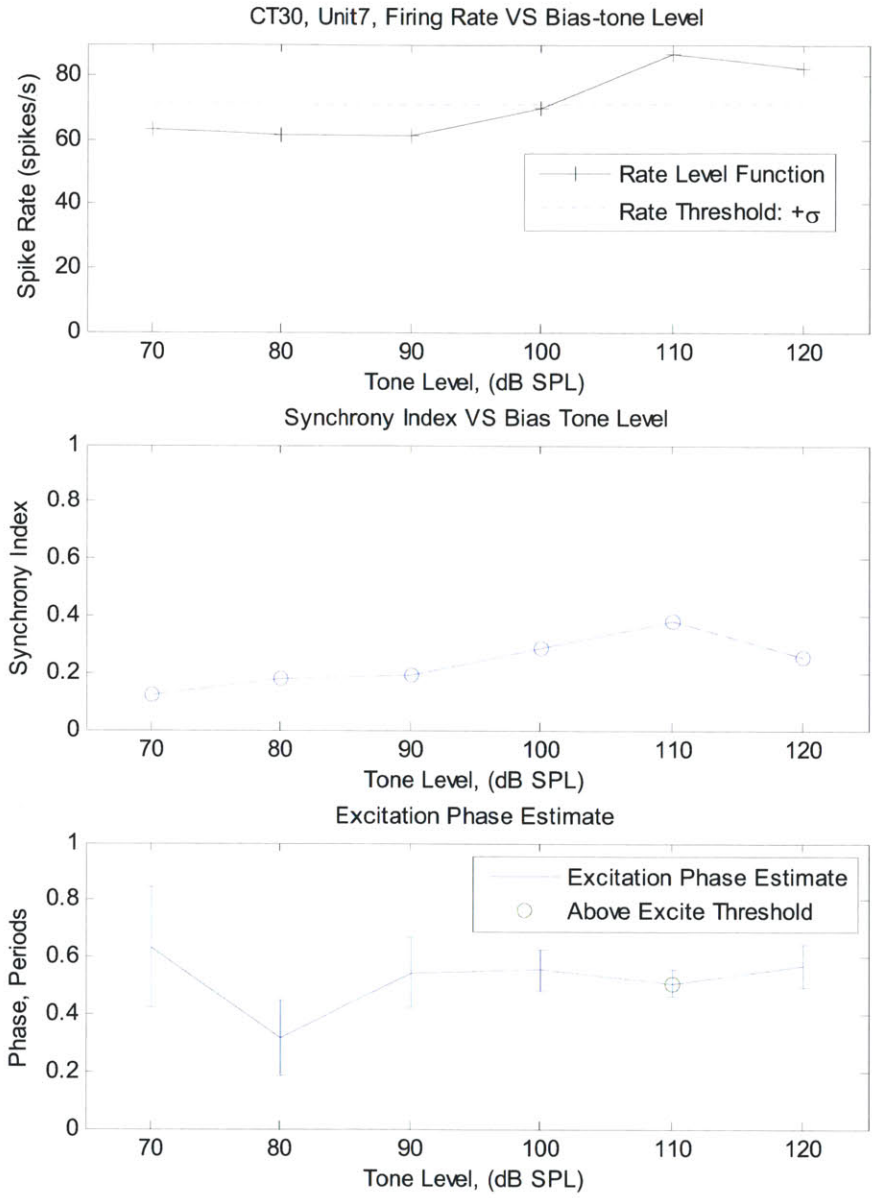

Fig. 4.7. Detailed data analysis metrics to determine bias-tone only response threshold & response phase. *Top*: Rate-level function from which the rate-threshold is determined when the spike rate exceeds one standard deviation; *Middle*: Level function of the synchrony index; *Bottom*: the excitation phase estimates with their standard error. The excitation phase & its standard error is determined by the vector phase method. The excitation threshold is met when both the rate threshold is met and also when the standard error on the phase estimate drops within 20°. In this example, the excitation criteria were met at 110 dB SPL.

E. Experimental Paradigm for Bias-tone Effects on Tone Responses: CF and Off-CF tones

Acoustic Stimulus and Data Collection

In this paradigm, a level series of 50 Hz bias-tone was presented together with a probe tone at a fixed level of 10 - 20 dB above the threshold of the probe tone. The frequency of the probe tone was either at the CF of the fiber or at the off-CF tone. As for the exact frequency of the probe-tone, it was not necessarily a harmonic of the bias-tone frequency, 50Hz, as done in previous studies [Sachs and Hubbard, 1981; Cai and Geisler, 1996a]. For the example fiber, the CF-tone was at the frequency of 1.88 kHz and the level of 33.6 dB SPL which is about 16 dB above threshold as shown in Fig. 4.8. The off-CF probe-tone for this fiber was at the frequency of 0.8 kHz and the level of 50 dB SPL which was ~10 dB re. the TC threshold at that frequency as shown in Fig. 4.8.

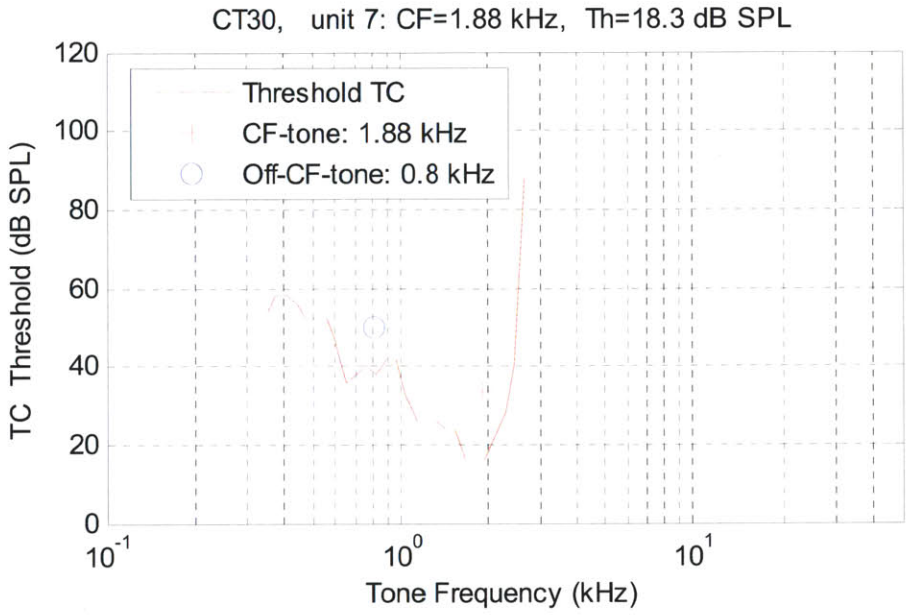

Fig. 4.8. The TC of the example fiber, CT030_U007, CF=1.88 kHz & SR=87.2 sps. The frequency and level of the CF and the off-CF probe tone applied in the bias-tone effect study are noted along with the TC.

Together with a probe-tone selected as described above, a randomized level series of 50 Hz bias-tone over the range of 70 dB SPL to 120 dB SPL was presented during the 50% ON duty cycle within the 500 ms trial period as shown in Fig. 4.9(a). Fig. 4.9(b) shows the post-stimulus time histogram (PSTH) resulting from this paradigm at the bias-tone level of 70 dB SPL presented together with the CF-tone from the example fiber.

The spike analysis window started at 25 ms for the duration of 220 ms spanning 11 cycles of the 50 Hz bias-tone during which the bias-tone and the low-level probe-tone are presented together for suppression effect analysis. The spike records from 24 of such trials were binned re. the bias-tone-period to form the bias-tone-period histogram. Note that spike records were initially time-stamped with the resolution of 10 μs which would yield bias-tone-period histograms with the sample size of 200000 if left unprocessed. Since spike data analysis for bias-tone effects on period histograms are concerned

mainly with low-frequency modulation on the spike records spanning first few harmonics of the bias-tone, the spike records were re-binned at a wider time bin width as follows. The initial time bin width of 10 μs was widened to a value close to the period of the CF-tone in order to reduce the bandwidth of the period histogram below the phase locking frequency to the CF of the fiber. Note that since the CF-tone frequency was not necessarily an integer multiple of the bias-tone frequency, the sample interval of the re-binned histograms was selected to be the bias-tone-period divided by an integer number whereby the resulting time bin width was closest to the period of the CF-tone. Finally, the sample size of the period histograms was limited at the maximum of 40 corresponding to the minimum time bin width of 0.5 ms. Note that the maximum sample size of 40 in this paradigm allowed spectral analysis up to the first 19 harmonics of the bias-tone as discrete Fourier transform was applied on the period histograms. The bias-tone level series of the PSTHs and the corresponding bias-tone-period histograms are shown in Fig. 4.10. In this example with the CF of 1.88 kHz, the period histogram consisted of 38 samples with the time bin width of 0.5263 ms.

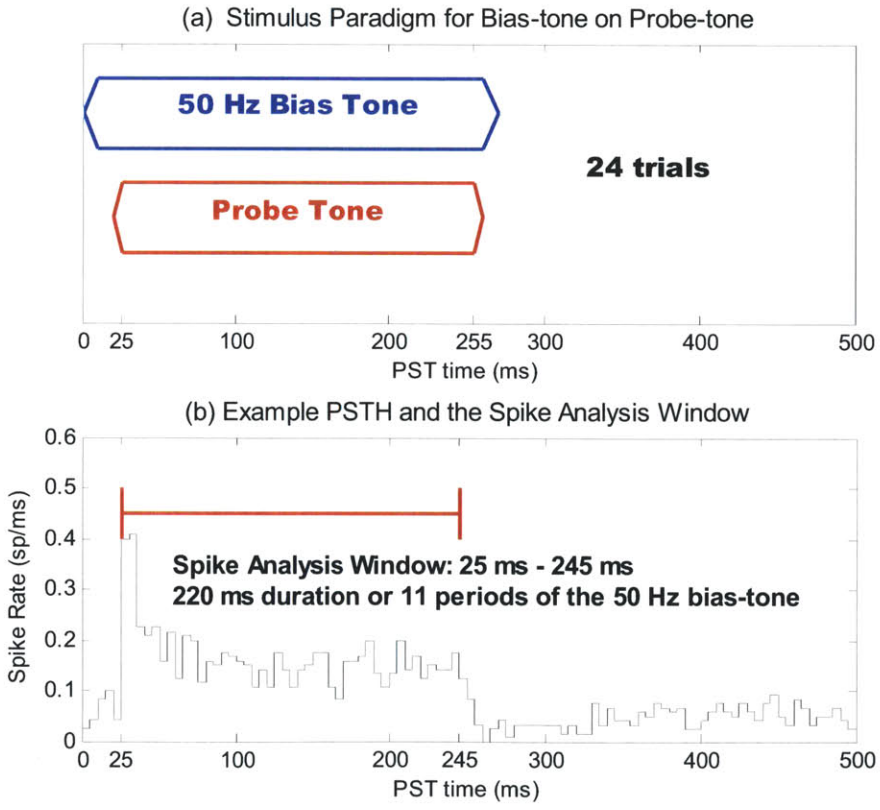

Fig. 4.9. Acoustic Stimulus Setup for the Bias-tone on Tone Burst Paradigm: *Top*: the probe tone & the 50 Hz bias-tone were presented together for 230 ms of spike analysis time within the total trial period of 500 ms. *Bottom*: The post-stimulus time histogram (PSTH) of the spikes over the entire 500 ms trial period. The data come from the example fiber, CT030_U007, CF=1.88 kHz & SR=87.2 sps. Note the ON duty cycle of ~50% corresponding to the stimulus setup diagram above. The spike analysis window covered the duration of 180 ms

or 9 periods of the 50 Hz bias-tone. Note that the analysis window starts at 65 ms which was 40 ms after the onset of the probe-tone in order to avoid the onset adaptation time of the probe-tone burst.

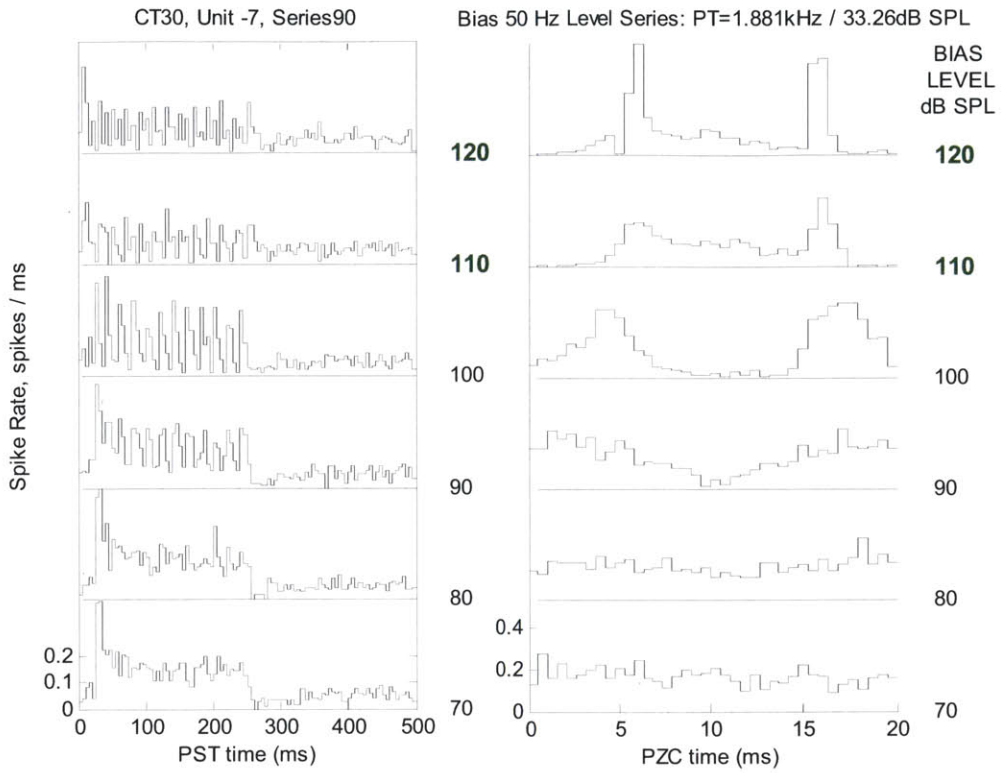

Fig. 4.10. Level series of PST histograms, *Left;* The corresponding the bias-tone-period histogram, *Right*. Spike records from the ON duty cycle from the PST histograms were binned re. the bias-tone-period to form the bias-tone-period histogram. The phase reference of the bias-tone-period histogram was the cosine phase of 50 Hz bias-tone earphone drive signal. Time bin width of the histogram was set at the probe-tone period to reduce the bandwidth of the data below the frequency of the probe tone.

Analysis of the Bias-tone-period Histograms for Suppression Effects

The period histograms were examined to detect significant suppression. Previous studies have shown that that the suppression effects by a low-frequency bias-tone predominantly result in either a single major suppression phase or two suppression phases at opposite phase locations [Patuzzi et al, 1984a; Cai & Geisler, 1996a; Temchin et al, 1997]. Detecting a period histogram with a single major suppression phase was done through the vector phase analysis for the first harmonic component. Specifically, significant suppression was detected when the standard error on phase estimate, $S.E.\phi$, for the first harmonic dropped below 20° (-20°≤ $S.E.\phi \leq$ 20°).

Period histograms with two peaks at opposite phase locations can be analyzed with the same basic framework of directional statistical analysis by examining the synchrony index, vector phase and the standard error on the phase estimate with respect to the second harmonic component of the period histogram [Mardia, 2000]. As with the first harmonic, maximum criterion of 40° on the standard error on phase for the second harmonic component, $S.E.\phi_2$, was applied to detect a period histogram with

two suppression phases at opposite phase locations; $-40° \leq S.E.\phi_2 \leq 40°$. Since the span of 40° of second harmonic phase is equivalent to 20° of the first harmonic phase, equivalent detection criteria were applied to the first and second harmonic.

Since the second harmonic phase points to two suppression phases within the period histogram separated by half a cycle, it was necessary to disambiguate major suppression phase between the two. The analysis procedure for this problem termed as "Half-period Synchrony Analysis" was based on the observation that the major suppression phase typically has a higher level of synchrony compared to the minor suppression phase. The analysis procedure first cuts the original period histogram into two half-period histograms of equal-length around the two suppression phase locations. The resultant two half-period histograms would have a single major suppression phase in each, and the depth of suppression in each were calculated as the synchrony index for the first harmonic of each half-period. Finally, the major suppression phase from the original full-period histogram was determined as the suppression phase with higher level of half-period synchrony index. This procedure is illustrated in Fig. 4.11 with the period histogram at the bias-tone level of 100 dB SPL on low-level CF-responses from the example fiber. In Fig. 4.11(a) the two suppression phase locations determined by the second harmonic phase are marked as a blue & red inverted triangle. The resulting two half-period histograms are shown in Fig. 4.11(b). Note that the half-period histogram centered at the blue triangle starts with the wrapped around data from the time window from ~16 ms to 20 ms. The synchrony index for the first harmonic of the half-period are shown in each of the half-period histograms. Due to the larger synchrony index value of the red half-period, the major suppression phase from the original full-period histogram is determined as the red triangle which is located in the middle of the period.

Finally, period histograms generated by bias-tone levels at or above the bias-tone alone excitation threshold were classified as "Excitation" and accordingly were not included in the suppression data pool. For the period histograms of the bias-tone effects on CF-tone responses from the example fiber, the period histograms at 110 and 120 dB SPL were not included in the suppression data pool.

The analysis procedures described above are illustrated on the bias-tone effects on the low-level CF-tone, 1.88 kHz, and the off-CF tone, 0.8 kHz, responses from the example fiber as shown in Fig. 4.12 and Fig. 4.13 respectively. In Fig. 4.12, the suppression threshold on the low-level CF-tone response was met 90 and 100 dB SPL for the first and the second harmonic respectively. The major suppression phase estimate at 90 and 100 dB SPL is noted by a blue and a red inverted triangle respectively. In this example, the major suppression phase would be determined by the first harmonic phase at the bias-tone level of 90 dB SPL. Further, note the drastic shift in the shape of the period histogram at 110 dB SPL and 120 dB SPL to a shape resembling the period histograms associated with bias-tone excitation. In Fig. 4.13, the suppression threshold on the off-CF-tone response was met at 100 dB SPL of the bias-tone level with the second harmonic criterion. The major suppression phase of the off-CF-tone response noted by a red inverted triangle in Fig. 4.13 is very similar to that of CF-tone response. Again, at the excitation threshold level of 110 dB SPL, the shape of the period histogram drastically shifts to resemble the pattern of excitation by the bias-tone alone.

Fig. 4.14 and Fig. 4.15 show the level functions of the spike rate, synchrony index and vector phase data for the first and second harmonic for the bias-tone effects on CF-tone and off-CF-tone response respectively. Note from both Fig. 4.14 and Fig. 4.15 that the firing rate started to decrease at the suppression threshold and leveled out at 110 dB SPL, the excitation threshold by the bias-tone alone. From the level function of the synchrony index, note the sharp increase of the synchrony index at the suppression threshold.

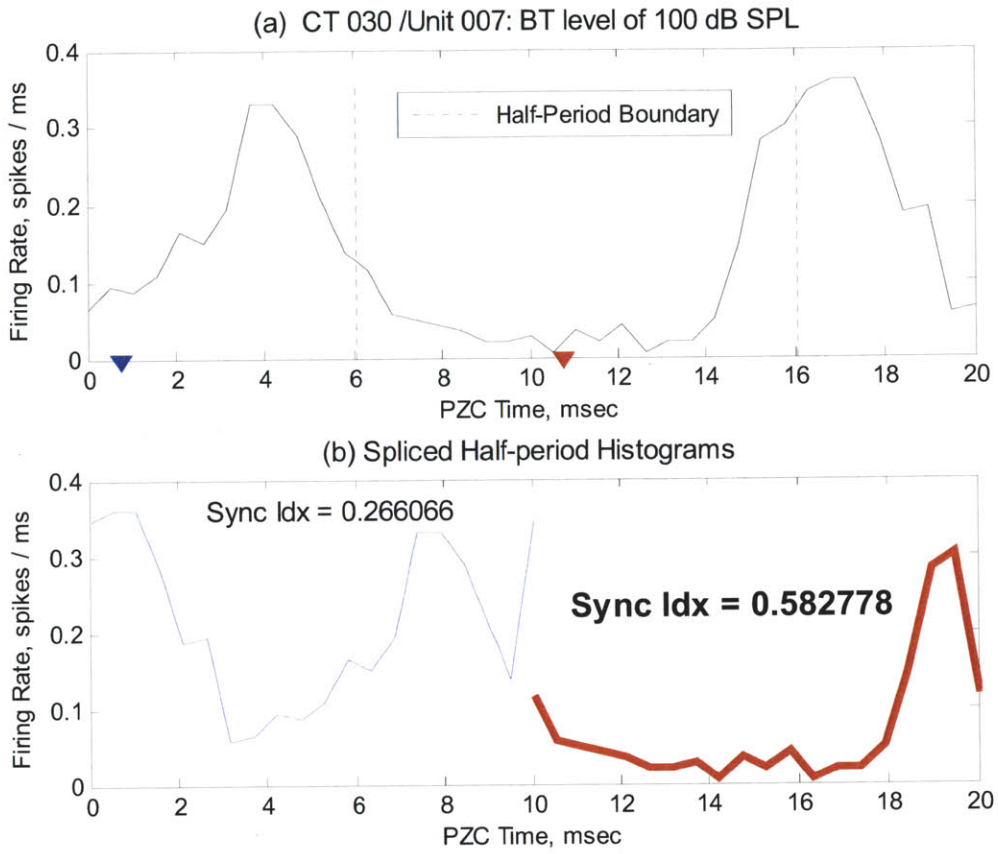

Fig. 4.11. Illustration of the "Half-period Analysis": method to determine the major suppression phase from a period histogram with a significant second harmonic component. The data came from the bias-tone-period histogram at 100 dB SPL from Fig. 4.10. *Top:* the two suppression phases based on the second harmonic phase are shown as blue & red inverted triangles. Half-period boundaries of equal width are formed around these two suppression phases in order to splice out the two half-period histograms. *Bottom:* the two half-period histograms & their first harmonic synchrony index are shown. The suppression phase noted with red has higher half-period synchrony index, and consequently, it is determined as the major suppression phase.

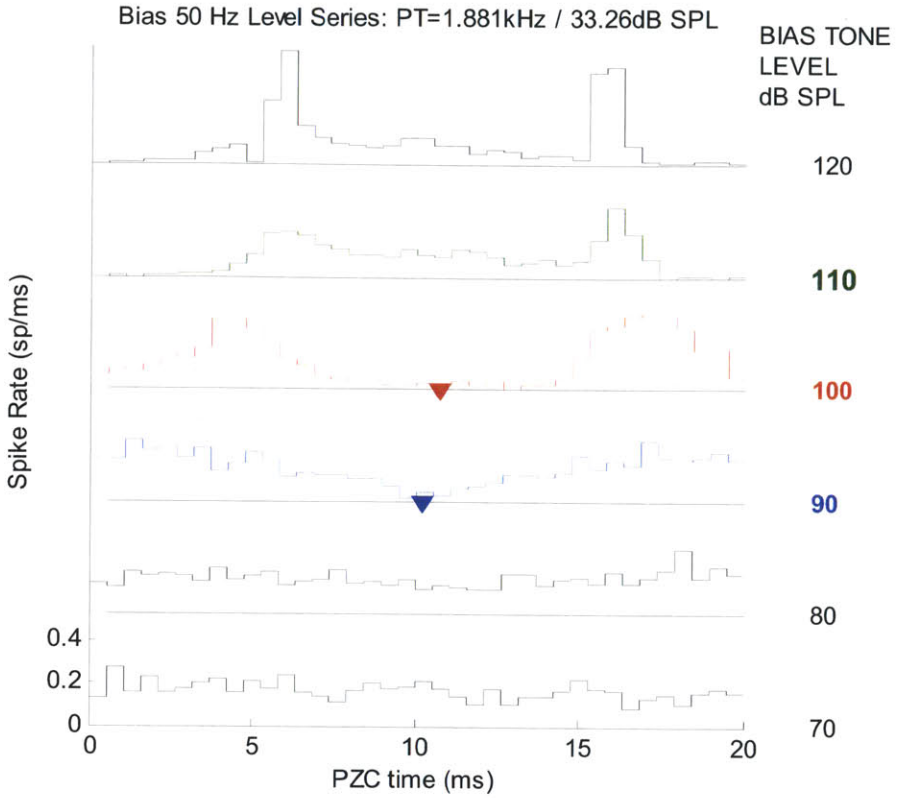

Fig. 4.12. The suppression phase analysis on the bias-tone-period histograms from the bias-tone level series of CF-tone response from the example fiber. The suppression thresholds based on phase estimate error bound was met at 90 & 100 dB SPL for the first and second harmonic respectively. The suppression phases are noted with inverted triangles on the period histogram. In this example, the major suppression phase would be determined by the first harmonic phase at the bias-tone level of 90 dB SPL. Further, note the drastic shift in the shape of the period histogram at 110 dB SPL & 120 dB SPL. Recall from Fig. 4.7. that the excitation threshold was reached at 110 dB SPL, which indicates that the spike pattern at 110 & 120 dB SPL are mainly due to the bias-tone excitation pattern.

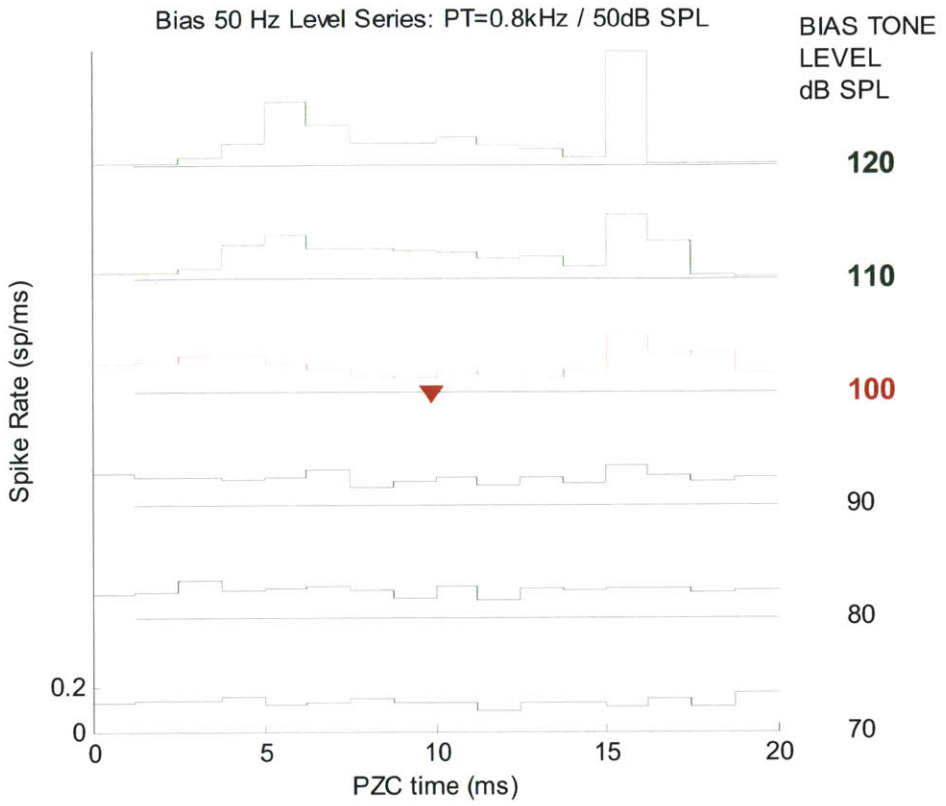

Fig. 4.13. The suppression phase analysis on the bias-tone-period histograms from the bias-tone effects on the responses to off-CF tone, 0.8 kHz, stimulus. The suppression threshold based on phase estimate error bound was met at 100 dB SPL for the second harmonic. The suppression phase is noted with a red inverted triangle on the period histogram. Note the drastic shift in the shape of the period histogram at 110 dB SPL & 120 dB SPL. Recall from Fig. 4.7. that the excitation threshold was reached at 110 dB SPL, which indicates that the spike pattern at 110 & 120 dB SPL are mainly due to the bias-tone excitation pattern

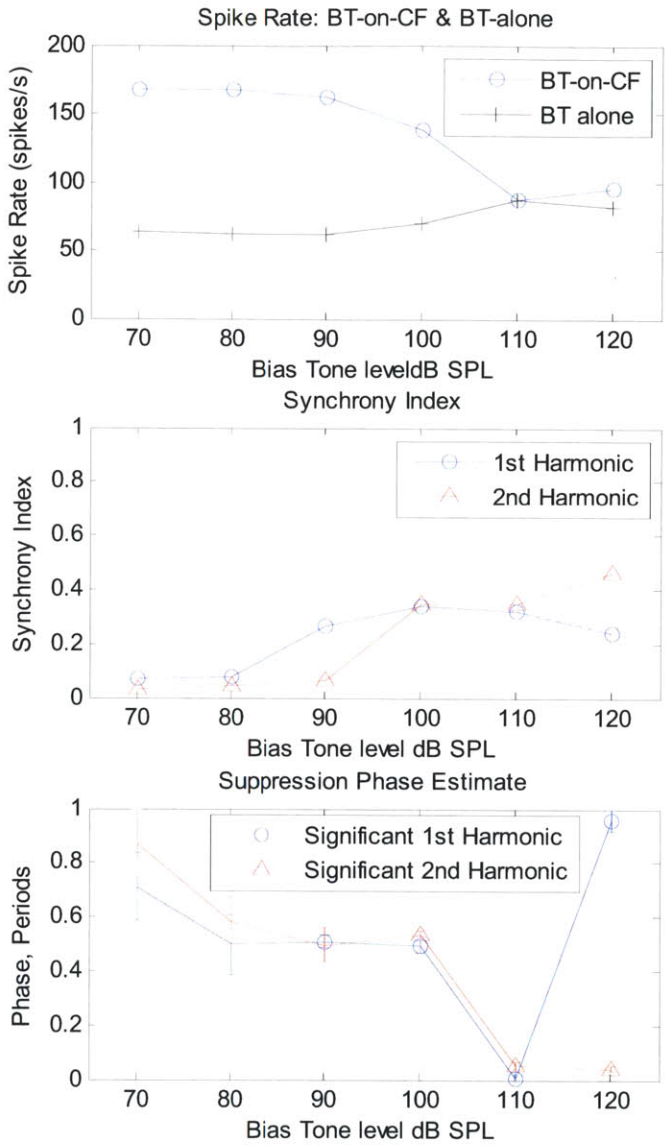

Fig. 4.14. The detailed data analysis on the bias-tone level functions from the suppression effects of CF-tone responses from the example fiber. *Top*: the rate-level function for the run with the bias-tone alone and for the bias on the probe tone run. Note that the firing rate started to decrease at the suppression threshold of 90 dB SPL and leveled out at the excitation threshold of 110 dB SPL. *Middle*: bias-tone level functions of synchrony index for 1st & 2nd harmonics. Note the sharp increase of the synchrony indices at the suppression thresholds. *Bottom*: level functions of suppression phase estimates for 1st & 2nd harmonics with their standard errors. The data points meeting the error criterion are noted with symbols labeled as "Significant 1st Harmonic" and "Significant 2nd Harmonic". The 1st & 2nd harmonic suppression thresholds are met at 90 & 100 dB SPL respectively.

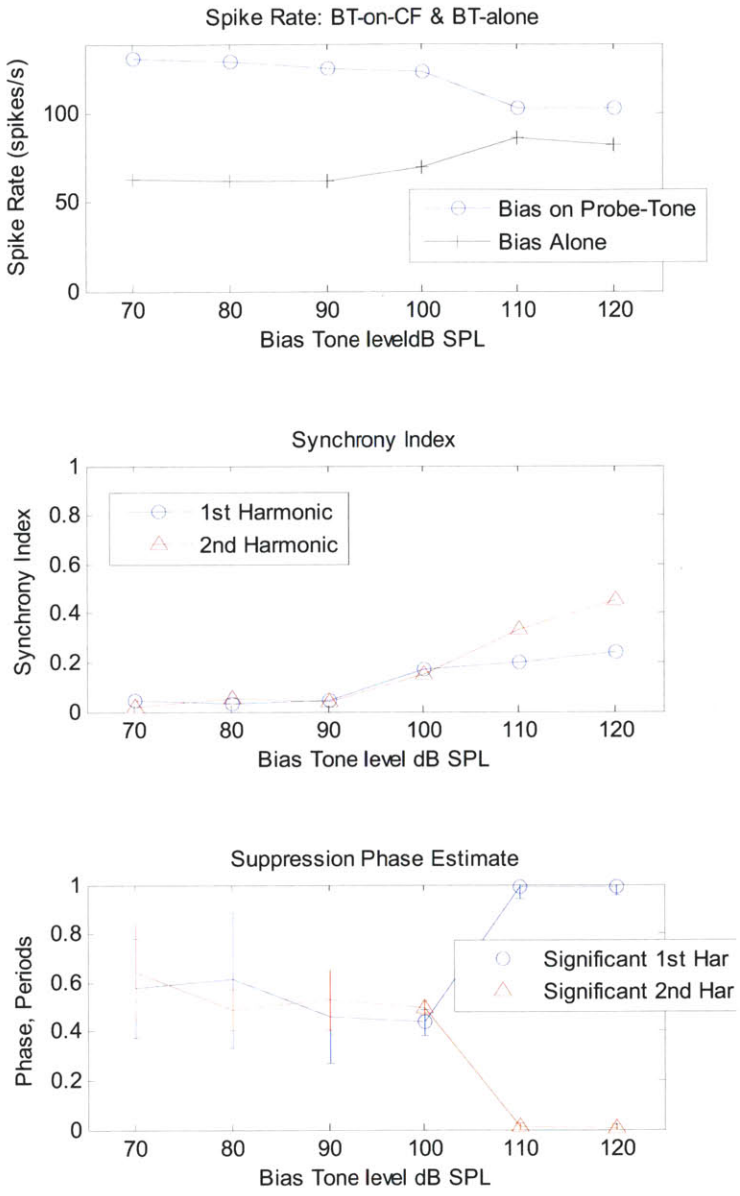

Fig. 4.15. The detailed data analysis on the bias-tone level functions from the suppression effects on off-CF-tone responses from the example fiber. *Top*: the rate-level function for the run with the bias-tone alone and for the bias-on-the-probe-tone run. Note that the firing rate started to decrease at the suppression threshold of 100 dB SPL and leveled out at 110 dB SPL which was the excitation threshold for this fiber. *Middle*: bias-tone level functions of the synchrony index for 1st & 2nd harmonics. Note the increase of the synchrony indices at the suppression thresholds. *Bottom*: level function of the suppression phase estimates for 1st & 2nd harmonics with

their standard errors. The data points meeting the error bound are noted with markers labeled as "Significant 1st Harmonic" and "Significant 2nd Harmonic". Both the 1st & 2nd harmonic suppression thresholds were met at 100 dB SPL, and the major suppression phase estimate was determined as the phase estimate based on the 2nd harmonic phase.

III. Results

A. Phase of Excitation by 50 Hz Bias-tone Alone and Phase of Suppression on Low-level CF-tone Responses

The phase of excitation of AN fibers in response to 50 Hz bias-tone throughout the entire range of CF is plotted in Fig. 4.16. Note that the zero phase reference of the plots was the cosine phase of the 50 Hz earphone drive signal. Also plotted in Fig. 4.16 is the phase of major suppression on low-level CF-tone responses at the suppression threshold level. As mentioned previously, the standard error on all phase estimates was within ±20° which is noted on the plot as the blue error bar.

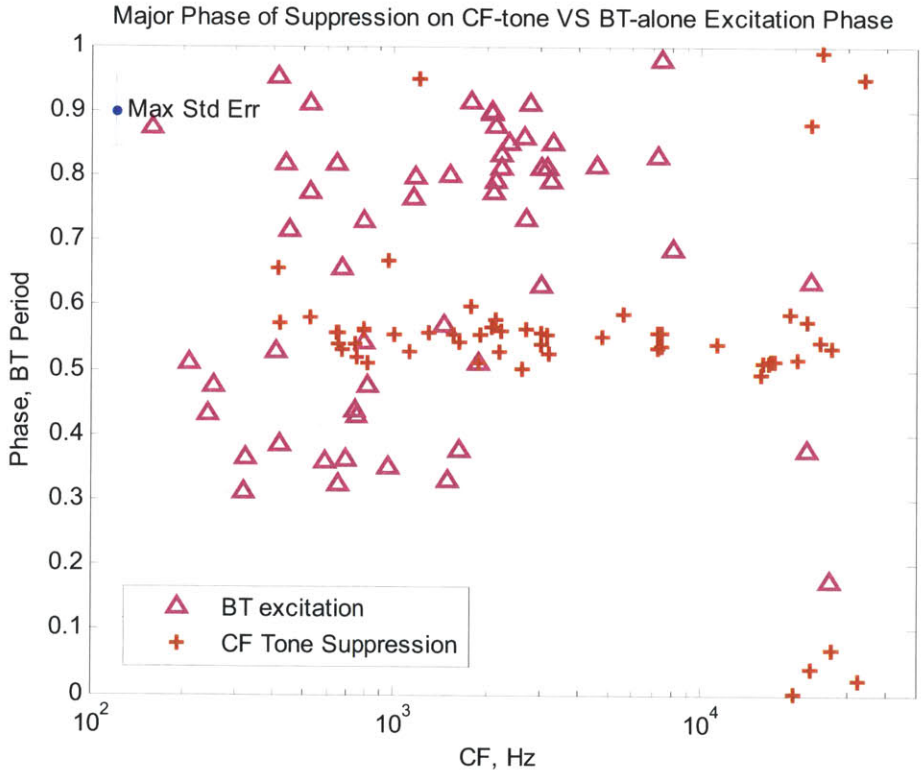

Fig. 4.16. Plot of the phase of excitation from the "bias-tone only" runs and the major suppression phase from the "bias-tone on CF-tone" responses. Note that the excitation phases formed two clusters separated by about ½ cycle, and the phase of suppression on the CF-tone response was located approximately in the middle separated by about ¼ cycle from the phase of excitation. Similar results have been reported in previous studies [Cai & Geisler, 1992a].

The two data groups formed distinctly separate clusters. The data for the major suppression phase of the low-level CF-tone responses were located tightly around the phase of 0.55 T within ± one standard error where T denotes a period of the bias-tone. In contrast, there was significantly wider spread in the phase of excitation in response to 50 Hz bias-tone. Further, the pattern of data scatter changed sharply across the CF boundary of about 2 kHz as shown in Fig. 4.17 where a histogram of fiber

count across the excitation phase are plotted first for fibers with CF < 2 kHz in Fig. 4.17(a) and for the fibers with CF ≥ 2 kHz in Fig. 4.17(b). For fibers with CF > 2 kHz, the phase of excitation data formed a single mode around 0.8 period whereas for CF < 2 kHz, the data were widely distributed with two main modes at 0.35 and 0.8 period that are approximately half a cycle apart. This bimodal distribution of the excitation phase for CF < 2 kHz can be explained by examining the details of the period histograms generated by 50 Hz bias-tone alone level series as shown in Fig. 4.6 and Fig. 4.18 where two peaks at about the opposite phases emerge from the period histogram at high levels of the bias-tone. Specifically, the typical pattern found throughout the animals showed a wider peak at about phase of 0.35 T in addition to a sharper peak at the opposite phase. Depending on the relative size of the two peaks, the excitation phase was determined as the middle of the peaks as in Fig. 4.6, the earlier peak in Fig 4.18(a), and the later peak as in Fig. 4.18(b). As mentioned earlier in methods section, similar results have been reported in previous work on cats AN fibers below 2 kHz as the "peak splitting" phenomenon [Cai & Geisler, 1996; Johnson, 1980; Kiang, 1984; Kiang, 1990].

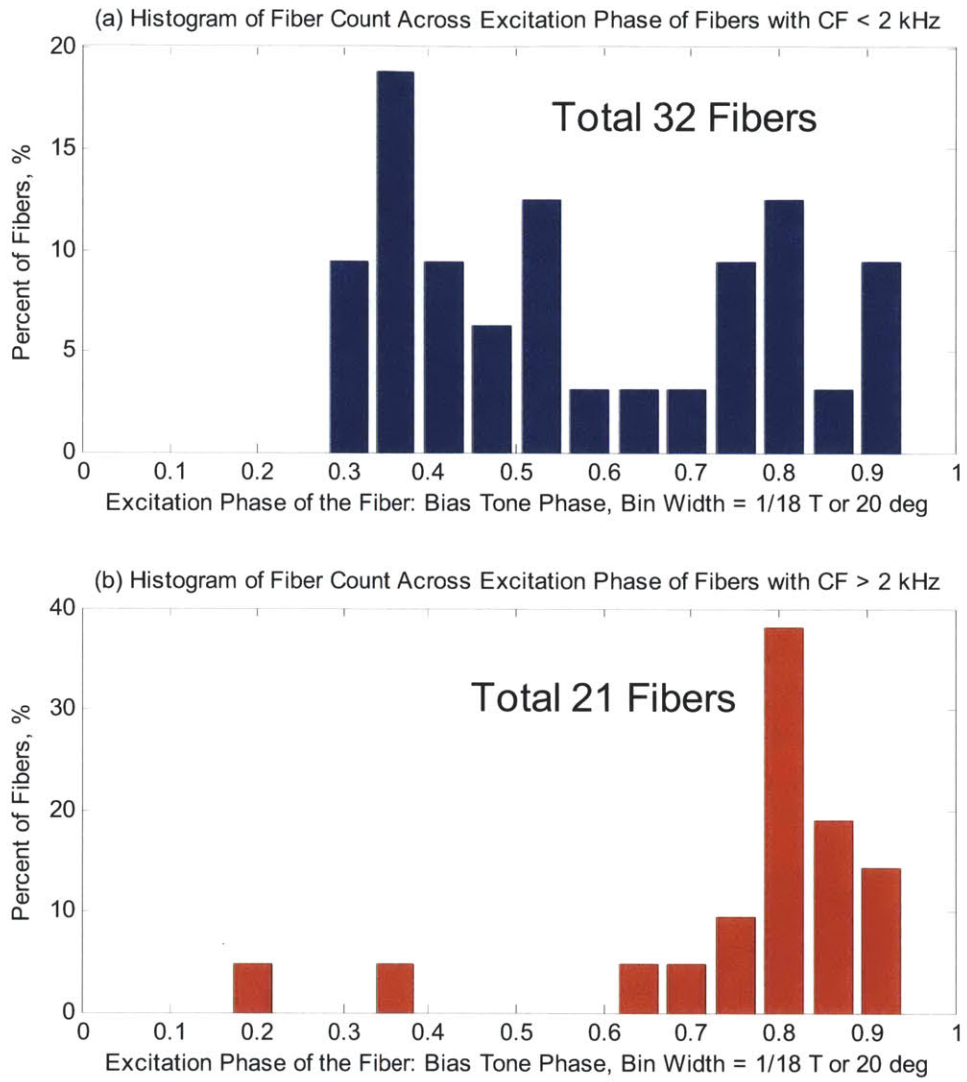

Fig. 4.17. Histograms of the AN fiber counts across phase of excitation of AN fibers in response to 50 Hz bias-tones presented alone. As shown in Fig. 4.16, the distribution drastically changes across the CF of about 2 kHz. (a) Histogram for fibers with CF < 2 kHz shows three modes at ~0.35 T, 0.53 T & 0.8 T where T denotes a period of the bias-tone; (b) Histogram for fibers with CF >= 2kHz shows a single prominent mode at 0.8T.

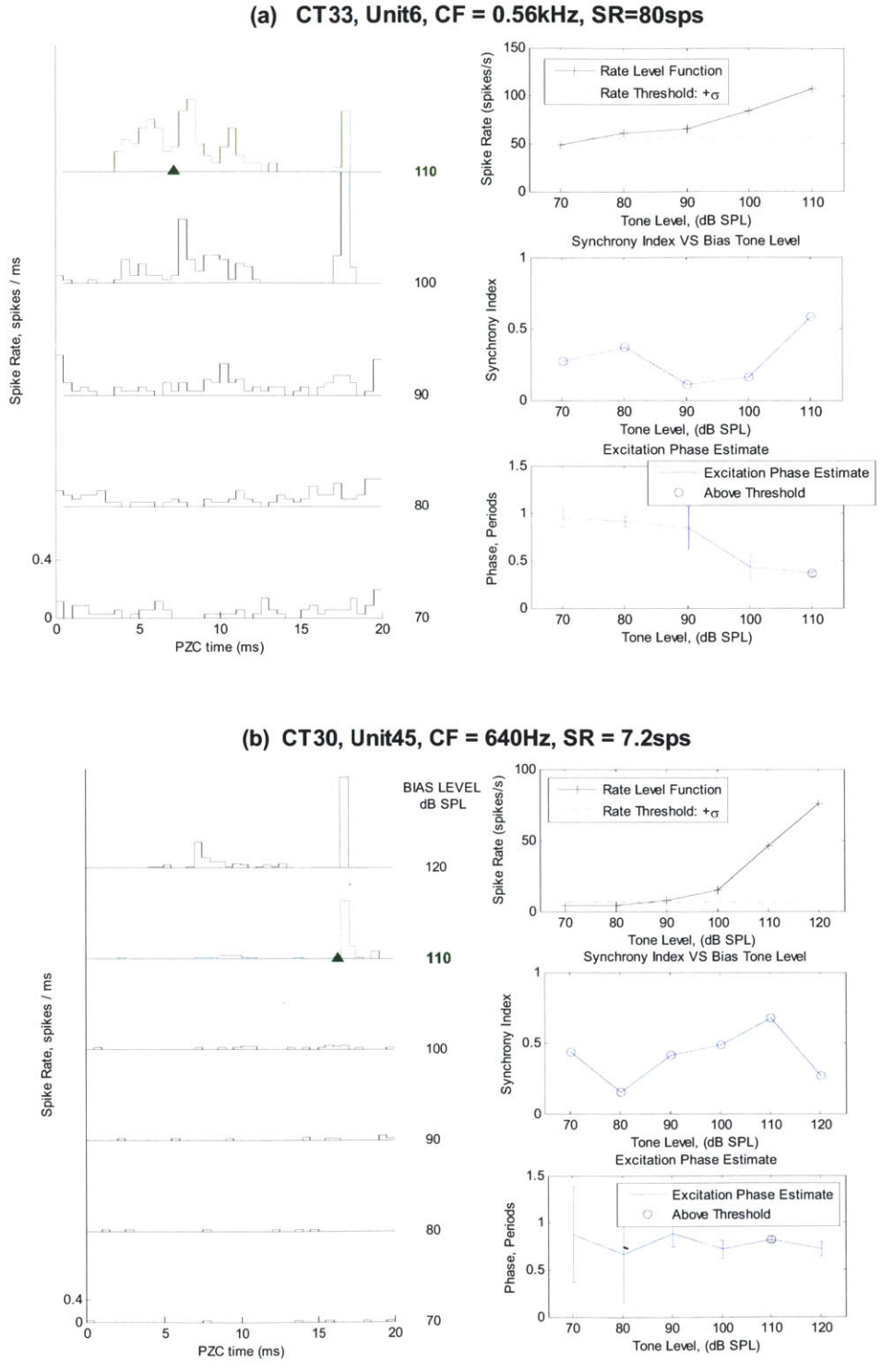

Fig. 4.18. Bias-tone alone excitation patterns for two AN fibers with CF < 2 kHz displaying the peak splitting phenomenon. Two main excitation peaks emerge at about half a cycle apart. Depending on the relative size of

the two modes, the first harmonic based vector phase estimate can select either the wider peak as in (a) or the narrower peak as in (b).

B. Suppression Effects by 50 Hz Bias-tone on Low-level CF-tone and Off-CF-tone Responses from Low-CF Fibers with CF < 4 kHz

Fig. 4.19 shows the major suppression phase of low-level CF-tone and off-CF-tone responses by 50 Hz bias-tone at the threshold of suppression. Note that the data for the off-CF-tone responses cover low-CF fibers with CF < 4 kHz while the data for CF-tone responses are plotted for all fibers which extend up to ~35 kHz. The major suppression phase of low-level CF-tone responses was similar to that of off-CF-tone responses except for a few outliers. Specifically, most data points with CF < 4 kHz for both CF-tone and off-CF-tone fell within ± 1 standard error (S.E), i.e., ± 20 deg, except for a few outliers located at ~1/2 cycle apart from the main data group. The detailed data analysis on these outlier data points as well as typical results are examined in the next section. Note that the frequency of the off-CF-tone stimulus for the data in Fig. 4.19 are shown in Fig 4.20 as octave spacing of the off-CF-tone frequency re. the CF of the fiber. Recall that the selection criterion for the off-CF-tone frequency of a fiber was for the selected frequency to be lower or higher than the CF by 0.7 – 2 octave for CF > 1 kHz and for CF < 1 kHz respectively.

Fig. 4.21 compares the 50 Hz bias-tone level at the threshold of suppression for the low-level CF-tone and off-CF-tone responses for fibers with CF < 4 kHz. Fig. 4.21(a) shows the distributions of the fiber count over the suppression threshold. The mode of the distribution for the CF-tone responses was ~10 dB lower than that of the off-CF-tone responses. Fig. 4.21(b) displays the suppression thresholds over the CF of the fiber. As in the Fig. 4.21(a), the suppression threshold of off-CF-tone responses was ~10 dB higher than that of CF-tone responses.

Fig. 4.22 plots the ratio of 2^{nd} harmonic VS 1^{st} harmonic synchrony index at the suppression threshold by the 50 Hz bias-tone for the CF-tone and off-CF-tone responses. A higher value of this ratio indicates stronger presence of the minor suppression phase at the threshold level of suppression thereby indicating more symmetrical location of the operating point of OHC mechano-electrical transduction function across the two saturation plateaus. In this plot, the data for CF-tone responses are plotted for the entire range of CF of the recorded fibers up to 35 kHz to serve as a reference. Note that most of the data for both CF-tone and off-CF-tone from low-CF fibers were located below 0 dB, and an appreciable difference was not found between the CF-tone and off-CF-tone data for fibers with CF < 4 kHz. Although an appreciable difference was not found between the data for the off-CF-tone VS CF-tone responses, a significant difference was found across the low-CF VS high-CF data for CF-tone responses. Specifically, most of the data for CF-tone response from high-CF fibers with CF > 20 kHz were located above 0 dB reference value in comparison to the data from the low-CF fibers thereby indicating more symmetrical location of the operating point of the mechanoelectric transduction function of OHCs for the high-CF fibers in comparison to the low-CF fibers. Similar results were found from cats AN fibers in [Cai and Geisler, 1996a].

The degree of symmetry of the location of the operating point within the OHC mechano-electrical transduction function was examined by another metric, "Half-period Symmetry Index", which tries to quantify the ratio of modulation depth of the minor VS major suppression phase at the threshold of

suppression. The range of this ratio is from 0 to 1 where values closer to 1 indicate more symmetrical depth of modulation between the two suppression phases thereby indicating more symmetric location of the operating point of the OHC transduction function. For this purpose, the "Half-period Synchrony Analysis" method described in the methods section which was used to disambiguate the major suppression phase from period histograms with two oppositely located suppression phases was adapted. Specifically, for period histograms which met the suppression threshold criteria of the second harmonic, the ratio of the minor VS major suppression phase was calculated as a part of the analysis procedure to determine the major suppression phase. For period histograms which met the suppression threshold criteria for the first harmonic, the "Half-period Synchrony Analysis" procedure was carried out with the suppression phase based on the first harmonic phase estimate, and the ratio of the synchrony indices of the two half-period histograms was calculated. The "half-period symmetry index" at suppression threshold for low-level CF-tone and off-CF-tone responses are plotted over the CF of the fiber in Fig. 4.23. As in Fig. 4.22, the data for CF-tone responses are plotted for the entire range of CF of the recorded fibers up to 35 kHz to serve as a reference. As in Fig. 4.22, no appreciable difference between the data for CF-tone and off-CF-tone responses could be found for fibers with CF < 4 kHz.

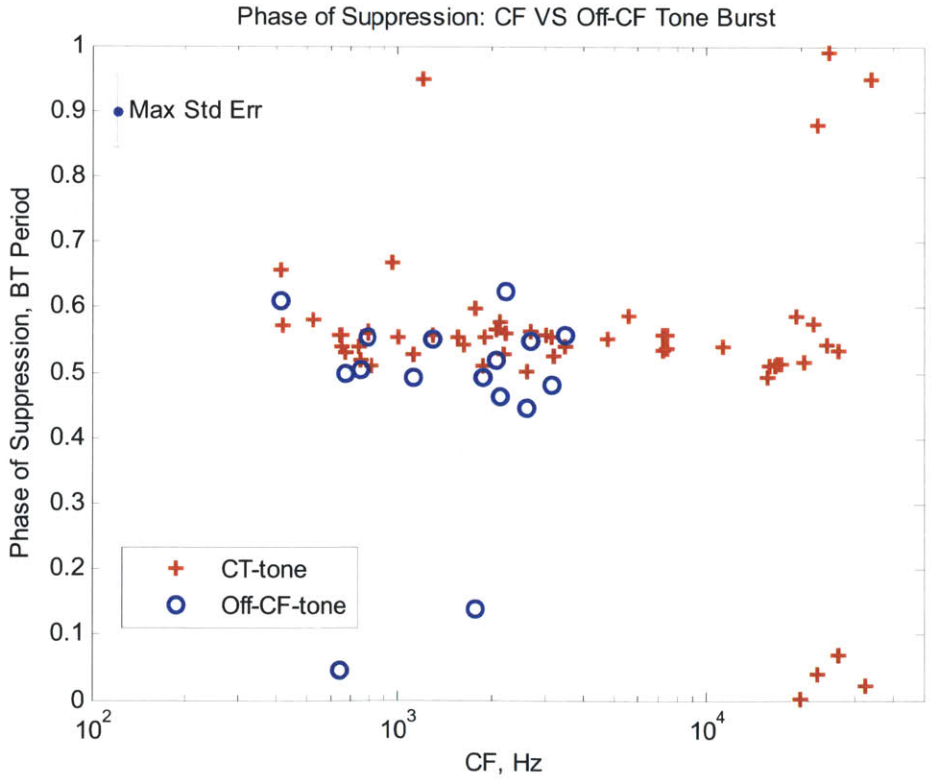

Fig. 4.19. The major suppression phase of low-level CF-tone and low-level off-CF-tone responses are plotted together. Note that the off-CF data extend up to 4 kHz while the suppression phase data on low-level CF-tone response are plotted for the entire range of CFs extending up to ~35 kHz. The major suppression phase of low-level CF-tone responses was similar to that of off-CF-tone responses except for a few outliers. Specifically, most data points with CF < 4 kHz for both CF-tone and off-CF-tone fell within ± 1 standard error (S.E), i.e., ± 20 deg,

except for a few outliers located at ~1/2 cycle apart from the main data group. Note that the frequency of the of the off-CF-tone stimulus for the off-CF-tone data points in this plot are shown in Fig. 4.20.

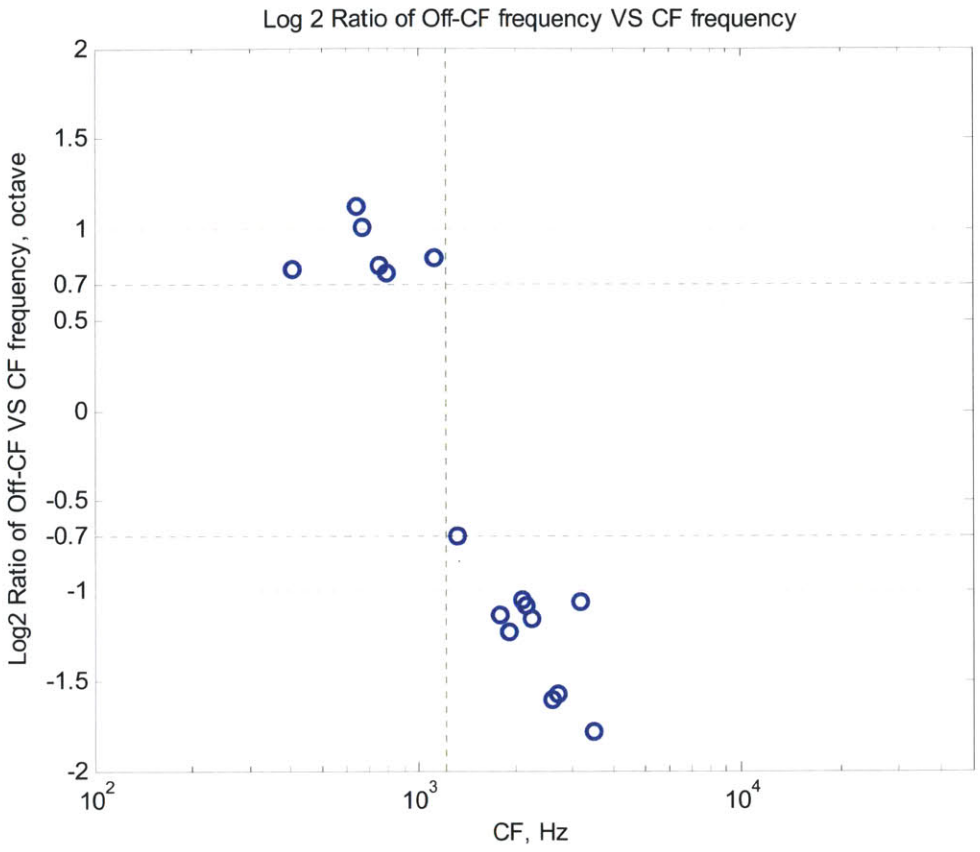

Fig. 4.20. The frequency of the off-CF-tone stimulus for the off-CF-tone data from Fig. 4.19 are plotted as the octave spacing of the off-CF-tone frequency from the CF of the fiber. Note that the selection criterion for the off-CF-tone frequency was for the selected frequency to be lower or higher than the CF by 0.7 – 2 octave for CF > 1.2 kHz and for CF < 1.2 kHz respectively. The selection criterion of ±0.7 octave are noted as black dashed lines.

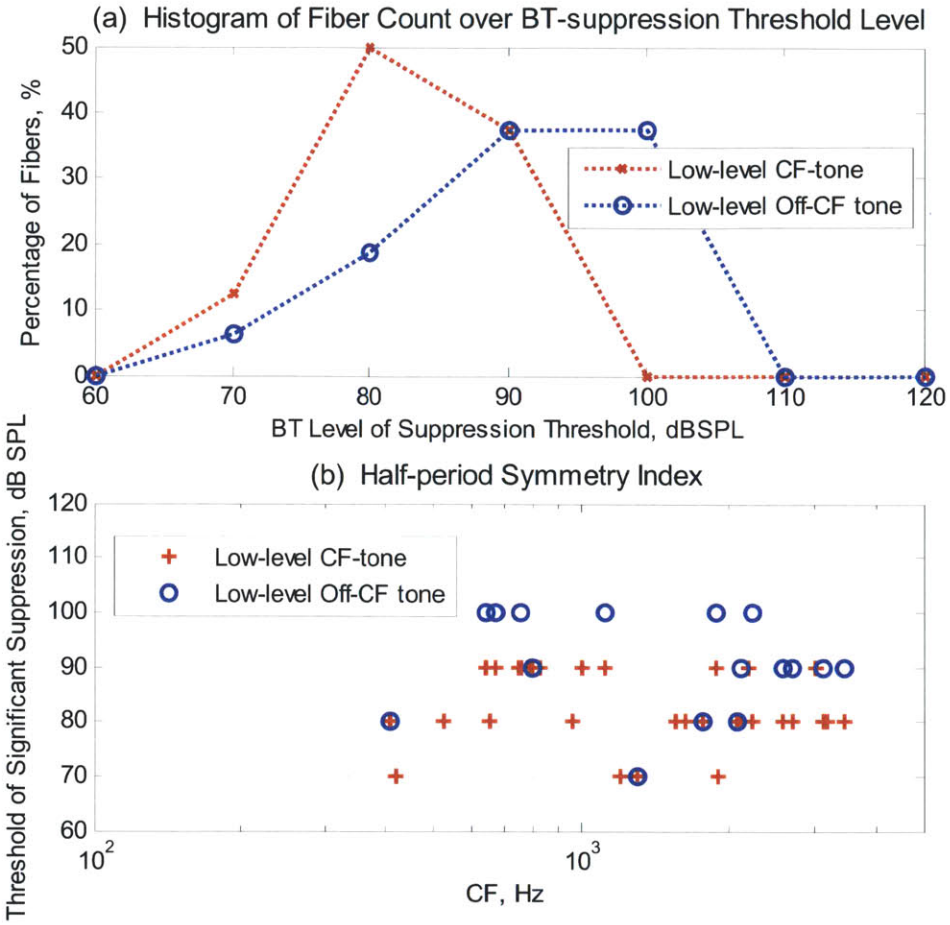

Fig. 4.21. The threshold of suppression on low-level CF-tone response and low-level off-CF-tone response for fibers with CF < 4 kHz: (a) Histogram of the fiber count over the suppression threshold; (b) the plot of the suppression thresholds over CF. The total fiber counts were 32 & 16 for the CF-tone and off-CF-tone respectively. Both data showed that the suppression threshold on the CF-tone responses was ~10 dB lower than that of the off-CF-tone responses.

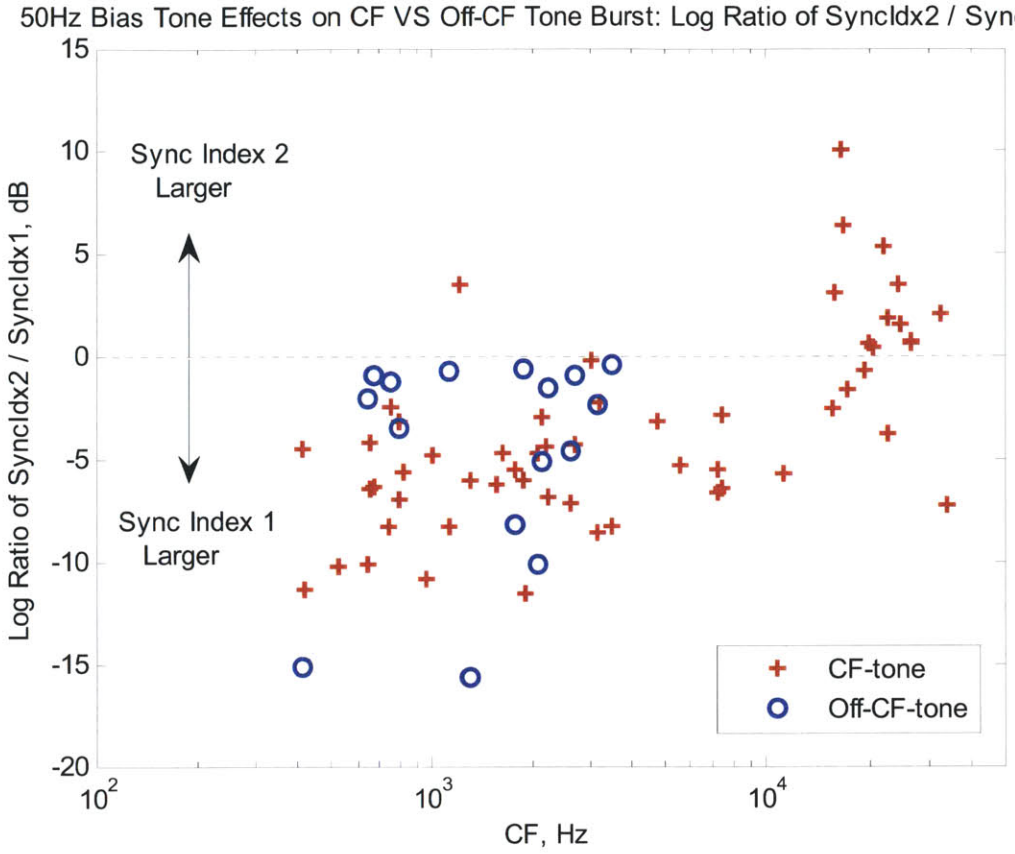

Fig. 4.22. Plot of the ratio of 2nd over 1st harmonic synchrony index at the suppression threshold VS CF of the fiber for CF-tone and off-CF-tone responses. Lower value of the ratio indicates more asymmetry in the suppression pattern between the two suppression dips; therefore, lower value of this ratio indicates more asymmetrical location of the operating point on the OHC mechano-electric transduction function. Appreciable differences were not be found between the data for the CF-tone and off-CF-tone responses for fibers with CF < 4 kHz.

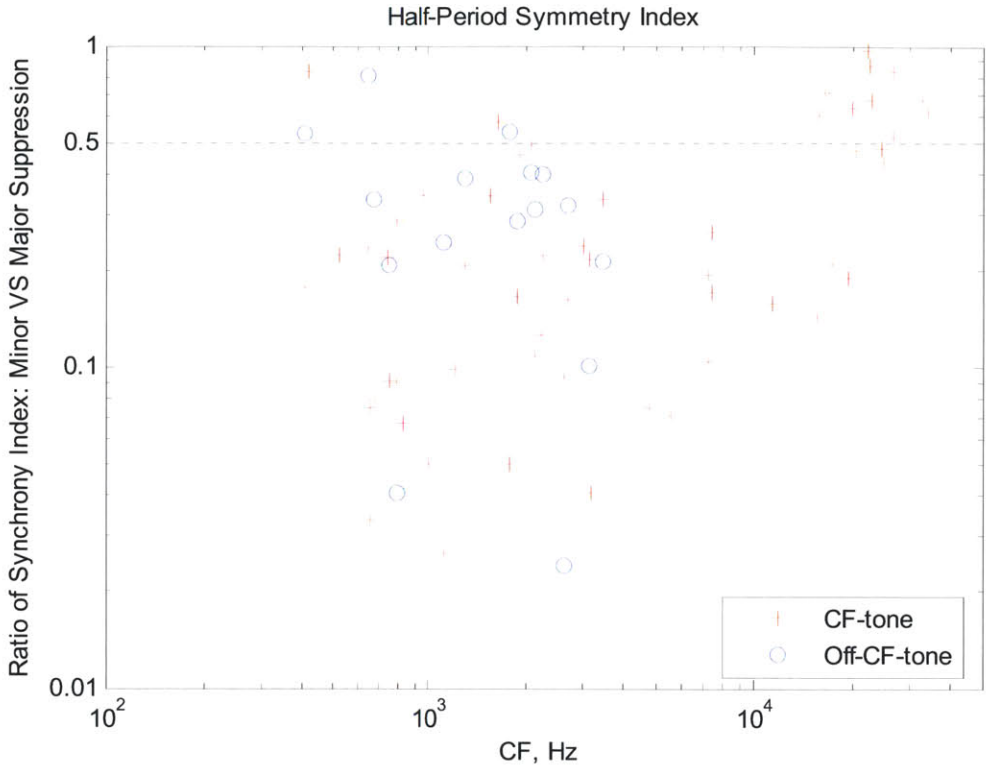

Fig. 4.23. Half-period Symmetry Index: is the ratio of the first harmonic synchrony index from the two "Half-period histograms", which tries to quantify the degree of symmetry in the modulation depth between the minor and major suppression phases. Specifically, the "Half-Period Analysis Method" shown in Fig. 4.11 has been adapted for this purpose. The range of this ratio is from 0 to 1 where 1 indicates perfectly matched modulation depth between the major and minor suppression phase. Refer to the main text for details. Note the reference value of 0.5 which indicates the 1 to 2 ratio of modulation index between the two suppression phases. Most of the data points are located below this value except for the data group for CF-tone response with CF > 20 kHz. Note that similar trend was seen from the Fig. 4.22. Also as in Fig. 4.22, appreciable difference was not found between the data for CF-tone and off-CF-tone responses for fibers with CF < 4 kHz.

C. Example Results of the 50 Hz Bias-tone Suppression Effects on Low-level CF-tone and off-CF-tone Responses from Low-CF Fibers

In order to aid the reader to appreciate how well the data from individual fibers fit with the data shown in the previous plots, this section documents examples of bias-tone induced suppression patterns on low-level CF-tone and off-CF-tone responses from individual fibers. Examples are presented from 7 normal AN fibers taken from 4 cats. Four of the example fibers are with CF < 1 kHz where the off-CF-tone was selected from the high-frequency-side of the CF. The remaining three fibers are with with CF > 1.7 kHz where the off-CF-tone was selected from the low-frequency-side of the CF of the fiber. Note that the two fibers with the CF of 0.64 kHz and 1.76 kHz with their major suppression phase located outside of the main data cluster in Fig. 4.19 are covered in Fig. 4.25 and Fig. 4.28 respectively.

For each example, the AN fiber is identified by its animal and unit number. Each example has three sets of plots. The first set shows, subplot (a) the threshold tuning curve (TC) of the fiber is plotted

along at the frequency and level of acoustic stimuli for the CF-tone and off-CF-tone. The second set of plots shows, subplot (b) at left, the 50Hz bias-tone-level-series period histograms from the bias-tone only responses, subplot (c) in the middle, the bias-tone-level-series period histograms from the responses to bias-tones plus low-level CF-tone, and subplot (d) the bias-tone-level-series period histograms from the responses to bias-tones plus low-level off-CF-tone. The third set of plots shows, at left, subplot (e) the detailed analysis the suppression effects on the low-level CF-tone response, and at right subplot (f) the detailed analysis the suppression effects on the low-level off-CF-tone response.

Example Result in Fig. 4.24: CT033, U012, CF=0.41 kHz, SR=93.6 sps

The data from this fiber show the typical pattern from the CF region below 1 kHz. The off-CF-tone was selected from the upper-side frequency of 0.7 kHz as shown in Fig. 4.24(a). The bias-tone only excitation threshold was met at 90 dB SPL with the excitation phase detected at the narrower peak in the period histogram as shown in Fig. 4.24(b). The suppression thresholds of the low-level CF-tone and off-CF-tone responses were reached at 80 dB SPL of the bias-tone for the second and first harmonic criterion respectively as shown in Fig. 4.24(c) and Fig. 4.24(d). The pattern of progression of suppression on CF-tone and off-CF-tone responses over the bias-tone levels were quite similar including the similar locations of the major suppression phase. Note that for the bias-tone levels above the excitation threshold at 90 dB SPL, the period histograms from both the CF-tone and off-CF-tone responses closely resemble the bias-tone only excitation pattern. The detailed data analysis of the suppression pattern are shown in Fig . 4.24(e) and 4.24(f) as the bias-tone level function of the spike rate, synchrony index and suppression phase estimates for the first and second harmonic. Significant changes occurred at around the suppression threshold from all three metrics. Specifically, the spike rates were suppressed, the synchrony indices rose, and the standard error on the phase estimates diminished significantly at around the suppression threshold of 80 dB SPL.

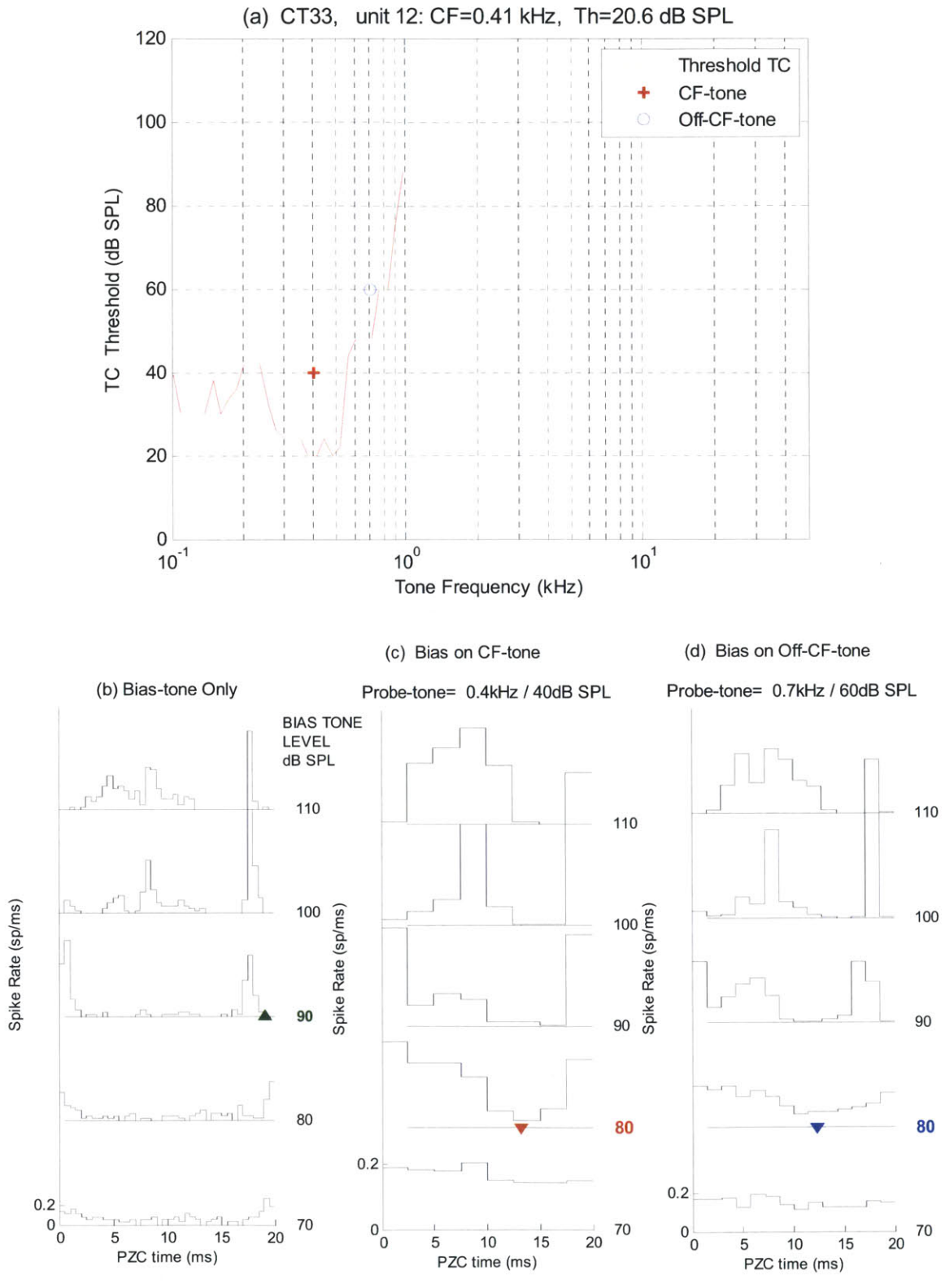
(a) CT33, unit 12: CF=0.41 kHz, Th=20.6 dB SPL
Threshold TC
CF-tone
Off-CF-tone
TC Threshold (dB SPL)
Tone Frequency (kHz)
(b) Bias-tone Only
BIAS TONE LEVEL dB SPL
(c) Bias on CF-tone
Probe-tone= 0.4kHz / 40dB SPL
(d) Bias on Off-CF-tone
Probe-tone= 0.7kHz / 60dB SPL
Spike Rate (sp/ms)
PZC time (ms)

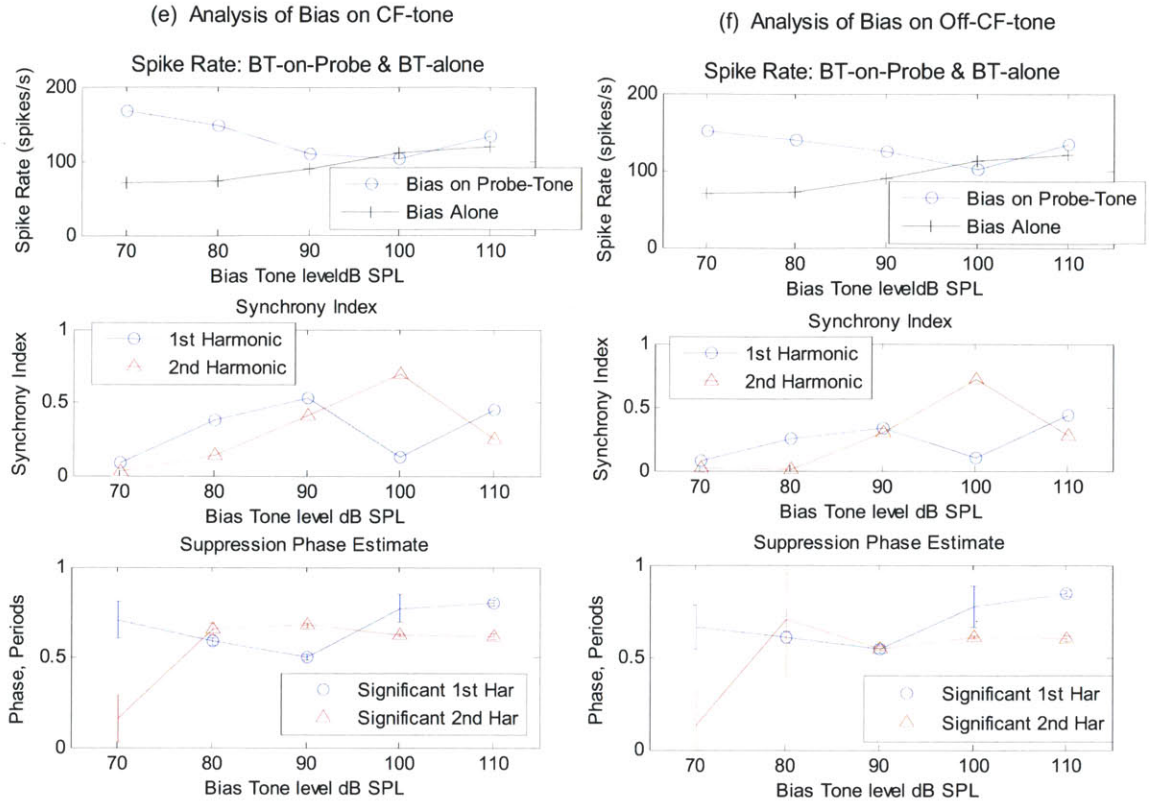

Fig. 4.24. Example Result: (a) Tuning Curve, CF=0.41kHz and SR= 93.6 sps. The acoustic stimulus for the CF and off-CF-tone are indicated as red '+' and blue 'o' together with the TC; (b) Bias-tone (BT) only level series, excitation threshold reached at 90 dB SPL. Excitation threshold level is indicated in green, and the excitation phase is indicated by a green triangle; (c) Bias-tone level-series on CF-tone response. The suppression threshold for the 2nd harmonic criterion was reached at 80 dB SPL as indicated in red text. The suppression phase of the 2nd harmonic is indicated by a red inverted triangle; (d) Bias-tone level-series on off-CF-tone response. Suppression threshold for the 1st harmonic was reached at 80 dB SPL as indicated by blue text. The suppression phase of the 1st harmonic is indicated by a blue inverted triangle. The major suppression phase of off-CF-tone responses was similar to that of CF-tone responses; (e) Detailed analysis of the bias-tone effects on CF-tone response, Bias-tone level functions of firing rate, synchrony indices and phase of major suppression for the 1st and 2nd harmonic in the top-bottom order; (f) Detailed analysis of the bias-tone effects on off-CF-tone response, Bias-tone level functions of firing rate, synchrony indices and phase of major suppression for the 1st and 2nd harmonic in the top-bottom order

Example Result in Fig. 4.25: CT030, U045, CF=0.64 kHz, SR=7.2 sps

This is one of the two fibers with the major suppression phase of off-CF-tone responses located at ~1/2 cycle away from the main data cluster. The off-CF-tone was selected from the upper-side frequency of 1.4 kHz as shown in Fig. 4.25(a). The bias-tone only excitation threshold was met at 110 dB SPL with the excitation phase detected at the narrower peak in the period histogram as shown in Fig. 4.25(b). The suppression threshold on the low-level CF-tone and off-CF-tone responses was reached at 90 dB SPL and 100 dB SPL respectively for the second harmonic criterion as shown in Fig. 4.25(c) and Fig. 4.25(d). The major suppression phase of off-CF-tone responses was opposite to that of the CF-tone responses. The next two examples show two fibers with a similar CF as this fiber which also came from the same cat as this fiber, CT030.

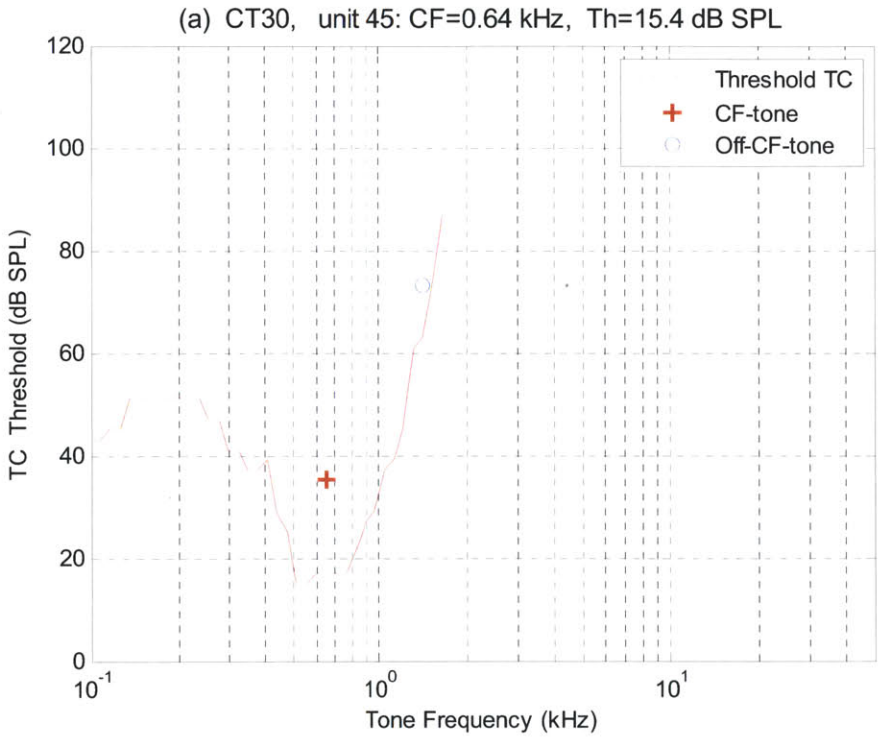

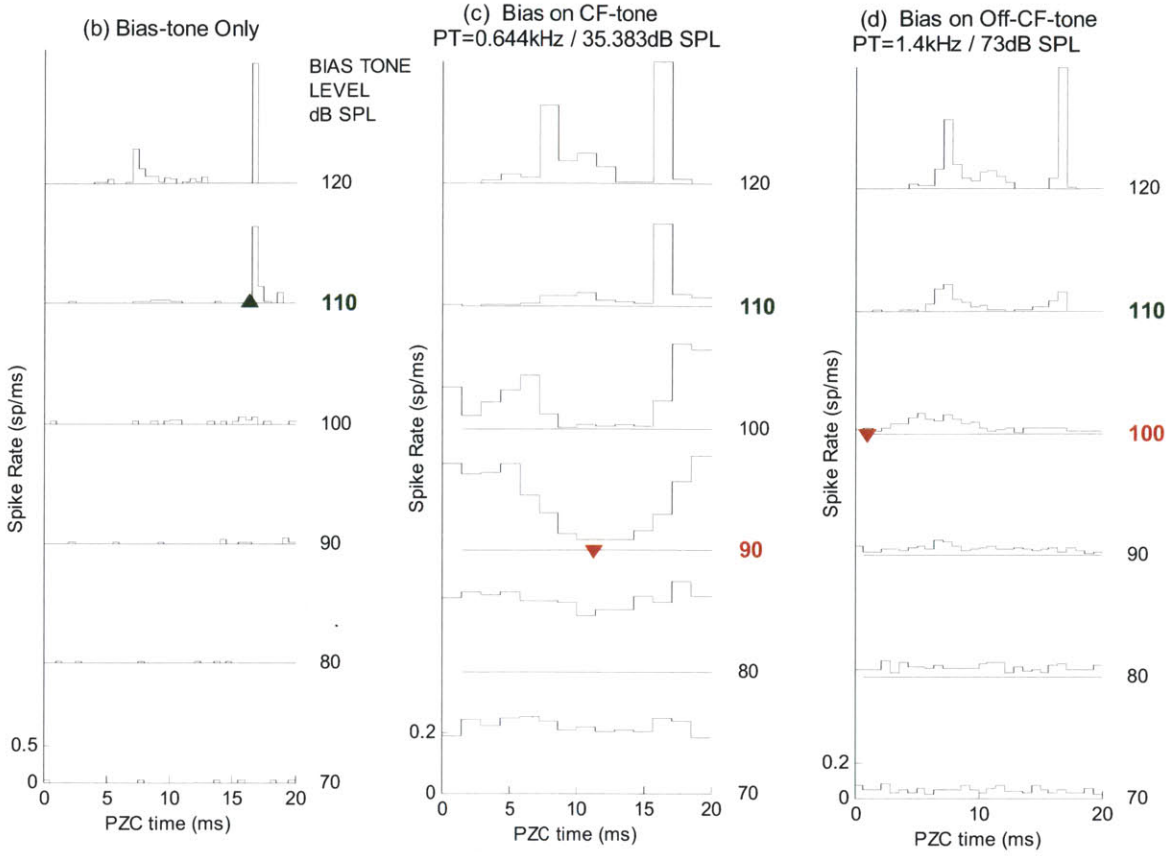
(b) Bias-tone Only
BIAS TONE LEVEL dB SPL
120
110
100
90
80
70
Spike Rate (sp/ms)
0.5
0
0 5 10 15 20
PZC time (ms)
(c) Bias on CF-tone
PT=0.644kHz / 35.383dB SPL
120
110
100
90
80
70
Spike Rate (sp/ms)
0.2
0
0 5 10 15 20
PZC time (ms)
(d) Bias on Off-CF-tone
PT=1.4kHz / 73dB SPL
120
110
100
90
80
70
Spike Rate (sp/ms)
0.2
0
0 10 20
PZC time (ms)

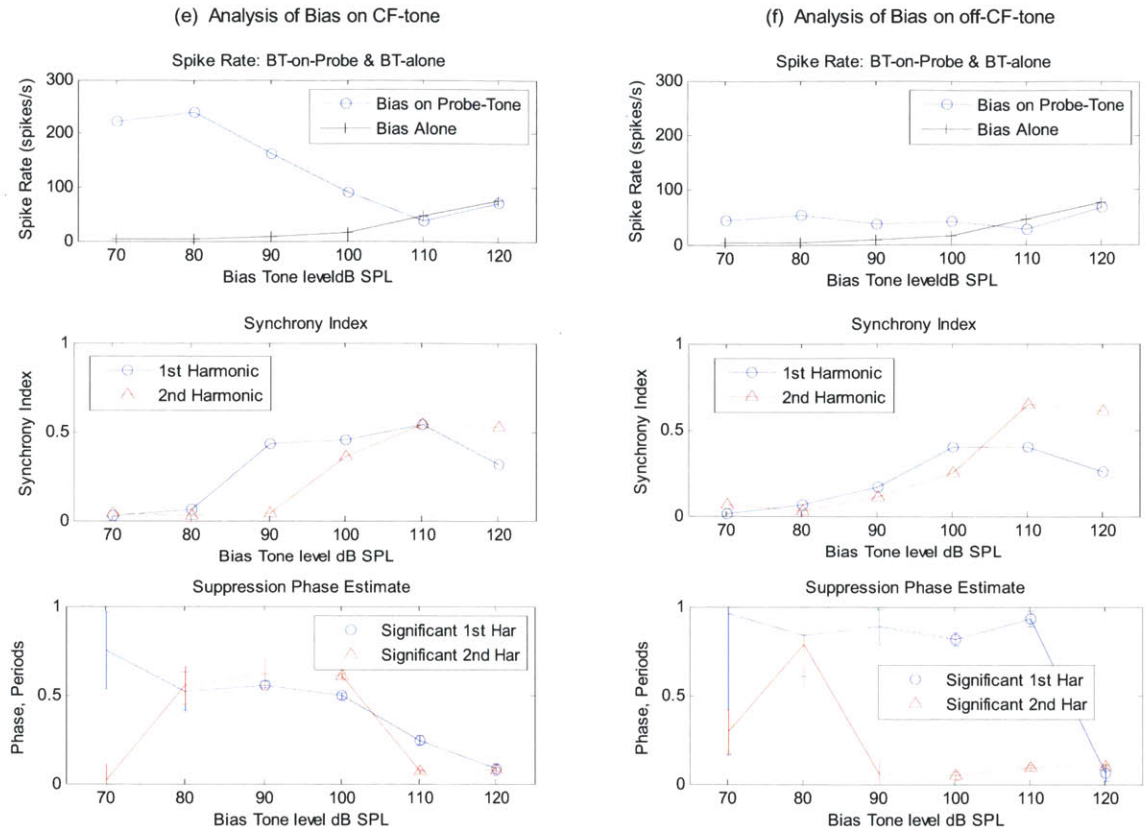

Fig. 4.25. Example Result: (a) Tuning Curve, CF=0.64kHz and SR= 7.2 sps. The acoustic stimulus for the CF and off-CF-tone are indicated as red '+' and blue 'o' together with the TC; (b) Bias-tone (BT) only level series, excitation threshold reached at 110 dB SPL. Excitation threshold level is indicated in green, and the excitation phase is indicated by a green triangle; (c) Bias-tone level-series on CF-tone response. The suppression threshold for the 2nd harmonic criterion was reached at 90 dB SPL. The suppression phase of the 2nd harmonic is indicated by a red inverted triangle; (d) Bias-tone level-series on off-CF-tone response. Suppression threshold for the 2nd harmonic was reached at 100 dB SPL. The oppositely located major and minor suppression phases are visible at the suppression threshold. Unlike most other fibers, the major suppression phase of off-CF-tone responses was opposite to that of CF-tone responses. At 10 dB lower than the suppression threshold, beginning of the major suppression phase seems to emerge at the opposite phase of the major suppression phase of CF-tone responses; (e) Detailed analysis of the bias-tone effects on CF-tone response, Bias-tone level functions of firing rate, synchrony indices and phase of major suppression for the 1st and 2nd harmonic in the top-bottom order; (f) Detailed analysis of the bias-tone effects on off-CF-tone response, Bias-tone level functions of firing rate, synchrony indices and phase of major suppression for the 1st and 2nd harmonic in the top-bottom order

Example Result in Fig. 4.26: CT030, U024, CF=0.688 kHz, SR=97 sps

This fiber had similar CF as the example in Fig. 4.25 and also came from the same cat as the example in Fig. 4.25 where the major suppression phase of off-CF-tone responses was located at approximately opposite phase to that of the main data group. The off-CF-tone was selected from the upper-side frequency of 1.35 kHz as shown in Fig. 4.26(a). The bias-tone only excitation threshold was met at 110 dB SPL. The suppression threshold on the low-level CF-tone and off-CF-tone responses was reached at 90 dB SPL and 100 dB SPL respectively for the second harmonic criterion as shown in Fig. 4.26(c) and Fig. 4.26(d). The major suppression phase of off-CF-tone responses was similar to that of the CF-tone responses as in the main data group.

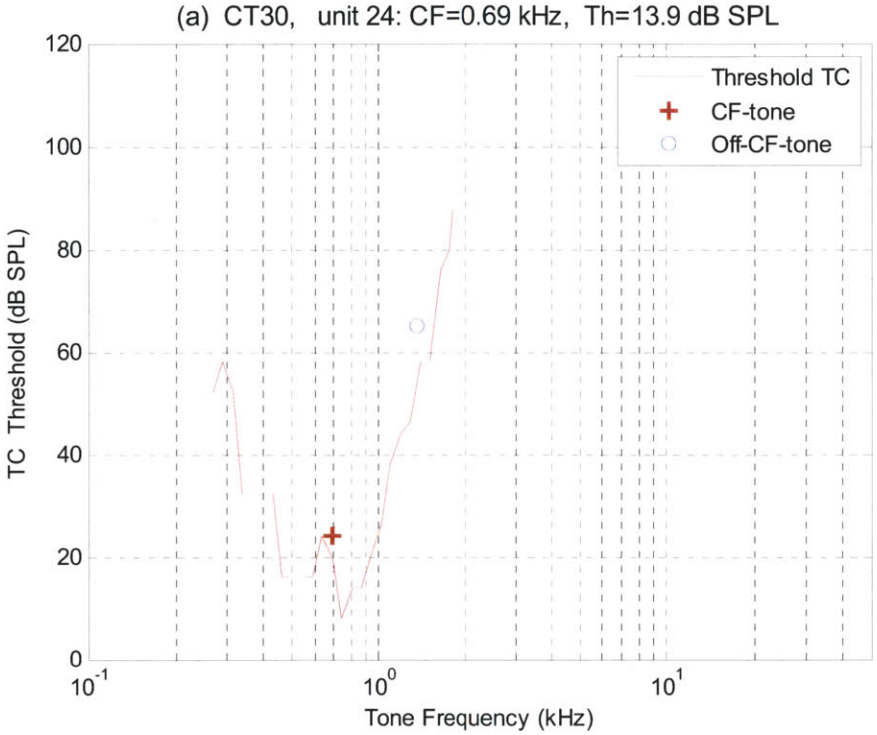

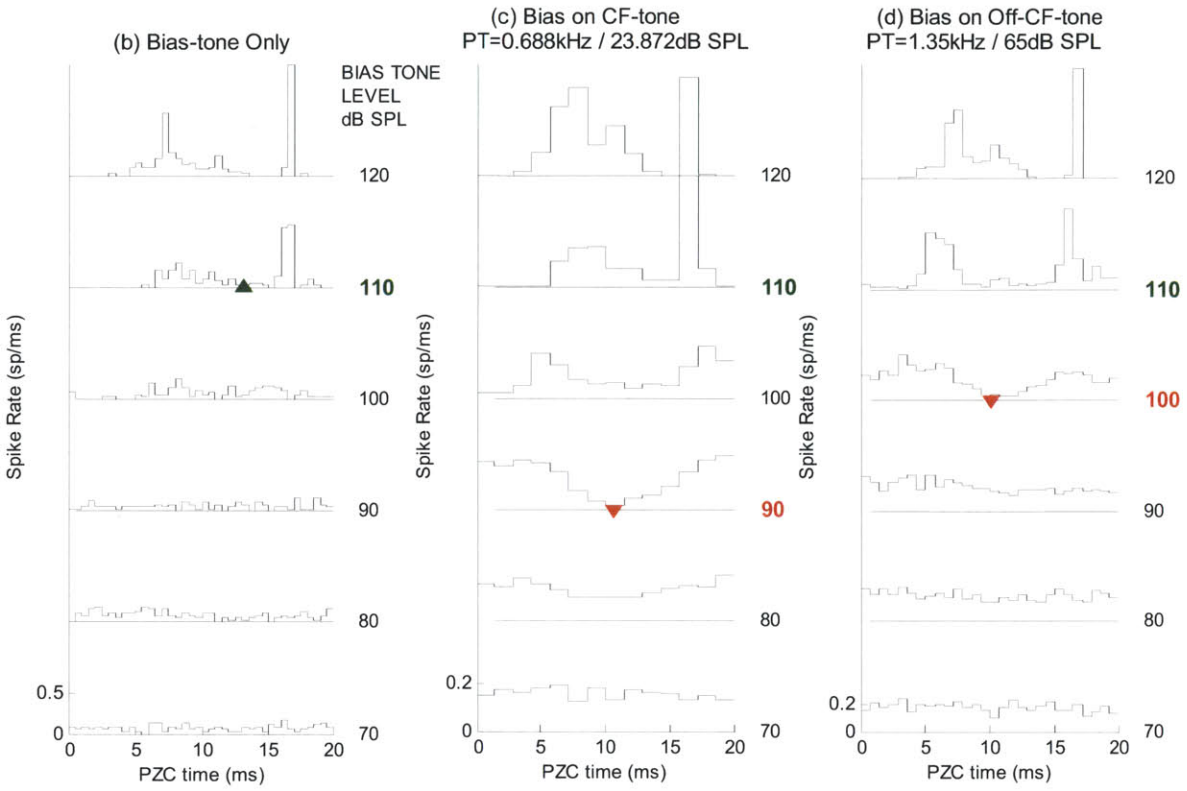
(b) Bias-tone Only
(c) Bias on CF-tone
PT=0.688kHz / 23.872dB SPL
(d) Bias on Off-CF-tone
PT=1.35kHz / 65dB SPL
BIAS TONE
LEVEL
dB SPL
120
110
100
90
80
70
Spike Rate (sp/ms)
0.5
0.2
0
5
10
15
20
PZC time (ms)

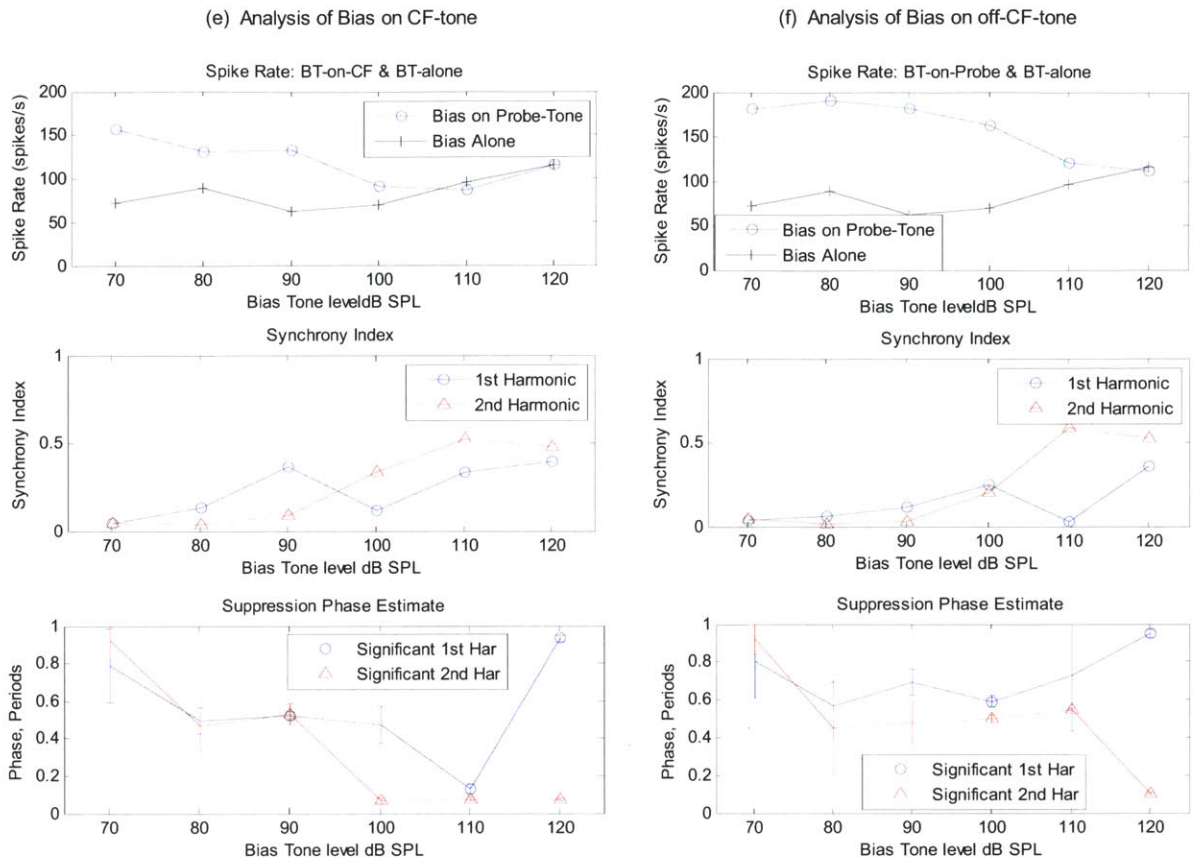

Fig. 4.26. Example Result: (a) Tuning Curve, CF=0.688kHz and SR= 97 sps. The acoustic stimuli for the CF and off-CF-tone are indicated as red '+' and blue 'o' together with the TC; (b) Bias-tone (BT) only level series, excitation threshold reached at 110 dB SPL; (c) Bias-tone level-series on CF-tone response. The suppression threshold for the 2nd harmonic criterion was reached at 90 dB SPL. The suppression phase of the 2nd harmonic is indicated by a red inverted triangle; (d) Bias-tone level-series on off-CF-tone response. Suppression threshold for the 2nd harmonic was reached at 100 dB SPL with the major suppression phase which was similar to that of CF-tone responses; (e) Detailed analysis of the bias-tone effects on CF-tone response, Bias-tone level functions of firing rate, synchrony indices and phase of major suppression for the 1st and 2nd harmonic in the top-bottom order; (f) Detailed analysis of the bias-tone effects on off-CF-tone response, Bias-tone level functions of firing rate, synchrony indices and phase of major suppression for the 1st and 2nd harmonic in the top-bottom order

Example Result in Fig. 4.27: CT030, U050, CF=0.791 kHz, SR=41 sps

This fiber had similar CF as the example in Fig. 4.25 and also came from the same cat as the example in Fig. 4.25 where the major suppression phase of off-CF-tone responses was located at approximately opposite phase to that of the main data group. The off-CF-tone was selected from the upper-side frequency of 1.34 kHz as shown in Fig. 4.27(a). The bias-tone only excitation threshold was met at 110 dB SPL. The suppression threshold on the low-level CF-tone and off-CF-tone responses was reached at 90 dB SPL for the second harmonic criterion as shown in Fig. 4.27(c) and Fig. 4.27(d). The major suppression phase of off-CF-tone responses was similar to that of the CF-tone responses as in the main data group.

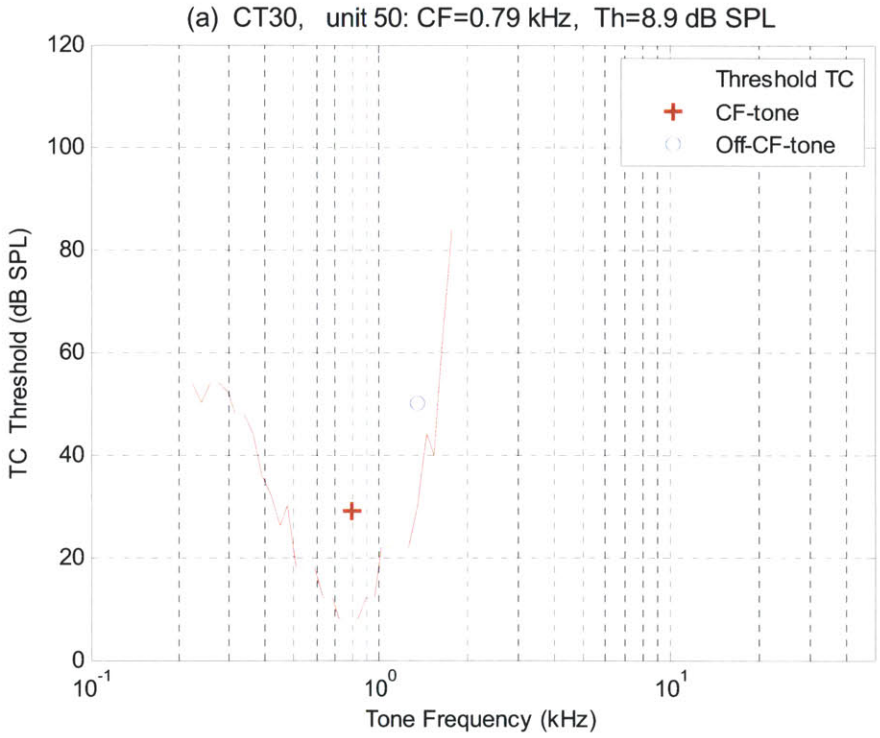

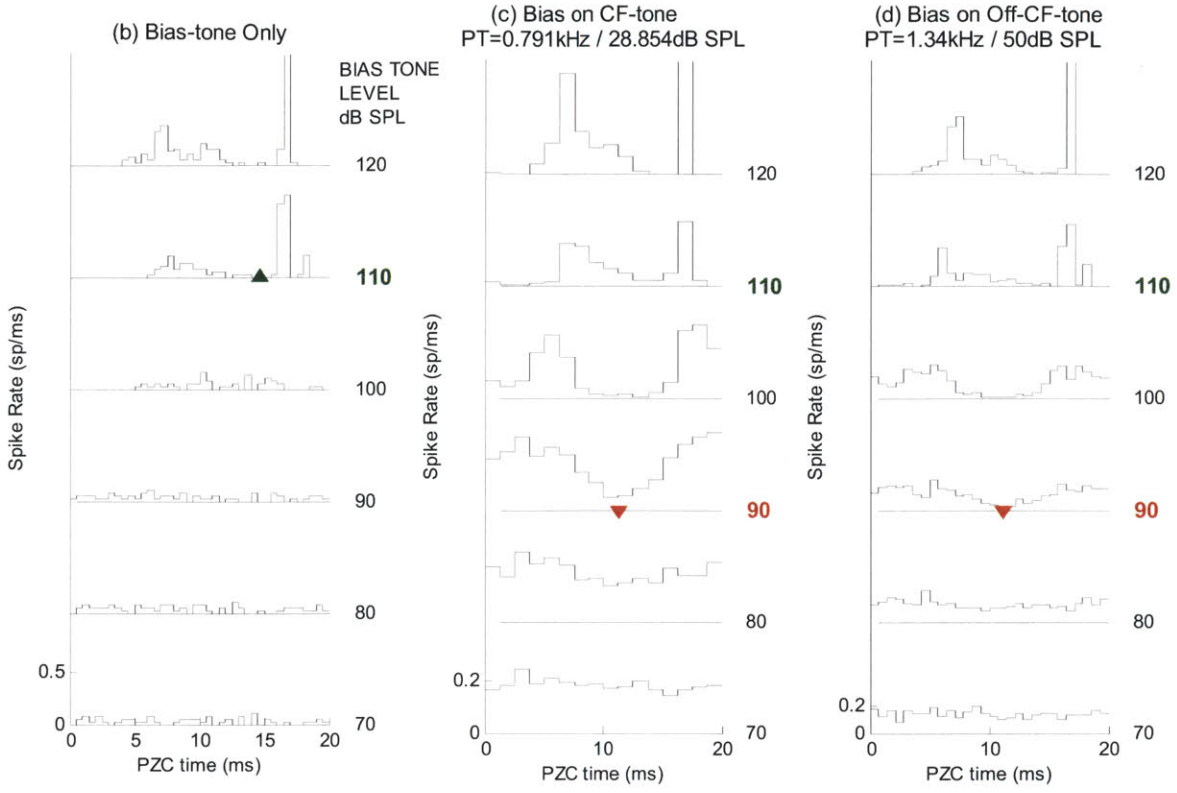
(b) Bias-tone Only
BIAS TONE LEVEL dB SPL
120
110
100
90
80
70
Spike Rate (sp/ms)
0.5
0
0
5
10
15
20
PZC time (ms)
(c) Bias on CF-tone
PT=0.791kHz / 28.854dB SPL
120
110
100
90
80
70
Spike Rate (sp/ms)
0.2
0
0
10
20
PZC time (ms)
(d) Bias on Off-CF-tone
PT=1.34kHz / 50dB SPL
120
110
100
90
80
70
Spike Rate (sp/ms)
0.2
0
0
10
20
PZC time (ms)

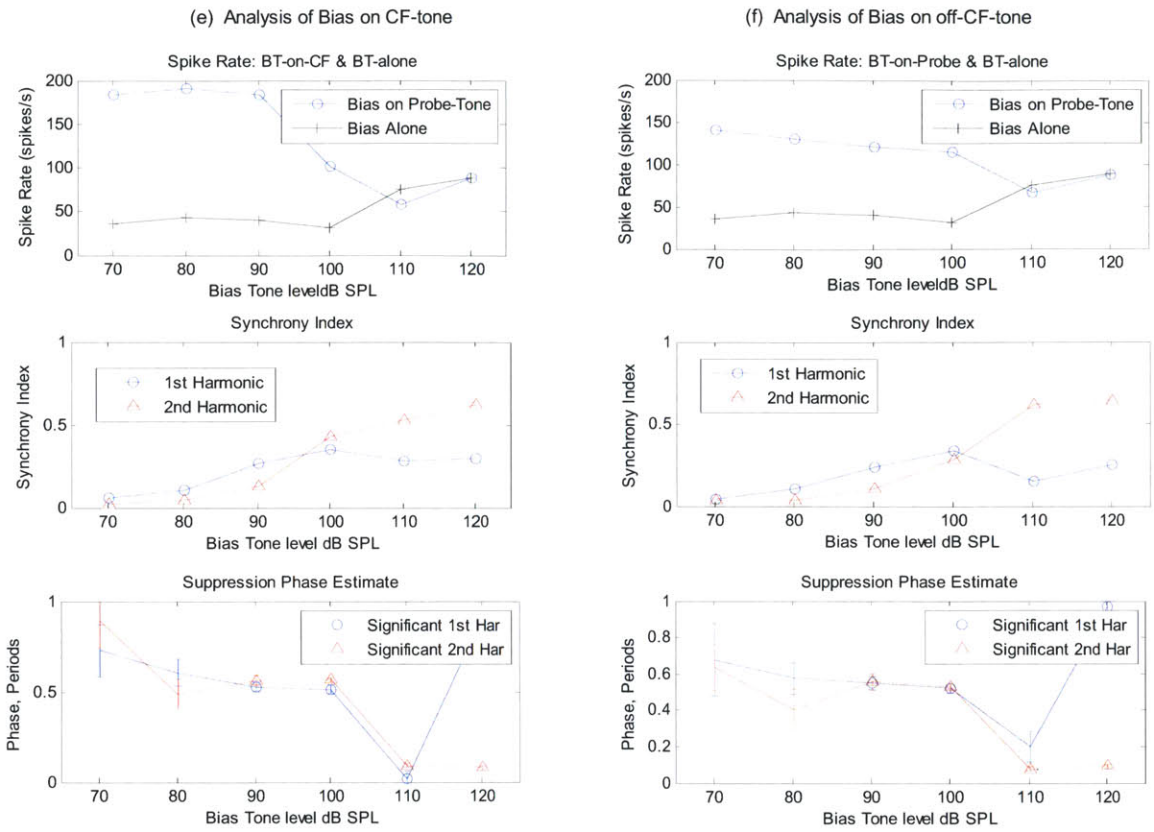

Fig. 4.27. Example Result: (a) Tuning Curve, CF=0.791kHz and SR= 41 sps. The acoustic stimuli for the CF and off-CF-tone are indicated as red '+' and blue 'o' together with the TC; (b) Bias-tone (BT) only level series, excitation threshold reached at 110 dB SPL; (c) Bias-tone level-series on CF-tone response. The suppression threshold for the 2nd harmonic criterion was reached at 90 dB SPL. The suppression phase of the 2nd harmonic is indicated by a red inverted triangle; (d) Bias-tone level-series on off-CF-tone response. Suppression threshold for the 2nd harmonic was reached at 90 dB SPL with the major suppression phase which was similar to that of CF-tone responses; (e) Detailed analysis of the bias-tone effects on CF-tone response, Bias-tone level functions of firing rate, synchrony indices and phase of major suppression for the 1st and 2nd harmonic in the top-bottom order; (f) Detailed analysis of the bias-tone effects on off-CF-tone response, Bias-tone level functions of firing rate, synchrony indices and phase of major suppression for the 1st and 2nd harmonic in the top-bottom order

Example Result in Fig. 4.28: CT031, U065, CF=1.76 kHz, SR=2.3 sps

This is one of the two fibers with the major suppression phase for off-CF-tone responses located at ~1/2 cycle away from the main data cluster. The off-CF-tone was selected from the lower-side frequency of 0.8 kHz as shown in Fig. 4.28(a). The bias-tone only excitation threshold was met at 100 dB SPL with the excitation phase detected at the narrower peak in the period histogram as shown in Fig. 4.28(b). The suppression threshold on the low-level CF-tone was reached at 80 dB SPL of the bias-tone for the second harmonic criterion with the major suppression phase located at a similar location as the main data group. As for the off-CF-tone responses, the suppression threshold was reached at 80 dB SPL with the major suppression phase located away from the main data group. Over the increasing bias-tone level, the period histogram did not follow the typical progression of suppression pattern. Specifically, at 100 dB SPL, which was the excitation threshold, the shape of the period histogram did not resemble the shape from the bias-tone alone runs but drastically shifted to resemble the suppression pattern on CF-tone responses at 90 dB SPL of the bias-tone. Further, the spike rate on the off-CF-tone responses remained relatively unchanged up to 100 dB SPL and started to decline for the bias-tone levels above 100 dB SPL. These observations suggest that the actual suppression effects on off-CF-tone responses due to the bias-tone effects on OHC transduction function did not start until 100 dB SPL of the bias-tone, and the actual value of the major suppression phase of the off-CF-tone responses from this fiber did not differ from the main data group. Note that the example fiber from the methods section had a similar CF of 1.88 kHz and the major suppression phase which was similar to the main data group.

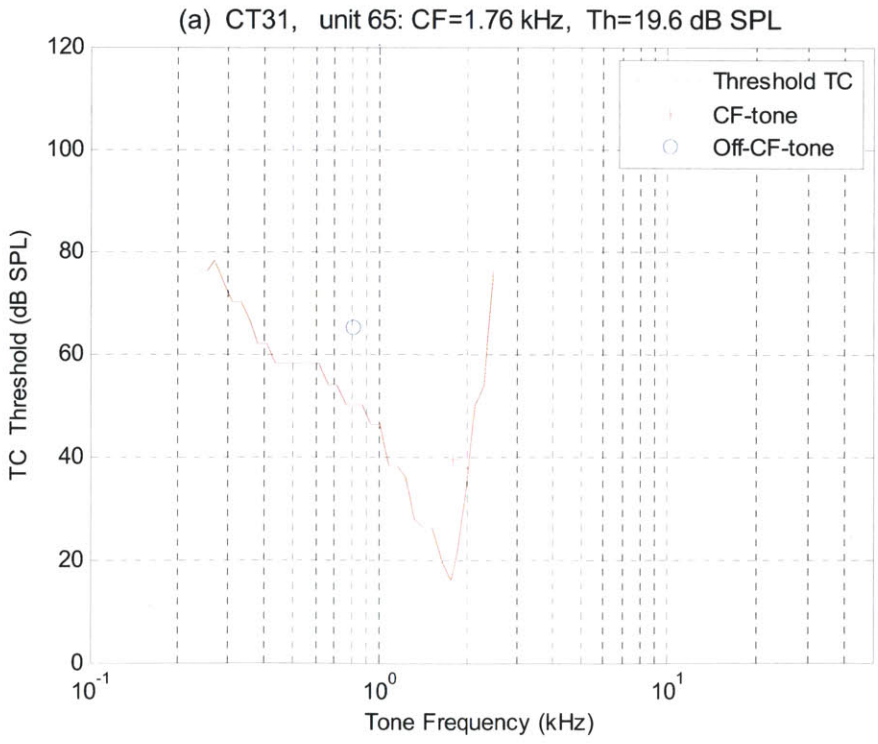

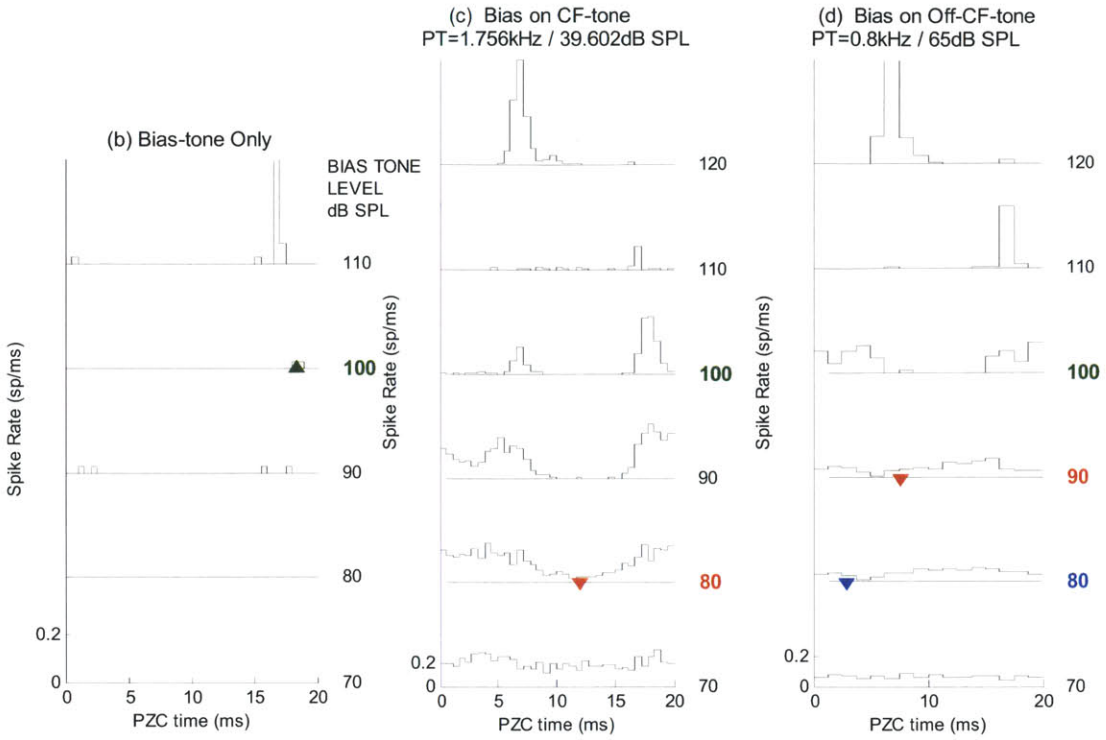
(b) Bias-tone Only
(c) Bias on CF-tone
PT=1.756kHz / 39.602dB SPL
(d) Bias on Off-CF-tone
PT=0.8kHz / 65dB SPL
BIAS TONE
LEVEL
dB SPL
110
100
90
80
70
120
Spike Rate (sp/ms)
0.2
0
0
5
10
15
20
PZC time (ms)

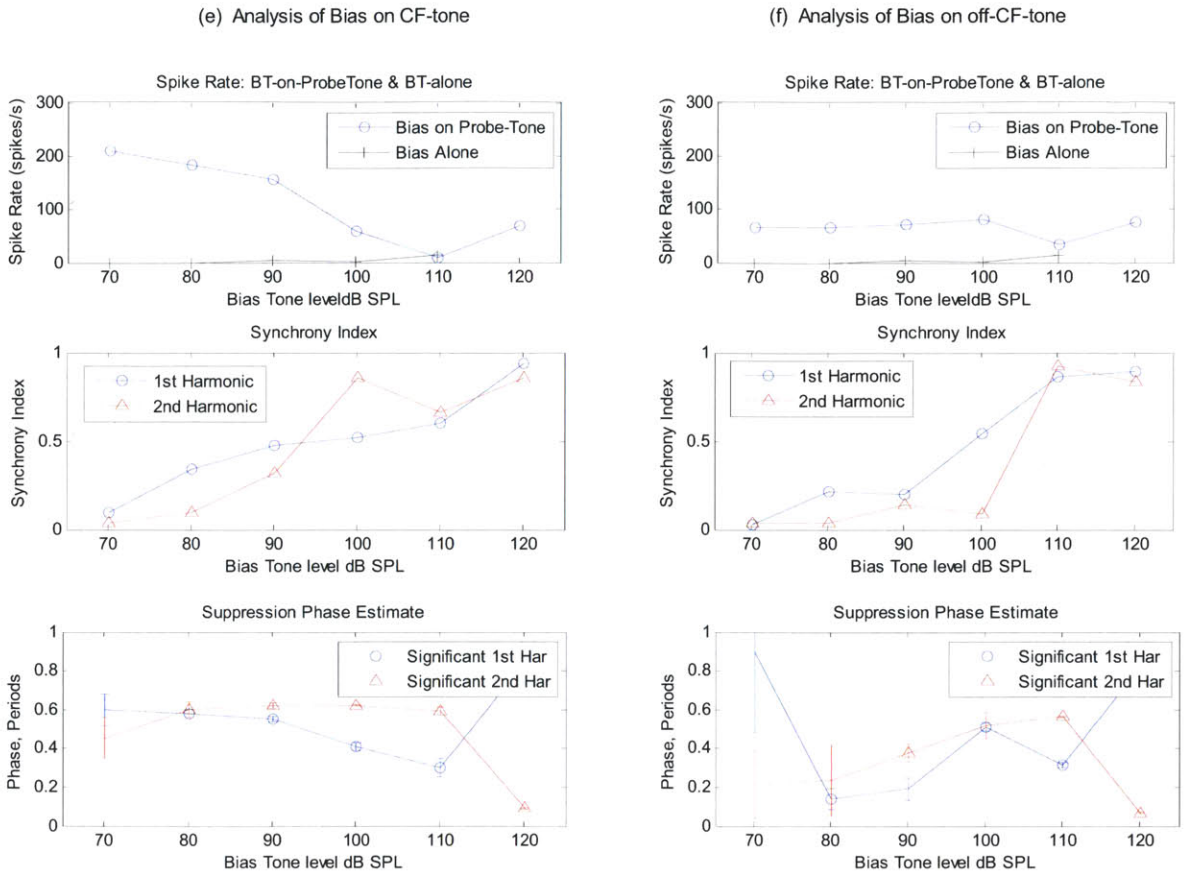

Fig. 4.28. Example Result: (a) Tuning Curve, CF=1.76 kHz and SR= 2.3 sps. The acoustic stimuli for the CF and off-CF-tone are indicated as red '+' and blue 'o' together with the TC; (b) Bias-tone (BT) only level series, excitation threshold reached at 100 dB SPL; (c) Bias-tone level-series on CF-tone response. The suppression threshold for the 2nd harmonic criterion was reached at 80 dB SPL. The suppression phase of the 2nd harmonic is indicated by a red inverted triangle; (d) Bias-tone level-series on off-CF-tone response. Suppression threshold for the 2nd harmonic was reached at 80 dB SPL with the major suppression phase which was opposite to that of the main data group; (e) Detailed analysis of the bias-tone effects on CF-tone response, Bias-tone level functions of firing rate, synchrony indices and phase of major suppression for the 1st and 2nd harmonic in the top-bottom order; (f) Detailed analysis of the bias-tone effects on off-CF-tone response, Bias-tone level functions of firing rate, synchrony indices and phase of major suppression for the 1st and 2nd harmonic in the top-bottom order.

Example Result in Fig. 4.29: CT028, U026, CF=2.07 kHz, SR=115.3 sps

This fiber with CF=2.07 kHz is a typical example for fibers with CF > 1.7 kHz where the off-CF-frequency was selected from the lower-side of the CF, i.e., 1.0 kHz for this fiber as shown in Fig. 4.29(a) The bias-tone only excitation threshold was met at 90 dB SPL. The suppression threshold on the low-level CF-tone and off-CF-tone was reached at 80 dB SPL for the first harmonic criterion with a similar value on the major suppression phase as with the main data group. Note that for this fiber, the bias-tone level function of the period histogram, spike rates and synchrony indices for the CF-tone and the off-CF-tone responses were quite similar to one another.

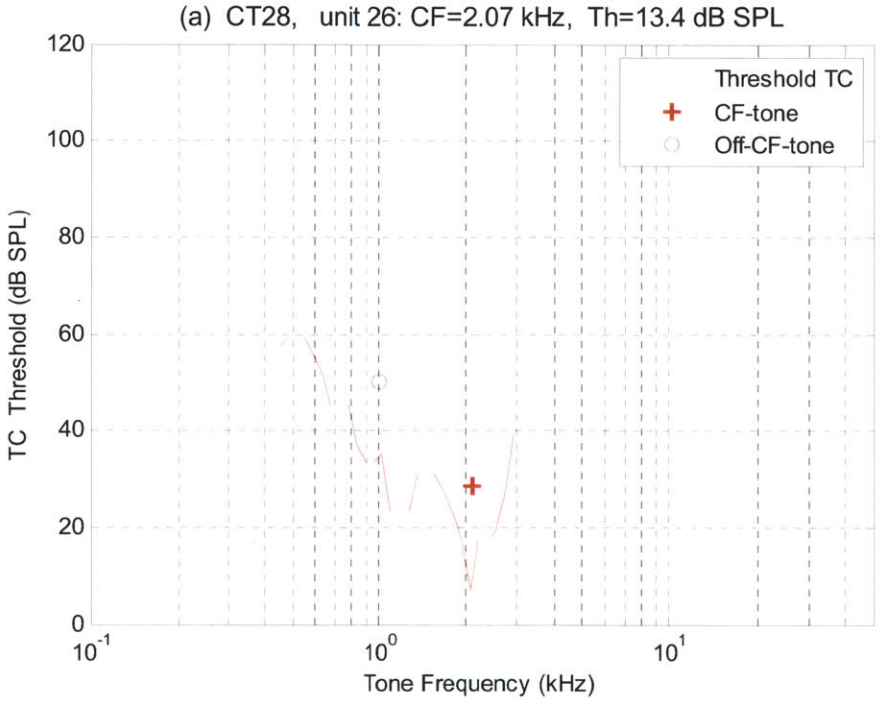

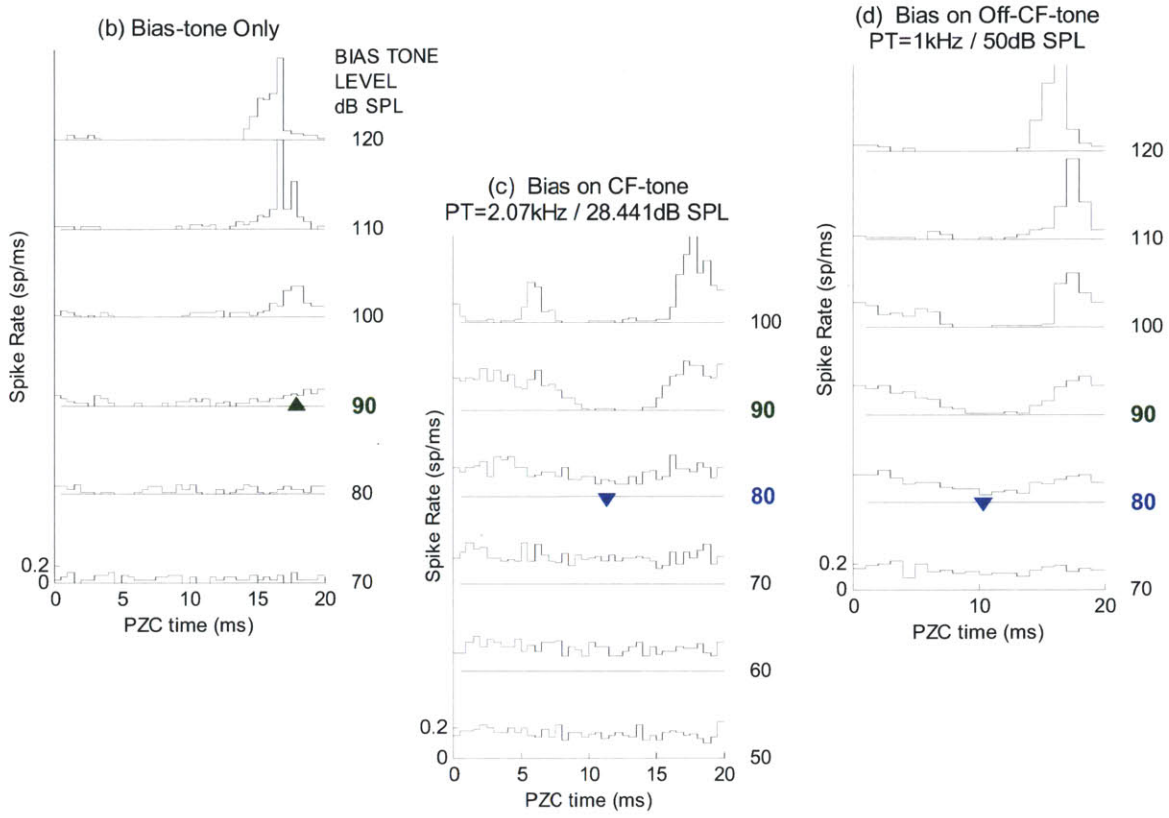
(b) Bias-tone Only
BIAS TONE
LEVEL
dB SPL
120
110
100
90
80
70
Spike Rate (sp/ms)
0.2
0
0
5
10
15
20
PZC time (ms)
(c) Bias on CF-tone
PT=2.07kHz / 28.441dB SPL
100
90
80
70
60
50
Spike Rate (sp/ms)
0.2
0
0
5
10
15
20
PZC time (ms)
(d) Bias on Off-CF-tone
PT=1kHz / 50dB SPL
120
110
100
90
80
70
Spike Rate (sp/ms)
0.2
0
0
10
20
PZC time (ms)

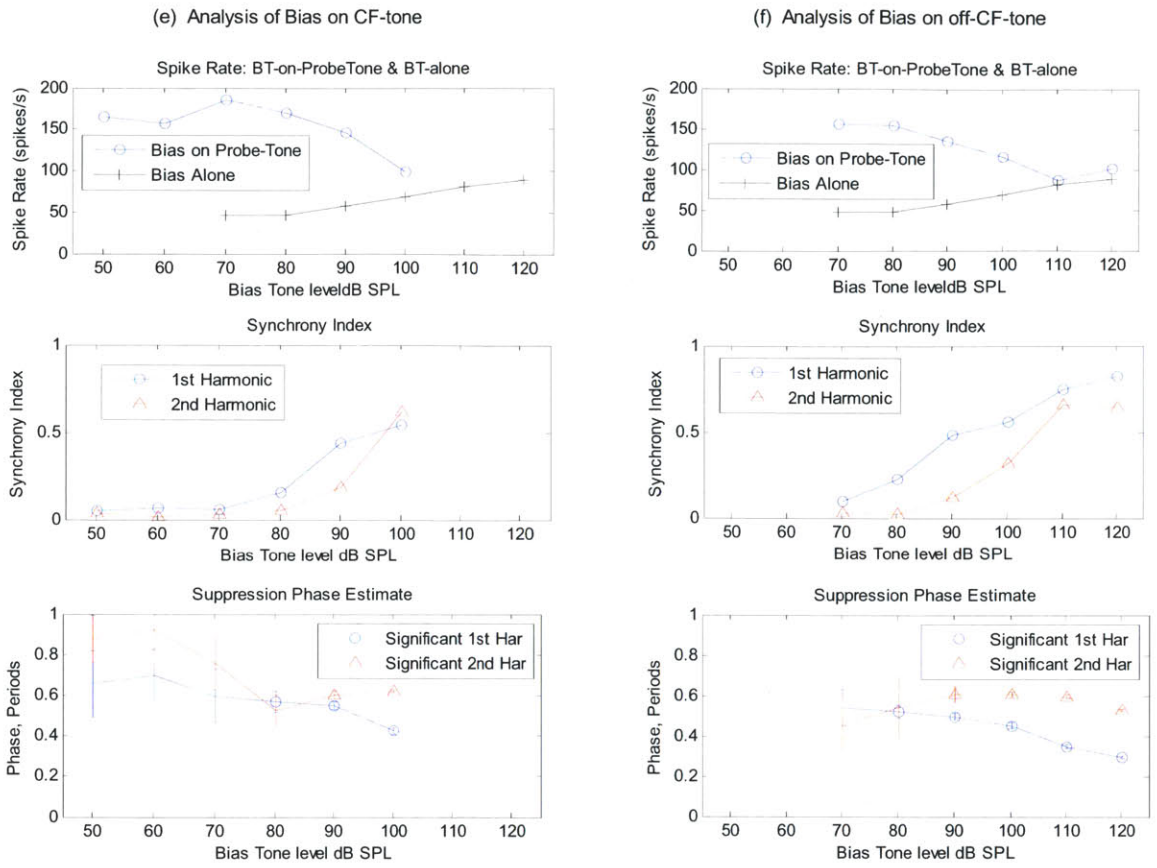

Fig. 4.29. Example Result: (a) Tuning Curve, CF=2.07kHz and SR= 115.3 sps. The acoustic stimuli for the CF and off-CF-tone are indicated as red '+' and blue 'o' together with the TC; (b) Bias-tone (BT) only level series, excitation threshold reached at 90 dB SPL; (c) Bias-tone level-series on CF-tone response. The suppression threshold for the 1st harmonic criterion was reached at 80 dB SP; (d) Bias-tone level-series on off-CF-tone response. Suppression threshold for the 1st harmonic was reached at 80 dB SPL with the major suppression phase which was similar to that of CF-tone responses as in the main data group; (e) Detailed analysis of the bias-tone effects on CF-tone response, Bias-tone level functions of firing rate, synchrony indices and phase of major suppression for the 1st and 2nd harmonic in the top-bottom order; (f) Detailed analysis of the bias-tone effects on off-CF-tone response, Bias-tone level functions of firing rate, synchrony indices and phase of major suppression for the 1st and 2nd harmonic in the top-bottom order.

Example Result in Fig. 4.30: CT031, U069, CF=3.44 kHz, SR=59.3 sps

This fiber had the highest CF among the fibers with significant suppression on both the CF-tone and off-CF-tone responses found in this study. The off-CF-tone was selected as 1.0 kHz from the lower-side frequency of the CF of the fiber as shown in Fig. 4.30(a). The bias-tone only excitation threshold was met at 100 dB SPL. Note that peak splitting was visible at 110 dB SPL of the bias-tone with the location of the wide and narrow peak reversed in comparison to fibers with CF < 1 kHz; for example, Fig. 4.27(b) with CF=0.791 kHz. The suppression threshold on the low-level CF-tone was reached at 80 dB SPL for the first harmonic criterion. The suppression threshold on the low-level off-CF-tone was reached at 90 dB SPL for the second harmonic criterion with the major suppression phase similar to that of CF-tone response as found in the main data group. Note that for this fiber, the bias-tone level function of the period histogram, spike rates and synchrony indices for the CF-tone and the off-CF-tone responses were quite similar to one another.

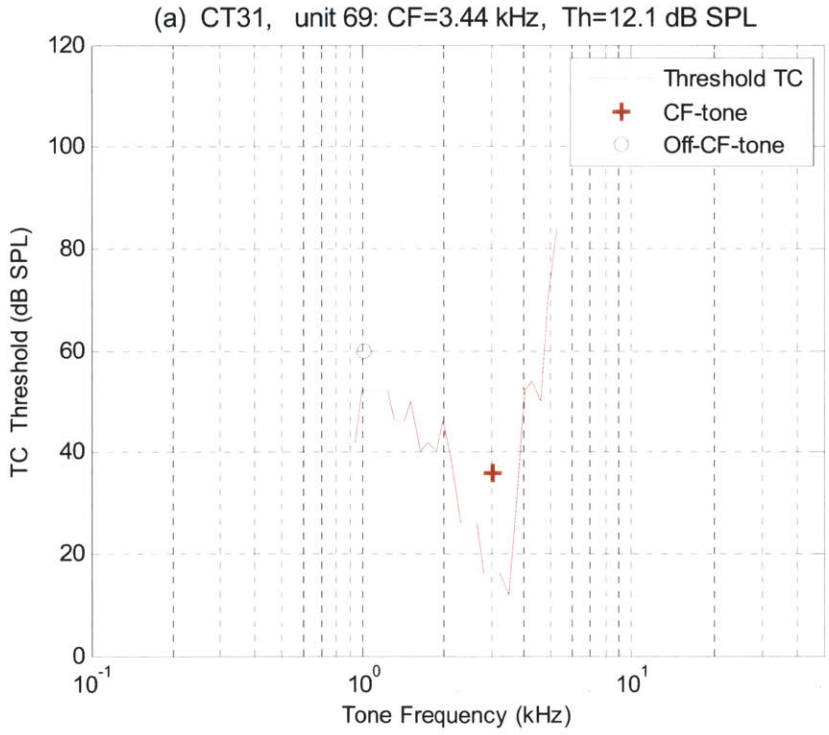

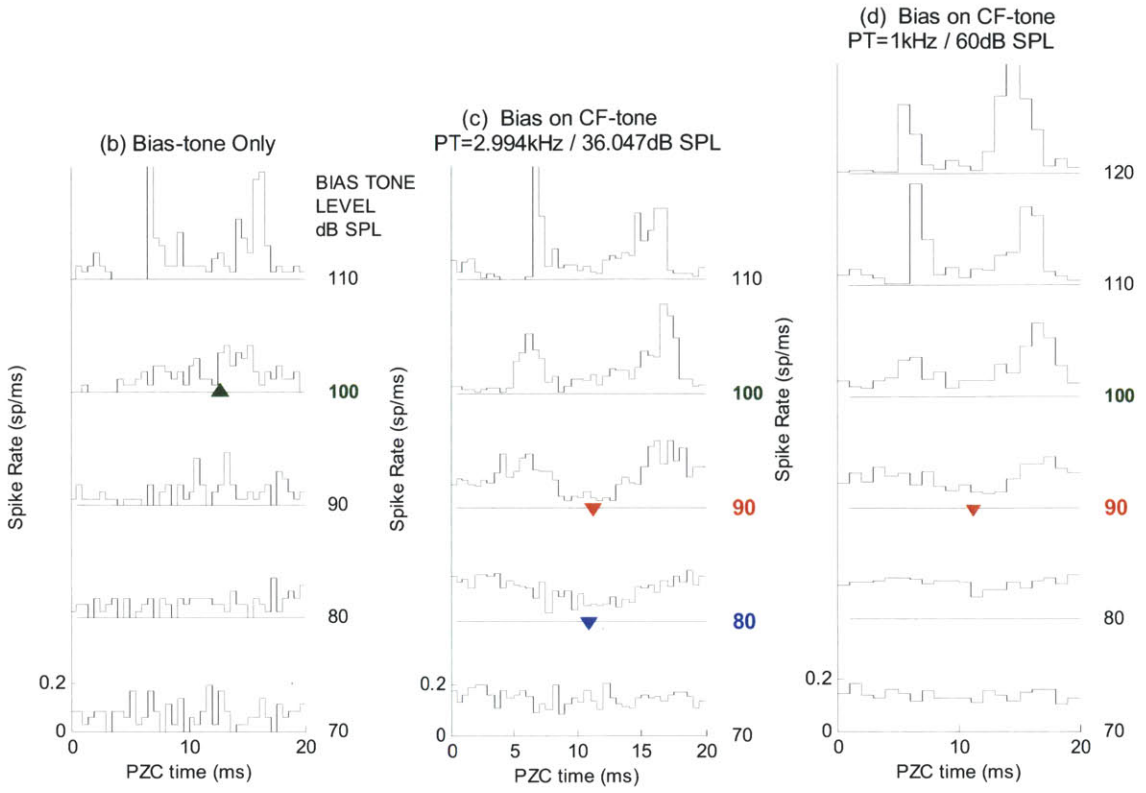
(b) Bias-tone Only
(c) Bias on CF-tone
PT=2.994kHz / 36.047dB SPL
(d) Bias on CF-tone
PT=1kHz / 60dB SPL
BIAS TONE
LEVEL
dB SPL
110
100
90
80
70
120
Spike Rate (sp/ms)
0.2
0
0
5
10
15
20
PZC time (ms)

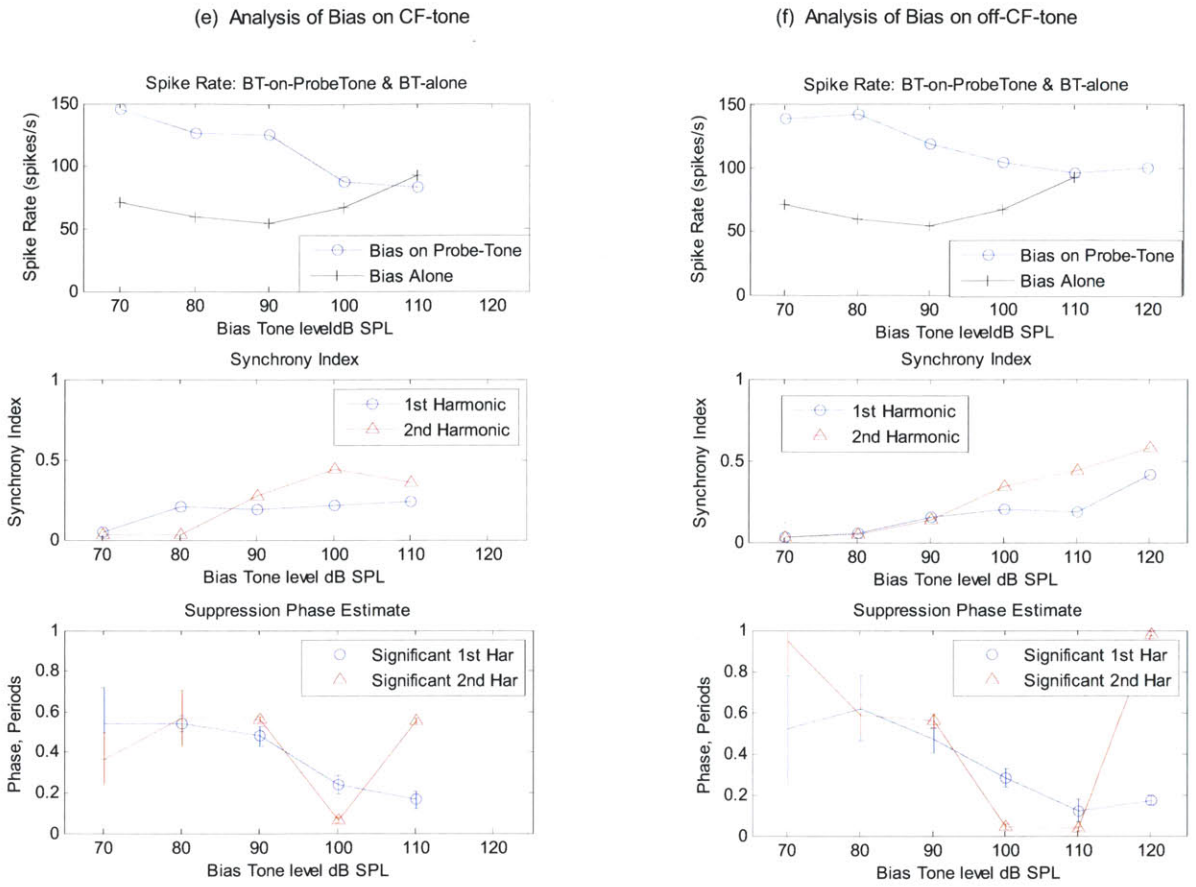

Fig. 4.30. Example Result: (a) Tuning Curve, CF=3.44 kHz and SR= 59.3 sps. The acoustic stimuli for the CF and off-CF-tone are indicated as red '+' and blue 'o' together with the TC; (b) Bias-tone (BT) only level series, excitation threshold reached at 100 dB SPL; (c) Bias-tone level-series on CF-tone response. The suppression threshold for the 1st harmonic criterion was reached at 80 dB SPL; (d) Bias-tone level-series on off-CF-tone response. Suppression threshold for the 2nd harmonic was reached at 90 dB SPL with the major suppression phase which was similar to that of CF-tone responses as in the main data group; (e) Detailed analysis of the bias-tone effects on CF-tone response, Bias-tone level functions of firing rate, synchrony indices and phase of major suppression for the 1st and 2nd harmonic in the top-bottom order; (f) Detailed analysis of the bias-tone effects on off-CF-tone response, Bias-tone level functions of firing rate, synchrony indices and phase of major suppression for the 1st and 2nd harmonic in the top-bottom order.

IV. Discussion

A. The Suppression Effects on AN Firing Reported in This Study Were Primarily Due to Stimulation of OHCs rather than Direct Stimulation of IHC Stereocilia by the 50 Hz Bias-tone

Although 50 Hz bias-tone used in this study is expected to stimulate the OHC stereocilia with higher amplitude than the IHC stereocilia [Russell and Sellick, 1983], it has been found in this study and elsewhere [Sellick et al, 1982; Patuzzi et al, 1984a; Cai and Geisler, 1996a] that AN responses to bias-tone level series with bias-tone alone do show both firing rate elevation and phasic modulation of period histograms at high enough levels of bias-tone. Consequently, it would be necessary to examine whether the results reported in this study as suppressive effects on OHC transduction function were not significantly affected by direct stimulation of the IHC stereocilia by the bias-tone.

In order to detect results with potential effects of direction stimulation of IHC stereocilia by the bias-tone, the excitation threshold level on AN firing by the bias-tone alone was measured from the AN response to level series of bias-tone alone from each AN fiber. Then, the results from the bias-tone level series on either low-level CF-tone or click responses were not included in the data pool for suppression effects.

The criteria to determine the excitation threshold of a AN fiber required firing rate elevation by a standard deviation and the standard error on the vector phase of firing to be within ±20°. Now, it would be necessary to examine whether the criteria applied on the reported results were appropriate. In order to examine the impact of the excitation threshold criteria on the suppression data, several iterations of data analysis were done with varying degrees of criteria around the values applied on the reported results. For example, the rate criteria with smaller increment such as ½ of standard deviation and the phase criteria with larger error bound such as ±30° are expected to lower the threshold of excitation by the bias-tone alone whereas a larger increment of firing rate such as two standard deviation and lower error bound on phase such as 10° would elevate the excitation threshold. Series of plots of the excitation phase and the major suppression phase of CF-tone and click response as shown in Fig. P and Fig. S with varying criteria on the excitation threshold did not show significant shifts in the results other than the number and scatter of data points around the same trend as shown in Fig. P and Fig. S. Considering these, the suppression Effects on AN Firing reported in this study were primarily due to stimulation of OHCs rather than direct stimulation of IHC stereocilia by the 50 Hz bias-tone

B. Comparison to Previous Studies on Low-frequency Bias-tone Effects on AN Responses to Low-level CF-tone

The previous study which is the most comparable to the results reported here for the bias-tone effects on low-level CF-tone responses comes from [Cai and Geisler, 1996a]. In their study, the temporal aspects of the suppressive effects of a low-frequency bias-tone on low-level CF-tone responses from cats AN fibers over the entire range of CFs were reported. Specifically, their results covered the bias-tone frequency of 50 Hz and comparison of the major suppression phase of the low-level CF-tone responses with the phase of excitation by the 50 Hz bias-tone alone as reported in this study. Overall, the results reported here were quite similar to the comparable results from [Cai and Geisler, 1996a] with no major discrepancies.

As reported in Fig 4.A and Fig. 5.A of [Cai and Geisler, 1996a] and in Fig. 4.16 of this study, the phase of major suppression by 50 Hz bias-tone on low-level CF-tone responses formed a smooth curve without significant discontinuities over the CFs of the AN fibers with a similar slope of ~-0.1 period of the 50 Hz bias-tone per decade of CF. Further, both studies showed that the major suppression phase was located ~1/4 cycle away from the phase of excitation by the bias-tone alone. Also both studies found that for the bias-tone frequency of 50 Hz, the phase of excitation by the bias-tone alone varied over the range of ~1/2 cycle for fibers with CF < ~2 kHz due to the peak-splitting phenomenon whereby a wide and a narrow peak separated by about ~1/2 cycle developed. With reference to the phase of the narrow peak, the major suppression phase was located with ~1/4 period lead as found by both studies. Further, similar results of ~1/4 cycle lead of the suppression phase of AN responses to low-level CF-tone in relation to the phase of excitation by the bias-tone alone have been found from low-frequency bias-tone studies on guinea pigs and chinchillas [Sellick et al, 1982; Temchin et al, 1997]. Note that the results on chinchillas' AN were obtained with the bias-tone frequency of 50 Hz as done in this study [Temchin et al, 1997] while the studies on AN fibers from guinea pigs were done with a similar frequency of 40 Hz [Sellick et al, 1982].

Despite the agreement among various studies on the relationship between the major suppression phase and the phase of excitation, relating the major suppression phase to the phase of BM vibration resulted in conflicting reports on cats [Cai and Geisler, 1996a; Rhode and Cooper, 1993]. Studies on low-frequency bias-tone effects on cats' BM vibration to low-level CF-tone by Rhode and Cooper reported that the major suppression phase corresponded to the phase of peak displacement of BM toward ST as found in both BM and AN studies on guinea pigs and chinchillas [Sellick et al, 1982; Patuzzi and Sellick, 1984b; Geisler and Nuttall, 1997; Temchin et al, 1997]. However, the studies on the bias-tone effects on cats' AN responses in [Cai and Geisler, 1996a] reported that the major suppression phase corresponded to the phase of peak displacement of BM toward SV which is opposite phase to the finding from studies on cats BM vibration. In [Cai and Geisler, 1996a], the phase of BM vibration corresponding to the phase of period histogram of AN firing was estimated from the gross potential recorded from the electrode placed near the round window. According to their estimate of the phase of BM vibration, the phase of excitation by the 50 Hz bias-tone as well as the major suppression phase were opposite to the results on guinea pigs [Sellick et al, 1982]. Consequently, if the BM phase estimates used in [Cai and Geisler, 1996a] were erroneous such that the phase of excitation actually corresponded to the phase of peak velocity of BM toward SV as found in other species, the major suppression phase would indeed correspond to the phase of peak displacement of BM toward ST which would be consistent with the studies on BM vibration measurements by Rhode and Cooper and also with the AN and BM studies on guinea pigs and chinchillas.

C. Comparison of the Bias-tone Suppression Patterns on Low-level CF–tone VS Off-CF-tone Responses Indicates that OHC Mechano-electrical Transduction Function Is Similarly Involved in Generating Low-level CF-tone Response and Low-level Off-CF-tone Response of Cats AN Fibers with CF < 4 kHz

The suppressive effects of 50 Hz bias-tone level series on AN responses to low-level CF-tone and low-level off-CF-tones were analyzed to compare the shape of the OHC transduction function behind the

two response types. Specifically, the major suppression phase and the degree of symmetry between the major and minor suppression phase at the suppression threshold were determined as shown in Fig. 4.19, Fig. 4.22 and Fig. 4.23.

Overall, comparison of the suppressive effects on low-level CF-tone VS low-level off-CF-tone responses in Fig. 4.19, Fig. 4.22 and Fig. 4.23 indicated that OHCs were involved in generating the low-level CF-tone and off-CF-tone responses with similar shape of mechano-electrical transduction function for AN fibers with CF up ~3.5 kHz. Particularly, significant differences were not found in the suppression data for the off-CF-tone responses across the break-frequency of ~1 kHz where the direction of the frequency glide in impulse responses of AN fibers is known to reverse [Carney et al, 1999; Shera, 2001]. As for the symmetry of the operating point of the OHC transduction function, most of the data points of the half-period symmetry index for both low-level CF-tone and off-CF-tone responses from fibers with CF < 3.5 kHz were located below the value of 1/2 as shown in Fig. 4.23 indicating a significantly asymmetric location of the operating point of the OHC transduction function resembling the model of Fig. 4.3(b) rather than Fig. 4.3(a) for both low-level CF-tone and off-CF-tone responses.

From the plot of the major suppression phase in Fig. 4.19, two data points with the CF of 0.64 kHz and 1.76 kHz for the off-CF-tone responses were located at ~1/2 cycle away from the main data group. These outlier cases for the off-CF-tone responses were analyzed in detail in Fig. 4.25 and Fig 4.28. The detailed analysis of the case with CF = 1.76 kHz revealed that the significant modulation on the period histogram detected as suppression effects at 80 dB SPL of the bias-tone is unlikely to be due to the bias-tone effects on the mechanoelectric transduction function on OHCs since the suppression on spike rates did not start until 100 dB SPL at which a typical pattern of bias-tone induced suppression started to emerge. Consequently, the bias-tone induced suppression effects on this fiber did not actually differ significantly from the main data group. As for the outlier case with CF = 0.64 kHz with the major suppression phase reversed from the main data group, detailed examination of the level function of the period histograms and the spike rate suggests that the reversed phase of major suppression at 100 dB SPL of the bias-tone for this fiber is indeed likely to be due to bias-tone effects on OHC transduction function. Since typical patterns were found with fibers with similar CFs from multiple animals in addition to this exceptional case as shown in detail in Fig. 4.29 and Fig. 4.30, this fiber does not significantly affect the main conclusion from this study that the OHC transduction function is similarly involved in generating AN responses to CF-tones and off-CF-tones from AN fibers with CFs < 3.5 kHz. However, due to the relatively small size of the data available from this study, the correlation of this exceptional behavior with the key parameters of the AN fibers or acoustic stimuli; for example, the spontaneous rate of the fiber, the range of the CF of the fiber, the frequency spacing of the off-CF-tone re. the CF of the fiber and the intensity of the off-CF-tone, could not be investigated thereby remains as an interesting issue for future studies.

As for the suppression thresholds, the thresholds on CF-tone response were ~10 dB lower than that of off-CF-tone responses for all fibers with CF < 3.5 kHz. Again, no significant shift in the difference in the suppression threshold between CF-tone VS off-CF-tone responses could be found across the break-frequency of 1 kHz. These data may suggest that application of a low-frequency bias-tone would result in broadening of the tuning curve for most of the fibers with CF < 3.5 kHz thereby suggesting a potential

conflict with results from some of the fibers from the MOC efferent stimulation studies where further sharpening of tuning was found from some fibers with CFs of 1 – 2 kHz [Guinan and Gifford, 1988c]. Note, however, since MOC efferent stimulation inhibits the electromotility of OHCs whereas a low-frequency bias-tone suppresses the gain of the mechanoelectric transduction function of OHCs, it is premature to conclude any conflicts in the results of these two studies. Therefore, this remains as an interesting issue for future studies.

In summary, comparison of the bias-tone suppression patterns on AN responses to low-level CF–tone VS the off-CF tones selected from the region where shorter group delays were reported in [Pfeiffer & Molnar, 1980; Kiang, 1984; Van der Heijden & Joris, 2006; Temchin et al, 2009] indicates that OHC mechano-electrical transduction function was similarly involved in generating AN responses to low-level CF-tones and low-level off-CF tones from the frequency region where shorter group delays were reported.

V. References

Cai Y, Geisler CD. (1996) Temporal patterns of the responses of auditory-nerve fibers to low-frequency tones. Hear Res. 1996 Jul;96(1-2):83-93.

Cai Y, Geisler CD (1996a) Suppression in auditory-nerve fibers of cats using low-side suppressors. I. Temporal aspects. Hear Res. 1996 Jul;96(1-2):94-112

Cai Y, Geisler CD (1996c) Suppression in auditory-nerve fibers of cats using low-side suppressors. III. Model results. Hear Res. 1996 Jul;96(1-2):126-40.

Carney LH, McDuffy MJ, Shekhter I. (1999) Frequency glides in the impulse responses of auditory-nerve fibers. J Acoust Soc Am. 1999 Apr;105(4):2384-91.

De Boer E, Nuttall AL. The mechanical waveform of the basilar membrane. I. Frequency modulations ("glides") in impulse responses and cross-correlation functions. J Acoust Soc Am. 1997 Jun;101(6):3583-92.

Goldberg, J. M., and Brown, P. B. (1969). "Response of binaural neurons of dog superior olivary complex to dichotictonal stimuli: some physiological mechanisms Of sound localization, "J. Neurophysiol. 32, 613-636.

Guinan JJ Jr, Gifford ML (1988c) Effects of electrical stimulation of efferent olivocochlear neurons on cat auditory-nerve fibers. III. Tuning curves and thresholds at CF. Hear Res. 1988 Dec;37(1):29-45.

Guinan JJ Jr, Lin T, Cheng H. (2005) Medial-olivocochlear-efferent inhibition of the first peak of auditory-nerve responses: evidence for a new motion within the cochlea. J Acoust Soc Am. 2005 Oct;118(4):2421-33

Guinan J.J., Jr. (2009). Bias-tone effects on auditory-nerve responses reveal three mechanical drives, two dependent on outer-hair-cell motility and one passive. Asso. Res. Otolaryngol. Abstr 33, #1109.

Johnson DH. (1980) The relationship between spike rate and synchrony in responses of auditory-nerve fibers to single tones. J Acoust Soc Am. 1980 Oct;68(4):1115-22.

Kiang NYS, Watanabe T, Thomas EC, Clark LF (1965) Discharge Patterns of Single Fibers in the Cat's Auditory Nerve (MIT, Cambridge, MA)

Kiang NYS (1984) Peripheral Neural Processing of Auditory Information, Handbook of Physiology, The Nervous System III, Chapter 15

Kiang NY. (1990) Curious oddments of auditory-nerve studies. Hear Res. 1990 Nov;49(1-3):1-16.

Liberman MC (1984) The cochlear frequency map for the cat: labeling auditory-nerve fibers of known characteristic frequency. J Acoust Soc Am. 1982 Nov;72(5):1441-9

Liberman MC, Kiang NY (1984) Single-neuron labeling and chronic cochlear pathology. IV. Stereocilia damage and alterations in rate- and phase-level functions. Hear Res. 1984 Oct;16(1):75-90

Lin T, Guinan JJ Jr. (2000) Auditory-nerve-fiber responses to high-level clicks: interference patterns indicate that excitation is due to the combination of multiple drives. J Acoust Soc Am. 2000 May;107(5 Pt 1):2615-30

Mardia KV (2000) Directional Statistics (Wiley, London)

Patuzzi R, Sellick PM, Johnstone BM (1984a) The modulation of the sensitivity of the mammalian cochlea by low-frequency tones. I. Primary afferent activity. Hear Res. 1984 Jan;13(1):1-8

Pfeiffer RR, Molnar CE (1970) Cochlear nerve fiber discharge patterns: relationship to the cochlear microphonic. Science. 1970 Mar 20;167(925):1614-6.

Ruggero MA, Robles L, Rich NC (1992) Two-tone suppression in the basilar membrane of the cochlea: mechanical basis of auditory-nerve rate suppression. J Neurophysiol. 1992 Oct;68(4):1087-99

Russell IJ, Sellick PM. (1983) Low-frequency characteristics of intracellularly recorded receptor potentials in guinea-pig cochlear hair cells. J Physiol. 1983 May;338:179-206.

Sachs MB, Hubbard AE. (1981) Responses of auditory-nerve fibers to characteristic-frequency tones and low-frequency suppressors. Hear Res. 1981 Jul;4(3-4):309-24.

Schoonhoven R, Keijzer J, Versnel H, Prijs VF (1994) A dual filter model describing single-fiber responses to clicks in the normal and noise-damaged cochlea. J Acoust Soc Am. 1994 Apr;95(4):2104-21

Sellick PM, Patuzzi R, Johnstone (1982) BM Modulation of responses of spiral ganglion cells in the guinea pig cochlea by low-frequency sound. Hear Res. 1982 Jul;7(2):199-221

Shera CA (2001) Frequency glides in click responses of the basilar membrane and auditory nerve: their scaling behavior and origin in traveling-wave dispersion. J Acoust Soc Am. 2001 May;109(5 Pt 1):2023-34

Temchin AN, Ruggero MA. (2009) Phase-locked responses to tones of chinchilla auditory nerve fibers: implications for apical cochlear mechanics. J Assoc Res Otolaryngol. 2010 Jun;11(2):297-318. Epub 2009 Nov 17

Van der Heijden M, Joris PX. (2006) Panoramic measurements of the apex of the cochlea J Neurosci. 2006 Nov 1;26(44):11462-73

Chapter 5 . Summary

I. Review of Thesis Objectives

The main objective of the thesis was to test the hypothesis from [Guinan et al, 2005] that the outer hair cell (OHC) mechanisms involved in generating auditory nerve (AN) initial peak (ANIP) and AN second peak (ANSP) responses are somehow different from the OHC mechanisms that produces AN responses to low-level clicks. The experimental strategy toward this objective was to measure AN responses while using the suppressive effects of a low-frequency bias-tone to change the OHC transduction function. The gain of the OHC mechano-electric transduction function and the resulting AN responses are suppressed at two opposite phases of the bias-tone period which correspond to traversals through low-gain regions in the OHC transduction function [Ruggero et al, 1992; Cai and Geisler, 1996c]. From the bias-tone-induced suppression patterns, the phase of the major suppression and the symmetry depth between the two suppression phases are expected to reveal similarities and differences in the OHC mechano-electric transduction functions that produce the AN response types of interest. Specifically, the focus of the investigation was on the following key issues which were explored in chapter 3 through the comparison of the suppressive effects of a 50-Hz bias-tone on ANIP versus ANSP versus AN responses to low-level clicks:

a. Is the OHC mechano-electric transduction function involved in the generation of ANIP and ANSP responses? If so, is the strength of involvement as robust as in the mechanism that produces AN responses to low-level clicks?
b. If the OHC mechano-electric transduction function is indeed involved in the generation of ANIP and ANSP responses, are there any significant differences in how the OHC mechano-electric transduction function is used in generating ANIP and ANSP responses at mid-to-high click levels versus AN responses to low-level clicks? If so, can we infer any details about the cochlear mechanisms that produce ANIP and ANSP responses versus the mechanisms that produce AN responses to low-level sounds?

Before delving into the main objective in chapter 3, the suppressive effects of a low-frequency (50 Hz) bias-tone on AN responses to low-level CF tones VS low-level clicks were studied in chapter 2. The bias-tone effects on these responses were expected to be similar since it is widely accepted that both are driven by a common mechanical drive, i.e., BM vibration enhanced by the cochlear amplifier. However, this similarity had not been shown previously since bias-tone effects on click responses had not been studied systematically.

In addition to the main objective in Chapter 3, Chapter 4 explored the hypothesis that different OHC-induced mechanical drives produce AN responses to low-level CF tones versus responses to low-level tones in tuning-curve side lobes. Responses in the side lobes were measured by using "off-CF" frequencies where "off-CF" means >0.7 octaves from CF. This hypothesis was explored by comparing the suppressive effects of a low-frequency bias-tone on AN response to low-level CF-tones versus off-CF-tones. The hypothesis was motivated by discontinuities in group delays from AN responses to tones in the tuning-curve CF region compared to the side-lobe region. Shorter group delays are seen in the side

lobes compared to delays at CF, and frequencies ~0.7 octave or further away from the CF are always in the side-lobe region [Liberman, 1978; Van der Heijden & Joris, 2006].

II. Summary of Chapter Conclusions

A. Chapter 2: Bias-tone Effects on Low-level Click Responses and Low-level CF-tone Responses

The suppressive effects of 50 Hz bias-tones on AN responses to low-level CF tones found in this thesis are quite similar (i.e. with no major discrepancies) to the most comparable study from the past [Cai and Geisler, 1996a]. Similar to the report in [Cai and Geisler, 1996a], the results in this thesis showed the well known pattern of two suppression dips at opposite phases of the bias-tone from most of the AN fibers recorded throughout the range of CFs from 408 Hz to 26.5 kHz. The major suppression phase as a function of CF (Fig. 2.18) formed a smooth curve located ~1/4 bias-tone period away from the phase of excitation by the bias-tone alone, as also reported in [Cai and Geisler, 1996a]. The difference of ~1/4 cycle between the phase of bias-tone excitation and phase of suppression of CF-tone responses has been explained through the difference in the coupling mechanism for a low-frequency tone to the IHC versus OHC stereocilia [Cai and Geisler, 1996a; Sellick et al, 1982; Temchin et al, 1997]. The symmetry between the two suppression phases was quantified as the ratio of the second harmonic to the first harmonic synchrony index as shown in Fig. 2.23. This shows a trend of increasing symmetry toward the base of the cochlea as also reported in [Cai and Geisler, 1996a].

Bias-tone effects on AN responses to low-level clicks were studied by analyzing the suppressive effects on the first peak of low-level click responses. As the bias tone level was increased, the characteristic progression of suppression from a single suppression phase to two suppression dips at opposite bias-tone phases was found over the CF range from 156 Hz to 7.2 kHz. For AN fibers with CFs > 10 kHz, the maximum level of the bias-tone available was not high enough to induce significant suppression of AN responses to low-level clicks. For AN fibers with CF < 10 kHz, the suppression patterns of AN responses to low-level clicks versus those to low-level tones were quite similar. In particular, the major suppression phases of the AN responses to low-level clicks and low-level tones were located close together, within one standard error of the phase estimate, i.e., ± 20 ° as shown in Fig. 2.21. These results support the widely accepted idea that AN responses to low-level tones and to low-level clicks are driven by a common OHC mechanism, i.e., the cochlear amplifier.

The failure to achieve criterion suppressions in the bias-tone effects on AN responses to low-level click responses for CF > 10 kHz is likely due to methodological limitations in the maximum level of the bias-tone and the bandwidth of the click stimulus. Accordingly, it would be desirable for a future study to extend direct comparison between the two response types beyond 20 kHz with an improved acoustic setup. In particular, it would be desirable to determine whether the trend of a rapidly increasing suppression symmetry from the AN responses to CF-tones for CF > 10 kHz is also seen in bias-tone effects on AN responses to low-level clicks. Such results would allow a more comprehensive test of the hypothesis that both low-level tone and low-level click responses are due to the same OHC mechanisms.

B. Chapter 3: Bias-tone Effects on AN Responses to Low-level Clicks and the Initial Peaks of Mid-to-high-level Clicks

The effects of low-frequency (50 Hz) bias tones on ANIP and ANSP responses from mid-to-high-level clicks were compared with the bias-tone effects on the first peak of AN responses to low-level clicks for AN fibers with CFs < 4 kHz. ANIP and ANSP were typically seen at 0.5 ms – 1.5 ms shorter latencies and ~30 dB higher click levels compared to low-level click responses. From most of the fibers recorded, as the bias level was increased the characteristic progression of the suppression pattern from a single suppression phase to two suppression dips at opposite phases of the bias-tone was found for all three types of click responses. These results indicate that the OHC mechano-electric transduction function is involved in the generation of ANIP and ANSP responses as well as in the generation of AN responses to low-level clicks.

The suppression threshold for AN responses to low-level clicks was ~5-10 dB lower than the suppression threshold of ANIP, and in turn the suppression threshold of ANIP was ~5-10 dB lower than the suppression threshold of ANSP (Fig. 3.21). Considering the results from Chapter 2 where the suppression threshold on AN responses to tones was ~5-10 dB lower than the suppression threshold of low-level click responses, the difference in the suppression threshold between ANIP and the low-level click responses can be considered as relatively small and is likely due to the difference in the click stimulus level between the two response types. Therefore, the relatively small difference in the suppression thresholds between ANIP and AN responses to low-level clicks suggest that the strength of involvement of the OHC mechano-electric function in ANIP response generation is as robust as in AN responses to low-level clicks. ANIP and ANSP responses were obtained at the same click level so the higher bias-tone thresholds for ANSP biasing compared to ANIP biasing are consistent with MOC efferent studies where the inhibitory effects by MOC efferents were significantly weaker on ANSP than on ANIP [Guinan et al, 2005]. The MOC results were interpreted in [Guinan et al, 2005] as that ANSP consists of a mixture of the active OHC drive that produces ANIP and the mostly passive drive that produces the later click-response peaks. The results in this thesis are consistent with that hypothesis.

In comparing the detailed suppression patterns of the three click-response types, the key data were the phase of the major suppressions as shown in Fig. 3.20. The major suppression phases of ANIP and ANSP were close, i.e. within one standard error (± 20°) from each other. The major-suppression phases for AN responses to low-level clicks, which were similar to those of AN responses to low-level CF-tones (Chapter 2), were ~1/2 cycle away from the major-suppression phases of ANIP and ANSP. These results indicate that OHC mechano-electric transduction is involved in the generation of ANIP and ANSP responses at mid-to-high click levels as well as in the generation of AN responses to low-level clicks. Furthermore, the significant difference in the major suppression phases of AN responses to low-level clicks VS to ANIP and ANSP supports the hypothesis in [Guinan et al, 2005] that the OHC mechanisms that produce ANIP and ANSP are different from the OHC mechanisms that produce AN responses to low-level clicks.

These results raise the question: "What is the detailed mechanism behind the reversal of the major suppression phases of AN responses from low-level clicks compared to ANIP and ANSP from mid-to-high level clicks?" Answers to this question require experimental data on cochlear mechanics from

the apex of the cochlea which are far from being abundant and reliable due to the challenges of maintaining the health of the cochlea during mechanical or intracellular recordings from the apex [Dallos, 1986]. However, it is desirable to review relevant studies from the base of the cochlea for any insights that they might provide [Cai and Geisler, 1996c; Cody and Russell, 1987; Russell and Kössl, 1992]. Particularly, it is of interest to examine the following points:

a. Are there similar reports of the key finding of this study from the base of the cochlea, i.e., reversals of the phase of the major suppression of AN responses produced by a low-frequency bias-tone?
b. If so, what are the cochlear mechanisms behind the reversals of the major suppression phase?

From the bias-tone effects on cat AN responses to low-level CF-tones, [Cai and Geisler, 1996a] reported variations in the bias-tone induced suppression patterns from basal fibers including reversals of the major suppression phase across AN fibers. They also reported that the symmetry between the suppression phases increased toward the base. In [Cai and Geisler, 1996c], the mechanism behind the varying location of the major suppression phase across basal fibers was attributed to a shift of the operating point of the OHC mechanoelectric-transduction function. Specifically, for the fibers with nearly symmetrical shapes of their suppression phases (as in Fig. 3.2(a)), small changes in the operating point of the OHC transduction function can shift the polarity of the major suppression phase. For fibers with a major suppression phase that was similar to apical fibers, the operating point is assumed to be away from the depolarizing voltage plateau as in Fig. 3.30(a). For fibers with the opposite major suppression phase, the operating point of the OHC transduction function is assumed to be away from the hyperpolarizing voltage plateau as in Fig. 3.30(b).

The cochlear mechanical explanation in [Cai and Geisler, 1996c] that links reversals of the major suppression phase with shifts in the operating point of the OHC mechano-electric transduction function is supported by in vivo measurements of the OHC receptor potentials from guinea pigs. These OHC receptor potentials showed differences in the operating point of the OHC mechano-electric transduction function from the apex to the base of the cochlea and also reversals over tone stimulus levels in the base of the cochlea [Cody and Russell 1987; Russell and Kössl 1992]. Due to the differences in species, stimulus paradigms and the CF regions of the recording in these studies compared to this thesis, the hypothesis that the shift of the operating point of the OHC mechano-electric transduction function explains the reversals of the suppression phase across low to mid-to-high click levels found in this thesis remains strictly a speculation. However, these related studies from the base of the cochlea do show that the key findings in this study, i.e., the reversals of the suppression phase, were previously observed in the base of the cochlea.

C. Chapter 4: Bias-tone Effects on Low-level CF-tone and Off-CF-tone Responses from Low-CF Fibers

The objective of this chapter was the exploration of possible differences in the OHC mechanisms that generate AN responses to tones from the CF VS the "side-lobe" regions of low-CF fibers. The motivation for thinking there might be a difference is that group delays are shorter in the side-lobe region than in the CF region. Shorter group delays at frequencies away from CF in comparison to delays

in the CF-tone region were reported in [Pfeiffer & Molnar, 1980; Kiang, 1984; Van der Heijden & Joris, 2006]. Selection of a tone frequency in the side-lobe region of an AN fiber was based on the frequency spacing from the CF of the fiber. Specifically, previous studies reported shorter group delays from the side-lobe frequency region for frequencies of 0.7 to 2 octaves from the CF of the fiber. For AN fibers with CF > 1.2 kHz, the side-lobe region was located on the low-side of the CF, and for AN fibers with CF < 1.2 kHz, the side-lobe region was located on the high-side of the CF. To study responses from the side-lobe region, we measured responses at "off-CF" frequencies, where "off-CF" is defined as frequencies >0.7 octaves away from CF.

From the comparison of the suppressive effects on low-level CF tone responses VS low-level off-CF tone responses, significant differences were not found in the major phase suppression phase or in the symmetry between the major and minor suppression phases, as shown in Fig. 4.19 and Fig. 4.22. Furthermore, no significant differences in the suppression data were found across the AN fibers with CF < 1.2 kHz VS CF > 1.2 kHz. These results indicate that the OHC mechano-electrical transduction function is similarly involved in generating AN responses to low-level CF tones and low-level side-lobe tones.

III. References

Cai Y, Geisler CD (1996a) Suppression in auditory-nerve fibers of cats using low-side suppressors. I. Temporal aspects. Hear Res. 1996 Jul;96(1-2):94-112

Cai Y, Geisler CD (1996c) Suppression in auditory-nerve fibers of cats using low-side suppressors. III. Model results. Hear Res. 1996 Jul;96(1-2):126-40.

Cody AR, Russell IJ. (1987) The response of hair cells in the basal turn of the guinea-pig cochlea to tones. J Physiol. 1987 Feb;383:551-69.

Guinan JJ Jr, Lin T, Cheng H. (2005) Medial-olivocochlear-efferent inhibition of the first peak of auditory-nerve responses: evidence for a new motion within the cochlea. J Acoust Soc Am. 2005 Oct;118(4):2421-33

Guinan JJ Jr. (2009) Bias-tone Effects on Auditory-Nerve Responses Reveal Three Mechanical Drives, Two Dependent on Outer-Hair-Cell Motility and One Passive. Asso. Res. Otolaryngol. Abstr 33, #1109

Kiang NYS (1984) Peripheral Neural Processing of Auditory Information, Handbook of Physiology, The Nervous System III, Chapter 15

Liberman MC (1978) Auditory-nerve response from cats raised in a low-noise chamber. J Acoust Soc Am. 1978 Feb;63(2):442-55.

Pfeiffer RR, Molnar CE (1970) Cochlear nerve fiber discharge patterns: relationship to the cochlear microphonic. Science. 1970 Mar 20;167(925):1614-6.

Russell IJ, Kössl M. (1992) Modulation of hair cell voltage responses to tones by low-frequency biasing of the basilar membrane in the guinea pig cochlea. J Neurosci. 1992 May;12(5):1587-601.

Ruggero MA, Robles L, Rich NC (1992) Two-tone suppression in the basilar membrane of the cochlea: mechanical basis of auditory-nerve rate suppression. J Neurophysiol. 1992 Oct;68(4):1087-99

Van der Heijden M, Joris PX. (2006) Panoramic measurements of the apex of the cochlea J Neurosci. 2006 Nov 1;26(44):11462-73